

Sheffield Hallam University

Phosphatase and tensin homologue deleted on chromosome ten (PTEN) gene mutations in haematological malignancies.

WELBOURN, John T.

Available from the Sheffield Hallam University Research Archive (SHURA) at:

<http://shura.shu.ac.uk/20514/>

A Sheffield Hallam University thesis

This thesis is protected by copyright which belongs to the author.

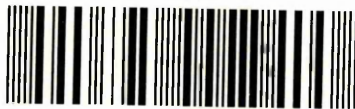
The content must not be changed in any way or sold commercially in any format or medium without the formal permission of the author.

When referring to this work, full bibliographic details including the author, title, awarding institution and date of the thesis must be given.

Please visit <http://shura.shu.ac.uk/20514/> and <http://shura.shu.ac.uk/information.html> for further details about copyright and re-use permissions.

Sheffield S11WB

101 895 493 7



Sheffield Hallam University
Learning and IT Services
Adsetts Centre City Campus
Sheffield S1 1WB

REFERENCE

Return to Learning Centre of issue
Fines are charged at 50p per hour



ProQuest Number: 10701161

All rights reserved

INFORMATION TO ALL USERS

The quality of this reproduction is dependent upon the quality of the copy submitted.

In the unlikely event that the author did not send a complete manuscript and there are missing pages, these will be noted. Also, if material had to be removed, a note will indicate the deletion.



ProQuest 10701161

Published by ProQuest LLC (2017). Copyright of the Dissertation is held by the Author.

All rights reserved.

This work is protected against unauthorized copying under Title 17, United States Code
Microform Edition © ProQuest LLC.

ProQuest LLC.
789 East Eisenhower Parkway
P.O. Box 1346
Ann Arbor, MI 48106 – 1346

Phosphatase and tensin homologue deleted on chromosome ten
(PTEN) gene mutations in haematological malignancies

John T Welbourn

A thesis submitted in partial fulfilment of the requirements of
Sheffield Hallam University
for the degree of Doctor of Philosophy

July 2007

Abstract

PTEN is a tumour suppressor protein named after its homology with phosphatase and tensin and its frequent deletion on chromosome 10.

PTEN was discovered to be mutated in several solid tumours such as breast brain and ovarian cancers. This study sought to establish the role of PTEN mutation in haematological malignancies. Methods were developed to extract DNA from archival material consisting of formalin-fixed, paraffin-embedded tissue sections and methanol-fixed, May-Grunwald and Giemsa-stained bone marrow smears. To optimise amplification of extracted DNA, PCR primers were developed to produce a range of product sizes from human β -globin, prothrombin and PTEN genes. Techniques were developed for RTPCR amplification of cDNA from cultured haematological cell lines. Electrophoresis methods were developed to demonstrate heteroduplex formation using non-denaturing concentrations of denaturing agents and different gel media and running temperatures. Primers were designed to flank exon sequences and a representative group of myeloid and lymphoid malignancies were screened for PTEN mutations. Exons 5, 7 and 8 were initially amplified for heteroduplex analysis following reports of frequent mutation. No heteroduplex bands were observed in samples assayed. The possible insensitivity of heteroduplex analysis to mutations in sub populations of mutant tumour cells led to the development of SSCP techniques. These techniques were optimised for analysis of DNA that was extracted from frozen archived bone marrow. PCR reactions were developed to amplify each PTEN exon. No suitable primers were found for exon 2 analysis due to extensive non-specific amplification. A total of 912 SSCP assays were performed, screening a range of lymphoid and myeloid malignancies for mutations in all PTEN exons except exon two. Only two possible aberrant conformations were indicated, both in exon 5. The exon 5 PCR product from both positive samples were DNA sequenced using forward and reverse primers. Exon 5 of seven other leukaemia samples were sequenced as controls to detect possible lack of sensitivity of SSCP analysis to PTEN mutations. All samples showed exon 5 DNA sequences in agreement with published sequences. These results suggest that small deletions and point mutations in the PTEN gene are very rare in haematological malignancy. The expression of PTEN mRNA in cultured haematological malignancy cells was established by the earlier RTPCR amplification using cultured cells. Western blotting was performed to establish PTEN protein expression in primary malignancies. All samples assayed showed protein expression. Concerns regarding the contribution from residual normal cells to the PTEN expression picture in tumour cell samples led to the assay of protein by immunofluorescence. PTEN protein was demonstrated in all successful reactions with one CGL and one AML M3 showing higher levels of expression than control cells. These results suggest that in haematological malignancy, the PTEN gene is not mutated and PTEN protein is expressed in leukaemic cells.

Research by other workers has demonstrated the importance of PTEN in normal haemopoiesis. In mouse models, normal PTEN expression is essential for normal compartmentalisation and to prevent the acquisition of a leukaemic picture. This study suggests that if PTEN dysfunction is involved in the development of haematological malignancy, then it is by a subtle mechanism such as a change in expressed protein levels. It may be that, with the small number of oncogenic mutations necessary to promote a leukaemic phenotype, mutated PTEN does not provide a selective advantage to promote further the survival of the malignant cell population.

Acknowledgments

I would like to thank the following: Dr Maria Blair for her supervision and advice whilst undertaking and writing up this thesis; Prof. Nicola Woodroffe for her support during the writing up of this thesis; Wirral Hospital NHS Trust for allocating time and resources to complete this thesis; The J K Douglas Research Laboratory for their help with DNA sequencing; Dr Paul Sherrington of The Royal Liverpool University Teaching Hospital for his general advice and provision of cell lines; The Wirral Hospitals League of Friends for the purchase of vertical eletrophoresis equipment.

Contents

	Page
Abstract	i
Acknowledgments	ii
Contents	iii
List of Abbreviations	xi
Chapter 1 Introduction	1
1.1 Cancer	1
1.1.1 Cell function in multi- and unicellular organisms	1
1.1.2 Development of cancer	1
1.1.3 Malignant and benign tumours	2
1.1.4 Historical Understanding of cancer	2
1.2 The Cell Cycle	4
1.3 Apoptosis	8
1.3.1 Induction of apoptosis	9
1.3.2 Apoptosis and neoplasia.	12
1.4 Gene regulation and DNA methylation	12
1.5 Genes involved in cancer	14
1.5.1 Proto-oncogenes	15
1.5.1.1 Oncogene Classification	16
1.5.2 Tumour suppressor genes	16
1.5.2.1 Rb	18
1.5.2.1.1 Rb in Apoptosis	21
1.5.2.1.1.3 Rb and promotion of differentiation	21
1.5.2.1.1.5 Rb and telomere length	22

	Page
1.5.2.1.1.5 Rb and maintenance of G0 phase	22
1.5.2.1.2 Interaction with PTEN	23
1.5.2.2 p53 Tumour protein	25
1.5.2.2.1 p53 function in oncogenesis	26
1.5.2.2.2 p53 and DNA damage	27
1.5.2.3 p16 and tumour suppression	28
1.5.2.4 Adenomatous Polyposis Of The Colon (APC) Gene	29
1.5.2.5 BRCA1 and BRCA2	30
1.5.2.6 WT1 and WT2	31
1.5.2.7 NF1	32
1.5.2.8 VHL	33
1.5.2.9 Men1	34
1.5.2.10 PTCH	34
1.5.2.11 SMAD4	35
1.5.2.12 E-Cadherin	35
1.5.2.13 LKB1/STK11	36
1.5.2.14 SNF5/INI1	36
1.5.2.15 EXT1 and EXT2	37
1.5.2.16 Tuberous sclerosis complex	37
1.6 Blood cell Production	37
1.7 Haematological malignancy	38
1.7.1 Chronic myeloid (or myelogenous) leukaemia (CML)	39
1.7.1.1 Abl	42
1.7.1.2 Bcr	43

	Page
1.7.1.3 Bcr/Abl and the PI3 kinase pathway	44
1.7.1.4 Bcr/Abl and Ras activation	45
1.7.1.5 STAT5 pathway	45
1.7.1.6 Apoptosis in CML	46
1.7.1.7 The cell cycle in CML	47
1.7.1.8 Progression to Blast Crisis	48
1.8 PTEN tumour suppressor protein	49
1.8.1 Structure of PTEN	50
1.8.2 Function of PTEN	51
1.8.2.1 PTEN Protein Phosphatase function	54
1.8.2.2 PTEN and p27 regulation	55
1.8.2.3 Role of PTEN in the Nucleus	56
1.8.2.4 PTEN and Chemotaxis	57
1.8.3 Regulation of PTEN	58
1.8.3.1 C terminus and PTEN regulation	58
1.8.3.2 N terminus and PTEN regulation	60
1.8.3.3 Regulation Of PTEN Expression and Ubiquitination	62
1.8.4 PTEN function in Leukaemia	63
1.9 Aims of thesis	65
Chapter 2 Materials and Methods	67
2.1 DNA extraction	67
2.1.1 Fresh cells, blood and bone marrow	67
2.1.2 Extraction of DNA from fixed, stained bone marrow smears	68
2.1.3 Microdissection of tumour cell DNA from stained bone marrow	69

	Page
2.1.4 Extraction of DNA from fixed paraffin-embedded tissue sections	70
2.1.4.1 Extraction of DNA from -fixed paraffin-embedded tissue sections using phenol/chloroform	70
2.1.4.2 DNA extraction from wax embedded tissue sections by de-waxing and proteinase K digestion	71
2.1.4.3 DNA extraction from wax embedded tissue sections by heat-based de-waxing and proteinase K digestion	71
2.1.5 RNA extraction from cultured cells	72
2.2 PCR primer design	73
2.3. PCR optimisation	74
Table 2.2 Primers used in the heteroduplex analysis reactions	75
2.3.1 RT PCR	76
2.4 Heteroduplex analysis	77
2.4.1 Sample disease types in the heteroduplex study of PTEN exons 5, 7 and 8	77
2.4.2 PTEN exon 5 7 and 8 Heteroduplex Analysis Electrophoresis	77
2.4.2.1 Heteroduplex sample generation	78
2.4.2.2 Heteroduplex gel preparation	78
2.4.2.3 Silver staining	78
2.4.2.4 Preparation of BAP/Glycerol/TTE Heteroduplex gels	79

	Page
2.4.2.5 Use of PagePlus Heteroduplex gels	79
2.4.2.5.1 PagePlus Gel preparation	80
2.5 Single Strand Conformation Polymorphism analysis of PTEN exons 1-9	80
Table 2.5.1 PCR primers for SSCP analysis	81
2.5.1 Generation of single stranded complexes	82
2.6 PCR product sequencing	84
2.6.1 PCR product sequencing using the Megabace sequence analyzer	84
2.6.1.1 Preparation of sequencing reaction	84
2.6.1.2 Post-reaction clean-up	84
2.6.1.3 Injection and run parameters	85
2.7 Western blotting of proteins by enhanced chemiluminescence	85
2.7.1 Protein purification for western blotting from bone marrow samples	85
2.7.2 Bradford assay for protein concentration	86
2.7.3 SDS Protein electrophoresis	87
2.7.4 Blotting to PVDF membrane	88
2.7.5 Western blot for PTEN/ β -Actin	89
2.8 Immunofluorescence and Immunocytochemistry	90
2.8.1 Immunocytochemistry	90
2.8.2 Immunofluorescence	91
Chapter 3 Results	92
3.1 Extraction of nucleic acids from fresh and archived tissue	92
3.1.1 Extraction of Nucleic acid from fresh cells	92

	Page
Table 3.1.1 Sample disease types, % tumour cells, DNA concentration and DNA purity of samples analysed in the SSCP reactions	93
Graph 3.1.1 Correlation of yield of DNA in $\mu\text{g ml}^{-1}$ with percentage purity of DNA extract	94
3.1.2 Extraction of DNA from fixed bone marrow tissue	95
3.1.3 Extraction of DNA from fixed, stained bone marrow smears and amplification with PTEN exon 5 and 8 primers	95
3.1.4 Extraction of DNA from fixed, Romanowsky stained bone marrow smears by micro dissection.	97
3.1.5 Extraction of DNA from formalin-fixed wax-embedded tissue sections.	97
3.1.6 Extraction of RNA and RTPCR of PTEN in cell lines	101
3.2 Optimisation of PCR reactions	104
3.2.1 Titre of magnesium concentration using primer pairs PTGS 5 and PTGS 8	104
3.2.2 Optimisation of magnesium concentration in RTPCR reaction	104
3.2.3 Titre of dimethylsulphoxide concentration in PCR reaction for PTEN exons 1 and 3 (PTGS1 and 3)	106
3.2.4 Annealing temperature gradient analysis for heteroduplex exon 2 primer pairs (PTGS 2 and 2.1)	108
3.2.5 RTPCR of cell lines derived from haematological malignancy and differentiation between PTEN cDNA and PTH2 homologous sequences.	111

	Page
3.3 Heteroduplex analysis.	113
3.3.1 Optimised heteroduplex PCR product for each PTEN exon22	113
3.3.2 Optimisation of Heteroduplex electrophoresis conditions	113
3.3.3 Heteroduplex analysis with modified cross-linker Bis-acryloyle piperazine.	116
3.3.4 Heteroduplex analysis with Bis-acryloyl piperazine and non- denaturing concentration of formamide and ethylene glycol and formamide.	116
3.3.5 Heteroduplex analysis with use of proprietary acrylamide- based gel mix PagePlus [®] with GelStar [®] or silver staining	118
3.3.6 Bis-acryloyl piperazine gel with silver staining.	118
3.3.7 Heteroduplex analysis of PTEN exons 5, 7 and 8	121
3.4 SSCP analysis of PTEN	127
3.4.1 PCR product specificity for SSCP analysis	127
3.4.2 SSCP of bone marrow samples	130
3.4.2.1 SSCP PTEN Exon1	130
3.4.2.2 SSCP PTEN Exon2	136
3.4.2.3 SSCP PTEN Exon3	136
3.4.2.4 SSCP PTEN Exon4	143
3.4.2.5 SSCP PTEN Exon5	150
3.4.2.6 SSCP PTEN Exon6	158
3.4.2.7 SSCP PTEN Exon7	165
3.4.2.8 SSCP PTEN Exon8	172
3.4.2.9 SSCP PTEN Exon9	179
3.4.3 SSCP gels stained with GelStar [®]	186

	Page
3.4.4 SSCP analysis – summary of results	188
3.5 DNA sequencing of PTEN exon 5 in samples with aberrant SSCP migration	189
3.6 Western blotting of PTEN protein	193
3.7 PTEN Immunocytochemistry and immunofluorescence	195
3.7.1 Immunofluorescence	196
3.7.2 Immunocytochemistry	198
Chapter 4 Discussion and Conclusion	
Discussion	199
Conclusion	218
Further Work	219
References	220
Appendix I WHO Classification of Haematological Malignancy	I
Appendix II French/American/British Classification of leukaemia	V
Appendix III Manual Staining Procedure For Blood Films	VI
Appendix IV Immunocytochemistry using Shandon Sequenza staining System	VIII

List of Abbreviations

5-Mc	5-Methyl Cytosine
ALL	Acute Lymphoblastic Leukaemia
ALL-CR	Acute Lymphoblastic Leukaemia in Complete Remission
AML	Acute Myeloid Leukaemia
Apc	Anaphase Promoting Complex
APC	Adenomatous Polyposis Coli
CD	Cluster of Differentiation
CDK	Cyclin Dependent Kinase
CFU	Colony Forming Unit
CGL	Chronic Granulocytic Leukaemia
CLL	Chronic Lymphatic Leukaemia
CML	Chronic Myeloid Leukaemia
CMLT	Chronic Myeloid Leukaemia Transformed
CMML	Chronic Myelomonocytic Leukaemia
CSF	Colony Stimulating Factor
CSGE	Conformation Sensitive Gel Electrophoresis
DGGE	Denaturing Gradient Gel Electrophoresis
EC	Endometrial Carcinoma
EDTA	Ethylenediamine Tetra-Acetic Acid
EGF	Epidemial Growth Factor
EPO	Erythropoietin,
FAK	Focal Adhesion Kinase
FAP	Familial Adenomatous Polyposis
FFPE	Formalin-Fixed Paraffin-Embedded
GDP	Guanosine Diphosphate

GTP	Guanosine Triphosphate
HD	Heteroduplex
HGF	Hepatocyte Growth Factor
HPV	Human Papilloma Virus
HSC	Haematopoietic Stem Cell
LSC	Leukaemic Stem Cell
LOH	Loss of Heterozygosity
MCR	Mutation Cluster Region
MDA	Multiple-Strand Displacement Amplification
MDS	Myelodysplastic Syndrome
MM	Multiple Myeloma
MMAC1	Mutated In Multiple Advanced Cancers 1
NGF	Nerve Growth Factor
NHL	Non-Hodgkin's Lymphoma
ORF	Open Reading Frame
PCR	Polymerase Chain Reaction
PDGF	Platelet Derived Growth Factor
PI	Phosphatidylinositol
PI2	PI(4,5)P2
PI3	PI(3,4,5)P3
PI3K	Phosphatidylinositol 3 Kinase
Pparg	Peroxisome Proliferator-Activated Receptor G
PTEN	Phosphatase And Tensin Homolog
PTP	Protein Tyrosine Phosphatase
RAEB	Refractory Anaemia with Excess Of Blasts
RAEBT	Refractory Anaemia with Excess Of Blasts Transformed

RARS	Refractory Anaemia with Ringed Sideroblasts
RCF	Relative Centrifugal Force
RTK	Receptor Tyrosine Kinase
SAHF	Senescence-Associated Heterochromatic Foci
SCLC	Small Cell Carcinoma of the Lung
SPF	S-Phase Promoting Factor
SSCP	Single Strand Conformation Polymorphism
TBE	Tris/Borate EDTA
TCR	T-Cell Receptor
TE	Tris EDTA
Temed	Tetramethylethylenediamine
TGF	Transforming Growth Factor
TNF	Tumour Necrotic Factor
TSG	Tumour suppressor gene
TTE	Tris Taurine EDTA
WHO	World Health Organisation
WM	Waldensrome's Macroglobulinaemia

Chapter 1 Introduction

1.1 Cancer

1.1.1 Cell function in multi- and unicellular organisms.

The millions of cells that comprise a complex multicellular organism are characterised by the property of differentiation to a mature state, followed by death. This process is associated with maintenance of a germline genotype in certain germ cells and stem cells, but for the vast majority of cells, their existence is limited to the service of the organism as a whole and with the eventual propagation of the genotype in the form of whole organism offspring. This cooperative system of multicellular organisms contrasts with that of single cell systems which function in a competitive environment purely for the benefit of individual cells (Alberts *et al.* 2002).

1.1.2 Development of cancer

The development of cancer has been described by Alberts *et al.* (2002) as a microevolutionary process. To coordinate their behaviour, the cells are subject to an elaborate set of signals that serve as social signals, controlling the action of each. In an organism such as *Homo sapiens*, consisting of approximately 10^{14} cells the maintenance of order is critical. A cell functioning outside the constraint of cooperation may acquire a growth advantage and begin to act “selfishly” at the expense of the neighbouring cells still constrained by the growth control mechanisms. The selective advantage may allow it to divide more vigorously than its neighbours and to become a founder of a growing mutant clone. The clone may undergo repeated rounds of mutation, further removing itself from the bounds of controlled cell growth

and function. These are the basic ingredients of cancer; it is a state in which individual cells begin by prospering at the expense of their neighbours, in an uncontrolled manner, possibly to the extent that the continued existence of the multicellular organism is untenable (Alberts *et al.* 2002).

1.1.3 Malignant and benign tumours

Tumour cell clones are classed as either benign or malignant. Benign tumours are encapsulated and are usually well differentiated and retain the characteristics of the cell of origin and are not usually life threatening.

Malignant tumours lose the ability to stay localised according to their original cell function and invade other tissue, often at a distant physical location within the organism, forming metastases that form further tumour masses. Tumour cells have several features that distinguish them from normal cells: they multiply independently of normal growth signals; they are anchorage independent; they may grow over or under each other without inhibition; they are less adhesive than normal cells; they continue to proliferate irrespective of population density (Blair M E, personal communication, January 2007).

1.1.4 Historical understanding of cancer

By the middle of the 20th century, the precise chemical structure of DNA was elucidated and found to be the basis of the genetic code. With the deciphering of the genetic code, workers were able to understand how genes worked and how they could be damaged by mutation. Chemicals, radiation, and viruses could cause cancer, and cancer could be linked to inherited genes. But, as understanding of DNA function increased, it became apparent that the

damage to DNA by chemicals and radiation or the introduction of new DNA sequences by viruses, often led to the development of cancer. It became possible to pinpoint the exact site of the damage to a specific gene (Brown 2002).

It became evident that sometimes, defective genes are inherited as germ-line defects and that sometimes these inherited genes are defective at the same points that chemicals exerted their effect via somatic mutation. Thus carcinogens caused genetic damage, mutations led to abnormal groups of cells (clones), mutated cell clones evolved to even more malignant clones over time and the cancer progressed by more and more genetic damage and mutation. Normal cells with damaged DNA senesce via programmed cell death or apoptosis (discussed in section 1.3); cancer cells with damaged DNA do not (Strachan and Read 2003).

Genes have been discovered that are associated with cancers of the colon, rectum, kidney, ovary, oesophagus, lymph nodes, and pancreas and skin melanoma. Familial cancer is less common than spontaneous cancer, causing less than 15% of all cancers; detection of cancer-associated genes in individuals makes possible the identification of persons at very high risk.

In the early twentieth century, cancer-causing elements in viruses that infected poultry were shown to be sufficient to cause tumour formation.

Peyton Rous at the Rockefeller Institute in New York reported the cell-free transmission of a sarcoma in chickens. The viral agent responsible for transmission was named after its discoverer; the Rous sarcoma virus and the gene responsible termed *src* (Coffin 1997). A short cDNA probe specific for the *src* viral oncogene was obtained by Stehelin in 1976 and was found to

hybridize to sequences in normal cellular DNA. This result showed that *src* was not originally a retroviral gene, but a gene of cellular origin carried in the viral genome and transduced by the virus from cell to cell. This finding led to an understanding of the molecular basis of cancer via discovery of several cellular homologues to cancer-causing elements in viruses. All retroviral oncogenes were found to be recent acquisitions from the cell. Many were eventually identified as cellular genes with normal functions in mitogenic signal transduction: coding for peptide growth factors, growth factor receptors, protein kinases, G proteins, and transcription factors (Stehelin *et al.* 1976, Weinberg 1994).

1.2 The Cell Cycle

Division in the eukaryotic cell requires a tightly regulated doubling of the genome into exact copies. The phases between cell division are denoted as G₁, S, G₂ (interphase) and M (metaphase). G₁ involves cell growth and preparation of genome for replication. S includes synthesis of genome copy and centromeres. G₂ is a second period of growth prior to M or mitosis (Gilbert 2000).

The cell cycle is controlled by a series of proteins termed cyclins (A, B, D and E) and their concentrations vary according to stages of the cycle. Cyclins are activated by phosphorylation under the influence of cyclin dependant kinases (Cdks) (Fig 1.2.1, Fig 1.2.2).

A rising level of G₁-cyclins signal to the cell to prepare the chromosomal DNA for replication by binding to their Cdks. A rising level of S-phase promoting factor (SPF) - which includes cyclin A bound to Cdk2 - enters the nucleus and

prepares the cell to duplicate its DNA (and its centrosomes). As DNA replication continues, cyclin E is destroyed, and the level of mitotic cyclins begins to rise (in G₂). M-phase promoting factor (the complex of mitotic cyclins with the M-phase CDK) initiates assembly of the mitotic spindle, breakdown of the nuclear envelope and condensation of the chromosomes within the nucleus. These events take the cell to metaphase of mitosis. At this point, the M-phase promoting factor activates the anaphase promoting complex (APC) which allows the sister chromatids at the metaphase plate to separate and move to the poles (anaphase), completing mitosis and destroys the mitotic cyclins. It does this by conjugating the cyclins with the protein ubiquitin which targets them for destruction by proteasomes. The APC also turns on synthesis of G₁ cyclin for the next turn of the cycle and degrades geminin, a protein that has kept the DNA freshly synthesized in S phase from being re-replicated before mitosis (Kimball 2006).

The cell has several systems for interrupting the cell cycle if errors in replication occur. The cell monitors the presence of the short discontinuous replicated sequences, termed Okazaki fragments, on the lagging strand during DNA replication. The cell is not permitted to proceed in the cell cycle until these have been made continuous by DNA ligase enzymes. DNA damage checkpoints (such as p53 tumour protein, Ataxia-Telangiectasia Mutated Gene (ATM) protein and the Max Dimerization (MAD) protein sense DNA damage before the cell enters S phase (a G₁ checkpoint), during S phase and after DNA replication (a G₂ checkpoint). A variety of CDK inhibitor proteins exist, such as CDKN1B/p27 which binds to and

Fig 1.2.1

The eukaryotic cell cycle

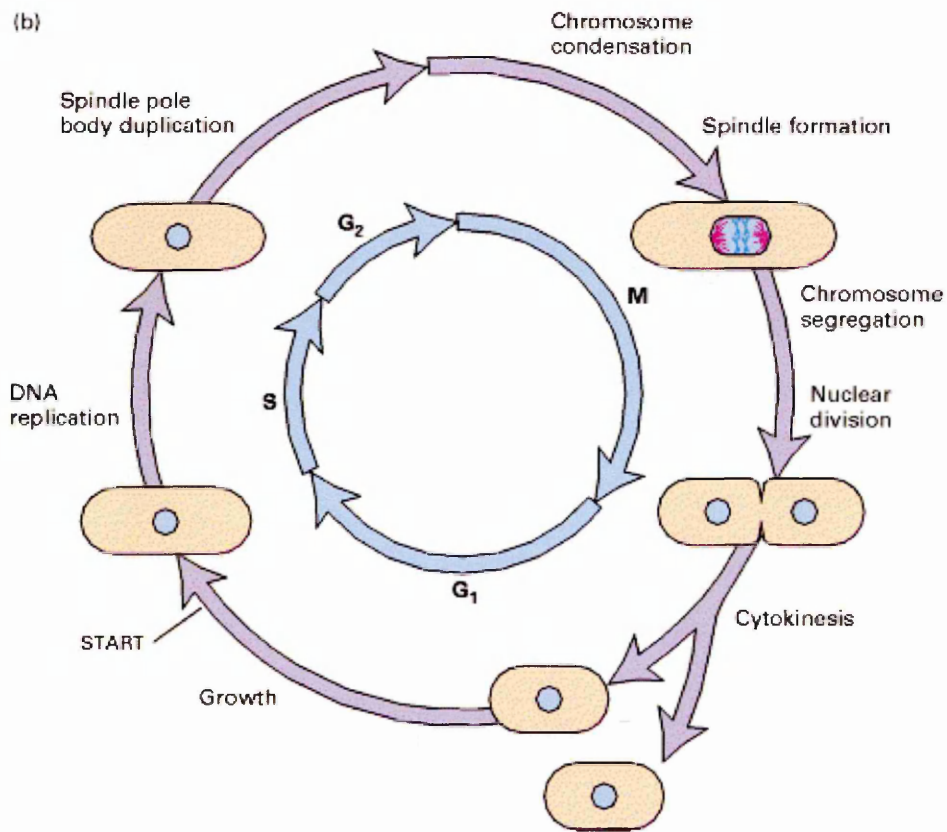


Fig 1.2.1
Figure shows eukaryotic cell cycle and associated events in cell. The G₁ growth phase is followed by DNA replication in S phase. The G₂ phase is associated with spindle pole body duplication and entry into M phase is associated with chromosome condensation, spindle formation, chromosome segregation then nuclear division and finally cell division. Cells may remain quiescent (G₀) or re-enter cell cycle under the influence of cytokines/growth factors (Nigg 1995)

Fig 1.2.2

Cyclins and cyclin dependent kinases expressed within the cell cycle.

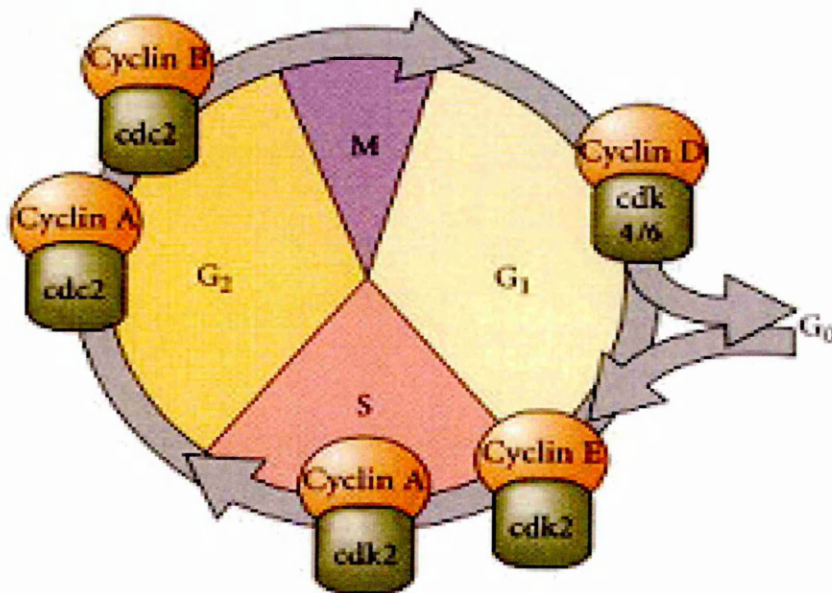


Figure 1.2.2 Figure shows cyclins A,B,D and E and their respective protein kinases (cdk2, 4 and 6 and cdc2) at their point of action in cell cycle regulation (Gilbert 2000).

prevents the activation of cyclin E-CDK2 or cyclin D-CDK4 complexes, and thus controls the cell cycle progression at G1. The degradation of this protein, which is triggered by its CDK dependent phosphorylation, is required for the cellular transition from quiescence to the proliferative state (Hall *et al.* 2004). A cell may leave the cell cycle temporarily or permanently. It exits the cycle at G1 and enters a stage designated G0. A cell in G0 phase is often called "quiescent", but G0 corresponds with a cell's functions in the organism. e.g., secretion, as in plasma cell immunoglobulin secretion, attacking pathogens. Often G0 cells are terminally differentiated: they will never re-enter the cell cycle but instead will carry out their function in the organism until they die. For other cells, G0 is followed by re-entry into the cell cycle. Most of the lymphocytes in human blood are in G0. However, with proper stimulation, such as encountering the appropriate antigen, they can be stimulated to re-enter the cell cycle (at G1) by cytokines and proceed on to new rounds of alternating S phases and mitosis. G0 represents not simply the absence of signals for mitosis, but an active repression of the genes needed for mitosis. Cancer cells cannot enter G0 and are destined to repeat the cell cycle indefinitely (Kimball 2006).

1.3 Apoptosis

The generation of new cell populations is normally carefully balanced by the destruction of an appropriate number of older cells. There are two mechanisms that govern cell death: Injury and programmed cell death (apoptosis or "suicide"). Injurious physical effects include mechanical, chemical, toxic, infection and radiation damage and are characterised by cell

swelling due to disruption of cell membranes, rupture and leakage of cellular contents and subsequently, inflammation (Kimball 2006).

Apoptosis is characterised by cell shrinkage, membrane blebbing, chromatin degradation by cleavage of DNA between nucleosomes, mitochondrial breakdown and release of cytochrome c and end-stage fragmentation of cell into membrane-wrapped fragments. Phosphatidylserine, which is normally preferentially expressed on the inner surface of the cytoplasmic membrane, is exposed on the exterior surface of these fragments. Phosphatidylserine earmarks the fragments for phagocytosis via specific receptors on phagocytic cells such as macrophages and dendritic cells, when the fragment is engulfed and inhibitors of inflammation are released. Apoptosis is part of a cell's normal physiology and is important in two cellular processes: firstly, in growth and development such as the formation of fingers and toes of the human foetus through the removal of tissue between them, the loss of the endometrium at the start of menstruation and the formation of synaptic junctions between neurons in the brain via the elimination of surplus cells. Secondly, programmed cell death is needed to destroy cells that threaten the normal function of an organism. Examples include induction of apoptosis in virus-infected cells by killer T cells, removal of effector cells once a cell-mediated immune response is completed (killer T cells are capable of inducing apoptosis in themselves as well as other T cells) and cells with damaged DNA (Kimball 2006).

1.3.1 Induction of apoptosis.

Apoptosis is induced in a cell by a change in the positive and negative

signalling mechanisms that maintain homeostasis. Negative signals that promote apoptosis include: increased intracellular oxidant concentration, UV and ionising radiation, cytotoxic drugs, accumulation of proteins with improper tertiary structure and binding of specific ligands or “death activators” (tumour necrosis factor (TNF) α , TNF β , CD95). TNF α and β bind to TNF receptors whilst CD95L binds to a CD95L receptor. Thus, apoptosis may be promoted by intracellular or extracellular stimuli. The internal or intrinsic pathway is induced by a change in Bcl2 protein expression on the surface of mitochondrial outer membranes. Bcl2 is normally bound to Apaf-1 protein (fig 1.3.1) (Allen *et al.*, 1998).

Internal cell damage, such as oxidation, causes Bcl2 to release Apaf1 whilst Bax, a Bcl2-related protein, penetrates the mitochondrial membrane causing leakage of cytochrome c from the mitochondria. Bcl2 and Bax seem to have opposing actions in regulating permeability of the mitochondrial membrane. The released cytochrome c and Apaf-1 bind to a further protein, caspase 9. This caspase 9-cytochrome c - Apaf-1 complex binds ATP to form an “apoptosome” The caspase 9 component of the complex is one of several caspase proteases that cleave protein at aspartic acid residues. The complex activates other caspases in the cytosol by proteolytic cleavage which, in turn, goes on to activate other caspases. This process of signal amplification is analogous to that of the blood coagulation cascade. The resulting widespread proteolytic activity leads to destruction of structural cytoplasmic proteins, degradation of DNA into 200bp fragments and ultimately, phagocytosis of the cell by macrophages (Algeciras-Schimnich *et al.* 2006).

The external/extrinsic/death receptor pathway is initiated by binding of

Fig 1.3.1

Signal transduction in apoptosis

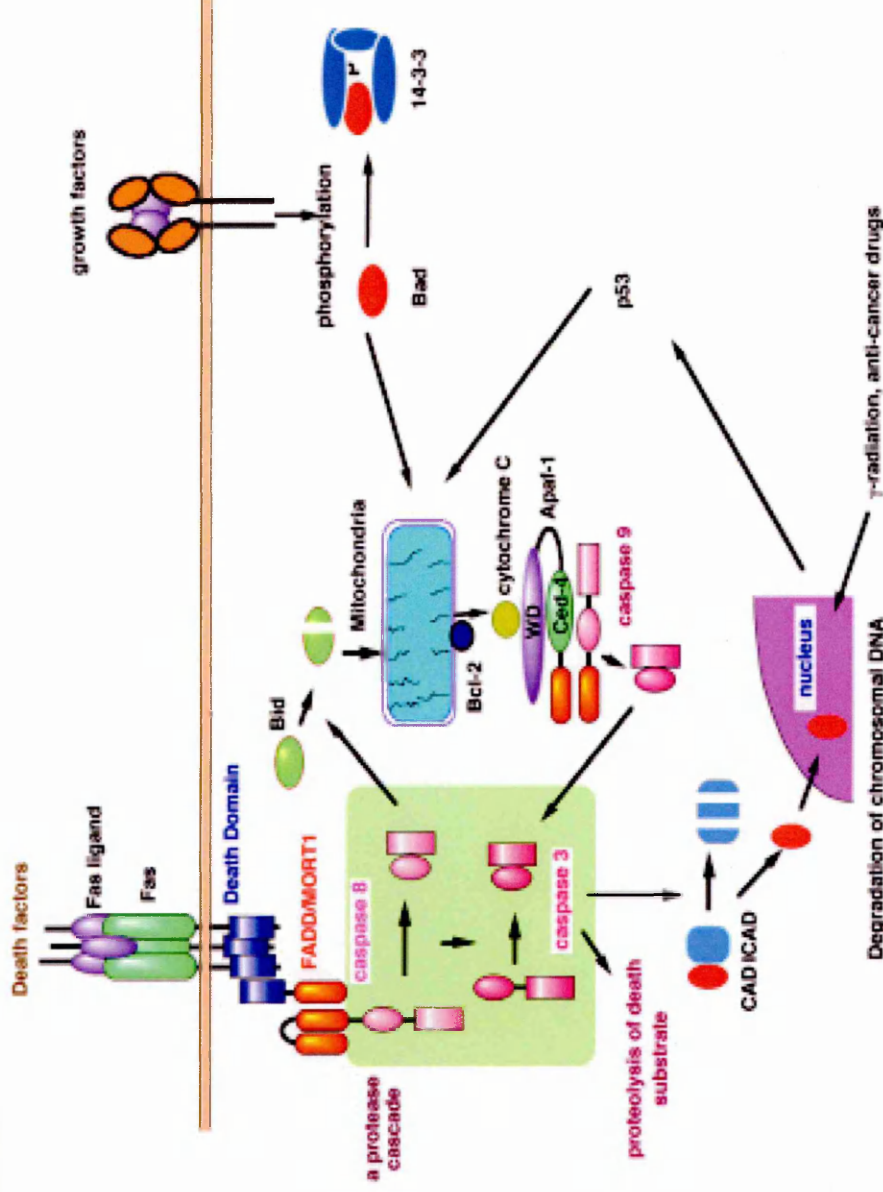


Fig 1.3.1
Figure shows the positive and negative signal transducers involved in apoptosis. Pro apoptotic signals can be extra cellular with the binding of Fas ligand to the Fas receptor or intracellular by activation of p53 and generation of the apoptosome complex around apaf-1. Both mechanisms result in the activation of the caspase protease cascade, proteolysis by CAD and degeneration of chromosomal DNA. Anti apoptotic signals are provided by growth factor binding and phosphorylation of BCL2 antagonist of cell death (BAD)
http://claim.springer.de/EncRef/CancerResearch/samples/0003_01.jpg

CD95/CD95 (found predominantly on the surface of activated T cells) and TNF to their respective receptors on the cell surface which span the cytoplasmic membrane. Binding of the signal molecule leads to activation of caspase 8. Caspase 8, like caspase 9, initiates a cascade of caspase activation, proteolysis and eventual phagocytosis by macrophages (Fig1.3.1.) (Cooper 2000).

1.3.2 Apoptosis and neoplasia.

Several oncogenic viruses exert their tumour-promoting influence by preventing apoptosis in transformed cells. The human papilloma virus (HPV) produces E6 protein that binds to p53 tumour protein and, as a result, targets it for rapid proteasome-mediated degradation. p53 is important in arresting the cell cycle and initiating apoptosis in damaged cells by promoting the expression of Bax, Apaf1 and many other genes (Wang 1999).

Some B cell lymphomas have raised levels of Bcl2 protein which block apoptosis. This may be achieved by translocation of the Bcl2 gene into a highly active immunoglobulin gene enhancer region (t14;18) or amplification of the Bcl2 locus by accumulation of repeated copies of the gene.

Melanoma tumour cells block apoptosis by blocking expression of the Apaf-1 gene. Other cancer cells may express high levels of CD95, essentially becoming effective killer cells that lead to the destruction of killer T cells that may attempt to bind with the tumour cell and induce apoptosis (Campioni *et al.* 2005).

1.4 Gene regulation and DNA methylation

The human genome contains approx. 25000 genes. Some are constitutively

expressed in all cells all the time. These “housekeeping” genes are responsible for the metabolic functions (e.g. respiration) common to all cells. Other genes such as the cyclin group of proteins are expressed in all cells, but only as cells enter a particular pathway of differentiation. Some are expressed constitutively only in cells that have differentiated in a specific lineage, such as specific immunoglobulin expression in plasma cells. Some have transient expression that occurs only in response to external stimuli, such as the binding of a growth factor to its specific receptor (Kufe 2006). The rate of transcription of a gene is the most common form of regulation in eukaryotes. Rate of expression pre-transcription is governed by the binding of a large group of transcription factor and repressor proteins such as myc and p53 to gene promoter, enhancer and silencer regions. Posttranscriptional mechanisms for gene regulation include modulation of 5'mRNA capping, exon splicing and poly-adenylation. Other control mechanisms include the stability of mRNA molecules (and their subsequent degradation) during transfer from nucleus to ribosome, and the rate at which the mRNA is decoded into a polypeptide during translation (Day and Tuite 1998).

The methylation of carbon 5 in cytidine groups (5-mC) by *cytosine5methyltransferase* in DNA is referred to as DNA methylation. All higher eukaryotes have some degree of methylated DNA. Methylation is heritable and occurs predominantly in areas of DNA rich in CpG palindromic sequences (CpG islands). These islands occur with greatest frequency in areas adjacent to highly transcribed genes. Following semi-conservative replication, DNA CpG sequences are hemi-methylated with the newly synthesised strand un-methylated. Heritability is achieved by the action of a

“maintenance methylase” which methylates all cytosine groups in the new strand that are diagonally opposite methylated cytosine groups in the template strand (Robertson 2005).

The degree of methylation for a given gene is not fixed and can vary in a tissue specific manner, or in the case of inactivation of the X chromosome in females, between chromosomes. DNA methylation represses transcription directly, by inhibiting the binding of specific transcription factors, and indirectly, by recruiting methyl-CpG-binding proteins and their associated repressive chromatin remodelling activities. Regulated DNA methylation patterns are essential for normal mammalian development and for the normal functioning of the adult organism. DNA methylation is a potent silencer of gene expression and maintains genome stability against a large quantity of repetitive DNA, which can otherwise give rise to illegitimate recombination events and cause transcriptional deregulation of nearby genes. The mechanism that allows changes in the degree of methylation to occur is unclear but it is suggested that maintenance of methylation requires constant remethylation by a yet unidentified methylase. The relative paucity of CpG groups in the human genome can be explained by the tendency of methylated C group to deaminate to thymine, leading to an accumulation of A-T pairs (Tucker 1996, Kudla 2004).

1.5 Genes involved in cancer

The viral DNA sequences associated with tumour formation that have high homology to genes that already exist in animal models are named proto-oncogenes, and their viral, cancer-causing counterparts are called

oncogenes. The distinction between proto-oncogene and oncogene relates to the activity of the protein product of the gene. A proto-oncogene is a gene whose protein product has the capacity to induce cellular transformation only if its normal expressed product is altered. An oncogene is a gene that has sustained some genetic damage and therefore, produces a protein capable of cellular transformation (Kufe *et al.* 2003)

1.5.1 Proto-oncogenes

The process of activation of proto-oncogenes to oncogenes can include retroviral transduction or retroviral integration, point mutations, insertion mutations, gene amplification, chromosomal translocation and/or protein-protein interactions (Strachan and Read 2003).

Proto-oncogenes are classified into many different groups based upon their normal function within cells or based upon sequence homology to other known proteins. Proto-oncogenes have been identified at all levels of the various signal transduction cascades that control cell growth, proliferation and differentiation. Proto-oncogenes that were originally identified as resident in transforming retroviruses are designated as c- indicative of the cellular origin as opposed to v- to signify original identification in retroviruses (Lodish 2000).

The change of an oncogene from normal to oncogenic function can be caused by a simple point mutation in the DNA sequence of a gene. A point mutation in the ras oncogene, located on human chromosome 11, from guanine to cytosine is associated with bladder cancer. This change results in a glycine to valine substitution at amino acid 12 of the translated protein. This dramatically changes the function of the G-protein encoded by the ras gene.

Normally, the protein switches from an inactive to active state by a change in phosphorylation of bound GDP and GTP. The mutation does not allow the release of GTP, and the protein is continuously active (termed a gain-of-function, as opposed to loss-of-function mutation). Because the growth signal delivered by the ras oncoprotein is permanently switched on, the cell continues to grow and divide. This unregulated growth leads to cancer (Alberts 2002).

1.5.1.1 Oncogene classification

Hundreds of specific oncogenes have been identified but they have classed by King (2003) according to their common function as shown in Table 1.5.1.

1.5.2 Tumour suppressor genes

Tumour suppressor genes encode protein products that inhibit mitosis and prevent the uncontrolled cell proliferation. Cell fusion experiments show that the transformed phenotype can often be corrected *in vitro* by fusion of the transformed cell with a normal cell. This provides evidence that tumourigenesis involves not only dominant activated oncogenes, but also recessive, loss-of-function mutations in other genes. When mutated (with rare exceptions) the mutant allele is recessive; as long as the cell contains one normal allele, tumour suppression continues. Knudson (1971) proposed this two-hit model of tumour suppressor gene inactivation, derived from mathematical modelling of cancer incidence. This implied that tumour suppressors were recessive, requiring mutations in both alleles. Recently it has become clear that mutations in tumour suppressor genes are not always

Table 1.5.1 Oncogene Class by Function (King 2003)

<p><u>Growth Factors:</u></p> <ul style="list-style-type: none"> • The c-Sis gene (the v-sis gene is the oncogene in simian sarcoma virus) encodes the PDGF B chain. The v-sis gene was the first oncogene to be identified as having homology to a known cellular gene. • The int-2 gene (integration of mouse mammary tumour virus) encodes an FGF-related growth factor. • The KGF/Hst) gene encodes an FGF-related growth factor.
<p><u>Receptor Tyrosine Kinases:</u></p> <ul style="list-style-type: none"> • The c-Fms gene encodes the colony stimulating factor-1 (CSF-1) receptor. • The Neu gene was identified as an epidemial growth factor (EGF) receptor-related gene. • The Trk genes (A,B and C) encode the NGF receptor-like proteins. • The Met gene encodes the hepatocyte growth factor (HGF)/scatter factor (SF) receptor. • The c-Kit gene encodes the mast cell growth factor receptor.cells.
<p><u>Membrane Associated Non-Receptor Tyrosine Kinases:</u></p> <ul style="list-style-type: none"> • The v-src gene was the first identified oncogene. • The Lck gene has been shown to be associated with the CD4 and CD8 antigens of T cells.
<p><u>G-Protein Coupled Receptors:</u></p> <ul style="list-style-type: none"> • The Mas gene was identified in a mammary carcinoma and has been shown to be the angiotensin receptor. • Membrane Associated G-Proteins • Three different homologies of the c-Ras gene, each of which was identified in a different type of tumour cell. Analogous to viral protein – v-Ras
<p><u>Serine/Threonine Kinases:</u></p> <ul style="list-style-type: none"> • The Raf gene is involved in the signaling pathway of most RTKs. It is likely responsible for threonine phosphorylation of MAP kinase following receptor activation.
<p><u>Nuclear DNA-Binding/Transcription Factors</u></p> <ul style="list-style-type: none"> • Myc gene. A disrupted human c-Myc gene is involved in numerous haematopoietic neoplasias. Disruption of c-Myc results from retroviral integration and transduction as well as chromosomal rearrangements. • Fos gene was identified in the feline osteosarcoma virus. Fos interacts with a second proto-oncogenic protein, Jun to form a transcriptional regulatory complex. • p53 The p53 gene is the single most identified mutant protein in human tumours. Mutant forms of the p53 protein interfere with cell growth suppressor effects of wild-type p53 indicating that the p53 gene product is actually a tumour suppressor.

completely recessive. Haploinsufficiency occurs when one allele is insufficient to confer the full functionality produced from two wild-type TSG alleles. Under some circumstances, one hit may be sufficient for inactivation (Payne and Kemp 2005).

Tumour suppressor genes have been discovered by three main routes: positional cloning of the genes causing rare familial cancers; examination of genes at chromosomal locations commonly deleted in tumour cells (by loss of heterozygosity analysis or comparative genomic hybridization); testing tumours for mutations in genes known to be involved in cell cycle regulation (Strachan and Read 2003).

Table 1.5.2 lists the tumour suppressor gene family members (Holland 2003) and shows the specific gene, the associated inherited cancer, cancers which occur as a result of somatic mutations and the presumed function of the protein product.

1.5.2.1 Rb

1.5.2.1.1 Rb Function

Retinoblastoma is a cancerous tumour of the retina. It occurs in two forms. In familial retinoblastoma, multiple tumours in the retinas of both eyes occur in the first weeks of infancy. In sporadic retinoblastoma, a single tumour appears in one eye sometime in early childhood before the retina is fully developed and mitosis in it ceases. (Holland 2003) A gene encoding a messenger RNA of 4.6 kb, located in the proximity of esterase D, was identified by Lee *et al.* (1987) as the retinoblastoma susceptibility gene on the basis of chromosomal location, homozygous deletion, and tumour-specific alterations in expression. Biochemical fractionation and immunofluorescence

Table 1.5.2
Classification of tumour suppressor genes (Holland 2003)

Gene	Associated inherited cancer	Cancers with somatic mutations	Presumed function
RB1	Familial retinoblastoma syndrome	Retinoblastoma, osteosarcoma, SCLC, breast, prostate, bladder, pancreas, oesophageal, others.	Transcriptional regulator; E2F binding
TP53	Li-Fraumeni syndrome	Approx. 50% of all cancers (rare in some types, such as prostate carcinoma and neuroblastoma)	Transcription factor; regulates cell cycle and apoptosis
*INK4a p16 /CDKN2/p19ARF	Familial melanoma, Familial pancreatic carcinoma	Approx. 25-30% of many different cancer types (e.g., breast, lung, pancreatic, bladder)	Cyclin-dependent kinase inhibitor (i.e., Cdk4 and Cdk6)
p19ARF	?Familial melanoma?	Approx. 15% of many different cancer types	Regulates Mdm-2 protein stability and hence p53 stability; alternative reading frame of p16/INK4a gene
APC	Familial adenomatous polyposis coli (FAP), Gardner syndrome, Turcot's syndrome	Colorectal, desmoid tumours	Regulates levels of , desmoid tumours. Regulates levels of β -catenin protein in the cytosol; binding to microtubules
BRCA1	Inherited breast and ovarian cancer	Ovarian (~10%), rare in breast cancer	DNA repair; complexes with Rad 51 and BRCA2; transcriptional regulation
BRCA2	Inherited breast (both female and male), pancreatic cancer, ?others?	Rare mutations in pancreatic, ?others	DNA repair; complexes with Rad 51 and BRCA1
WT-1	WAGR, Denys-Drash Syndrome	Wilms' tumour	Transcription factor
NF-1	Neurofibromatosis type 1	Melanoma, neuroblastoma	p21ras-GTPase
VHL von-Hippel Lindau syndrome		Renal (clear cell type), hemangioblastoma	Regulator of protein stability

Table 1.5.2 continued...

Gene	Associated inherited cancer	Cancers with somatic mutations	Presumed function
MEN-1	Multiple endocrine neoplasia type 1	Parathyroid adenoma, pituitary adenoma, Endocrine tumours of the pancreas	Not known
PTCH	Gorlin syndrome, hereditary basal cell carcinoma syndrome	Basal cell skin carcinoma, medulloblastoma	Transmembrane receptor for sonic hedgehog factor; negative regulator of smoothed protein
PTEN/MMAC1	Cowden's syndrome; sporadic cases of juvenile polyposis syndrome	Glioma, breast, prostate, follicular thyroid carcinoma, head and neck squamous carcinoma	Phosphoinositide 3-phosphatase; protein tyrosine phosphatase
DPC4	Familial juvenile polyposis syndrome	Pancreatic(~50%), approx. 10–15% of colorectal cancers, rare in others	Transcriptional factor in TGF- β signaling pathway
E-CAD	Familial diffuse-type gastric cancer; Lobular breast cancer	Gastric (diffuse type), lobular breast carcinoma, rare in other types (e.g. ovarian),	Cell-cell adhesion molecule
LKB1/STK1	Peutz-Jeghers syndrome	Rare in colorectal, not known in others	Serine/threonine protein kinase
SNF5/INI1	Rhabdoid predisposition syndrome choroid plexus carcinoma medulloblastoma; central primitive neuroectodermal tumours)	Rare in rhabdoid tumours, choroid plexus carcinoma, medulloblastoma	Member of the SWI/SNF chromatin ATP-dependent remodeling complex
EXT1	Hereditary multiple exostoses	Not known	Glycosyltransferase; heparan sulfate chain elongation
EXT2	Hereditary multiple exostoses	Not known	Glycosyltransferase; heparan sulfate chain elongation
TSC1	Tuberous sclerosis	Not known	Not known; cytoplasmic vesicle localization
TSC2	Tuberous sclerosis	Not known	Putative GTPase activating protein for Rap1 and rab5; golgi localization

from DNA-cellulose columns, suggesting a DNA binding activity. Chen *et al.* (1989). demonstrated that the RB1 gene product has the properties of a cell cycle regulatory element and that its function is modulated by a phosphorylation/dephosphorylation mechanism during cell proliferation and differentiation. In G₀/G₁ cells, virtually all the Rb protein is unphosphorylated, whereas during S and G₂ phases, it is largely, if not exclusively, phosphorylated.

1.5.2.1.1.1 Rb in Apoptosis

Yap *et al.* (1999) showed that the binding of Rb to MDM2 is essential for Rb to overcome both the antiapoptotic function of MDM2 and the MDM2-dependent degradation of p53. Since Rb specifically rescues the apoptotic function but not the transcriptional activity of p53 from negative regulation by MDM2, transactivation by wild type p53 is not required for the apoptotic function of p53.

Hill *et al.* (2006) showed that inactivation of the pRb family proteins in genetically engineered mice induced epithelial proliferation and was sufficient to produce prostatic intraepithelial neoplasia lesions. Apoptosis was dependent on PTEN function and not p53, PTEN hemizyosity reduces apoptosis by 50%, accelerating progression to adenocarcinomas with heterogeneous composition in the Rb deficient model.

1.5.2.1.1.3 Rb and promotion of differentiation

The incidence of osteosarcoma is increased 500-fold in patients who inherit mutations in the Rb gene. To understand why the Rb protein is involved in osteosarcoma, Thomas *et al.* (2001) studied its function in osteogenesis.

Loss of Rb but not p107 or p130 blocked late osteoblast differentiation. Rb physically interacted with the osteoblast transcription factor, CBF (core binding factor) A1 and is associated with osteoblast-specific promoters *in vivo* in a CBFA1-dependent fashion. Association of Rb with CBFA1 and promoter sequences resulted in synergistic transactivation of an osteoblast-specific reporter. This transactivation function was lost in tumour-derived Rb mutants, underscoring a potential role in tumour suppression. Thus, Rb functions as a direct transcriptional coactivator promoting osteoblast differentiation, which may contribute to the targeting of Rb in osteosarcoma (Thomas *et al.* 2001).

1.5.2.1.1.5 Rb and telomere length

Garcia-Cao *et al.* (2002) reported a connection between members of the retinoblastoma family of proteins, Rb1, RbL1 and RbL2 and the mechanisms that regulate telomere length. In particular, mouse embryonic fibroblasts doubly deficient in RbL1 and RbL2 or triply deficient in all three genes had markedly elongated telomeres compared with those of wildtype or Rb1-deficient cells. This deregulation of telomere length was not associated with increased telomerase activity. The abnormal elongated telomeres in double or triple deficient cells retained their end-capping function, as shown by the normal frequency of chromosomal fusions and thus demonstrated a connection between the RB1 family and the control of telomere length in mammalian cells (Garcia-Cao *et al.* 2002).

1.5.2.1.1.5 Rb and maintenance of G0 phase

Cellular senescence is a stable form of cell cycle arrest that limits proliferation of damaged cells and may act as a natural barrier to cancer progression.

Narita *et al.* (2003) described a distinct heterochromatic structure that accumulates in senescent human fibroblasts, designated senescence-associated heterochromatic foci (SAHF). They found that SAHF formation coincides with recruitment of heterochromatin proteins and the RB1 protein to E2F-responsive promoters and is associated with the stable repression of E2F target genes. Both SAHF formation and the silencing of E2F target genes depended on the integrity of the Rb pathway and did not occur in reversibly arrested cells. This prevents E2F from binding to the promoters of proto-oncogenes such as c-myc and c-fos. Transcription of c-myc and c-fos is needed for mitosis so blocking the transcription factor needed to turn on these genes prevents cell division (fig 1.5.2.1). If cell damage is minor, p53 protein halts the cell cycle by stimulating expression of p21 until the damage is repaired (Narita *et al.* 2003).

1.5.2.1.2 Interaction with PTEN

Bai *et al* (2006), in a study of how the Rb pathway interacts with other pathways in tumour suppression, characterized mice with double mutations of an INK4 cyclin dependent kinase inhibitor and PTEN (expression of INK4 retains Rb proteins in their growth-suppressive states). Double mutant mice developed a wider spectrum of tumours with nearly complete penetrance in anterior and dorsolateral lobe prostate cancer. PTEN protein expression was lost in 9 out of 11 prostate tumours from PTEN^{+/-} mice whilst loss of PTEN protein expression was not detected in any tumours from 5 pituitary, 12 thyroid and 9 adrenal gland tumours. Bai *et al* (2006) suggested that p18

Fig 1.5.2.1
Function of Rb

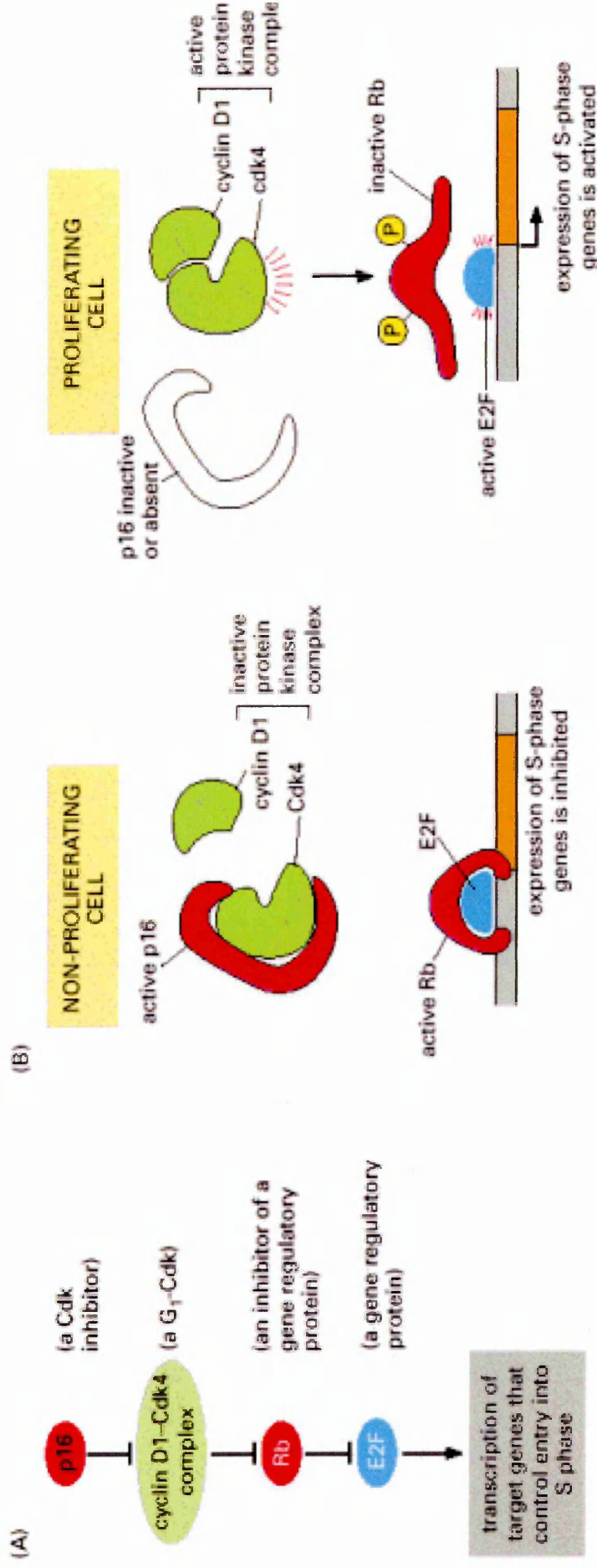


Fig 1.5.2.1 shows order of events (A) and mechanism of inactivation (B) of Rb protein in proliferating cells by phosphorylation via protein kinase complex and role of p16 (see section 1.5.2.3) in activation of cdk4 and cyclin D1 complex. In a non-proliferating cell, active p16 binds Cdk4 and active Rb protein binds E2F transcription factor and inhibits expression of S-phase genes. In a proliferating cell, p16 is inactive and Cdk4 binds cyclin D1 and forms an active protein kinase complex which phosphorylates Rb protein. Phosphorylated Rb falls to bind E2F which initiates expression of S phase genes. (Lodish 2003, Alberts 2002)

and PTEN cooperate in tumour suppression by constraining a positive regulatory loop between cell growth and cell cycle control pathways. Their results indicated a tissue-specific haploinsufficiency in the tumours studied.

1.5.2.2 P53 Tumour protein

The p53 tumour antigen is found in increased amounts in a wide variety of transformed cells. The protein is also demonstrated in many actively proliferating normal cells, but it is only present at low levels in resting cells. Wild type p53 plays a role in DNA repair and expression of mutant forms of p53 may alter cellular resistance to the DNA damage caused by gamma-radiation. p53 functions as a cell cycle checkpoint after irradiation, suggesting that mutant p53 might change the cellular proliferative response to radiation (see section 1.5.2.2.2). p53 is not required for normal development, but under conditions such as DNA damage or other cellular stress, p53 expression is stimulated. In turn, p53 tetramers bind to p21 regulatory elements and transcriptionally activate its expression. The p21 protein subsequently binds to and inhibits cyclin-dependent kinase activity, preventing phosphorylation of critical cyclin-dependent kinase substrates and blocking cell cycle progression. In tumour cells with inactive p53, this pathway is absent, permitting unregulated growth. The mechanism by which p53 mediates apoptosis is a 3-step process: first, the transcriptional induction of redox-related genes; second the formation of reactive oxygen species; and third, the oxidative degradation of mitochondrial components, culminating in cell death. Thus, p53 has a cytoplasmic and nuclear role in preventing cell proliferation. p53 functions in the nucleus to regulate proapoptotic genes, whereas cytoplasmic p53 directly activates proapoptotic BCL2 proteins to permeabilize

Fig 1.5.2.2 Function of p53

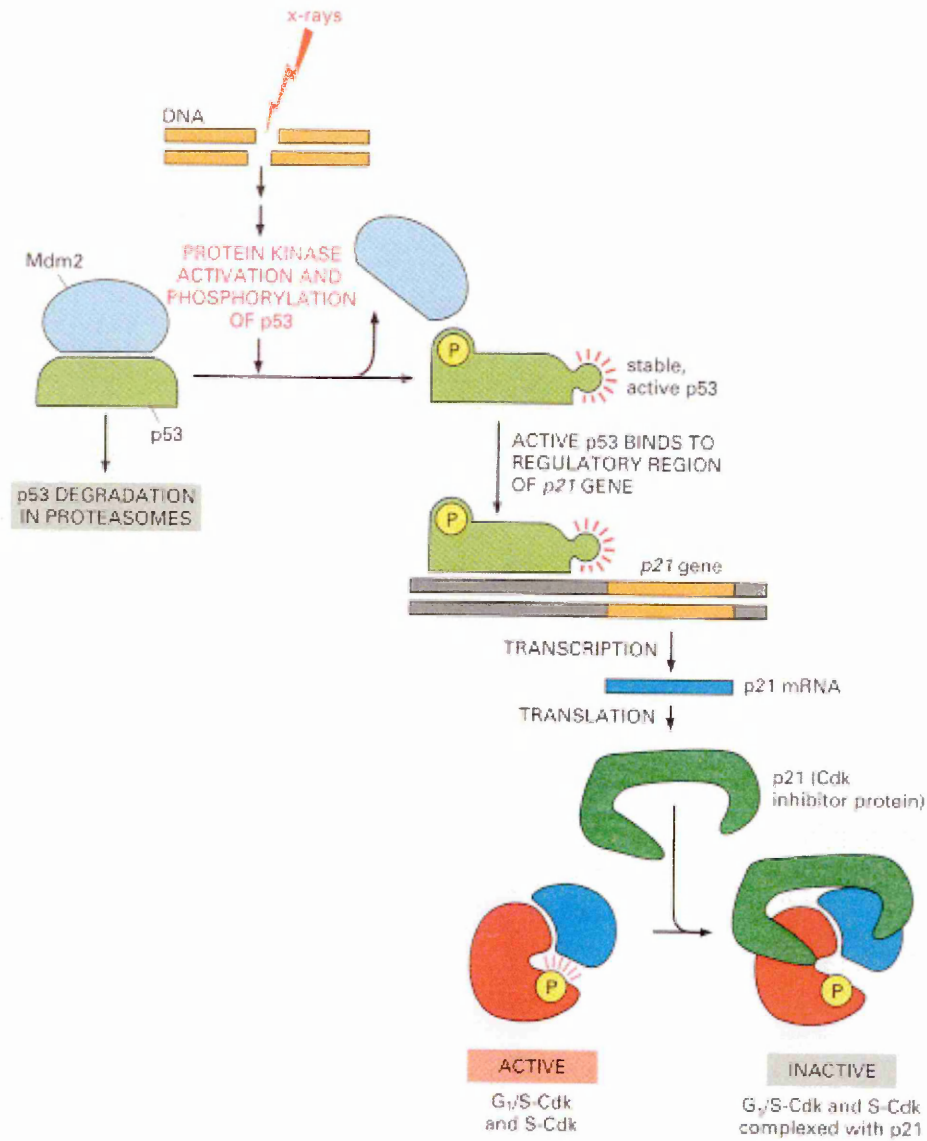


Fig 1.5.2.2 shows action of p53. DNA is damaged; p53 levels rise, protein kinases that phosphorylate p53 are activated. MDM2 (or E6 produced by mucosal specific papilloma viruses) bind and target P53 for proteolytic degradation. Phosphorylation of p53 blocks its binding to Mdm2; p53 accumulates to high levels and stimulates transcription of the gene that encodes the Cdk inhibitor protein p21. The p21 binds and inactivates G₁/S-Cdk and S-Cdk complexes, arresting the cell in G₁. (Alberts et al 2003, Iliakis 1997)

mitochondria and initiate apoptosis (fig 1.5.2.2) (Kufe 2003) .

1.5.2.2.1 P53 function in oncogenesis

Vogelstein and Kinzler (2004) outlined 5 mechanisms for p53 inactivation:

In the first mechanism, p53 binds as a tetramer to a p53-binding site and activates the expression of adjacent genes that inhibit growth. Deletion of one or both p53 alleles reduces or abolishes the expression of tetramers, resulting in decreased expression of the growth inhibitory genes (such as p21). This mechanism is found in tumours of several types.

Secondly, nonsense or splice site mutations that result in truncation of the protein do not allow oligomerization, thus resulting in a reduction of p53 tetramers. Mutations of this gene are common in lung, oesophagus, and other cancers.

The third mechanism involves missense mutations resulting in dominant-negative effects which mimic and oncogene function due to an even greater reduction of functionally active tetramers. Such missense mutations are common in colon, brain, lung, breast, skin, bladder, and other cancers.

Fourthly, a mechanism by which p53 is involved in oncogenesis is common in cervical and anal cancers where the expression of the E6 gene of human papilloma virus (HPV) results in the functional inactivation of p53 through binding and rapid degradation.

Finally, the p53 pathway may also be disrupted by alteration of a cellular oncoprotein gene, MDM2 (Kufe 2003).

1.5.2.2.2 p53 and DNA damage.

DNA damage by UV radiation leads to an increase in production of protein

kinase directed at p53, which is phosphorylated at ser15 and also lead to a transient rise in p53 levels due to posttranslational modifications that increase its half-life. The phosphorylation causes a conformational change in p53, which leads to reduced interaction of p53 with MDM2, its negative regulator. Association of p53 with MDM2 results in ubiquitination and subsequent degradation of p53 by cellular proteases (Iliakis 1997).

If the cell damage is major and cannot be repaired, degradation does not occur, p53 levels increase, and cell senescence is triggered by apoptosis. These functions make p53 a key player in protection against cancer. More than half of all human cancers harbour p53 mutations and have no functioning p53 protein, which, as with Rb, tips the balance of cell growth in favour of proliferation (Alberts 2002).

1.5.2.3 p16 and tumour suppression

The involvement of 9p21 in chromosomal inversions, translocations, heterozygous deletions, and homozygous deletions in a variety of malignant cell lines indicates that this region may contain a gene with tumour suppressor function. Lukas *et al.* (1995) showed that wildtype p16 arrests normal diploid cells in late G1 phase of the cell cycle, whereas a tumour-associated mutant of p16 does not. Furthermore, the ability of p16 to induce cell cycle arrest was lost in cells lacking functional retinoblastoma protein. This suggests that loss of p16 and loss of retinoblastoma protein have similar effects on G1 progression, and may represent a common pathway in the promotion of oncogenesis. Stott *et al.* (1998) stated that p16 was a recognised tumour suppressor that induces a G1 cell cycle arrest by inhibiting the phosphorylation of the Rb protein by the cyclin-dependent kinases CDK4

and CDK6 and that the protein was able to generate a p53 response. p16 protein binds to CDK4 and inhibits the ability of CDK4 to interact with cyclin D (see Fig 1.5.2.1) and stimulate passage through the G1 phase of the cell cycle. p16 protein exists as 2 distinct transcripts from different promoters. The transcripts have been designated p16(INK4A) and p14(ARF). Each has a 5-prime exon that is spliced into common exons 2 and 3. Deletions, mutations and inactivation by hypermethylation in the p16 gene may affect the relative balance of functional p16 and cyclin D, resulting in abnormal cell growth. p16 dysfunction has been particularly associated with malignant melanoma and pancreatic adenocarcinoma. You *et al.* (2002) found evidence of collaboration between PTEN and p16/Ink4a in constraining the growth and oncogenic transformation of cultured cells and in suppressing a wide spectrum of tumours *in vivo* such as pheochromocytoma, prostatic intraepithelial neoplasia, and endometrial hyperplasia.

1.5.2.4 Adenomatous Polyposis Coli (APC) Gene

This is a multidomain protein containing 2,843 amino acids and is strongly associated with Familial Adenomatous Polyposis coli (APC). It plays a major role in tumour suppression by antagonizing the WNT signalling pathway (WNT signaling molecules regulate cell-to-cell interactions during embryogenesis) where APC is thought to act as a scaffold for a protein complex that regulates the phosphorylation and thus degradation of β -catenin in the WNT pathway. Inappropriate activation of this pathway through loss of APC function contributes to cancer progression (Nathke 2004).

APC also has roles in cell migration, adhesion, chromosome segregation, spindle assembly, apoptosis, and neuronal differentiation. Mutations in the

APC gene are an initiating event for both familial and sporadic colorectal tumours. Most of these mutations accumulate in the central region of the APC gene, called the mutation cluster region (MCR), and result in expression of carboxy-terminally truncated proteins. APC mutations in the first or last third of the gene are associated with an attenuated polyposis with a late onset and a small number of polyps (Solomon and Burt 2005).

1.5.2.5 BRCA1 and BRCA2

BRCA1 and *BRCA2* encode large proteins of 1,863 and 3,350 amino acids, respectively. They are both complex genes made up of more than 20 exons. Neither gene bears significant homology with other known genes, with the exception of the BRCT domain in the C-terminus of *BRCA1*, a domain found in more than 40 other genes associated with response to DNA damage.

BRCA1 and *BRCA2* are important components of the pathway that protects cells from the effects of DNA damage. The majority of mutations identified thus far lead to protein truncation, and it is believed that cancer then develops when the second copy is lost, with *BRCA1* and *BRCA2* behaving like classic tumour-suppressor genes, with the loss of one copy predisposing the carrier to the development of the characteristic cancers of this classic cancer syndrome (Petrucelli 2005).

Several lines of investigation have implicated *BRCA1* and *BRCA2* in DNA damage-response pathways. An association between *BRCA1* and p53 and the subsequent enhancement of p53 activity incriminates *BRCA1* in p21-mediated cell-cycle arrest following DNA damage. In addition, *BRCA1* forms complexes with both *BRCA2* and Rad51 the human homolog of the *Escherichia coli* gene *RecA*, which is essential to normal recombination and

genome stability. Co-localization of *BRCA1*, *BRCA2*, and Rad51 in “nuclear dot” structures is seen to disappear following treatment of cells with DNA-damaging agents that cause double-stranded chromosome breaks. In addition, mouse embryonic stem cells that are homozygous for *BRCA1* null and *BRCA2* truncations are hypersensitive to ionizing radiation and other forms of oxidative damage (Jin 1997, Kufe 2003).

BRCA1 may also play a role in transcription regulation, cell-cycle control, and development. Both *BRCA1* and *BRCA2* are nuclear proteins. *BRCA1* associates with a RNA polymerase holoenzyme and binds CREB implicating it in transcriptional regulation. *BRCA1* protein levels are also altered by variations in hormone levels. During the cell cycle, *BRCA1* and *BRCA2* mRNA levels increase from low levels at the start of G1 to maximum levels at the G1/S transition in parallel to cyclin A levels. Phosphorylation of *BRCA1* also occurs in a cell-cycle-dependent manner in sporadic breast cancer. Thompson *et al.* (1995) found that *BRCA1* mRNA levels are markedly decreased during the transition from benign tumour to invasive cancer. Experimental inhibition of *BRCA1* expression with antisense oligonucleotides produced accelerated growth of normal and malignant mammary cells but had no effect on non-mammary epithelial cells. They interpreted these results as indicating that *BRCA1* may normally serve as a negative regulator of mammary epithelial cell growth and that this function is compromised in breast cancer, either by direct mutation or by alterations in gene expression.

1.5.2.6 WT1 and WT2

The principal gene for Wilms Tumour (*WT1*) is located on chromosome 11p13. There is a second predisposition locus (*WT2*) at 11p15.5. The

WT1 gene encodes a protein that suppresses transcription downstream from epidermal growth factor receptor 1 and insulin-like growth factor II. It is a zinc finger DNA-binding protein and acts as a transcriptional activator or repressor depending on the cellular or chromosomal context. It has 4 major isoforms, due to the insertion of 3 amino acids between zinc fingers 3 and 4, and the insertion of an alternatively spliced 17-amino acid segment encoded by exon 5 in the middle of the protein (Hossain and Saunders, 2001). The conservation in structure and relative levels of the 4 WT1 mRNA species suggests that each encoded polypeptide makes a significant contribution to normal gene function. Haber *et al.*, (1991) suggested that the control of cellular proliferation and differentiation exerted by the WT1 gene products may involve interactions between the 4 polypeptides with distinct targets and functions .

The candidate Wilms tumour gene was expressed specifically in the condensed mesenchyme, renal vesicle, and glomerular epithelium of the developing kidney, in the related mesonephric glomeruli, and in cells approximating these structures in tumours. Niksic *et al.* (2004) found that WT1 protein is not restricted to the nucleus and shuttles continuously between the nucleus and cytoplasm. The other main sites of expression were the genital ridge, fetal gonad, and mesothelium. This was interpreted as indicating that the anomalies of the urinary tract and genitalia, which are frequent in both sporadic and syndrome-associated Wilms tumours, are a pleiotropic effect of the WT1 gene.

1.5.2.7 NF1

NF1 is a large gene (59 exons) located on chromosome 17q11.2. The NF1

gene encodes a GTP-activating protein known as neurofibromin. The gene product negatively regulates signals transduced by ras proteins. NF1 functions as a tumour-suppressor gene in immature myeloid cells but inactivation of both NF1 alleles has not been demonstrated in leukaemic cells from patients with neurofibromatosis type 1 (Friedman 2002) .

1.5.2.8 VHL

The von Hippel-Lindau tumour suppressor protein (pVHL) has been implicated in a variety of functions including transcriptional regulation, post-transcriptional gene expression, protein folding, extracellular matrix formation, and ubiquitinylation Normal pVHL binds to elongin C, which forms a complex with elongin B and cullin-2 (CUL-2). This complex resembles the SCF ubiquitin ligase or E3 complex in yeast that catalyzes the polyubiquitinylation of specific proteins and targets them for degradation by proteosomes. Under normoxic conditions, HIF1 α is hydroxylated at two specific proline residues by a member of the EGLN family of prolyl hydroxylase enzymes. The VHL protein then binds to hydroxylated HIF1 α and targets it for degradation. Under hypoxic conditions, HIF1 α is not hydroxylated, pVHL does not bind, and HIF1 α subunits accumulate. HIF1 α forms heterodimers with HIF1 β and activates transcription of a variety of hypoxia-inducible genes (i.e., *VEGF*, *EPO*, *TGF α* , *PDGF β*). Likewise, when pVHL is absent or mutated, HIF1 α subunits accumulate, resulting in cell proliferation and the neovascularization of tumours characteristic of VHL disease (Kaelin 2002).

1.5.2.9 Men1

Menin is a protein of 610 amino acids and is localised in the nucleus and has

two nuclear localization signals near the carboxyl terminus. Menin does not show similarity with any other known protein. The *MEN1* transcript has been detected in all human tissues.

Menin is widely expressed and may play different roles in different tissues. It is involved in the regulation of several cell functions, including DNA replication and repair, and in transcriptional machinery. Menin inhibits JunD-mediated transcriptional activation, as studies of deletion mutants have shown the existence of interacting regions of both the proteins. Menin inhibits JunD-mediated transcription by modification of chromatin structure recruiting a specific histone deacetylase targeted to a promoter by binding JunD.

Moreover, when compared to controls, lymphocytes from individuals with a heterozygous *MEN1* mutation show both premature division of the centromere and hypersensitivity to alkylating agents. Thus, menin is a negative regulator of cell proliferation after DNA damage

Most germline or somatic mutations in the *MEN1* gene predict truncation or absence of encoded menin. Similarly, 11q13 loss of heterozygosity in tumours predicts inactivation of the other *MEN1* copy. Neither the finding of a tumour suppressor mechanism nor the identification of binding partners has established the ultimate pathways of menin action in normal tissues or in tumours (Agarwal et al 2004).

1.5.2.10 PTCH

Johnson *et al.* (1996) cloned the human *Drosophila* patched (PTC) homologue gene by screening a human lung cDNA library with mouse PTC cDNA clones. They assembled 5.1 kb of contiguous sequence containing a 4.5-kb open reading frame that encodes a 1,447-amino acid protein. The

predicted amino acid sequence has 96% identity to mouse and a 40% identity to *Drosophila* PTC proteins. The hydrophobic PTC protein is predicted to contain 12 membrane-spanning domains and 2 large hydrophilic extracellular loops. PTC acts as a receptor for Sonic hedgehog (Shh) proteins, which are a family of secreted signal molecules that act as local mediators in many developmental processes in both invertebrates and vertebrates.

Abnormalities in the hedgehog pathway during development can be lethal and in adult cells can also lead to cancer. High levels of PTC induced by Shh serve to sequester free Hh and therefore create a barrier to its further movement. (Chen and Struhl 1996).

1.5.2.11 SMAD4

The protein product of this gene is a tumour suppressor that is critical for transmitting signals from TGF β by mediating transcriptional activation of target genes by interaction with Smad4-interacting transcriptional co-activator (SMIF) protein. The proteins form a mRNA de-capping complex, a key factor in the regulation of mRNA decay (Haidle & Howe 2006).

1.5.2.12 E-Cadherin

Cadherins are transmembrane glycoproteins that mediate extracellular calcium-dependent cell-cell interactions (Jou et al 1995). E-Cad is involved in epithelial cell-cell communication and is localised to the cell membrane in adherent junctions. E-Cad functions as a metastasis suppressor molecule in several cell lines. Semb and Christofori (1998) showed that loss of gene expression was correlated with increased invasiveness and metastatic potential, and replacement or augmentation of gene expression resulted in

suppression of the invasive phenotype.

1.5.2.13 LKB1/STK11

Loss of STK11 is associated with gastrointestinal polyposis. This serine/threonine-protein kinase has a prenylation motif suggesting that it is involved in protein-protein interactions and membrane binding. The predicted protein structure also shows an autophosphorylation domain along with a cyclic AMP-dependent protein kinase phosphorylation site. STK11 expression was shown to cause apoptosis in epithelial cells. The transport of STK11 to the mitochondria appears to be an early step in apoptosis. STK11 co-localises with p53 during apoptosis. The ability of STK11 to induce apoptosis also depends upon p53. These results suggest that signalling through STK11 may be an early event leading to apoptosis through p53 pathways.

Truncating mutations prior to amino acid 311 abrogate the kinase activity of STK11 (Jenne *et al.* 1998).

1.5.2.14 SNF5/INI1

The INI1 gene encodes a member of the SWI/SNF ATP-dependent chromatin-remodelling complex and is the target of recurrent loss-of-function alterations in renal and extra renal malignant rhabdoid tumour (MRT), a highly aggressive Wilms-like tumour. The observation of biallelic, truncating mutations on chromosome 22 in tumours strongly supports the hypothesis that hSNF5/INI1 is a new tumour-suppressor gene consistently inactivated in MRT. In addition to somatically acquired alterations, constitutional mutations of this gene also have been observed very recently in patients with MRT (Versteeg 1998).

1.5.2.15 EXT1 and EXT2

These two genes are associated with d-glucuronyltransferase and N-acetyl-d-glucosaminyltransferase reactions in heparan sulfate biosynthesis, Heparan sulphate (HS) proteoglycans occur at cell surfaces and in the extracellular matrix of most tissues. A two-hit mutational model was proposed for EXT1 and EXT2 in the formation of exostoses, based on the observation of loss of heterozygosity in chondrosarcomas. The protein product also participates in cell signalling and chondrocyte proliferation and differentiation, roles which are thought to give rise to their tumour suppressor function (Schmale 2005).

1.5.2.16 Tuberous sclerosis complex

The TSC1 gene at 9q34 encodes the protein hamartin and TSC2 at 16p13.3 encodes the protein tuberin. Tuberin has GTPase-activating protein functions for the small G-proteins (Rap1a and Rab5) and functions as a major regulator of small G-protein Rheb and downstream pathway on protein translation, growth and cell proliferation. Hamartin interacts with the ezrin-radixin-moesin (ERM) family of actin-binding proteins Hamartin also regulates the cell cycle through interacting with CDKs. The two proteins form heterodimers, suggesting that they may act in concert to regulate cell proliferation. Most recently, tuberin and hamartin were shown to be key regulators of the AKT pathway and to participate in several other signaling pathways including the MAPK, AMPK, b-catenin, calmodulin, MTOR/S6Kinase, CDK, and cell cycle pathways. (Crino *et al.* 2006)

1.6 Blood cell Production

All cells in the blood cell compartment are produced from a quiescent

undifferentiated “stem” cell. Subsequent stimulation leads these cells to self-renew or differentiate into cells of the appropriate lineage. This differentiation is associated with a loss of self renewal capacity and increased proliferation rates (Hoffbrand *et al.* 2006). The progenitor cells are named according to their ability to form colonies of haemopoetic cells in a semi-solid growth medium. The earliest colony forming unit (CFU) BLAST contains cells that give rise to a progenitor termed the CFU-GEMM (granulocyte, erythroid, macrophage and megakaryocytic). These cells are capable of differentiating into other lineages (but no longer have the capacity of self renewal) via more terminally differentiated CFUs such as CFU-GM. The entire differentiation process in normal haematopoiesis is modulated by a series of growth factors or colony stimulating factors, some with broad spectrum modes of action, some specific for a particular lineage (Hoffbrand *et al.* 2006)

1.7 Haematological malignancy

All of the cellular components of the haemopoetic system, composed of erythroid, myeloid, lymphoid and megakaryocytic lineages, are affected by malignancy. The various disorders have historically been classified, grouped and sub-grouped according to the cell type from which the malignant clone arose and the degree of maturation/differentiation of the malignant cells. More recent classification systems have veered towards classes delineated in terms of common genetic lesions in the first instance and then levels of differentiation as a secondary class (Appendix I and II).

Whatever the cell of origin, the malignant phenotype results in mitotic division in successive generations until, when sufficiently large, the clonal population causes clinically apparent disease. Diffuse tumours such as leukaemias

display a smaller number of mutations than solid tumours and this is borne out by the more rapid appearance of leukaemia after the initial mutagenic episode than solid tumours (Volgstein and Kinzler 1998). Because a normal haemopoietic stem cell (HSC) and leukaemic stem cell (LSC) share various developmental pathways and the ability to self-renew, it is possible that LSCs are HSCs that have become leukaemic as the result of accumulated mutations. In contrast to other more differentiated cells, HSCs have the machinery for self-renewal already activated and therefore may require fewer mutations to maintain a leukaemic phenotype. HSCs also persist throughout life and therefore have greater opportunities to accumulate mutations than more mature cells, which persist only for a short period (Passegué *et al.* 2003).

1.7.1 Chronic myeloid (or myelogenous) leukaemia (CML)

CML occurs with greatest frequency at age > 50 years. It has an incidence of 1-2 per 100000 per person per annum. Although the condition is rare it constitutes 20% of all types of adult leukaemia (Faderl 1999). Patients with CML are often asymptomatic at diagnosis, and present incidentally with an elevated white blood cell count on a routine laboratory test. CML must be differentiated from reactive neutrophilia due to infection, which can have a similar appearance on a blood smear (Faderl 1999).

Symptoms of CML may include: tiredness, low-grade fever, susceptibility to infections, anaemia, and thrombocytopenia with easy bruising and, paradoxically, thrombocytosis in some CML cases. Splenomegaly may also be present (Savage *et al.* 1997) .

CML is amongst the most studied of leukaemias, if not all cancers, in terms of

its cellular and molecular biology. It serves here as a useful model to describe the events surrounding the generation of neoplastic disease. The intensity of study was prompted by the fact that CML was the first neoplastic disease to be associated with a consistent chromosomal abnormality and the first to be characterised as a clonal disorder. The chromosomal abnormality was described by Nowell and Hungerford (1960) as a loss of the long arm of what was thought to be chromosome 21. Improved Giemsa banding techniques allowed Rowley (1973) to identify accurately the "Philadelphia chromosome" (Ph) as involving a reciprocal translocation between the long arms of chromosomes 9 and 22 (fig. 1.7.1). The presence of the translocated chromosome in myeloid erythroid and megakaryocytic cell lineages suggested that the disease resulted from a defect in a "pluripotent" or non-terminally differentiated progenitor cell. Fialkow et al (1977) demonstrated the clonal nature of CML by observing a single glucose 6 phosphate dehydrogenase isoform in CML affected cells of a patient that were otherwise heterozygous for this disease.

The typical course of the disease is presentation with the "chronic" phase consisting of an indolent leukocytosis consisting predominantly of mature polymorphonuclear neutrophils in bone marrow, peripheral blood, and extramedullary sites. These cells have essentially normal morphology and function but are present in blood at 10-100 times their normal numbers. The myeloid progenitor cell constituting the majority of the tumour load has, like its normal counterpart, a normal response to positive and negative growth and differentiation stimulants. The median duration of the chronic phase has historically been about 3 years after which the biology of the disease

Figure 1.7.1

Schematic view of the formation of the Philadelphia chromosome with the reciprocal translocation of chromosomes 9 and 22

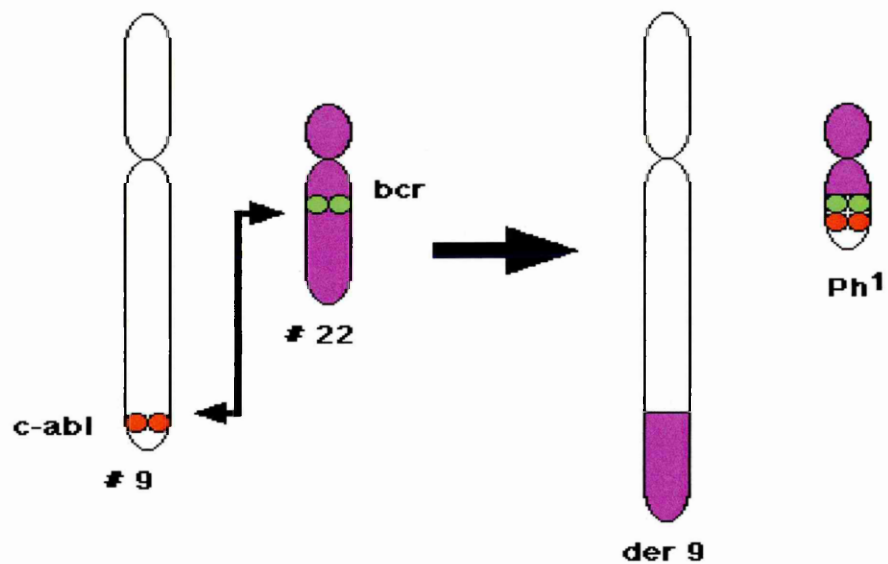


Fig 1.7.1 Schematic view of formation of Philadelphia chromosome.
Reciprocal translocation occurs between chromosomes 9 and 22 resulting in a longer chromosome 9 and shorter (Philadelphia) chromosome 22. Chimeric fusion genes *Bcr/Abl* and *Abl/Bcr* result from translocation (Kimball 2003)

becomes more aggressive. The “accelerated phase” phase lasts 4 to 6 months and is characterized by an increase in disease burden and in the frequency of progenitor/precursor cells rather than terminally differentiated cells. Bone marrow progenitors progressively lose their ability to differentiate leading to a proliferation of undifferentiated blast cells that fill the bone marrow cavity and lead to the final phase and bone marrow failure. This phase is referred to as “blast crisis” and is morphologically similar to acute leukaemia. The variable lineage of the blast cells at this stage confirms the primary disorder as a stem cell defect with cells appearing from myeloid, lymphoid, erythroid, megakaryocytic or T cell lineages (Geary 2000).

The Ph chromosome is present in 95% of CML cases and a smaller proportion of other acute leukaemias and, at the molecular level, leads to the translocation of a proto-oncogene, *c-abl* from chromosome 9 to 22. *c-abl* is the human equivalent of the transforming element of the Ableson murine leukaemia virus, known as *v-abl*, which causes pre B-cell leukaemia in mice. The translocation leads to the formation of a chimeric gene with the 3' section of the Abl sequence and the 5' section of a gene termed Bcr (breakpoint cluster region) (Sawyers1999).

1.7.1.1 Abl.

The human Abl gene encodes a tyrosine kinase that is a ubiquitously-expressed 145-kd protein with 2 isoforms arising from alternative splicing of the first exon (Deininger et al 2000). Several structural domains can be defined within the protein. Three homology domains (SH1-SH3) are located toward the N terminus. The SH1 domain carries the tyrosine kinase function, whereas the SH2 and SH3 domains allow for interaction with other proteins.

Proline-rich sequences in the centre of the molecule can, in turn, interact with SH3 domains of other proteins. Nuclear localization signals and DNA-binding and actin-binding motifs are encoded toward the 3' end of the Abl gene.

Studies in fibroblasts have revealed that Abl serves a complex and ill-defined role as a cellular element that modulates signals from various extra-cellular and intra-cellular sources that influence the cell cycle and apoptosis (Barila and Superti-Furga 1998).

1.7.1.2 Bcr

The 160-kd Bcr protein, like Abl, is ubiquitously expressed and encodes a serine-threonine kinase in the first N-terminal exon. The substrate of this kinase may be Bcr itself as a coiled-coil domain at the N-terminus of Bcr allows dimer formation *in vivo*. Bcr contains a binding site for growth factor receptor binding protein (GRB-2) (Calabretta and Perrotti 2004) and in addition, Bcr can be phosphorylated on several tyrosine residues, especially tyrosine 177. The exact physiological role of Bcr is unclear and confounded by the fact that Bcr knockout mice are viable. Maru and Witte (1991) reported that the first exon of Bcr encodes a novel serine/threonine kinase domain.

Regardless of the exact location of the translocation breakpoint, splicing of the primary hybrid transcript yields an mRNA molecule in which Bcr sequences are fused to Abl exon a2 giving rise to a chimeric protein of between 190 and 230 Daltons, (commonly 210). The variable character of the Bcr component and constant nature of Abl suggests Abl is responsible for the transforming principle.

The transforming ability of Abl mutants is activated by loss of the SH3 domain which appears to regulate the activity of the protein. In v-abl, the domain is

replaced by viral gag sequences; in CML, by Bcr sequences. Mechanisms implicated in the pathogenesis of CML include decreased adhesion to bone marrow stroma cells and extracellular matrix, deregulated mitogenic signaling and reduced apoptosis (Pane *et al.* 2002) .

Adhesion to stroma negatively regulates cell proliferation, and CML cells escape this regulation by virtue of their perturbed adhesion properties.

Interferon- α (IFN- α), an active therapeutic agent in CML, appears to reverse the adhesion defect (Karti *et al.* 2002)

1.7.1.3 Bcr/Abl and the PI3 kinase pathway.

PI3 kinase activity is required for the proliferation of Bcr/Abl-positive cells.

Bcr/Abl forms multimeric complexes with PI3 kinase, Cbl, and the adapter molecules Crk and Crkl, in which first, PI3 kinase and then Akt is activated.

Akt is implicated in anti-apoptotic signalling (see fig 1.8.2) (García 2006). Akt is in the downstream cascade of the IL-3 receptor and the pro-apoptotic protein Bad is a key substrate of Akt. Phosphorylated Bad is inactive because it is no longer able to bind anti-apoptotic proteins such as Bcl_{XL} and it is trapped by cytoplasmic 14-3-3 proteins. Together this indicates that Bcr/Abl might be able to mimic the physiologic IL-3 survival signal in a PI3 kinase-dependent manner. Ectopic expression of a mutant form of BAD, which cannot be phosphorylated by Akt, induces massive apoptosis, suggesting that inactivation of BAD proapoptotic effects is important for survival of Bcr/Abl - expressing cells. Ship and Ship-2 inositol phosphatases modulate PI3-kinase signalling and are activated in response to growth factor signals and by Bcr/Abl . Bcr/Abl interacts indirectly with the p85 regulatory subunit of PI-3K via GRB-2/Gab2 and this appears pathologically relevant because Gab2-

deficient marrow cells are resistant to Bcr/Abl transformation (Sattler *et al.* 2002). Thus, Bcr/Abl has a profound effect on phosphoinositol metabolism, which might mimic growth factor stimulation.

1.7.1.4 Bcr/Abl and Ras activation

Bcr/Abl activates several substrate proteins that are in turn responsible for holding Ras in its phosphorylated conformation. Unlike most other solid tumours affected by Ras, CML cells show low rates of Ras mutation. Ras is expressed constitutively in CML without direct activation by mutation and down-regulation of this pathway *in vitro* suppresses proliferation and sensitizes cells to apoptotic stimuli (Sawyers *et al.* 1995). Negative signalling through the SHIP phosphatases discussed above appears to inhibit the Ras pathway by competition with Grb2 and Shc for SH2 domain binding (Kashige 2000)

1.7.1.5 STAT5 pathway

STAT5 is activated by Bcr/Abl via the Src family haematopoietic cell kinase (Hck). On interaction with the SH3 and SH2 domains of Bcr/Abl, Hck is activated and phosphorylates tyrosine 699 of STAT5B, leading to its translocation to the nucleus where it functions as a transcription factor. Nieborowska-Skorska *et al.* (1999) showed that mutants defective in STAT5 activation were less efficient than the wild-type form in transformation of 32Dcl3 myeloid precursor cells. Furthermore, a constitutively active STAT5 mutant rescued the leukemogenic potential of STAT5 activation-deficient Bcr/Abl mutants and ectopic expression of a dominant-negative STAT5 mutant suppressed Bcr/Abl-dependent transformation of primary mouse

marrow cells. The role of STAT5 is likely to depend on transcriptional activation of the target genes potentially involved in Bcr/Abl leukaemogenesis, such as the antiapoptotic Bcl-XL gene (Horita *et al.* 1999).

1.7.1.6 Apoptosis in CML

The effect of Bcr/Abl expression on apoptosis is demonstrated by the failure of apoptosis in response to removal of growth factors in factor dependent cell lines expressing the Bcr/Abl protein and this resistance to apoptosis has been shown to correlate with activation of Ras. Bcr/Abl positive cells also show resistance to apoptosis induced by DNA damage. It is suggested that Bcr/Abl may inhibit apoptosis by blocking the release of cytochrome c from mitochondria, thus blocking caspase activation (Wang 2000). Bcr/Abl has been shown to up-regulate Bcl-2 in a Ras or a PI3 kinase-dependent manner in Baf/3 and 32D cells, respectively. Another link between Bcr/Abl and the inhibition of apoptosis might be the phosphorylation of the pro-apoptotic protein Bad. In addition to Akt, Raf-1, immediately downstream of Ras, phosphorylates Bad on 2 serine residues. Two studies (Neshat *et al.* 2000, Keeshan *et al.* 2002) provide evidence that the survival signal provided by Bcr/Abl is at least partially mediated by Bad and requires targeting of Raf-1 to the mitochondria. It is also possible that Bcr/Abl inhibits apoptosis by down-regulating the interferon consensus sequence binding protein (ICSBP). Furthermore, ICSBP knockout mice develop a myeloproliferative syndrome, and haemopoietic progenitor cells from ICSBP^{2/2} mice show altered responses to cytokines (Hao and Ren 2000).

Thus, Bcr/Abl may shift the balance towards the inhibition of apoptosis while simultaneously providing a proliferative stimulus. This is in line with the

concept that a proliferative signal leads to apoptosis unless it is counterbalanced by an anti-apoptotic signal, and Bcr/Abl fulfils both requirements at the same time.

1.7.1.7 The cell cycle in CML

Early reports of higher than normal frequency of actively cycling progenitors in CML (Eaves *et al.* 1986) coexist with studies that failed to find increased cell proliferation rates in CML (Kramer *et al.* 2001). Subsets of very immature CML progenitors survive and proliferate *in vitro* in the absence of exogenous growth factors, whereas their normal counterparts die rapidly under the same conditions. By contrast, more differentiated subsets appear to lack the capacity for autonomous growth *in vitro*. Expansion of myeloid progenitors is caused by p210B^{cr/Abl} expression in primitive progenitors; that is these cells would normally remain quiescent, but Bcr/Abl may promote cell division to maintain the pool of stem cells and to generate committed late progenitors. Primitive CML progenitor cells appear to have a greater proportion of cycling cells than normal progenitors, whereas Clarkson *et al.* (1998) found the more abundant, committed CML progenitors might have a lower proliferative potential of their normal counterpart.

Exit from quiescence induced by Bcr/Abl in primitive progenitor cells may depend on its effect on cyclins and Cdk inhibitors (Deininger *et al.* 2002). Cyclin D2 levels are increased in Bcr/Abl -expressing lymphoblasts and are required for stimulation of proliferation induced by Bcr/Abl in these cells, and down-regulation or cytoplasmic relocation of CdkN1B/p27 has been demonstrated in mouse and human lymphoid and myeloid Bcr/Abl -expressing cells (Jena *et al.* 2002). As mentioned above, p27 Cdk inhibitor

maintains quiescence and thus regulates the expansion of haematopoietic stem cells and early progenitors. The ability of Bcr/Abl to modulate levels of cyclin and Cdk inhibitors may promote the entry of primitive haematopoietic cells into the cell cycle. Autocrine production of interleukin 3 (IL-3) by primitive CML progenitors is proposed as a mechanism causing the initial expansion of these cells and would, in turn, increase cyclin D2 and down-regulate p27 levels, possibly allowing CML primitive progenitors to leave quiescence and start cycling (Eaves *et al.* 2003).

A possible explanation for the different effects induced by endogenous Bcr/Abl in the CD34⁺ and CD34⁻ subset may rest in its levels of expression; low levels of Bcr/Abl expression typically found in most CML cells may be sufficient for anti-apoptotic, but not for proliferative signals, whereas higher levels of Bcr/Abl expression in the more primitive subsets of CD34⁺ cells may be sufficient for both anti-apoptotic and proliferative signals (Calabretta and Perrotti 2004).

1.7.1.8 Progression to Blast Crisis

The mechanisms underlying the blast phase/crisis (BC) process are poorly understood. There is no specific genetic change associated with disease transformation, though p16 p53 and Rb have been implicated. It is suggested that a variety of cooperating genetic lesions are responsible (Melo 1996). p53 is mutated in approximately 30% of blast cell crisis cases Bcr/Abl expression leads to enhanced expression of the low fidelity DNA polymerase β , and it is suggested that this in turn leads to the accumulation of genetic lesions amongst the rapidly proliferating cells of the chronic phase (Calabretta and Perrotti 2004). This is compounded by the possibility that Bcr/Abl inactivates

(by phosphorylation) the error prone DNA repair mechanism associated with xeroderma pigmentosum group B protein (Takeda *et al.* 1999). Bcr/Abl may also deregulate expression of critical genes involved in monitoring and repair of DNA damage such as RAD51, DNA-PK_{CS}, and BRCA-1. Thus, Bcr/Abl expression is consistent with the phenotype of these cells and implicates reduced apoptosis susceptibility and enhanced proliferative potential of specific cell subsets in progression to blast phase. The vast majority of secondary changes leading to blast crisis involve genes encoding nucleus-localized proteins that directly or indirectly regulate gene transcription; mutations/loss of function of tumour suppressor genes is predominant over mutation/activation of oncogenes; and p53 is genetically or functionally inactivated in a large fraction of CML BC cases (Melo and Deininger 2004) Several other haematological malignancies are associated with varying degrees to specific genetic lesions, though with the exception of the recently-discovered V617F mutation in the Jak2 Janus kinase gene and polycythaemia vera, few show the same specificity for a given phenotype as that seen in CML (Kralovics *et al.* 2005)

1.8 PTEN tumour suppressor protein

The common involvement of phosphorylation in the activation of oncogenes led to the hypothesis that a tumour suppressor protein with phosphatase function may exist. This was confirmed with the discovery of PTEN. Li *et al.* (1997) noticed loss of heterozygosity (LOH) at 10q23 as an alteration that occurred at high frequency in a variety of human tumours. Although rarely seen in low-grade glial tumours and early-stage prostate cancers, LOH at 10q23 occurs in approximately 70% of glioblastomas (the most advanced

form of glial tumour) and approximately 60% of advanced prostate cancers. (Li *et al.* 1997) The finding that wild-type chromosome 10 suppresses the tumourigenicity of glioblastoma cells in mice suggested that 10q23 may encode a tumour suppressor gene. Li *et al.* (1997) mapped homozygous deletions on 10q23 and isolated a candidate tumour suppressor gene that they called PTEN for “phosphatase and tensin homolog” deleted on chromosome ten. Steck *et al.* (1997) independently isolated the same gene (termed MMAC1) by exon trapping.

1.8.1 Structure of PTEN

Sequence analysis of the predicted 403-amino ORF revealed a protein tyrosine phosphatase domain with a large homologous region to chicken tensin, a protein that interacts with actin filaments at focal adhesions and bovine auxilin. The preliminary homologies discovered in PTEN structure suggested a tumour suppressor function exerted by opposing tyrosine kinases action and by modulating tumour cell metastases by interaction at focal adhesions.

Lee *et al.* (1999) determined PTEN's crystalline structure and revealed an N-terminal phosphatase domain and a tightly associated C-terminal C2 domain. These two domains together form a minimal catalytic unit, and comprise almost the entire protein, excluding only a very short N-terminal tail and a longer 50-amino-acid C-terminal tail. The phosphatase and C2 units form the catalytic domain, whilst the terminal sections appear to regulate function and localisation. The N-terminal sequence contains a polybasic motif, extending into the start of the phosphatase domain, with sequence similarity to that found in proteins that have been proposed to bind PI2 (Walker *et al.* 2004).

PTEN is a member of the PTP enzyme family, all of which have a reactive active-site cysteine residue for catalysis, which are sensitive to oxidation involving the formation of a disulphide bond between the active site and an adjacent cysteine residue (fig 1.8.1) (Lee *et al.* 2002).

The longer C-terminal tail in PTEN contains a cluster of serine and threonine residues that become phosphorylated in many cells. Raftopoulou *et al.* (2004) have shown that expression of the C2 domain of PTEN alone, in the absence of the phosphatase domain, is able to suppress cellular motility. These findings suggest a function for PTEN in addition to its ability to remove phosphate groups from its substrate molecule. Their study also provided evidence that a weak protein phosphatase activity in PTEN acts to dephosphorylate its own C-terminal phosphorylation sites.

1.8.2 Function of PTEN

PTEN has been shown to be primarily a lipid phosphatase and a ubiquitous regulator of the cellular PI (phosphoinositide) 3-kinase signalling pathway. This signalling pathway is characterized by the regulated activation of class I PI3-kinase enzymes, producing the second messenger PI3 from its relatively abundant precursor PI2 which is profuse in the interior of the phospholipid cell membrane. Inositol is a sugar-like molecular having a circular six-carbon ring structure that can be reversibly

Fig 1.8.1

Proposed structure of PTEN

PTEN

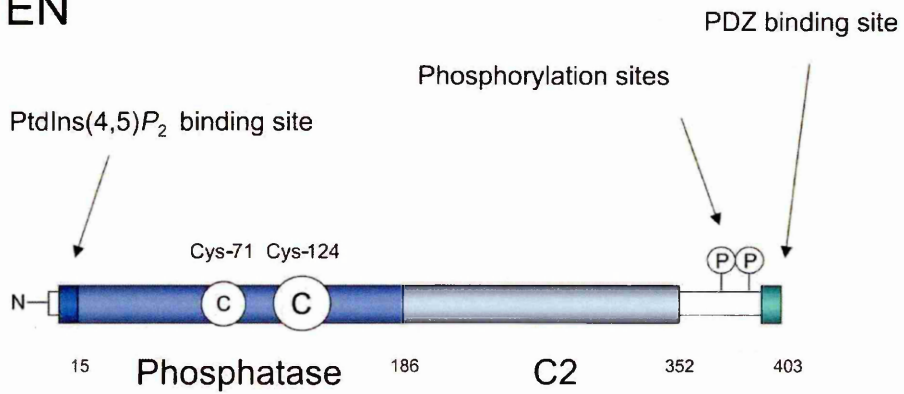


Fig 1.8.1
Proposed PTEN structure showing N terminal PI binding site, catalytic phosphatase site and phosphorylation sites on tail at carboxy terminus end (Leslie and Downes 2004)

phosphorylated at free carbon groups. PI3 mediates downstream signalling through a range of effector proteins, including the proto-oncogene product Akt/protein kinase B that are able to recognize this lipid and bind it selectively. PTEN antagonizes PI3-kinase signalling by dephosphorylating the 3-position of the inositol ring of PI3 and thus inactivating downstream signalling (Fig 1.8.2). Although other 3-phosphorylated inositol lipids and phosphates have been proposed as substrates for PTEN, current evidence indicates that PI3 may well be its only important physiological substrate of this type (Leslie and Downes 2004).

Over expression of PTEN in MCF-7 breast cancer cells causes G1 arrest followed by cell death. Weng *et al.* (2001a) demonstrated increased PTEN-mediated cell death of MCF-7 breast cancer cells cultured in low levels of growth factors. The caspase-9-specific inhibitor ZVAD blocked PTEN-induced cell death without altering the effect of PTEN on cell cycle distribution. Over expression of dominant-negative Akt, a downstream protein kinase, induced more cell death but had less effect on the cell cycle than over expression of PTEN. The authors suggested that the apoptotic cells induced by the over expression of PTEN are not derived from the G1-arrested cells. Further, they hypothesized that the effect of PTEN on cell death is mediated through the PI3K/Akt pathway, whereas PTEN-mediated cell cycle arrests depend on both PI3K/Akt-dependent and -independent pathways (Weng *et al.* 2001b).

Fig 1.8.2

Proposed function of PTEN

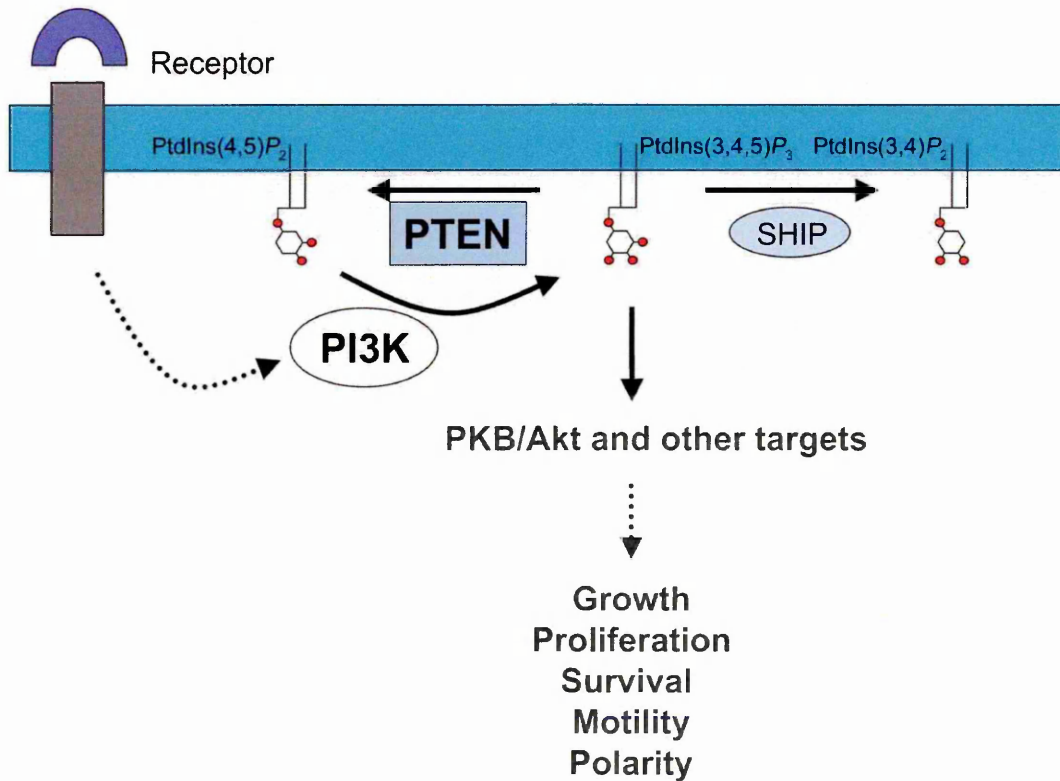


Fig 1.8.2

Proposed function of PTEN (Leslie and Downes 2004). Binding of extracellular ligand stimulates phosphorylation (by PI3 kinase PI3K) and activation of membrane phospholipid – phosphatidylinositol. Phosphorylation results in downstream activation of Akt and subsequent growth/proliferation signal.

PTEN phosphatase returns membrane phospholipids to inactive form by removing the 3' inositol ring phosphate and abrogating proliferation/growth signal. Src-homology 2-containing inositol 5' phosphatase (SHIP) also dephosphorylates PI3 at the 1' site but may not abrogate activation of Akt (Choi *et al.* 2002)

1.8.2.1 PTEN Protein Phosphatase function

PTEN also has a weak protein phosphatase activity, and several target proteins have been proposed, including PTEN itself (see below) and the platelet-derived growth factor receptor, which may form a complex with PTEN. Resolving whether these proteins are physiological substrates for the phosphatase is an important area for future work. Leslie *et al.* (2007) reported that a PTEN mutant (G129E) with only protein phosphatase activity is capable of inhibiting the epithelial-to-mesenchymal transition of chick embryo mesoderm cells ingressing through the anterior and middle primitive streak during embryo development. Directional motility of mesoderm cells during embryo development was dependent on PTEN's lipid phosphatase activity.

The PI3K/Akt pathway is also involved in down-modulating the expression or the function of the CDK inhibitor p27. Akt directly phosphorylates p27 and prevents its nuclear translocation. Activated mutants of Akt induce down-regulation of p27, which is prevented by proteasome inhibitors, suggesting that Akt modulates p27 stability. It is unclear whether phosphorylation by Akt leads to p27 degradation or whether other Akt-dependent mechanisms are involved in this process. Regardless of the mechanisms, Bcr/Abl-activated Akt may enhance the proliferative potential of Bcr/Abl-expressing cells by disruption of p27 activity (Wu *et al.* 2003). Weng *et al.* (2001b) further demonstrated that over expression of wildtype PTEN leads to the suppression of cell growth through the blockade of cell cycle progression, an increase in the abundance of p27, a decrease in the protein levels of cyclin D1, and the inhibition of Akt phosphorylation.

1.8.2.3 Role of PTEN in the Nucleus

Shen *et al.* (2007) reported a function for PTEN in the nucleus in controlling chromosomal integrity. Mutation of PTEN leads to centromere breakage and increased chromosomal translocations. PTEN was physically associated with CENP-C (an integral component of the kinetochore) at the centromeres. Shen *et al.* (2007) reported that PTEN with C-terminal mutations disrupted the association of PTEN with centromeres and caused centromeric instability. PTEN null cells also exhibit spontaneous DNA double-strand breaks. The group suggested that PTEN maintains chromosomal stability by physical interaction with centromeres and control of DNA repair, possibly by stimulation of Rad51 expression.

Denning *et al.* (2007) identified a short sequence in the N-terminal region of PTEN required for cytoplasmic localization which they denoted as a cytoplasmic localization signal. Mutations within this region induced nuclear localization and impaired growth suppression activities of PTEN while maintaining lipid phosphatase activity. Denning *et al.* (2007) ascribed to this signal a function as a nuclear export or as a cytoplasmic retention signal of PTEN.

Trotman *et al.* (2007) suggested that nuclear PTEN is essential for tumour suppression and that PTEN nuclear import is mediated by its monoubiquitination. A lysine mutant of PTEN, associated with Cowden syndrome, retains catalytic activity but fails to accumulate in nuclei of patient tissue due to an import defect. The group identified several lysine residue as major monoubiquitination sites essential for PTEN import. While nuclear PTEN was stable, polyubiquitination lead to its degradation in the cytoplasm. Thus, mutations of PTEN target its posttranslational modification and controls

tumour progression by differentiating between degradation and protection of PTEN. The group suggested that failure of tumour suppression could occur in PTEN with normal enzyme activity but incorrect post translational modification and subsequent ubiquitination leading to aberrant localisation in the nucleus.

1.8.2.4 PTEN and Chemotaxis

Cell migration is inhibited by overexpression of PTEN but is enhanced when low levels of PTEN are induced by an antisense silencing method. Integrin-mediated cell spreading and the formation of focal adhesions are down regulated by wildtype PTEN but not by PTEN with an inactive phosphatase domain. PTEN interacts with the focal adhesion kinase FAK , reducing its tyrosine phosphorylation. Overexpression of FAK partially antagonizes the effects of PTEN. Thus, PTEN phosphatase may function as a tumour suppressor by negatively regulating cell interactions with the extracellular matrix Tamura *et al.* (1998)

Raftopoulou *et al.* (2004) demonstrated that PTEN inhibits cell migration through its C2 domain, independent of its lipid phosphatase activity. This activity depends on the protein phosphatase activity of PTEN and on the dephosphorylation at a single residue, threonine-383. Raftopoulou *et al.* (2004) suggested that the ability of PTEN to control cell migration through its C2 domain is likely to be an important feature of its tumour suppressor activity. Nishio *et al.* (2007) showed that, in contrast to their study of the phosphatase SHIP1, bi-allelic loss of PTEN had no impact on neutrophil chemotaxis. Subramanian *et al.* (2007) studied PTEN function in cells in which PTEN was disrupted only in myeloid-derived cells. Neutrophils studied in chemotaxis assays displayed small but significant errors in directionality.

Chemoattractant-stimulated myeloid cells lacking PTEN showed significantly higher Akt phosphorylation and actin polymerization. Overall, chemotaxis was not affected. Because of the increased responsiveness of PTEN deficient neutrophils, the *in vivo* recruitment to the inflamed peritoneal cavity was significantly enhanced (Subramanian *et al.* 2007).

1.8.3 Regulation of PTEN

1.8.3.1 C terminus and PTEN regulation

PTEN lacks obvious regulatory domains, and appears to have relatively high constitutive phosphatase activity, both *in vitro* and *in vivo* (Leslie and Downes 2004). This contrasts with other PI3 phosphatases such as the SHIP phosphatases, that are tightly regulated, with low basal cellular activity. Cells lacking PTEN expression have been found to have greatly elevated basal PI3 levels, whereas cells lacking SHIP demonstrate a greater magnitude and duration of stimulated rises in the levels of this lipid (Stambolic *et al.* 1998). Stambolic *et al.* (2001) identified a p53-binding element directly upstream of the PTEN gene. Deletion and mutation analyses showed that this element is necessary for inducible transactivation of PTEN by p53. A p53-independent element controlling constitutive expression of PTEN was also identified. In contrast to p53 mutant cell lines, induction of p53 in primary and tumour cell lines with wildtype p53 increased PTEN mRNA levels. Thus, the primary control of PTEN levels may be exercised by modulation of protein production levels.

Other studies suggest a model for PTEN regulation in which phosphorylation plays a major role through induction of a conformational switch. Most cellular PTEN appears to be phosphorylated at a cluster of serine and threonine

residues in the acidic stretch of the C-terminal tail. In this form, PTEN appears monomeric and cytosolic (Vazquez *et al.* 2000)

Using PTEN mutants in which the putative phosphorylation sites were changed to alanine residues, it has been inferred that dephosphorylation makes PTEN highly susceptible to proteolysis, increases its affinity for anionic lipids and enhances its localization to the plasma membrane. Also, non-phosphorylatable PTEN mutants have greatly enhanced biological activity in cells, presumably due to co-localization with their membrane-incorporated substrate. It has been proposed that the dephosphorylation of these C-terminal residues causes a conformational opening up of the protein that mediates many of these effects of phosphorylation (Leslie and Downes 2004). Dephosphorylated PTEN is more sensitive to protease digestion *in vitro*, it interacts much more efficiently with some protein binding partners and also associates more effectively with cellular membranes. It is likely that the opening up of the dephosphorylated PTEN structure reveals the basic regions in PTEN that can mediate its binding to acidic membranes, and that in the phosphorylated protein, these basic regions are hidden, perhaps through direct interaction with the highly acidic phosphorylated C-terminus tail region (Leslie and Downes 2004).

It has been proposed that the PTEN C-terminus is phosphorylated by the protein kinase CK2 (Torres and Pulido 2001), which is constitutively active. This kinase phosphorylates PTEN at several C-terminal residues *in vitro*, and inhibitors of CK2 greatly decrease PTEN phosphorylation in cells, though the inhibitors are weak and non-specific, so this mechanism is putative.

Nevertheless, most cellular PTEN appears to be maintained in a phosphorylated, inactive state, and its transient activation can be mediated

through dephosphorylation (Sarno *et al.* 2003).

The above mechanism suggests a potential feedback control mechanism and it is possible that PTEN may initiate this regulatory switch itself (Fig 1.8.3), through dephosphorylation of Thr-383, by its own weak protein phosphatase activity. This idea is supported by the finding that phosphatase-inactive PTEN mutants are found to be more highly phosphorylated upon C-terminal residues than the wild-type enzyme (Birle *et al.* 2002).

Odrizola *et al.* (2007) investigated the role of PTEN C-terminal tail domain in regulating its membrane-targeting and catalytic functions. Characterization of a panel of PTEN phosphorylation site mutants revealed that mutating Ser385 to alanine (S385A) promoted membrane localization *in vivo*, and phosphatase activity *in vitro*. S385A mutation was associated with a substantial reduction in the phosphorylation of the Ser380/Thr382/Thr383 cluster.

1.8.3.2 N terminus and PTEN regulation

PTEN has greater activity towards substrates incorporated into lipid surfaces that have an acidic character, such as the inner surface of the cell plasma membrane. PTEN shows increased activity *in vitro* against substrates presented in vesicles that include non-substrate acidic lipids.

The polybasic motif at the PTEN N-terminus plays an important role in both the binding to anionic vesicles and the enhancement of activity, such that a mutation in this motif identified in a human glioblastoma specifically impairs this binding and activation, and removes the ability of the enzyme to regulate cellular proliferation in culture.

Fig 1.8.3

Proposed self-regulation mechanism of PTEN

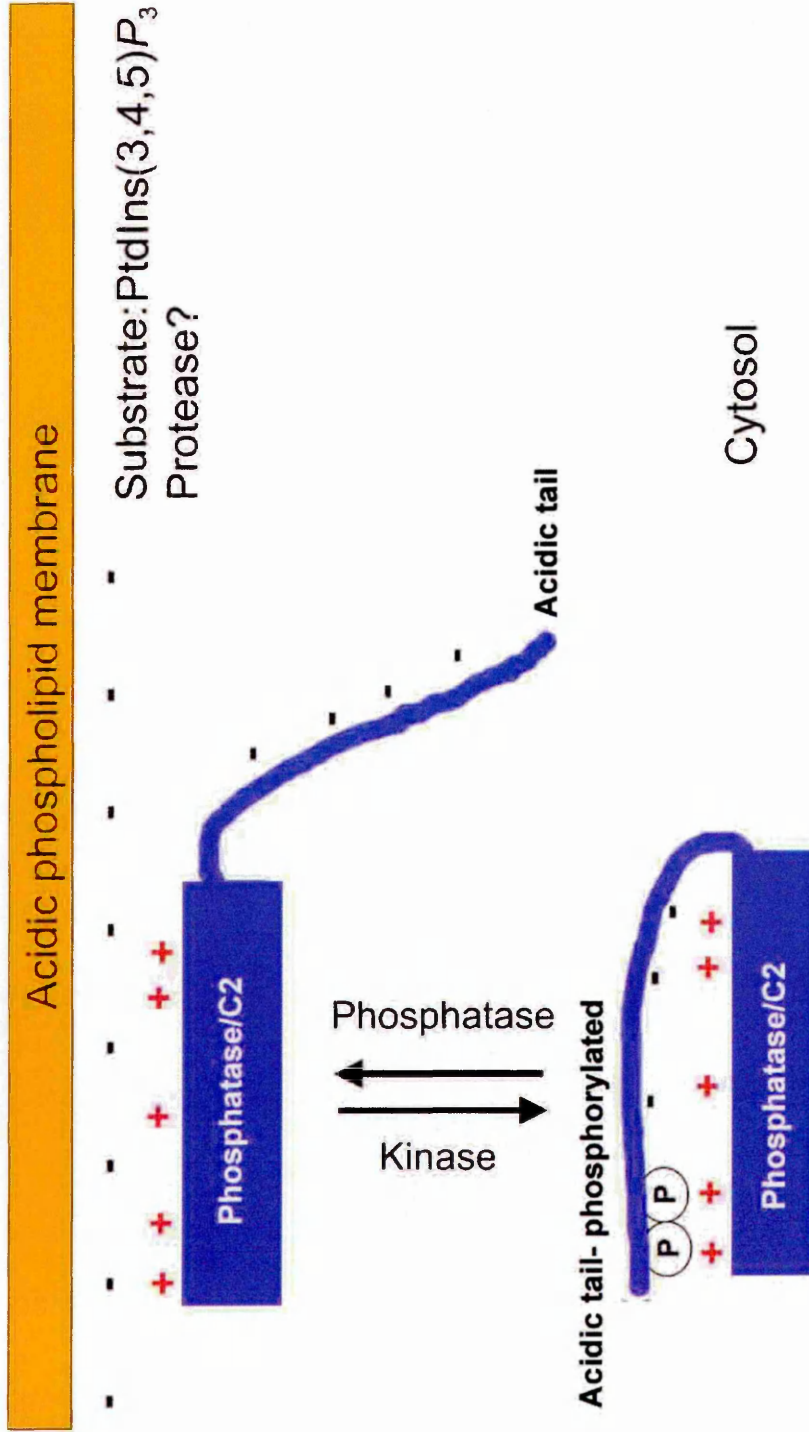


Fig 1.8.3 Proposed self-regulation mechanism of PTEN by binding of negatively charged phosphorylated acidic tail at C terminus to positively charged phosphatase region.

Leslie and Downes (2004) suggest a model where PTEN is preferentially recruited to, and active against, lipids within membranes that contain relatively high levels of anionic lipids, such as PI2 and phosphatidylserine and that PTEN is active only against substrates located within the acidic plasma membrane, but not within internal membranes such as the less charged endoplasmic reticulum.

1.8.3.3 Regulation of PTEN Expression and Ubiquitination

The importance of correct regulation of the expression of PTEN is demonstrated by the developmental abnormalities and numerous benign polyps that appear to result from reduced expression of the PTEN protein in experimental animals and human subjects with inherited PTEN defects such as Cowden syndrome (Marsh *et al.* 1997). Several transcription factors have been demonstrated to regulate PTEN. The PPARg (peroxisome proliferator-activated receptor g) agonist rosiglitazone, and egr-1 have been shown to bind the PTEN promoter and regulate its expression, and it appears that p53 and egr-1 may play a role in the up-regulation of PTEN expression caused by irradiation. (Stambolic *et al.* 2001, Virolle *et al.* 2001).

The constitutive expression of PTEN may be regulated by factors that affect the stability of the protein. Vazquez *et al.* (2002) showed that the protein phosphorylated at the C terminus is relatively stable. Dephosphorylation of these residues leads to a functional activation of the protein as described above but also to dramatic destabilization. Several studies have implicated proteosomal degradation as a control mechanism, since in some circumstances PTEN stability appears to be increased by proteasome inhibitors (Vazquez *et al.* 2001) and the detection of ubiquitinated forms of PTEN has been reported (Tolkacheva 2001). Nedd4 (Neural precursor cell Expressed Developmentally Downregulated) modifies substrate proteins by the addition of ubiquitin groups in a process known

as ubiquitination. Wang *et al.* (2007) reported that Nedd4 regulates PTEN levels by ubiquitin-mediated proteosomal degradation. Wang *et al.* (2007) suggested that aberrant upregulation of NEDD4-1 can post translationally suppress PTEN in tumour cells. They also suggested that the role Nedd4 played in PTEN regulation was analogous to that of MDM2 in P53 regulation.

During apoptosis, it appears that PTEN protein becomes cleaved at several C-terminal sites, probably by caspase 3, sensitising the protein to further degradation, and blocking interaction with PDZ domain-containing scaffold proteins (Torres *et al.* 2003).

Salmena and Pandolfi (2007) suggested that the monoubiquitylation of PTEN described by Denning *et al.* (2007) and Trotman *et al.* (2007) coupled to nuclear-cytoplasmic shuttling might be a novel regulatory mechanism that directly influences the function of PTEN

1.8.4 PTEN function in Leukaemia

Yilmaz *et al.* (2006) noted the functional similarities between normal and cancer stem cells and the associated difficulty of eliminating tumour stem cells without affecting normal stem cells. The group also reported that deletion of PTEN in a murine model causes the generation of transplantable leukaemia-initiating cells and causes the depletion of normal haemopoietic stem cells (HSCs). Their data suggested that PTEN promotes quiescence in HSCs and that in the absence of PTEN, HSCs are driven into cell cycling but the increase is transient as the cells are unable to sustain themselves after depletion of PTEN. Irradiated mice were rescued with transplantation of PTEN-deficient cells but failed over eight weeks to develop full lineage reconstitution, although they did not develop leukaemia.

Yimaz *et al.* (2006). suggested that HSC depletion resulted from inhibition of self-renewal rather than promotion of apoptosis. The mammalian target of rapamycin

(mTOR) is a protein kinase that controls cell growth by modulation of upstream growth factor signals and is also a sensor of cellular nutrient and energy levels and redox status (Hay & Sonenberg 2004). The observations that the PI3 kinase pathway initiated mTOR kinase pathway, led the group to administer the mTOR inhibitor, rapamycin to PTEN deficient leukaemic mice to assess whether rapamycin depleted the leukaemic cell population. When administered concurrently with leukaemic cells, rapamycin-treated mice showed no evidence of leukaemia. Rapamycin also restored the multilineage reconstitution in irradiated mice treated with PTEN deficient HSCs. This group suggest that persistent activation of the PI3 kinase pathway leads to the depletion of PTEN-deficient HSCs via a gradual increase in the rate at which HSCs exit the stem cell pool or alternatively, the depletion of PTEN may lead to the acquisition of secondary mutations that inactivate the senescence response (Yilmaz *et al.* 2006). In a study of HSC numbers in PTEN deficient mice, Zhang *et al.* (2006) demonstrated a two to three-fold decrease in the proportion of HSCs in G0 phase and a parallel increase in the proportion in S, G2 and M phase and that the proportion of cycling HSCs was aberrantly high. The group suggested that PTEN helps control the transitions that stem cells make between the quiescent and active states and whether to progress further through the cell cycle or return to a quiescent (G0) state. Disrupting PTEN in stem cells results in more active cycling and a loss of the quiescent pool of stem cells that is necessary for long-term stem cell maintenance. PTEN's role in cell adhesion and migration might lead to a mobilisation of HSCs into the peripheral circulatory system, though *in vitro* assays of PTEN deficient cells' ability to bind to fibronectin collagen and laminin were normal. *In vivo* homing assays showed that PTEN mutants were less efficient at populating bone marrow niches when in competition with fully competent cells. Zhang *et al.* went on to suggest that the ability to lodge within bone marrow was

linked to quiescent stages of cell cycling irrespective of PTEN status but the reduced ability of PTEN deficient cells to lodge in bone marrow may be a reflection of their activated state.

Cheong *et al.* 2003 observed that phosphorylation of PTEN affects the protein's stability and function. In this study, phosphorylated PTEN (pPTEN) was observed in 45 (73.8%) of 61 cases with acute myeloid leukaemia (AML). Phosphorylation of Akt and its downstream molecules (Forkhead (Drosophila) homologue 1; and glycogen synthase kinase 3 beta) was significantly associated with pPTEN. The complete remission rates were not different with respect to pPTEN, but overall survival was significantly shorter in patients with pPTEN. The group suggested that PTEN phosphorylation may add insight into the molecular pathogenesis of AML, and may be a parameter for an unfavourable outcome.

1.9 The aims of this thesis

Frequent mutations in PTEN have been detected in several types of human cancer, including glioblastoma, prostate cancer and endometrial cancer (reviewed in Introduction). The main aim of this thesis was to investigate the occurrence of PTEN mutations in leukaemia. For this purpose a range of unpaired normal and primary haematological malignancy samples from the stored archives of the Department of Haematology, Wirral Hospitals NHS Trust was studied. Ethical approval for this study was obtained from the Wirral Hospitals Research and Development Committee. Immortalised cell lines were obtained from the Department of Haematology, Royal Liverpool Hospital.

The project involved several objectives:

1. Developing DNA extraction methods for formalin-fixed and paraffin wax embedded cells and for cells micro-dissected from Romanowsky-stained bone marrow smears.

2. Optimisation of PCR conditions for amplification of the nine exons of the PTEN gene.
3. Conformation-based screening of PCR products by SSCP and DGGE to detect point mutations, small deletions and insertions in primary haematological malignancies.
4. DNA sequencing of samples identified as possessing mutation(s) to precisely determine their nature and location and evaluate their effect on PTEN protein.
5. Studies of PTEN gene expression at the mRNA level in cell lines by RT-PCR.
6. Investigation of PTEN protein expression in primary haematological malignancies by immunohistochemistry and Western blotting-based techniques.
7. Analysis of results to correlate DNA mutation and protein expression with disease classification.

Materials and Methods

2.1 DNA extraction

DNA was extracted from a variety of fresh, fixed, stained cells and tissue.

Heterogeneity between and within source material and degree of fixation prompted the development of several differing methods for DNA extraction of the cells.

2.1.1 Extraction from fresh and frozen cells, blood and bone marrow

These cells were unfixed and unstained but had been collected in Starsted tri-potassium EDTA blood collection tubes to prevent coagulation. DNA was extracted from blood or bone marrow samples and cultured cell suspensions according to the following protocol modified from that originally suggested by Wilcockson (1973).

Total nucleated cell numbers in samples were not calculated as PCR has the ability to generate large quantities of amplified DNA, potentially from single copy sequences. Cultured cells which had been grown to confluence were pelleted by centrifugation in a 50ml centrifuge tube at a relative centrifugal force (RCF) of 1000g in a MSE Micro Centaur centrifuge for 5 mins, and started at the point of sodium perchlorate addition step in the extraction procedure below.

Blood and bone marrow samples were collected in EDTA- or Citrate-anticoagulant and centrifuged at 2000g RCF for 5min at room temperature. The Buffy coat was removed with a sterile disposable pipette and transferred to a 2ml microcentrifuge tube. 1.5ml of RBC lysis buffer (8.3g NaCl; 1.0g KHCO₃; 0.3g Na₂EDTA in 1l sterile water) was added to lyse RBCs. The tube was vortex-mixed and incubated at room temp for 5 min. The tube was centrifuged for 5 min at 12 000g RCF in a MSE Micro Centaur centrifuge to pellet the nucleated cell fraction

and the supernatant discarded into 2% Virkon solution (Anachem Ltd UK). The RBC lysis wash process was repeated. 500µl of 5M sodium perchlorate was added to the cell pellet which was homogenized by repeated pipetting with a 100µl Anachem M100 direct displacement pipette and incubated at RT for 5min. The extracted samples were transferred to an air extraction fume cupboard and 700µl of chloroform (-20⁰C) was added and thoroughly vortex-mixed at maximum speed for 15 min. The tube was centrifuged at 12 000g for 5 min and the supernatant transferred to a clean micro-tube. 1ml of isopropanol (-20⁰C) was added and mixed thoroughly prior to centrifugation at 12 000g for 15 min. The supernatant was removed and 1.5ml of 70% ethanol (-20⁰C) was added and mixed by gentle inversion. The tube was centrifuged at 12000g for 1 min and the supernatant ethanol decanted. The nucleic acid pellet was re-suspended in 500µl of TE buffer pH 8.0 (10 mM Tris HCL, 1mM EDTA). DNA concentration of extract was estimated by measuring the ratio of 260/280nm absorption on a GeneQuant UV spectrophotometer (Biochrom UK).

2.1.2 Extraction of DNA from fixed, stained bone marrow smears

This object of this procedure was to develop a method to extract PCR-amplifiable DNA from archived bone marrow smears.

Archived bone marrow smears had been fixed in methanol and ethanol then stained in May-Grunwald and Geimsa stain (Raymond A Lamb Ltd UK) following routine lab procedures SOP (Appendix 1). Several procedures were utilized including proteinase K digestion, phenol/chloroform extraction, chloroform extraction, extraction without removal of stain and extraction of dry scrapings. Slides were de-stained in methanol for 5 min then washed in deionised water. 100µl of PCR buffer (Bioline Ltd, UK) was spread out over the surface of the slide with a second glass slide and soaked for 5 min. The entire slide surface was

scraped off with a scalpel and collected into a 2ml microtube. 200µl of PCR buffer (Bioline Ltd, UK) plus 5µl of proteinase K solution 10mg ml⁻¹ (Amresco Inc, USA) was added and incubated for 60 min. at 55⁰C then 5 min at 100⁰C. The sample was centrifuged for 5 min. at 12 000g and the supernatant collected in a conical 1.5ml micro-tube. 5µl of extract was used per 100 µl of PCR mix.

The following optimised protocol with an added ethanol precipitation step was adopted:

Slides were de-stained in methanol for 5 min then washed in water.

100µl of PCR buffer was spread out over the surface of the slide with a second glass slide and soaked for 5 min. The entire slide surface was scraped off with a scalpel and collected into a 2ml microtube. 200µl of PCR buffer (Bioline Ltd UK) plus 5µl of proteinase K solution 10mg ml⁻¹ (Amresco Inc USA) in PCR buffer was added and incubated for 60 min. at 55⁰C then 5 min at 100⁰C. The sample was centrifuged for 5 min at 12 000g and the supernatant collected in a conical 1.5ml micro-tube. 0.1 volume of 3M sodium acetate solution and 2 volumes of -20⁰C ethanol was added. The tube was placed at -20⁰C for 15 min then centrifuged at 12 000g for 15 min.

The pellet was then washed in 70% ethanol and resuspended in 50µl of TE buffer (10mM Tris HCl, 1mM EDTA pH 8.0).

DNA concentration was measured by spectrophotometric absorption at 260 nm using a GeneQuant spectrophotometer.

2.1.3 Microdissection of tumour cell DNA from stained bone marrow smears

This technique made use of the fact that nucleated cells in stained blood and bone marrow smears appear as discrete cells surrounded by non-nucleated red blood cells and platelets. Mature red cells could be collected with the nucleated tumour cells without contributing to the nucleic acid component of the sample

whilst avoiding the collection of normal cells.

The smear was dipped in PCR buffer and blotted lightly on filter paper then placed on an inverted stage (subject illuminated from above, viewed from below). A narrow gauge insulin syringe needle was tapped on a glass slide to produce a slight "hook" at the sharp end. Using the 20 times magnification objective, an area of smear was found with well spaced-out, nucleated cells. Using the microscope stage as a hand rest, the tip of the needle was brought into the field of view. With a mixture of slight hand movements and the fine adjustment wheel of the microscope stage, the slide was "trawled" for tumour cells whilst avoiding normal nucleated cells.

Approximately 100 cells were collected and placed in 50µl of proteinase K buffer (5µl 10mg ml⁻¹ proteinase K plus 45µl PCR buffer) in a 0.5 ml PCR tube.

The tube was incubated at 55⁰C for 1 hour and 100⁰C for 5min then centrifuged at 12000g for 1min. The supernatant was transferred to a fresh tube and 10µl 3M sodium acetate, and 200µl of -20⁰C ethanol was added. Tube was incubated at -20⁰C for 15 min then centrifuged at 12 000g for 15 min.

PCR components were added directly to this tube.

2.1.4 Extraction of DNA from fixed paraffin-embedded tissue sections

2.1.4.1 Extraction of DNA from formalin-fixed paraffin-embedded tissue sections using phenol/chloroform

10 x10µm sections were cut from the tissue block using a microtome.

Microtome blade was washed with extreme care between block samples using a tissue soaked in xylene. Sections were placed in a 2ml microtube and xylene added (to approx 1.5ml) to de-paraffinise the sections.

After 30 mins at room temp, tube was centrifuged at 12000g for 1 min and the xylene was discarded. The tissue was washed with three consecutive changes of

ethanol.

DNA was extracted by the phenol/chloroform method (Sambrooke *et al* 1998).

2.1.4.2 DNA extraction from wax embedded tissue sections by de-waxing and proteinase K digestion

Trial PCR reactions using beta globin primers yielded poor levels of 438 bp specific product with a high level of non-specific amplification. The method was modified by using proteinase K digestion in place of phenol/chloroform after de-paraffinisation:

Sections were cut and de-waxed as in 2.1.4.1. 0.5ml Proteinase K buffer (5µl 10mg ml⁻¹ proteinase K plus 45µl PCR buffer) was added and incubated at 55°C for 30min. Tube was incubated at 95 °C for 5min to destroy proteinase activity. 5µl of extract was added to a 50µl PCR reaction.

This extraction technique gave an increased yield compared to the phenol chloroform method.

2.1.4.3 DNA extraction from wax embedded tissue sections by heat-based de-waxing and proteinase K digestion

To further increase the yield of specific product, the following protocol was applied:

Sections were cut as in 2.1.4.1. Samples were placed in a 2ml microcentrifuge tube 1.5ml of TE buffer pH 8.0 and incubated for 5 mins at 95°C. The tube was centrifuged at 12 000g then the solidified wax and TE buffer was discarded.

0.5ml Proteinase K buffer (5µl 10mg ml⁻¹ proteinase K plus 45µl PCR buffer) was added and incubated at 55°C for 30min. The tube was incubated at 95°C for 5 mins to destroy proteinase activity. 5µl of extract was added to a 50µl PCR reaction.

This extraction method gave optimum PCR product levels with minimum non-specific amplification and was used for subsequent PCR.

2.1.5 RNA extraction from cultured cells

This technique was modified from Sambrooke *et al.* (2000) and was designed to isolate total cellular RNA.

Total RNA was extracted from the following cell lines: CV605, K260, THP1, JURKAT, HL60, K562. Cells had been grown to confluence. Cell numbers were not estimated as the subsequent RTPCR amplification was not a quantitative procedure and RTPCR has the theoretical ability to generate billions of target sequences from a single copy template .

The cell suspension was centrifuged at 2000g for 5min and supernatant discarded into 2% Virkon. 500µl of 5M guanidine HCL was added per 100µl of cell pellet.

The cell pellet was homogenised by repeated pipetting with a fine-tip 100µl direct-displacement pipette (Gilson M100, Anachem Ltd UK) and incubated at RT for 5min. The sample was transferred to an air extraction cabinet and 500µl of phenol/chloroform/iso-amyl alcohol 45:45:10 pH 6.0 was added and mixed by inversion then incubated for 5min at RT. The sample was centrifuged at 12 000g for 5 min. The supernatant was transferred to a new micro-tube and the procedure repeated from the "500µl of phenol/chloroform/iso-amyl alcohol" step until the organic/aqueous interface was clear. The supernatant was transferred to a new micro-tube and 500µl of chloroform added. The sample was mixed by vigorous shaking and centrifuged at 12 000g for 5 min. The supernatant was removed and 1 volume of ice-cold isopropanol and 0.1 vol. of 3M sodium acetate added. The tube was incubated at -20⁰C for 15 min and centrifuged at 12 000g

for 15 min. The RNA pellet was washed in 70% ethanol.

Ethanol was decanted and the pellet was re-suspended in 50µl of RNase-free water (Amresco Inc. USA). RNA concentration was established by measuring spectrophotometric absorption at 260nm.

2.2 PCR Primer design

PTEN DNA sequences for spanning exons 1-9 including the intron exon boundary region (Nucleotide, <http://www.ncbi.nlm.nih.gov>) were used to design intronic PCR primers for amplification of each exon. Primers were designed to produce PCR products of a size greater than 300bp to achieve maximum CSGE sensitivity (Ganguly *et al.* 1995). Primers were designed manually with a target melting temperature of 60°C using the formula $T_m = 4(G + C) + 2(A + T)^\circ\text{C}$ (Thein and Wallace 1986). Primer regions were selected that had <60% GC base content and primer length was dictated by the target annealing temperature. Primer sequences were then checked with a computer program (Primer - Whitehead Institute for Biomedical Research, USA) to detect self complementarity and 3' overlaps that might generate primer dimers. The use of primers situated within the intron sequences 50 bp from the intron/exon boundary on each side of the exon, was necessary to prevent amplification of PTEN homologous sequences (which lack intron sequences) and also to counter reduced sensitivity of the proposed Conformation Sensitive Gel Electrophoresis (CSGE) to heteroduplex (HD) mismatches occurring within 50 bp of the 5' and 3' ends of the target exon sequence.

To confirm the expression of PTEN mRNA in cultured cells, the PTEN mRNA sequence (Entrez, NCBI <http://www.ncbi.nlm.nih.gov>) was used to design cDNA primers including as much of the transcribed sequence as possible using the methods as per exon 1-9 primers. The DNA sequence for the PTEN homologous

sequence *PTH2* was obtained (Entrez, NCBI <http://www.ncbi.nlm.nih.gov>) and compared to the cDNA sequence for PTEN using a computer program (DNASIS, *Hitachi Software Engineering Company, Ltd*). Subsequent sequence differences were used to identify restriction endonuclease (RE) recognition sites that would be useful in differentiating PTEN cDNA amplification products from PTH2 amplification products. An Mse1 RE site was identified 235bp from the 5' end of the mRNA coding sequence that was present in PTEN gene cDNA but not in the PTH2 homologue.

The cDNA primers were designed to give a 397bp amplicon that would give MSE1 digest fragments of 143, 194 and 60bp for PTEN cDNA plus 337 and 60bp fragments for PTH2 DNA. Human Beta globin primers were supplied by JK Douglas Research Laboratories, Clatterbridge Cancer Research Trust UK, Control primer set. PCR Primers for the SSCP reactions are shown in Table 2.2. All sequences are 5'→3'.

2.3 PCR optimisation

A "standard" reaction was used to establish the initial conditions of reaction. If a specific product of the expected molecular weight was evident, optimisation was limited to magnesium chloride concentration. Magnesium concentration was titred in 0.5mM steps initially. If the titre results showed a narrow range of optimum magnesium concentration, a fine titre was performed using 0.2 mM increments. Other more problematical reactions such as the PCR of exons 1 and 3 were optimized as indicated with betaine and DMSO additives. Initial PCR reactions were carried out in a Biometra Uno thermocycler using the following parameters: Initial denaturation 3min - 95⁰C, then 35 cycles of: denaturation 30 sec - 95⁰C, annealing 60 sec - 55⁰C, extension, 60 sec - 70⁰C, Using the following 50µl PCR

Table 2.2 Primers used in the heteroduplex analysis reactions

Primers for β -globin DNA (J K Douglas research labs.)

Forward: AGT CAG GGC AGA GCC ATC TA

Reverse: GCC CAG TTT CTA TTG GTC TTC

Primers for Prothrombin gene (Bioline UK Ltd.)

Forward: ATA GCA CTG GGA GCA TTG AAG

Reverse: AGA AGG TCA TTG ATA AGC TTG GAG AG

Primers for PTEN cDNA/PTH2 DNA (Bioline UK Ltd.)

Forward: GCT ATG GGA TTT CCT GCA GA

Reverse: CTC CCT TTT TGT CTC TGG TCC

Primers for Heteroduplex analysis PTGS 1-9 (Bioline UK Ltd.)

Exon 1 forward: ATC AGC TAC CGC CAA GTC CA

Exon1 reverse: TGA CCT AGC AAC CTG ACC AG

Exon 2 forward: CCC CTG TGC AGT TGA AAA TT

Exon 2 reverse: AAC TGT ATC CCC CTG AAG TC

Exon 3 forward: AAA ATC TGT CTT TTG GTT TTT CTT G

Exon 3 reverse: TCT GTG CCA ACA ATG TTT TAC C

Exon 4 forward: GTG TCA CAT TAT AAA GAT TCA GGC

Exon 4 reverse: CCT GAC AAT ATT AAT AGC TTT ATG CA

Exon 5 forward: GCA ACA TTT CTA AAG TTA CCT ACT TG

Exon 5 reverse: AAG AAA CCC AAA ATC TGT TTT CC

Exon 6 forward: GTT GTG ACC TTT GAA TAA ATG GG

Exon 6 reverse: ACA GTG CCA CTG GTC TAT AAT C

Exon 7 forward: GTT TTT GAC AGT TTG ACA GTT AAA GG

Exon7 reverse: ACA CCT GCA GAT CTA ATA GAA AAC A

Exon 8 forward: TGT TTA ACA TAG GTG ACA GAT TTT C

Exon 8 reverse: TTC ATC AGC TGT ACT CCT AGA ATT

Exon 9 forward: AAT TAA TAT GTT CAT CTG CAA AAT GG

Exon 9 reverse: AAA AAG GTC CAT TTT CAG TTT ATT C

mixture: 15 pMole forward primer; 15 pMole reverse primer; 1x PCR buffer (with 1.5mM Fermentas MgCl₂); 1x Fermentas dNTP mix; 2U Fermentas Taq supreme; 1µl DNA extract (Approx 100ng µl⁻¹).

Samples for heteroduplex analysis were amplified using the following optimised 50µl reaction: 15 pMole forward primer; 15 pMole reverse primer; 1x Bioline PCR buffer; 1x Bioline dNTP mix; 2U Bioline Taq polymerase; 2.0 mM Bioline MgCl₂; 1µl DNA template solution (Approx 100ng).

2.3.1 RTPCR

cDNA synthesis was carried out using a Gibco/BRL superscript kit using a random hexamer primer in a 20µl reaction:- 100 pMoles random hexamer primer (Pharmacia); 10µg total RNA; 4µl 5x First Strand Buffer; 2µl 0.1M DTT; 1.0µl dNTP mix (Bioline); 20U RNase inhibitor (Amresco); 200U SuperScript RT (Life Technologies UK). The cDNA PCR step was titred for optimum Mg⁺⁺ concentration as for PCR and performed in a 50µl reaction as follows: 15 pMole forward primer, 15 pMole reverse primer, 1x PCR buffer (Bioline), 1x dNTP mix (Bioline), 1.5 mM Mg⁺⁺ (Bioline), 1U Taq polymerase Fermentas, 5µl cDNA mix -using the following programme: Initial denaturation 3min at 95⁰C to allow complete dissociation of target sequences. Then 35 cycles of: denaturation 30 sec - 95⁰C annealing - 60 sec at 55⁰C extension - 60 sec at 70⁰C, followed by Final extension 180 sec 70⁰C

2.3.2 Analysis of PCR products

PCR products were analysed by electrophoresis through a 2% agarose minigel prepared and run in 1 x TBE buffer (0.045M Tris-borate, 0.001M EDTA) at 100V for 60 mins. PCR fragments were visualised by 312nm UV trans-illumination of gels stained initially with 10µg ml⁻¹ ethidium bromide in TBE buffer and

subsequently by the less mutagenic and more sensitive GelStar (FMC Ltd USA)

stain 1:10000

2.4 Heteroduplex (HD) analysis

2.4.1 Sample disease types in the heteroduplex study of PTEN exons 5, 7 and 8

All lymph node samples were non-Hodgkin's lymphoma. Initial bone marrow smear samples for heteroduplex analysis consisted of 3 chronic myelogenous leukaemia, 10 chronic lymphocytic leukaemia, 12 acute myelogenous leukaemia, 2 hairy cell leukaemia, 10 non-Hodgkins lymphoma, 13 myelodysplasia, 13 myeloma and 2 Waldenstrom's macroglobulinaemia. Smears with a tumour load of less than 10% of nucleated cells were excluded. PTEN exons 5,7 and 8 were examined initially.

2.4.2 PTEN exon 5 7 and 8 Heteroduplex Analysis Electrophoresis

Heteroduplex analysis or conformation sensitive gel electrophoresis (Körkkö *et al.* 1998) is designed to detect differences in electrophoretic migration between homo- and heteroduplex sequences. Heteroduplexes are formed when amplicons with one or more point mutations are mixed with wild type sequences. They were first described by Nagamine *et al.* (1989) as PCR artefacts. Heat denaturation, followed by slow annealing allows the formation of heteroduplex DNA.

Heteroduplex control DNA consisted of a heterozygous HbS commercial control sample (Helena Biosciences). This preparation was heterozygous for the point mutation associated with sickle haemoglobin which yielded a heteroduplex sequence when subjected to PCR amplification of the area of the β -globin gene containing the mutated allele. This yielded a 438bp sequence with an A/T allelic site 92 bp from the 5' end.

2.4.2.1 Heteroduplex sample generation

Residual polymerase activity was inhibited in the PCR product with 1mM EDTA (final concentration). 10µl of sample and normal control PCR product were mixed in a 0.5 ml PCR tube. Samples and controls were heated to in a Biometra thermocycler to 95⁰C and cooled in steps of 2.5⁰C at 15 sec intervals to RT.

2.4.2.2 Heteroduplex gel preparation

Gel mix (for six 0.1 x 15 x 20cm or two 0.1 x 50 x 20cm gels) was prepared in a 250ml plastic Universal bottle: 130ml Pure water, 20ml ethylene glycol (Amresco), 30ml formamide (Amresco), Acrylamide/bis acrylamide 19:1 40% 60ml.

Gel solution was filtered through a 0.45 µm filter just before use then degassed under vacuum. One plate was treated with silane substitute to ease disassembly. 500µl 10% ammonium persulphate, (Amresco) and 50µl TEMED (Amresco) was added.

The gel was poured and allowed to polymerize for 1hr at RT.

HD analysis was initially run on a standard 50cm 6% acrylamide gel at 500v for 6 hours in 1x TBE buffer with fan-driven air cooling. Migrant bands were visualized prior to excision for silver staining with 1 mg ml⁻¹ ethidium bromide solution.

2.4.2.3 Silver Staining

The area of gel containing the heteroduplex fragments was excised and stained with silver staining adapted from protocol of Silver Stain Kit, Pharmacia Ltd., according to the following protocol:

Gel was fixed in fixative/stop reagent (10% acetic acid) for 10min with constant mixing. Gel was rinsed three times for 2min in pure water then stained in staining solution (1g l⁻¹ AgNO₃ in pure water with 1.5ml 40% formaldehyde per litre) for

30min with constant mixing. The gel was then rinsed briefly in pure water (10 sec max) and developed in developing solution (30g Na₂CO₃ (Prepared fresh for each staining); 1.5ml 40% Formaldehyde; 200µl of 10mg ml⁻¹ Sodium Thiosulphate in 1l of pure water) until the first bands were visible. Gel was then transferred to fresh developer for 2 min and placed in reagent fixative/stop reagent to stop the staining reaction. Gels were rinsed 2 x 2 mins in water and photographed using a cold white light viewer. The digital image was transferred to a personal computer and using Adobe PhotoShop software, the cyan and magenta channels were deleted to enhance the contrast of the yellow/brown silver stain.

2.4.2.4 Preparation of BAP/Glycerol/TTE Heteroduplex gels

Bis-acrylamide was replaced with Bis acryl piperazine (BAP) in 0.5x Tris-Taurine EDTA (TTE) buffer at 19:1 ratio of acrylamide and bis-acrylamide using a 10% gel as specified by Ganguly and Prockop (1995). TTE Glycerol Tolerant Buffer (20X) is a concentrated Tris-Taurine-EDTA buffer solution prepared in distilled/deionised water.

TTE (20X) eliminates the band distortion associated with DNA samples in glycerol run with borate containing buffers. With TTE Buffer (20X), DNA/glycerol samples can be used without diluting the samples (Product instruction sheet, Geneflow Ltd, UK).

2.4.2.5 Use of PagePlus Heteroduplex gels

A commercial poly-acrylamide preparation with a modified cross-linking agent of unknown formulation (10% PagePlus, Amresco Inc, USA) was used in place of acrylamide/BAP in an attempt to improve resolution and prevent diffusion.

Running conditions of 600V for 20 hours with fan-assisted cooling at room temp provided optimum separation and resolution of HD bands.

2.4.2.5.1 PagePlus Gel preparation

Gel mix (for six 0.1 x 15 x 20cm or two 0.1 x 50 x 20cm gels) was prepared by combining: 180ml Pure water, 60 ml 40% Page-plus stock solution, Gel solution was filtered and degassed as previously. 500µl 10% ammonium persulphate and 50µl TEMED was added. The gel was poured and allowed to polymerize for 1hr at RT.

2.5 Single Strand Conformation Polymorphism analysis of PTEN exons 1-9

SSCP is designed to detect conformational differences in single stranded species that have been generated by heat denaturation of PCR product followed by rapid cooling. (Ganguly *et al.* 1993). Folding of single stands into a particular conformation is defined by order of bases and is sensitive to single base changes. PCR primers (Table 2.5.1) were redesigned manually as for heteroduplex analysis and checked for self-complementary regions and hairpin loops using a computer programme (PCR Primer, Rozen and Skaletsky,

Table 2.5.1 PCR primers for SSCP analysis

PCR Primers for SSCP analysis (Life technologies, UK) 5'>3'
Exon1forward: AGT CCA GAG CCA TTT CCA TC
Exon1 reverse: GAC CTA GCA ACC TGA CCA GG
Exon 2 forward: TTG AAC AAC ACA GAG GGT AGG
Exon 2 reverse: CAT CAC AAA GTA TCT TTT TCT GTG G
Exon 2.1 forward alternate1: CCT GTG CAG TTG AAA ATT CAC
Exon 2.2 forward alternate: 2 TAT CCA TGA CAG TTG ACC CTT G
Exon 2.1 reverse alternate1: ATC ACA AAG TAT CTT TTT CTG TGG C
Exon 3 forward: GGA AAA AGA AAA TCT GTC TTT TGG
Exon 3 reverse: CTT GGC CTT CTT GAC TTA ATC GG
Exon 4 forward: TGG GGG TGA TAA CAG TAT CTA CTT
Exon 4 reverse: CTG GAT GAC TCA TTA TTG TTA TGA CA
Exon 5 forward: TGC AAC ATT TCT AAA GTT ACC TAC TT
Exon 5 reverse: GGA AGA GGA AAG GAA AAA CAT C
Exon 6 forward: AGG GAG GAG AGT TAT TCT GAT ATC C
Exon 6 reverse: CAT CTT GTG AAA CAA CAG TGC C
Exon 7 forward: CAT TAA AAT CGT TTT TGA CAG TTT G
Exon 7 reverse: TAG CTT TTA ATC TGT CCT TAT TTT GG
Exon 8 forward: ATG TCA TTT CAT TTC TTT TTC TTT TC
Exon 8 reverse: TCA CAT ACA TAC AAG TCA CCA ACC
Exon 9 forward: ATG TCC ATC TGC AAA ATG GA
Exon 9 reverse: TGG TAA TCT GAC ACA ATG TCC TA

Whitehead Institute. 2000) to achieve fragment sizes of approx 200-300 base

pairs for each of PTEN exons 1-9.

This technique was employed as a result of the very low number of samples with results indicating the presence of sequence mutations obtained with heteroduplex analysis. All DNA samples screened were from fresh frozen bone marrow samples. 114 samples of various disease classifications (Table 3.1.1, Results chapter) were PCR amplified using the SSCP primers for PTEN exons 1-9. Each exon was amplified as a run of 2 x 55 samples using a microtitre format in a Eppendorf Gradient Multicycler thermocycler using a 50µl reaction under optimised reaction conditions of: 15pmole forward and reverse primer; 1x Immolase buffer (Bioline); 1x dNTP mix; 1U Immolase (Bioline); 2.0mM Mg⁺⁺; approximately 100ng DNA template.

Vertical gel electrophoresis was performed using a Biorad Protean multi cell unit and power supply with an LKB cooling unit and 6 x 20 sample combs. The sample loading buffer consisted of: 800µl formamide; 100µl of 1% Bromophenol blue; 100µl of 1% Xylene cyanol; 2µl 0.5 M EDTA; 1µl 10 M NaOH;

2.5.1 Generation of single stranded complexes

50µl of sample loading buffer was added to the PCR reaction tube and placed in a thermocycler to denature the samples at 95 °C for 5 min. The reaction was snap cooled in a methanol ice bath at -20°C, and then transferred to an ice block until electrophoresis.

5µl of each sample was loaded onto the SSCP gel. Running conditions were: 1 x TBE buffer at 13°C at 12 W constant power for 16hours using a Protean (Biorad UK) vertical electrophoresis system cooled by a refrigerated circulation unit (LKB UK). A lane of double-stranded DNA ladder (PCR ladder Amresco Inc USA) was included to indicate the likely position of the faint staining single strand

complexes.

Different concentrations of Gene-page (1x and 2x manufacturer's recommended concentration) and standard 19:1 bis/acrylamide mixes were tried with and without added glycerol and ethylene glycol at 10% concentration, using exon 7 primers and an NIH 33 (which contained a mutated PTEN allele cell line DNA as positive control). Optimum resolution of single strand complexes was obtained with: 10% Gene-page; 10% ethylene glycol; 1 x Tris-Borate-EDTA buffer pH 8.3.

A range of running temperatures were tried using a refrigerated coolant recirculation unit (LKB UK) varying from 5 °C to 25 °C as recommended by Ganguly *et al.* (1993). The optimized conditions adopted were 12 W constant power for 16h at a plate temperature (measured in the centre of the plate) of 13°C, which corresponded to a coolant temperature of 10 °C. The cooling unit was switched on for 30 mins prior to electrophoresis to prevent overheating at the start of the run. Gels were removed and provisionally stained with 2x GelStar (FMC bio-products USA) and examined under UV at 312nm light to reveal the position of the single strand complexes. The width of gel containing the complexes was excised as a strip of approx 10cm length to ease the silver staining process as though the PagePlus gels were more resilient than standard acrylamide-based gels they were still prone to tearing during the agitation steps of the silver staining process. Gels were silver stained as in section 2.4.2.3 for the heteroduplex gels and dried under vacuum in a gel drier at 50°C overnight to enhance visualization of staining. Dried gels were scanned into a PC running Adobe Photoshop and the cyan and magenta colour channels deleted to enhance the yellow silver stain. Gel images were converted to greyscale, magnified and contrast increased as necessary then images were visually inspected for aberrant band migration.

2.6 PCR product sequencing

2.6.1 PCR product sequencing using the Megabace sequence analyzer

The exon five PCR products that displayed aberrant migration bands were sequenced along with four adjacent samples with normal conformers on either side of the gel.

A Biometra thermocycler was pre-programmed as per cycling times below.

All kit reagents (DYEnamic ET Amersham Pharmacia) were thawed and placed on ice prior to use.

2.6.1.1 Preparation of sequencing reaction.

DNA sequencing was performed using a DYEnamic DNA sequencing kit (Amersham UK). Template DNA (PCR product) was diluted 1:10 in pure water to a volume of 12 μ l.

For each template to be sequenced, the following were combined in a 0.5 ml microcentrifuge tube: DYEnamic ET terminator reagent premix 8 μ l forward Primer (5 μ M) 1 μ l; DNA template 11 μ l; Total volume 20 μ l.

Reagents were mixed thoroughly by gentle pipetting and centrifuged briefly to bring contents to the bottom of the tube. Capped tubes were placed into the pre-programmed thermocycler. Cycling program was started using the following cycling parameters: 95°C for 20s; 50°C for 15s; 60°C.1 min for a total of 30 cycles
After cycling, reactions were centrifuged to collect the reaction mixtures at the bottoms of the tubes .

2.6.1.2 Post-reaction clean-up

2 μ l of 7.5 M Ammonium acetate was added to each reaction tube.

2.5 volumes (55 μ l) of 95% ethanol were added to each reaction and mixed well.

tubes were centrifuged at 13000g in a microcentrifuge for 5 min and the supernatant removed by aspiration then samples were washed in 70% ethanol and left to air dry at RT.

The pellet was re-suspended in 10 µl of loading solution and vortexed vigorously for 10-20 sec to ensure complete re-suspension then briefly centrifuged to collect the sample at the bottom of the tube.

2.6.1.3 Injection and run parameters for the Megabace sequencing system

Samples were loaded into the Megabace capillary system using run parameters of 3 kV for 40 s with run conditions of 100 min at 9 kV. After completion of the sequencing run the electropherogram was downloaded into a Macintosh computer and the automated base calling checked for accuracy. The published DNA sequence for each exon was checked against the sample sequence: (<http://www.ncbi.nlm.nih.gov/entrez/viewer.fcgi?val=51467897&from=8371711&to=8474918&view=gbwithparts>) to identify possible point mutations, small deletions or additions.

2.7 Western blotting of proteins by enhanced chemiluminescence.

The lack of evident sequence mutation in the samples screened by both HD and SSCP ruled out small-scale deletions and point mutations in the PTEN gene, but protein expression could be reduced or abolished by other mechanisms such as large scale deletions and mutations, or by epigenetic mechanisms such as methylation of promoter regions. These mechanisms would not be detected by the PCR-based methods used for the PTEN exons studied. Therefore, western blotting performed to establish whether PTEN protein was being expressed in the leukaemic cell samples studied.

2.7.1 Protein purification for western blotting from bone marrow samples

Protein purification/white blood cell lysis buffer: 5ml glycerol (Sigma UK), 0.5g sodium dodecyl sulphate (SDS) (Sigma UK), 0.5g dithiothreitol(Sigma UK), 5ml 1MNaF (Sigma UK), 0.5ml 2m $\text{Na}_4\text{P}_2\text{O}_7$ (Sigma UK), 0.05ml 1M Na_3VO_4 (Sigma UK), 0.5ml PMSF(Sigma UK), 300UI Sigma protease inhibitor cocktail(Sigma UK), 3.125ml 1M TRIS HCl buffer pH6.8 (Sigma UK), sterile water to 50ml.

The red cell lysis buffer consisted of: 9g ammonium chloride, 100 ml 10x tris EDTA pH 7.2, sterile water to 1l.

The samples consisted of approximately 1ml of fresh and frozen bone marrow samples anticoagulated with Tri-potassium EDTA in Starstedt blood collection tubes.

The sample was centrifuged at 3000g for 10 mins. The Buffy layer (approx. 0.5ml) was added to a 2ml microcentrifuge tube with 1.5ml red cell lysis buffer and mixed gently, incubated at RT for 5 mins then centrifuged at 12000g for 1 min in a Sanyo microcentaur centrifuge. The supernatant was removed into 2% Virkon solution. A further 1.5ml of RBC lysis solution was added and the process repeated. 150 μ l of protein purification lysis buffer was added on ice.

The cell lysates were transferred to sterile 1.5 ml Eppendorf tubes and incubated on ice for 30 minutes to allow complete lysis of the cells. The lysates were cleared of insoluble material by centrifugation for 10 mins at 12,000g at 4°C and the supernatant transferred to clean tubes on ice.

2.7.2 Bradford assay for determination of protein concentration.

Protein concentration was determined to ensure uniform application of sample to eletrophoresis gels. Protein concentration in each sample was determined using the Bradford Assay (Friedenauer & Berlet, 1989). This method quantitates the

amount of protein in a sample by the proportional binding of Coomassie blue dye to the protein, which can be measured at an absorbance of 595nm.

Each protein sample was diluted 1:200 in sterile water. 500µl protein dilution was added to 500µl Bradford reagent (Sigma) and incubated at room temp for 5 min. Absorbance was read at 595nm. Protein concentration was interpolated from an albumin standard curve from 0-10 µg ml⁻¹

2.7.3 SDS Protein gel electrophoresis

SDS-polyacrylamide gels were prepared based on the Laemmli system of protein separation (Laemmli, 1970) using an 8cm BioRad miniprotein II vertical electrophoresis system. Proteins separated by SDS electrophoresis are denatured and differences in native charge are abolished by the presence of SDS. Electrophoresis of proteins is then based on molecular weight only. The separated proteins are then transferred by electro-blotting to a PVDF membrane for detection by specific antibodies.

Buffers used were: R Buffer - 1.5M Tris/HCl pH 8.8; S Buffer - 0.5M Tris/HCl pH 6.8; 10x Running Buffer- 0.25M Tris/HCl, 2M glycine, 1% SDS(w/v) pH 8.3.

8% Resolving Gel mix (2x minigels of 0.75mm thickness) consisted of: 3.0ml R-Buffer; 1.6ml 19:1 acrylamide/bis-acrylamide (Amresco); 3.2ml deionised water; 80 µl 10% SDS.

The gel solution was de-gassed under vacuum for 2 mins before polymerization was initiated by adding 100 µl 10% Ammonium persulphate solution and 40µl TEMED

Stacking gel consisted of: 1.25 ml S-Buffer; 0.5 ml 40% bis/Acrylamide 19:1; 3.1ml H₂O; 20 µl 10% SDS. The gel solution was de-gassed under vacuum for 2

mins before polymerization as previously described for the resolving gel.

Biorad Protean glass plates were cleaned with 1M HCl then ethanol and assembled according to the manufacturer's instruction. The resolving gel was prepared in the proportions shown (8% for PTEN), and overlaid with ethanol. After 1 hour, the ethanol was poured off and the gel surface washed three times with water. The stacking gel was prepared and poured over the resolving gel. Ten-well combs were inserted and left for 30 mins. The combs were removed and the wells washed thoroughly with 1x running buffer. The gels were inserted into the tank and filled with buffer.

The protein samples were prepared by mixing 10µg of each sample with 1µl of loading buffer and boiling at 100°C for 1 minute on a thermocycler. A coloured molecular weight (C1992 Sigma UK) marker was also boiled at 100°C for 1 minute, according to the manufacturer's instructions.

The entire 11µl volume of each sample was loaded into the wells of the SDS-PAGE gel using gel loading pipette tips, ensuring that the samples sank to the bottom of each well. To one well of each gel was added 4ul of boiled colour marker and 0.5ul of a biotinylated molecular weight marker (b2787 Sigma). Gels were connected to a power supply and electrophoresed at 120 V for 90 minutes.

2.7.4 Blotting to PVDF membrane

Transfer buffer (pH8.3) consisted of: 25mM Towbin Buffer- 3.0 g Tris base; 14.4g glycine; 200 ml methanol -20°C. PVDF membrane (immunoblot Biorad UK) was wetted in methanol, then covered with Towbin Buffer. The polyacrylamide gels were separated from plates and covered with Towbin buffer. PVDF, gels, fibre pads and blotting paper were soaked in buffer for 10 min.

The gel sandwich was assembled with blotting paper and pads in cassette and

inserted into the tank. Buffer, an ice pack and magnetic bar was added. The run conditions were 150v for 1 hour with constant stirring. After the run sandwiches were removed and PVDF placed on a towel to air dry. The gel was stained with Coomassie blue to detect residual protein and thus assess the efficiency of protein transfer process

2.7.5 Western blot for PTEN/ β -Actin

Buffers used in the Western Blot were: 1x Phosphate buffered saline (PBS); PBST- PBS with 0.1% Tween 20 (Amresco USA); Blocking buffer- 3% marvel dried milk powder in PBST.

Developing solutions used were: Anti PTEN mouse monoclonal clone a2b1 (Becton Dickinson Bio-sciences UK); Vector elite anti mouse IgG detection kit; Anti mouse kit (Vector labs UK); Lumiglo ECL kit (Amersham UK); anti β -actin mouse monoclonal clone ac5 (Sigma UK).

PVDF membrane from electrophoresis step was pre-wetted with methanol and washed three times with PBST for 5mins each. The colour marker was used to orientate the membrane so that the proteins faced upwards and to indicate the portion of the membrane to be cropped prior to processing. The membrane was placed in blocking solution for 1 hour then washed 3 times in PBST, then incubated with anti-PTEN (1:300) or anti-actin (1:20,000) in PBST, for 90 mins. Membrane was washed 3 times then Incubate with anti-mouse antibody, 1:800 for 40mins then Vector ABC complex for 30 mins (prepared 30 mins before use). After a further 3 washes, ECL reagent was added and agitated for 1 min. Excess was drained and PVDF wrapped in Saran wrap.

The membrane was exposed to photographic x-ray film for 1 min and the film developed.

2.8.1 Immunocytochemistry

Bone marrow smears were subjected to immunostaining using a Shandon Sequence staining system and a double dilution titre of primary antibody in TBS. Positive control without primary antibody was included as a reagent control. The titre was started at the maximum concentration recommended by the manufacturer. The degree of immunostaining staining, characterised by a brown DAB precipitate, was assessed microscopically. The diaminobenzidine hydrochloride technique was chosen because DAB produces a precipitate that is very stable, not subject to diffusion away from the site of enzyme activity, and is insoluble in organic solvents which permits the use of non-aqueous mounting media. This media allows clearer resolution of the magnified image in microscopy.

The streptavidin/biotin complex (StrepABC) immunostaining was carried out using the following protocol:

Slides were fixed in ice-cold methanol/acetone for 5 min and then immersed in 0.5% hydrogen peroxide in methanol for ten minutes to inhibit endogenous peroxidase activity, then washed in running tap water. Slides were loaded onto a Shandon Sequenza staining rack and wash with Tris Buffered Saline (TBS) 100 mM Tris·Cl, pH 7.5;

0.9% NaCl) for five min. All slides were incubated with normal goat serum (1:5 with TBS) for 20 min to block non specific binding of primary antibodies then treated with 1:300 dilution of PTEN primary antibody (Becton Dickinson UK) for 60 min at room temp. Slides were washed in TBS for five min then incubated in Biogenex Streptavidin Multilink (Biomen Ltd., UK) diluted 1:60 in TBS for 30 min. Slides were washed in TBS for 5 min then incubated in "Biogenex"

StrepABC/horse radish peroxidase label diluted 1:60 in TBS for 30 min. Slides

were washed in PBS for 5 min then incubated in Diamino benzidine DAB solution (Sigma UK) for 5 min then washed in running tap water before counterstaining with Harris's Haematoxylin (Merck UK) for 10 seconds. The blue counterstain was enhanced by immersion for 1 min in tap water. Slides were then dehydrated through consecutive changes of ethanol (BDH, UK) (70→100%), cleared in xylene (BDH, UK) and mounted in non aqueous mounting media (Sigma UK). (Internal Standard Operating Procedure, Dept of Histopathology, Arrowe Park Hospital.1998 (Appendix))

2.8.2 Immunofluorescence

Bone marrow smear slides (Haematology Department, Arrowe Park Hospital) used for immunofluorescence were methanol-fixed slides selected at less than one month old. Slides were rinsed in PBS for 2x2 min then incubated in normal goat serum for 30min. Slides were incubated in anti PTEN (1:100) Primary Antibody: for 1 hour at room temperature then rinsed in PBS for Rinse 3x2 min. Slides were incubated sections in biotinylated secondary antibody (1:500, Vector Labs UK) for 30 minutes at room temperature. Slides were rinsed in PBS for 3x2 min Slides were incubated in FITC-Avidin D (1:500, Vector Labs UK) in PBS for 30 minutes at room temperature in a black box. Slides were rinsed in PBS for 3x2 min and counterstained with DAPI (Sigma) for 20-30 minutes at room temperature. Slides were rinsed in PBS for 3x2 min then mounted with Vector aqueous anti-fade fluorescent mounting medium and examined under UV using an Olympus epi-fluorescence microscope.

Results

3.1 Extraction of nucleic acids from fresh and archived tissue3.1.1 Extraction of Nucleic acid from fresh cells

The DNA sodium perchlorate/chloroform extraction method provided high yields of high purity DNA from all 114 SSCP samples tested with no failed extractions (Table 3.1.1). $>50 \mu\text{g ml}^{-1}$ concentrations of extracted DNA could be achieved from lower yields by adding smaller quantities (approx 50ul) of TE buffer to the precipitated DNA pellet during reconstitution. Occasional samples of very cellular nature such as CML and CLL produced very viscous sodium perchlorate homogenates, and this is reflected by the skewed correlation of DNA extract concentration and DNA purity (corr. coef.= -0.36) (Chart 3.1.1).

This method replaces phenol with 5M sodium perchlorate solution and avoids the use of the toxic and corrosive chemical used in conventional nucleic acid extraction methods. The concentrated salt solution acts as a chaotropic agent and causes rupture of the cell and nuclear membranes and the dissociation of nucleic acid/protein complexes. The resulting cellular homogenate was mixed with chloroform, which disrupts protein tertiary structure and exposes hydrophobic groups that reduce the protein solubility and cause protein precipitation. Lipid-based cell components dissolve in the organic phase and precipitated protein can be removed by centrifugation. DNA was precipitated from the resulting aqueous phase by the addition of isopropanol. The alcohol dehydrates the DNA molecule. The solubility of DNA depends on the highly soluble, polar deoxy-ribose group and the highly soluble, negatively charged phosphate group. DNA is insoluble in alcohol and partial exclusion of water by alcohol results in DNA precipitation. The purine and pyrimidine base groups in DNA are hydrophobic and the presence of 30% water in the ethanol wash prevents relaxation of torsion pressure in the DNA

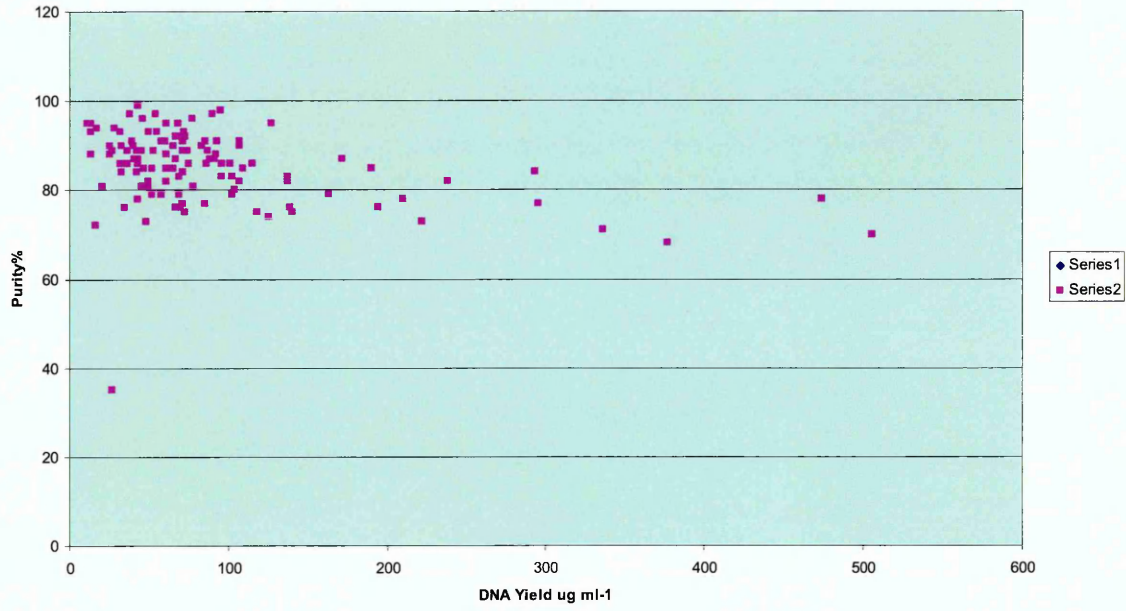
Table 3.1.1 Sample disease types, % tumour cells, DNA concentration and DNA purity of samples analysed in the SSCP reactions

Samp. No.	Leukaemia/ lymphoma type	% tumour cells	DNA concentration, $\mu\text{g ml}^{-1}$	Purity of DNA %
1	CML	70	104	80
2	CML	>80	336	71
3	CML	>80	127	95
4	CML	80	101	86
5	CML	90	71	89
6	CML	>80	92	88
7	CML	>80	72	93
8	CML	80	107	82
9	CMLT	100	194	76
10	CML	75	140	75
11	CML	75	107	91
12	CLL	100	91	87
13	CLL	100	73	92
14	CLL	100	107	90
15	CLL	82	115	86
16	CLL	75	139	76
17	CLL	100	61	95
18	CLL	57	377	68
19	CLL	73	102	83
20	CLL	64	74	89
21	CLL	83	67	92
22	CLL	95	46	96
23	CLL	84	40	90
24	CLL	87	293	84
25	CLL	71	83	90
26	CLL	77	222	73
27	CLL	81	125	74
28	CLL	71	88	87
29	AML M1	100	61	82
30	AML M1	30	28	94
31	AML M1	100	137	82
32	AML M0	90	190	85
33	AML M0	100	25	90
34	AML M0	90	39	91
35	AML M2	70	295	77
36	AML M2	70	32	93
37	AML M3a	100	118	75
38	AML4	30	238	82
39	AML4	45	210	78
40	AML M1	75	109	85
41	AML M1	87	474	78
42	AML M1	81	506	70
43	AML M1	88	36	86
45	AML M1	96	67	76
46	AML M1	69	43	86
47	AML M1	82	69	79
48	HCL	20	43	87
49	HCL	60	27	35
50	NHL	22	35	76
51	NHL LG	51	43	99
52	NHL LG	30	43	78
53	NHL LG	52	25	88
54	NHL LG	11	13	93
55	NHL LG	60	60	91
56	NHL LG	18	53	89
57	NHL LG	45	13	95
58	NHL LG	22	16	72
59	NHL LG	18	96	86
60	NHL LG	31	45	89
61	NHL LG	29	102	79
62	NHL LG	11	45	81
63	NHL LG	22	42	84
64	NHL LG	14	21	81
65	NHL LG	28	70	76
66	NHL LG	24	137	83
67	NHL LG	17	68	92
68	NHL LG	15	33	90
69	NHL LG	25	38	97
70	NHL HG	63	50	82
71	NHL HG	58	68	95
72	NHL HG	43	67	87
73	NHL HG	53	71	91
74	NHL HG	47	87	89
75	NHL HG	50	78	81
76	NHL HG	45	58	79
77	NHL HG	68	11	95
78	RARS	20	36	89
79	RARS	10	61	85
80	RARS	10	85	77
81	RARS	10	65	85
82	RARS	15	52	85
83	RARS	10	52	79
84	RARS	13	73	75
85	RARS	15	17	94
86	RAEB	20	95	98
87	RAEB	29	86	86
88	RAEB	22	65	90
89	RAEB	23	41	87
90	RAEB	18	50	81
91	RAEBT	58	90	97
92	RAEBT	16	55	93
94	RAEBT	23	69	83
94	RAEBT	20	61	88
95	RAEBT	20	77	96
96	RAEBT	33	75	86
97	MYELOMA	31	93	91
98	MYELOMA	39	71	77
99	MYELOMA	28	33	86
100	MYELOMA	23	163	79
101	MYELOMA	>30	48	73
102	MYELOMA	10	13	88
103	MYELOMA	23	27	89
104	MYELOMA	26	85	91
105	MYELOMA	18	54	97
106	MYELOMA	unk	71	84
107	MYELOMA	10	42	89
108	MYELOMA	20	33	84
109	MYELOMA	20	96	83
110	MYELOMA	19	58	91
111	MYELOMA	31	171	87
112	MYELOMA	26	32	86
113	WM	45	50	93
114	WM	64	47	85

Table 3.1.1 shows the disease type of leukaemia/lymphoma; tumour cells as a percentage of the total sample nucleated cells, the concentration of DNA extract established by spectrophotometry at 260nm; the purity of DNA extract using the ratio of absorbance at 260nm and 280nm

Graph 3.1.1

Correlation of yield of DNA in $\mu\text{g ml}^{-1}$ with percentage purity of DNA extract



molecule and prohibits the formation of alternative helical conformations which is essential for binding of DNA binding proteins. The method was used for all fresh bone marrow DNA extractions and examples of amplified product are shown in the PTEN heteroduplex analysis and SSCP analysis sections. (Calladine et al 2004).

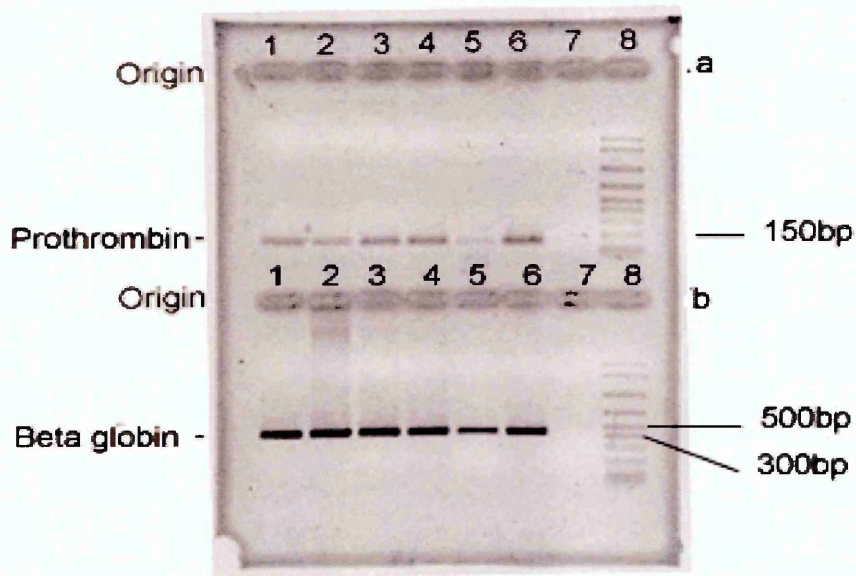
3.1.2 Extraction of DNA from fixed unstained bone marrow tissue

Amplification of DNA by PCR reaction using DNA extracted from archived, methanol-fixed, unstained DNA smears used a Proteinase K based method. In this method, DNA was extracted by the action of Proteinase on membrane proteins and nuclear DNA binding proteins. The use of organic solvents was avoided though digested protein was not removed prior to precipitation with alcohol and the purity of the DNA extract was reduced in comparison to the method used for fresh cells. Varying levels of amplification products were obtained from samples (Fig 3.1.2) but with lower levels of staining in the smaller prothrombin gene product. The prothrombin gene sequence amplified was relatively gc rich compared to the β -globin sequence and may be amplified less efficiently. The prothrombin primers also have miss-matches two bases from the 3' end of the forward primer which may reduce the efficiency of primer binding. Also, ethidium bromide staining occurs in proportion to the size of the DNA product (Sambrooke et al 1988). The lower levels of staining seen in the prothrombin gene product may be a reflection of its smaller size (149bp) compared to the β -globin product.

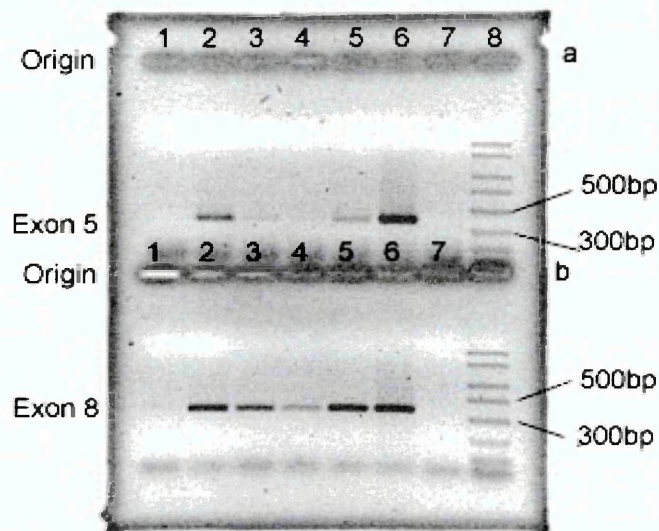
3.1.3 Extraction of DNA from fixed, stained bone marrow smears and comparison with unstained smears.

Fig 3.1.2 Amplified DNA from fixed stained and unstained smears

A



B



A Amplified DNA from random normal, fixed, unstained bone marrow smears. Acceptable levels of amplification are present in all samples. Top lanes (a) 147 bp human Prothrombin PCR product. Bottom lanes (b) 438bp human β globin gene PCR product. Lanes 1-6: (a and b) random normal bone marrow smears. Lane 7: Blank. Lane 8: 100bp Ladder (8cm Agarose minigel, ethidium bromide stain, negative image)

B Amplified DNA from PTEN gene exon 5 and 8 using heteroduplex primers and DNA extracted from random normal fixed, stained bone marrow smears. Amplification was less successful compared to unstained smears using the PTEN primers. In this reaction, exon 8 primers show higher levels of amplification than exon 5 primers. Top lanes (a) - PTEN exon 5, bottom lanes (b) - PTEN exon 8. Lanes 1-6: (a and b) random normal bone marrow smears. Lane 7: Blank. Lane 8: 100bp Ladder (8cm Agarose minigel, ethidium bromide stain, negative image)

Amplification of DNA by PCR reaction using DNA extracted from archived, methanol-fixed, Romanowsky-stained bone marrow smears by proteinase K based extraction from total cell content of the slide (Fig 3.1.2) shows varying levels of specific product amplification with no product evident in lane 1. The gel shows lower levels of product compared to unstained smear DNA extraction. Exon 8 products appear brighter than exon 5 despite similar fragment sizes. Levels of amplification are reduced compared to unstained smear extracts.

3.1.4 Extraction of DNA from fixed, Romanowsky stained bone marrow smears by micro dissection

DNA was extracted and amplified by PCR using DNA extracted from archived, methanol-fixed, Romanowsky-stained bone marrow smears by an improvised micro-dissection procedure using an ultra fine, hooked needle and inversion microscope.

The gel (Fig 3.1.3 A) shows the β -globin product with varying levels of amplification and no amplification at all in lane 1 and 5. Products are specific but amplification levels were poor and not considered sufficient for heteroduplex analysis which required high levels of amplified product to offset band diffusion during the extended electrophoresis run.

3.1.5 Extraction of DNA from formalin-fixed wax-embedded tissue sections.

Amplification of β -globin DNA by PCR reaction using DNA extracted from archived formalin-fixed wax-embedded tissue sections (FFPE) was performed using three methods of DNA extraction: deparaffinisation with xylene and DNA extraction using organic solvents; deparaffinisation using xylene followed by proteinase K treatment; heat-based deparaffinisation followed by proteinase K

treatment . The gel in fig 3.1.3 B shows varying levels of specific amplification with very little product in lane 2 and non in lane 5 but acceptable levels of specific amplification in lanes 1, 3, 4 and 6. A characteristic smear of higher molecular weight DNA was evident in all PCR reactions using FFPE and amplification levels were lower than fresh cells. Lehmann et al (2001) have reported that tissue storage in formaldehyde solution for more than one week might damage nucleic acids, because fixation in formaldehyde induces extensive cross-linking of tissue proteins, and nucleic acid fragmentation. The smear of background DNA may represent DNA subject to the high rate of fragmentation

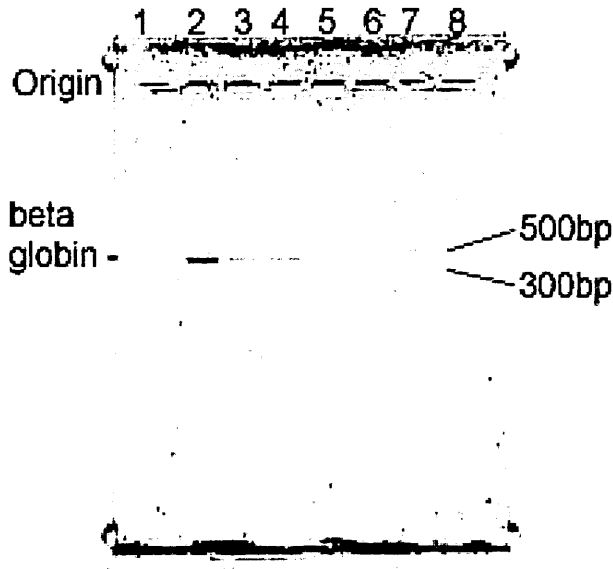
Other extractions showed similar levels of amplified product (not shown) with similar rates of successful amplification. The PCR products obtained with the heat-based de-waxing technique were amplified as successfully as xylene-treated sections. The use of proteinase k gave similar levels of amplification to extraction with phenol and chloroform. De-waxing by boiling for 15 min followed by proteinase K digestion overnight was the method used for subsequent DNA extractions from FFPE. The FFPE subjected to boiling only has a characteristic odour of formaldehyde after processing which was not present in the other methods. This could explain the lack of amplification if the thermostable polymerase protein was denatured by formaldehyde as indicated by Lehmann *et al.* (2001). Fig 3.1.4 shows a titre of DNA template levels from boiling extraction and demonstrates the inhibition.

The level of amplification was poor throughout the titre but decreases with increasing template, which suggests an inhibition of the reaction. Interestingly, primer dimer formation present in the reaction decreases in proportion to the added template and at the same rate as the specific product which further suggests the presence of an inhibitory factor such as formaldehyde.

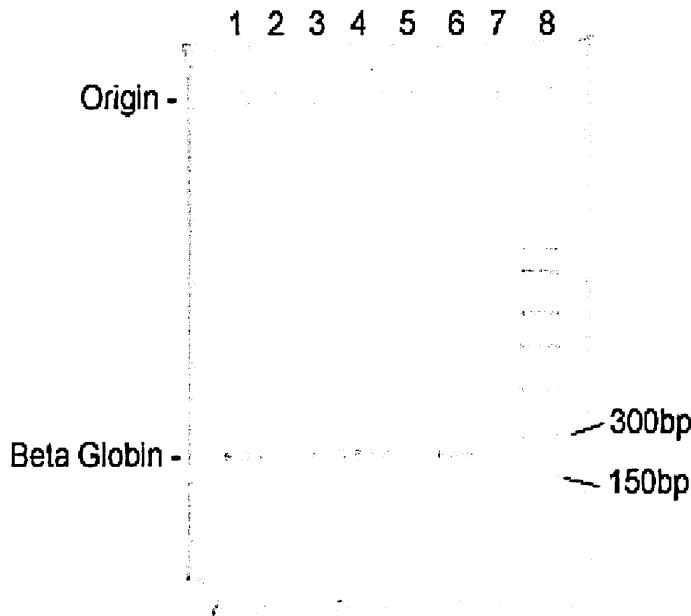
Fig 3.1.3 PCR amplification of DNA extracted from fixed, stained bone marrow

smears and FFPE tissue

A -



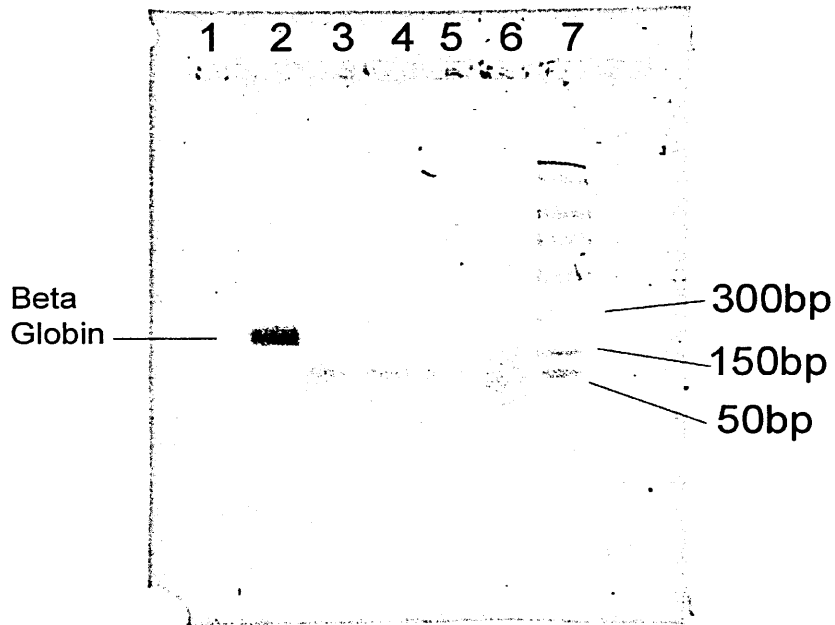
B -



A
PCR amplification of 438bp beta globin gene DNA extracted from fixed, stained bone marrow smears by micro dissection. Amplification was variable and only reaches acceptable level in lane 2. Two of six reactions have failed (lanes 1 and 5), two (lanes 3 and 4) show low level amplification.
Lane 1-5: Random normal bone marrow Lane 6: blank. Lane 7: DNA ladder (8cm Agarose minigel, ethidium bromide stain, negative image).

B
PCR amplification of 219bp β globin gene DNA extracted from wax embedded tissue sections (pooled adeno carcinoma samples)
Amplification of 219bp product was adequate for heteroduplex analysis in four out of six samples. A background smear of DNA was evident in all successfully amplified samples. Extraction with proteinase K only gave similar levels of amplification to the organic solvent extracts in lanes 4, 5 and 6. boiling without proteinase K treatment was unsuccessful with or without organic solvent DNA extraction
Lane 1 – boil plus proteinase K, Lane 2 - 15 minute boil only, Lane 3 – xylene dewax + Proteinase K, Lane 4, 5 and 6 as per lanes 1,2 and 3 but with phenol chloroform extraction. Lane 7 – blank control. Lane 8 150bp ladder. (8cm Agarose minigel, ethidium bromide stain, negative image)

Fig 3.1.4 Amplification of 219bp β -globin gene DNA extracted from wax embedded tissue sections – titre of template DNA



PCR amplification of 219bp beta globin gene DNA extracted from wax embedded tissue sections (pancreas) by boiling technique – a titre of template DNA.
The gel shows the inhibitory effect of increasing quantities of DNA template in the PCR reaction. Lane 2 was the product amplified from the commercial control DNA used as the heteroduplex control.
Lane 1- blank; lane2 – control blood DNA extract; lane 3-6 2.5, 5, 7.5, 10ul of DNA template respectively; lane 7 – ladder

3.1.6 Extraction of RNA and RTPCR of PTEN in cell lines

This reaction was designed to demonstrate RTPCR was possible using the PTEN cDNA primers and thus demonstrate the production of mRNA in the HL60, JURKAT, K562, K620, THP1 and CV605 cell lines studied. Total cellular RNA was extracted by an acidic phenol chloroform method then precipitated with alcohol. cDNA synthesis was carried out using a random hexamer primer and SuperScript reverse transcriptase. The PCR stage used primers that generated a 397bp product. The gel in fig 3.1.6 shows successful amplification of all cell line cDNA. The K562 cell sample was had been stored at -20°C for several months but still showed an amplified product but with reduced band intensity compared to other cell lines. HL60 and CV605 show highest levels of amplification. K562, K620 and THP1 show lower levels of product. There was faint staining in Jurkat PCR reaction (lane 2) despite the fact that Jurkat cells contain two mutated PTEN alleles in exon 7 (a 2bp deletion plus a 9 bp insertion and a 39 bp insertion) that introduce premature stop codons which should abolish RTPCR product (Georgescu *et al.* 1999). This could represent amplification of PTHS sequences or PTEN cDNA. The possibility of carry over whilst loading the gel was ruled out by the lack of product in the blank lane and by similar results obtained with subsequent reactions. Contamination with full length mRNA was the most likely explanation. This could have been introduced at any part of the procedure between cell culture and RTPCR amplification. The reproducibility of the faint signal in subsequent extracts suggests the initial cell culture was contaminated with a small population of cells expressing full-length mRNA. No distinction was possible here between PCR products of PTEN cDNA and PTHS genomic DNA.

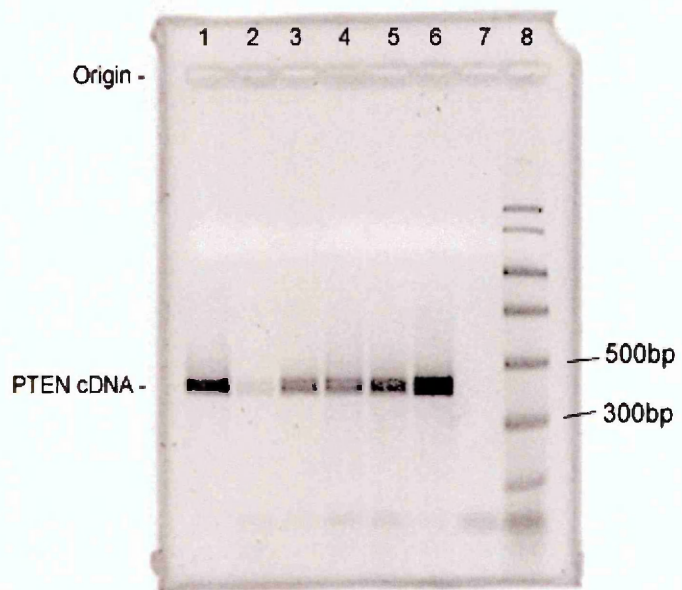
Table 3.1.6

Nucleic acid concentration of cell line total RNA extractions

Cell line	Leukaemia Cell type	Cell count $\times 10^7 \text{ ml}^{-1}$	Nucleic acid concentration $\mu\text{g ml}^{-1}$
CV605	AML M2	8.1	162
K620	Plasma cell	0.5	82
THP1	Acute Monocytic	0.8	265
Jurkat	Acute lymphoblastic	2.5	137
HL60	AML M2	1.2	808
K562	CML blast phase	--	--

Table shows high levels of nucleic acid extracted from each cell line. Quantity of nucleic acid extracted is not proportional to cell count with 8.1×10^7 CV605 cells yielding 162 μg whilst 1.2×10^7 HL60 cells yielded 808 μg . RNA of the K562 cells had been extracted previously by the same method

Fig 3.1.6 RTPCR amplification of PTEN mRNA in cell lines



Gel shows 397 bp RTPCR product PTEN gene from cultured cells. Amplification was achieved for all cell lines with very weak amplification in the Jurkat cells

Lanes 1-8: HL60, JURKAT, K562, K620, THP1, CV605, RTPCR Blank, 150bp Ladder respectively. (8cm Agarose minigel, ethidium bromide stain, negative image)

3.2 Optimisation of PCR reactions

3.2.1 Titre of magnesium concentration using primer pairs PTGS 5 and PTGS 8.

These titres were designed to optimise reaction magnesium concentration for the problematic exon 5 and 8 (PTGS 5 and 8 primers) for heteroduplex analysis.

These primers tended to give lower levels of amplification than other exon primers. The magnesium concentration titre was performed over the range of 0.5 to 3.0 mM magnesium chloride in 0.5 mM increments (fig 3.2.1).

The exon 5 reaction shows increasing product levels from 1.0mM Mg^{++} with a maximum at 2.5mM with a slight decrease in product levels at 3mM. Non-specific products are evident at 1.0mM but decrease with increasing Mg^{++} concentration.

2mM Mg^{++} was selected for use in subsequent reactions using the exon 5 primers as amplification at this level provided specific amplification with acceptable product levels for heteroduplex analysis (Fig 3.2.1A).

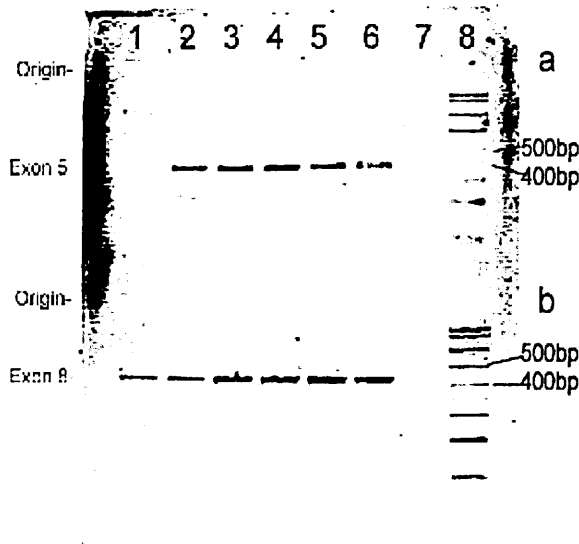
The exon 8 reaction shows increasing levels of product from 0.5mM Mg^{++} to a maximum at 2.5mM with a slight decrease in product levels at 3mM. Non-specific products were only evident at 0.5mM Mg^{++} . 2mM magnesium was also chosen for subsequent exon 8 reactions for heteroduplex analysis. The exon 2 magnesium titre fails to amplify a specific product but produces two non-specific products at approximately 600bp and 1400bp (Fig 3.2.1B)

3.2.2 Optimisation of Magnesium concentration in RTPCR reaction

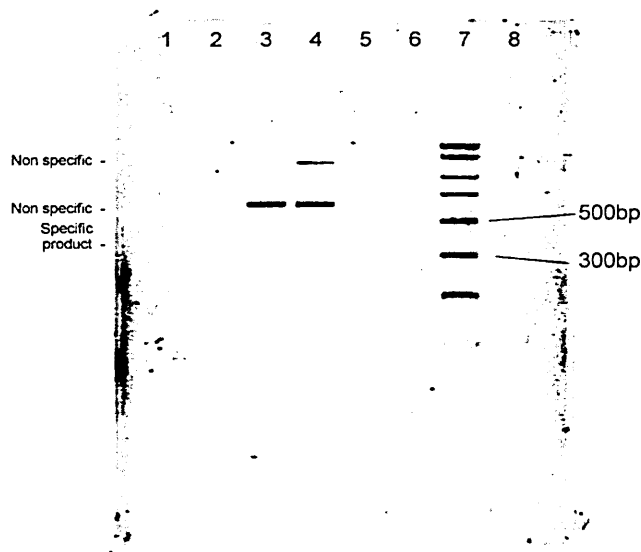
The RTPCR reaction had shown a sudden onset of successful reaction magnesium concentration between 1 and 1.5 mM. A further reaction titre was performed to assess optimum magnesium concentration for PCR step of RTPCR reaction by using a finer range of magnesium concentrations over the range 0.8-2.0 mM magnesium chloride

Fig 3.2.1 Titre of PCR magnesium concentration for PTEN exons

A



B



A

Titre of PCR magnesium concentration for PTEN exon 5 (a) and 8 (b)

Using PTGS 5 and 8 primers, optimum amplification of maximum product levels and minimum non-specific amplification was achieved at 2mM Mg⁺⁺ for both primer sets

Lane 1-6: 0.5, 1.0, 1.5, 2.0, 2.5, 3.0, mM Mg⁺⁺ respectively, Lane 7 blank, lane 8: 100bp ladder. (8cm Agarose minigel, ethidium bromide stain, negative image)

B

Titre of PCR magnesium concentration for PTEN alternative exon2 primer pair (PTGS2.1)

Gel shows PCR Mg⁺⁺ titre using alternative exon 2 primers. Expected product was missing from the 400bp region. Two non-specific products are present at approx 600 and 1400bp

Lane 1-6: 0.5, 1.0, 1.5, 2.0, 2.5, 3.0, mM Mg⁺⁺ respectively, Lane 7 100bp ladder, lane 8 blank. (8cm agarose minigel, ethidium bromide stain, negative image)

Amplification product was evident at 1.2mM magnesium chloride and band intensity increases with concentration to a maximum at 2mM Mg^{++} and this concentration was used for subsequent reactions (Fig 3.2.2).

No distinction possible here between PCR products of PTEN cDNA and PTHS genomic DNA but the extraction procedure was assumed to be specific for PTEN total RNA. Fig 3.2.4 shows a non specific amplification product approximately 30bp behind the specific product increases with magnesium concentration at same rate as specific product. The non-specific product was not evident on later gels (c.f. Fig 3.2.5).

3.2.3 Titre of dimethylsulphoxide concentration in PCR reaction for PTEN exons 1 and 3 (PTGS1 and 3)

These titres measured the effect of dimethylsulphoxide (DMSO) concentration on the specificity of PCR reaction for the PTEN exon 1 and 3 reactions, which showed non-specific amplification products in the additive free PCR . Titres were performed from 0-10% DMSO in 2% increments.

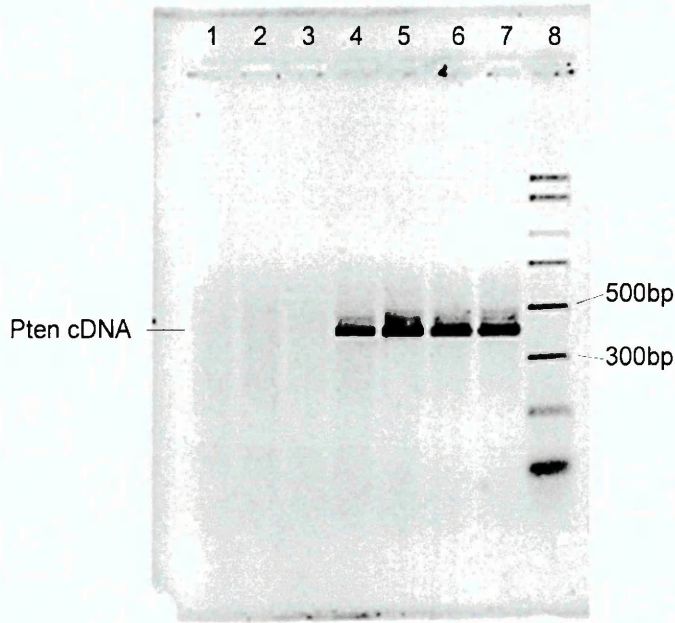
The exon 1 reaction shows product level increases with DMSO concentration up to 4% then falls to zero at 10%. Specificity increases with DMSO concentration up to 10%. Optimum product level and specificity was obtained at 6% and this concentration was used in subsequent reactions.

The exon 3 reaction shows product level decreases with increasing DMSO concentration until no product was visible at 10%. Specificity increases with DMSO concentration. Optimum product level and specificity occurs with no added

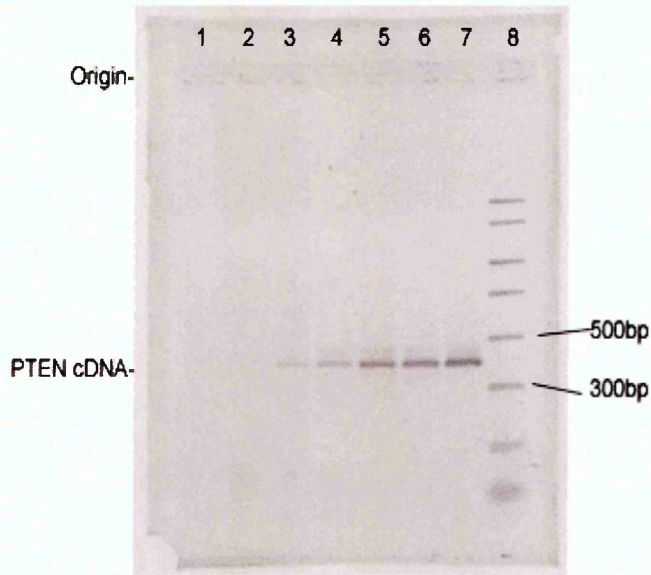
Fig 3.2.2 Coarse titre of reaction magnesium concentration for PTEN cDNA

primers

A



B



A
Coarse titre of reaction magnesium concentration for PTEN cDNA primers.
Amplification product was not evident until 1.5 mM Mg⁺⁺. Product level above this concentration does not vary significantly.
Lane 1-7: 0.0, 0.5, 1.0, 1.5, 2.0, 2.5, 3.0 mM Mg⁺⁺ respectively, lane 8: ladder. (8cm agarose minigel, ethidium bromide stain, negative image)

B
Fine titre of reaction magnesium concentration for PTEN cDNA primers.
Amplification was evident using 1.2 mM Mg⁺⁺ and rises to maximum amplification at 2.0mM.
Lane 1-7: 0.8, 1.0, 1.2, 1.4, 1.6, 1.8, 2.0 mM Mg⁺⁺ respectively, lane 8: ladder. (8cm agarose minigel, ethidium bromide stain, negative image)

DMSO. Amplification was weak compared to the exon 1 reactions. Interestingly, the level of primer-dimer formation evident in the exon 3 reaction also falls with increasing DMSO concentration (Fig 3.2.3).

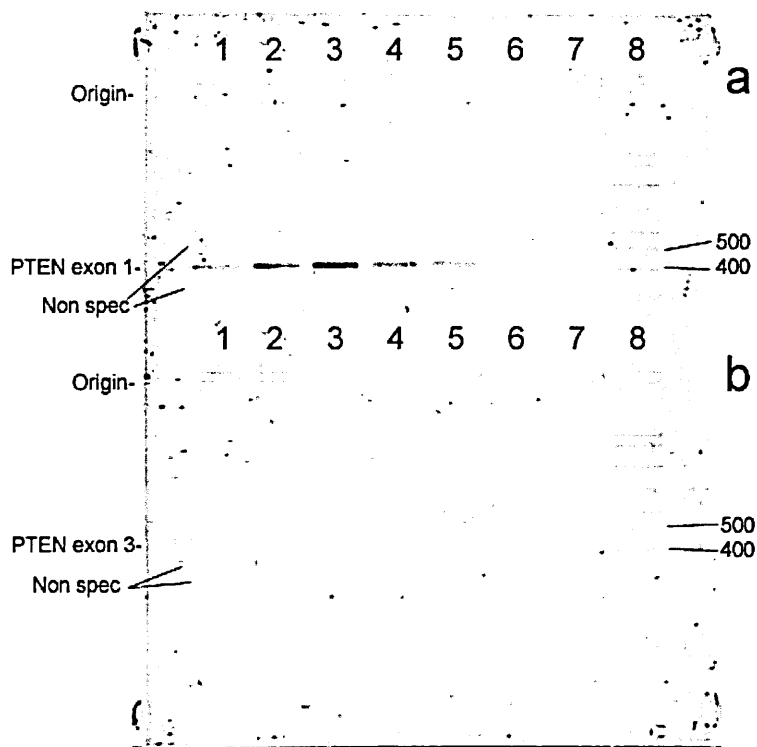
3.2.4 Annealing temperature gradient analysis for heteroduplex exon 2 primer pairs (PTEN genomic sequence (PTGS) 2 and 2.1)

Analysis of the effect of annealing temperature in the PCR reaction using the exon 2 primers which showed poor specificity by performing the reaction over a range of annealing temperatures - plus and minus 5^oC of the suggested annealing temperature of 55^oC. The exon 2 primers showed high levels of non-specific product and appeared to generate different length products in different reaction runs using identical reaction conditions. The analysis of the effect of annealing temperature was performed using an Eppendorf gradient thermocycler which generated a gradient of temperature of 10^oC across the thermocycler block during the annealing stage of PCR.

The gel in Fig 3.2.4 shows a range of products across the temperature gradient. At 51^oC, large amounts of non specific product were produced along with some smaller bp non-specific products. As annealing temperature increases towards the predicted optimum temperature of 55^oC, the quantity of specific product produced decreases and higher bp non-specific products start to appear.

At 56^oC very little specific product was produced and the 1000bp non-specific product starts to accumulate with a maximum yield at 59^oC. Alternative exon 2 primer pairs (PTGS 2.1) showed similar low specificity with very low levels of specific product and high levels of higher bp non-specific products . Optimisation of magnesium ion concentration and use of additives DMSO and betaine in PCR did not increase specificity (not shown).

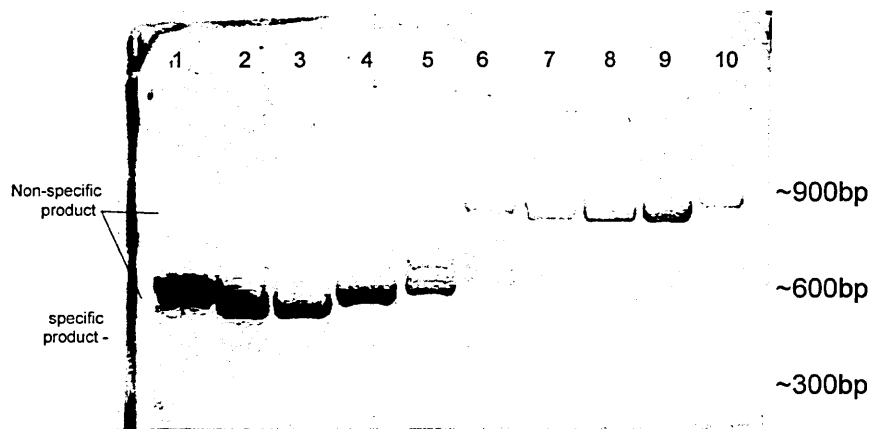
Fig 3.2.3 DMSO titres for PTEN exons 1 and 3



DMSO titres for PTEN exons 1 and 3.

PCR amplified DNA from pooled normal human DNA. For exon 1, maximum product specificity was obtained using 3% DMSO whilst exon 3 shows maximum product with no added DMSO. The non-specific product can be seen for both exons. Primer dimer and non specific amplification decrease with increasing DMSO concentration with both reactions. Lane 1-7: 0%,2%,4%,6%,8%,10%, DMSO respectively. Lane 8 100bp ladder. Exon1 top row (a), exon 3 bottom row (b) (8cm agarose minigel, ethidium bromide stain, negative image)

Fig 3.2.4 Annealing temperature gradient analysis of exon 2 reaction (PTGS2 primers)



Gel shows products produced at annealing temperatures of 51°C, 52°C, 53°C, 54°C, 55°C, 56°C, 57°C, 58°C, 59°C and 60°C in lanes 1-10 respectively. Very low levels of specific product are present at 51-53°C. A single specific product was not obtained at any temperature and there was a change in product sizes obtained at 56°C annealing temperature from a range of products around 600 bp to a single product of around 900 bp (top half of 8cm agarose minigel, ethidium bromide stain, negative image)

3.2.5 RTPCR of cell lines derived from haematological malignancy and differentiation between PTEN cDNA and PTH2 homologous sequences.

RTPCR of leukaemia/lymphoma cell lines CV605, K260, THP1, K562, HL60 and Jurkat was designed to amplify PTEN cDNA and establish that amplification of cDNA was achieved without contamination with genomic DNA from the PTH2 homologous sequence by using digestion with MseI restriction endonuclease (RE).

Fig 3.2.5 shows the 397bp sequence amplified from both sequences. The RTPCR product from cell lines was fully digested into fragments of 143 and 194 bp, with only a faint trace of undigested product (337bp) in lane 2, the CV605 lane which could be product carry over from lane 1.

Lanes 1 and 8 show the PTH2 PCR product amplified from genomic DNA which was only partially digested into a 337bp sequence. Lane 9 shows undigested/full-length PCR product.

All cell lines show similar levels of product except Jurkat cells in (lane7), which shows a very faint amplified product (as previously mentioned, Jurkat cells contain two mutated PTEN alleles in exon 7 - a 2bp deletion plus a 9 bp insertion and a 39 bp insertion - that introduce premature stop codons which should abolish RTPCR product (Georgescu *et al.* 1999)). The presence of faint but fully digested product in the Jurkat lane indicated the presence of RT PCR product not amplified PTH2 product as the product had been digested by MseI.

Fig 3.2.5 Differentiation between PTEN cDNA and PTHS sequences by MseI digest

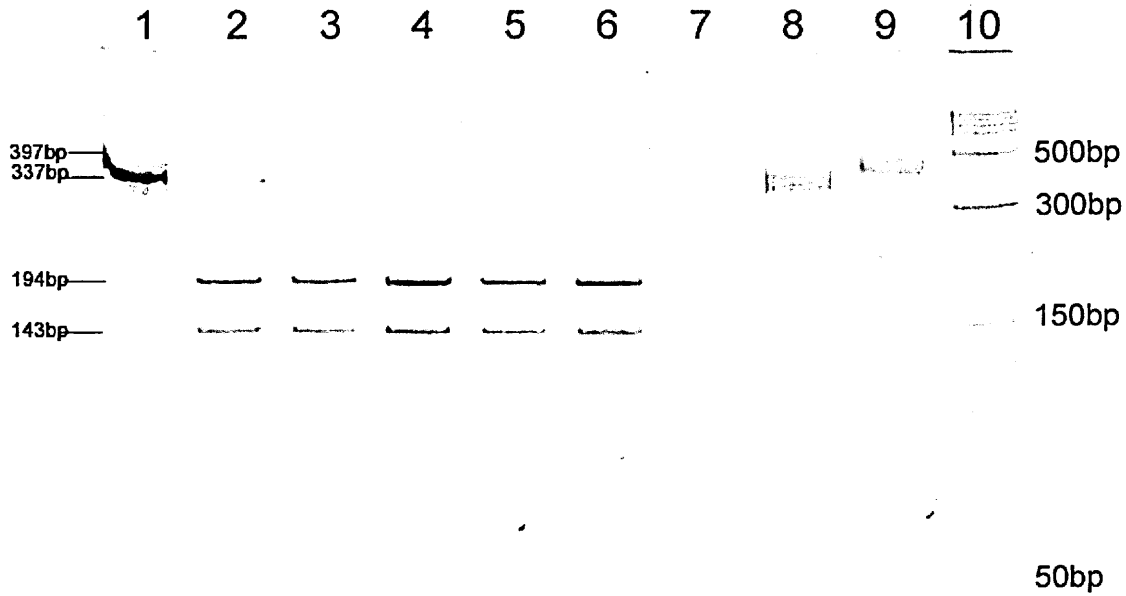


Fig 3.2.5 shows RTPCR of cell lines digested with MSE1 plus a pooled DNA extract. Lane 1&8: pooled normal DNA. Lane 2-7: CV605, K260, THP1, K562, HL60 and Jurkat RNA. Lane 9 uncut 397bp PCR product Lane 10 PCR DNA ladder. All cells show amplified cDNA including weak amplification in the Jurkat cell sample, which should not show amplification due to a deletion of PTEN expression in both alleles. (10cm, 10% polyacrylamide gel stained with ethidium bromide. Negative image)

3.3 Heteroduplex analysis.

3.3.1 Optimised heteroduplex PCR for each PTEN exon.

The gel in Fig 3.3.1 shows the optimised PCR product after magnesium concentration titres, DMSO titres for exons 1,2 and 3 and annealing temperature gradient analysis for exon 2. The reactions used normal pooled control DNA as a template for each PTEN exon used in the heteroduplex analysis reactions. The gel shows the relative quantity of product produced by each reaction. Exons 1,3,8 and 9 amplicons show less intense staining than exons 2,4,5,6 and 7. The size variation between reactions was necessary to achieve efficient PCR. The exon 2 product shows several non-specific products of increased fragment size compared to the specific product (approx 1000 and 600bp). Optimisation of the exon 2 reaction to yield only specific product proved very difficult despite the use of additives and optimisation of magnesium ion concentration and annealing temperature gradient studies. Exons 1 and 3 still have some low level non-specific product despite addition of DMSO but the non-specific product level was considered acceptable for heteroduplex analysis.

3.3.2 Optimisation of Heteroduplex electrophoresis conditions

This gel was designed to show that 19:1 acrylamide/bis acrylamide was suitable for resolution of heteroduplex bands using a PCR-amplified section of the β globin gene heterozygous for the a \rightarrow t mutation coding for haemoglobin S (fig 3.3.2) Separation of heteroduplex and homoduplex bands was not apparent and resolution was very poor. Heat generated during the electrophoresis has induced “smiling” effect. Gel star[®] stain demonstrates bands faintly.

Fig 3.3.1 Optimised PCR product for each PTEN exon

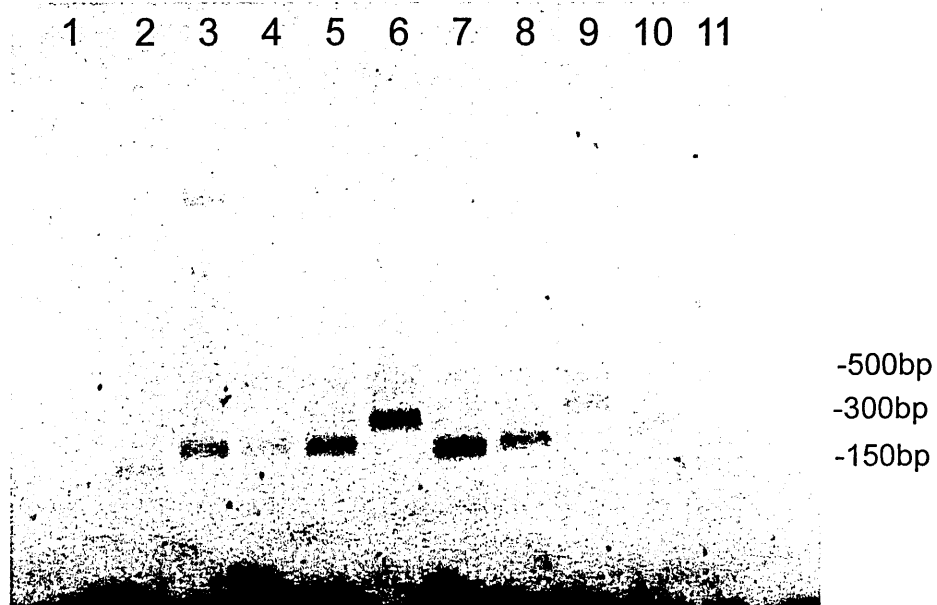


Fig 3.3.1 Gel shows optimised PCR product for each PTEN exon used for the heteroduplex analyses. Lane 1-11 Blank, Exon 1, Exon 2, Exon 3, Exon 4, Exon 5, Exon 6, Exon 7, Exon 8, Exon 9, 150 bp ladder respectively. (10cm-long section of 15x15cm Agarose gel, ethidium bromide stain, negative image)

Fig 3.3.2 Heteroduplex analysis with acrylamide/bis gel

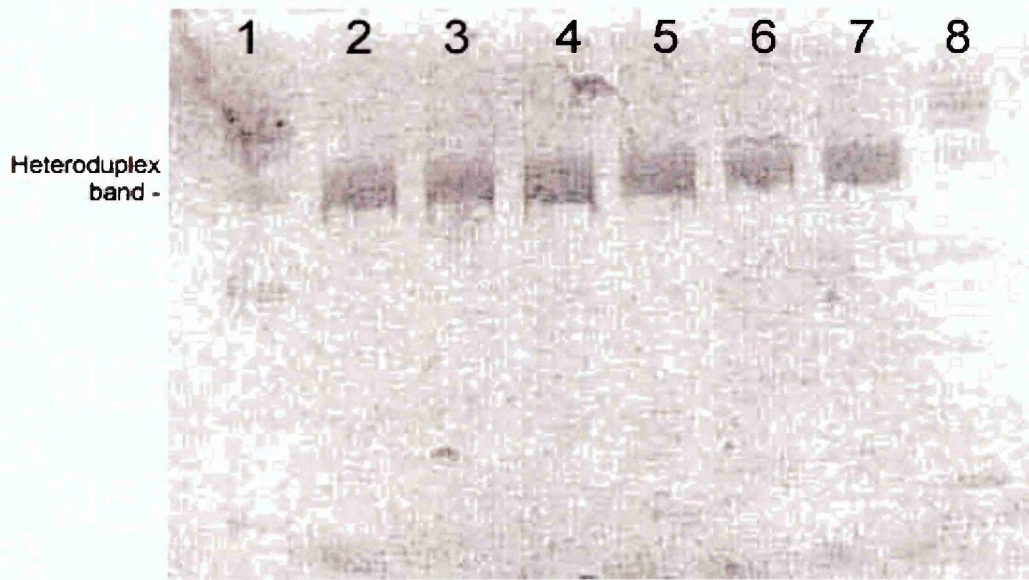


Fig 3.3.2 Gel shows 7cm long area of 50cm heteroduplex gel using 6% 19:1 bis acrylamide/acrylamide gel. Lane 1 and 8: Φ X174/*Hinf*I digest Lanes 2-7 β globin PCR product heterozygous for a/t allele responsible for sickle haemoglobin mutation. (Gelstar® stain, negative image)

3.3.3 Heteroduplex analysis with modified cross-linker Bis-acrylole piperazine

In an attempt to increase band sharpness Bis-acrylamide was replaced with Bis acryl piperazine (BAP) in 0.5x Tris-Taurine EDTA (TTE) buffer at 19:1 ratio of acrylamide and bis/acrylamide using a 10% gel as specified by Ganguly *et al.* (1993) with 10% glycerol. TTE Glycerol Tolerant Buffer (20X) is a concentrated Tris-Taurine-EDTA buffer solution. The use of TTE buffer eliminates the band distortion obtained during electrophoresis of DNA samples in glycerol-containing gels run with borate-containing buffers (Product instruction sheet, Geneflow Ltd, UK).

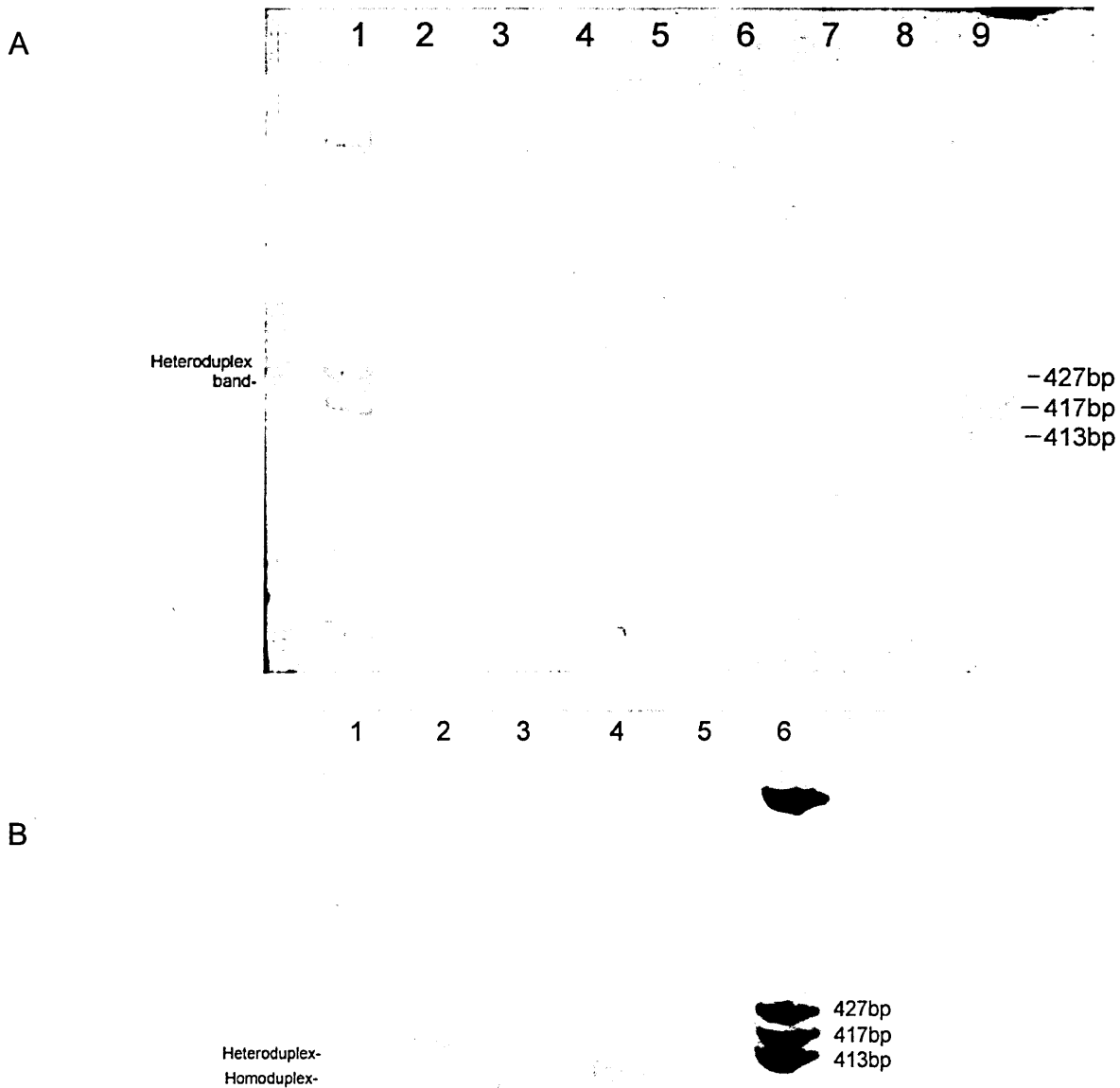
The use of TTE buffer dramatically increased band separation but resolution of heteroduplex bands was still poor.

Separation of heteroduplex and homoduplex bands was not apparent but there was a detectable increase in resolution of heteroduplex bands compared to bis-acrylamide (fig 3.3.4 A).

3.3.4 Heteroduplex analysis with Bis-acryloyl piperazine and non denaturing concentration of ethylene glycol and formamide.

Electrophoresis was performed with and without non denaturing concentrations of ethylene glycol and formamide to demonstrate the effect on resolution of heteroduplex bands. The gel shows improved separation and sharper resolution of heteroduplex bands and a clear distinction possible between homo- and heteroduplexes was obtained but unacceptable levels of band diffusion remained (Fig 3.3.4 B).

Fig 3.3.4 Heteroduplex gels with and without formamide and ethylene glycol



A
Gel A was a 7cm long area of 50cm heteroduplex gel using 6% 19:1 acrylamide with bis acryl piperazine (BAP) modified cross-linker.
Heteroduplex bands are highly diffused and only partially discernable
Lanes 1 and 9: Φ X174/*Hinf*1 digest. Lanes 3-8 β globin PCR product carrying a/t allele responsible for sickle haemoglobin mutation. (Gelstar © stain, negative image)

B
Gel shows 4cm long area of 50cm heteroduplex gel 6% 19:1 acrylamide with bis-acryloyl piperazine (BAP) with non denaturing concentration of formamide and ethylene glycol.
Resolution of heteroduplex bands was improved but was still insufficient for accurate delineation of bands
Lane 1- normal homoduplex , Lanes 2-5 Positive heteroduplex control β globin PCR product carrying a/t allele. Lane 6- Φ X174/*Hinf*1 ladder.
(Gelstar © stain, negative image)

3.3.5 Heteroduplex analysis with use of proprietary acrylamide-based gel mix

PagePlus[®] with GelStar[®] or silver staining

The PagePlus media was used in an attempt to improve heteroduplex band resolution and produced dramatically improved resolution of stained bands. The relationship between fragment size and distance migrated appeared more linear than standard acrylamide gels. Gel 3.3.5 shows very clear bands with low levels of diffusion and a clear distinction between homo- and heteroduplex bands in the HbS control lane.

The gel was stained with GelStar at manufacturers' recommended concentration then silver stained. GelStar stained gel shows very clear distinct bands whilst the silver stained gel shows increased staining levels but some loss of resolution. The silver stained gel also shows some non-specific product in the PTEN exon 8 reactions. Silver staining also appears more quantitative with larger differences in staining intensity between exons compared to GelStar.

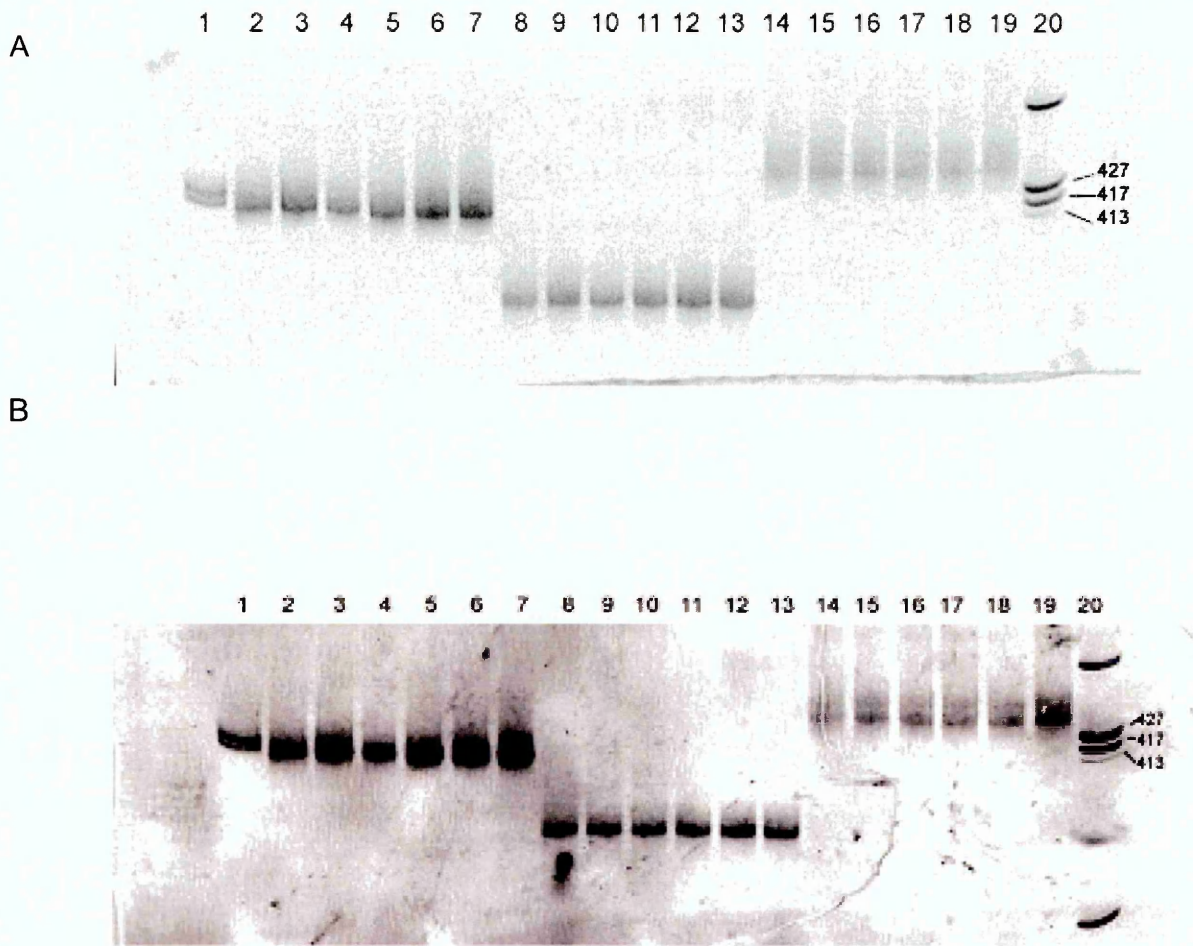
3.3.6 Bis-acrylole piperazine (BAP) gel with silver staining.

Difference between migration distance and fragment size obtained with BAP gel.

The products of each exon show a greater relative difference in migration distance than when compared to the PagePlus gels in Fig 3.3.5

Silver stained gel shows intense staining of PCR heteroduplex fragments and this represents an over-developed gel. Individual bands of hetero- and homoduplexes in control fragments were visible during initial development of stained gel but became indistinct as development of the image continued. Exon 5 reactions show more intense staining and overall resolution of the gel was poor due to overdeveloping of the silver stain. GelStar was used in subsequent runs to identify the position of the heteroduplex bands then photographed prior to

Fig 3.3.5 Comparison of GelStar staining and silver staining.



A Gel was stained with GelStar and shows excellent delineation of heteroduplex bands in the control (lane 1) background staining was very low.

B Gel was silver stained. Staining was more intense showing greater sensitivity to quantity of DNA in each band.

Delineation of the heteroduplex control was adequate but inferior to GelStar staining

7cm section of 50cm heteroduplex gel using PagePlus® medium at concentration recommended by manufacturer.

Lane 1 HbS HD control. Lanes 2-7 samples PTEN exon 5(400bp). Lanes 8-13 samples exon7 (351). Lanes 14-19 samples exon 8 (420bp). Lane 20 Φ X174/*Hinf*I Ladder. (Gelstar stain, negative image).

Fig 3.3.6 Silver stained BAP gel heteroduplex reactions



Random stained bone marrow smear samples and Jurkat cells. 20x50cm, bottom 20cm of gel shown. This gel shows the relative increased difference in distance migrated by the exon 5 7 and 8 products on the BAP gel when compared to the PagePlus media. Silver staining was over developed on this gel. The heteroduplex bands in the control have merged despite being visible in the early stages of development. Lane 1 heteroduplex control . Lanes 2-6 are bone marrow smears PTEN exon 5 (400bp).. Lanes 7-10 are bone marrow smears PTEN exon 7 (351bp). Lane 11 was Jurkat exon 7. Lanes 12-15 are bone marrow smears PTEN exon 8 (420bp). Lane 9 300 & 500bp marker.

excision of the region for silver staining. Interestingly, the 438bp heteroduplex control migrates at approximately the same rate as the 427bp ladder fragment. This effect was a feature of polyacrylamide gel electrophoresis where fragment secondary structure affects migration rate. Jurkat cells contain two mutated PTEN exon 7 alleles: a 2bp deletion plus a 9 bp insertion and a 39 bp insertion (Sakai *et al* 1998)

3.3.7 Heteroduplex analysis of PTEN exons 5, 7 and 8

All lymph node samples screened were non-Hodgkin's lymphoma. Initial bone marrow smear samples for heteroduplex analysis consisted of 3 chronic myelogenous leukaemia, 10 chronic lymphocytic leukaemia, 12 acute myelogenous leukaemia, 2 hairy cell leukaemia, 10 non-Hodgkins lymphoma, 16 myelodysplasia, 13 myeloma and 2 Waldenstrom's macroglobulinaemia

All lymphoma samples in all exon 5, 7 and 8 PCR reactions for lymph nodes migrated as homoduplexes. The proportion of PCR product representing DNA amplified from the tumour cell clone varied between samples. Figures for the percentage of tumour and normal cells were unavailable for the FFPE and depended on the size of the tumour in relation to the individual lymph node. The very low positive screen rate and concerns that a sub population of mutated tumour cells would not produce a visible heteroduplex band led to the abandonment of heteroduplex screening in favour of SSCP after 18 lymph node and bone marrow samples

The heteroduplex gels showed a high failure rate for exon 8 PCR reactions characterized by faint, diffused or absent product (fig 3.3.7.1) in expected region of gel with only 8 of 18 lymph node FFPE samples showing product in which a heteroduplex band would be apparent against the diffused background signal.

Exon 5 and 7 reactions were less variable with 3 and 1 failed reactions respectively. Failed reactions in the 50cm heteroduplex gel often showed some reaction products in the screening procedure using short runs on agarose gel. Loss of staining intensity was marked when comparing the same product in 8cm agarose and 50 cm Page Plus gels.

FFPE samples 1-6 (Fig 3.3.7.1 A) show good resolution of exon 5 and 7 products with no amplification products for exon 8. All visible bands have migrated as expected with no evidence of heteroduplex bands. The control band shows formation of heteroduplex.

FFPE samples 7-12 (Fig 3.3.7.1 B) show resolution of exon 5 and 7 and 8. Samples 9, 11 and 12 show fainter products in each exon and heteroduplex generation would not be apparent. All bands have migrated as expected with no evidence of heteroduplex bands. The control band shows formation of heteroduplex.

FFPE samples 13-18 (Fig 3.3.7.2 A) show good resolution of exon 5 and 7 products with no amplification products for exon 8. All bands have migrated as expected with no evidence of heteroduplex bands. The control band shows formation of heteroduplex.

Stained bone marrow samples 1-6 (Fig 3.3.7.2 B) show resolution of exon 5 and 7 and 8. Samples 2,4,5 and 6 show no products in exon 8. All bands have migrated as expected with no evidence of heteroduplex bands but sample 1 in lane 14 shows two bands with aberrant retarded migration patterns that were not

Fig 3.3.7.1 Heteroduplex analysis of lymph node samples 1-12 exons 5,7 and 8

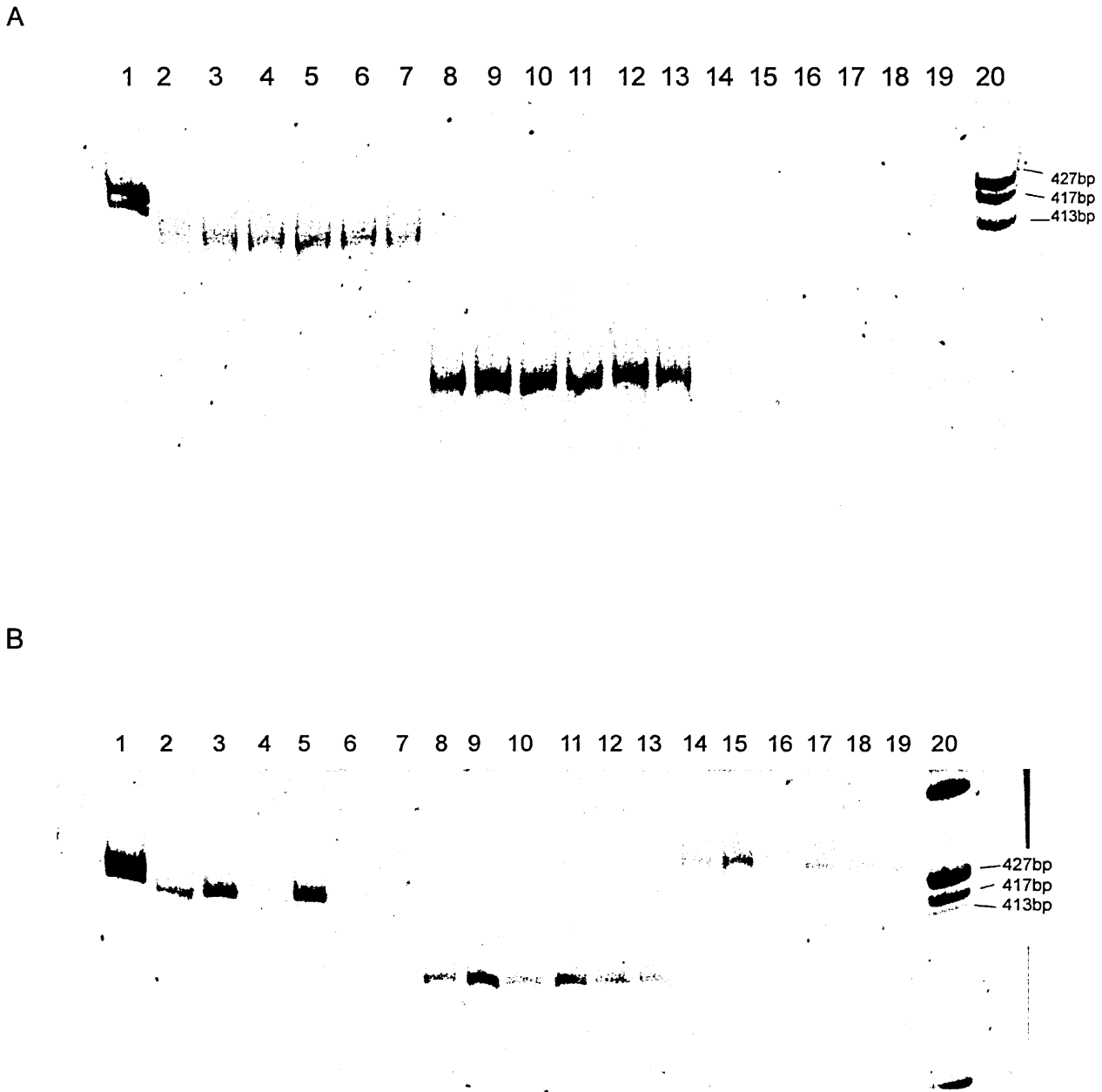


Fig 3.3.7.1 A

Gel A shows heteroduplex analysis of lymph node samples 1-6.

No heteroduplex bands are evident. Exon 8 samples are highly diffused.

lane 1: heteroduplex control, in lane 2-19: lymph node samples 1-6 of exons 5, 7 and 8 respectively. lane 20: Φ X174/*Hinf*I Ladder (7cm section of 50cm heteroduplex PagePlus[®] gel, Gelstar[®] stain, negative image).

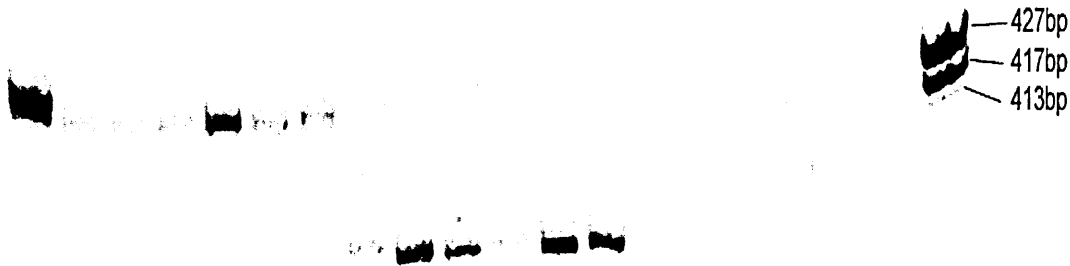
Fig 3.3.7.1 B shows heteroduplex analysis of lymph node samples 7-12. lane 1: heteroduplex control, in lane 2-19: lymph node samples 7-12 exons 5, 7 and 8 respectively. Exon 8 reactions were prone to failure at the heteroduplex electrophoresis stage despite adequate levels of amplification in agarose gels lane 20: Φ X174/*Hinf*I Ladder (7cm section of 50cm heteroduplex PagePlus[®] gel, Gelstar[®] stain, negative image).

Fig 3.3.7.2 Heteroduplex analysis of lymph nodes 13 – 18 and bone marrow

samples 1-6

A

1 2 3 4 5 6 7 8 9 10 11 12 13 14 15 16 17 18 19 20



B

1 2 3 4 5 6 7 8 9 10 11 12 13 14 15 16 17 18 19

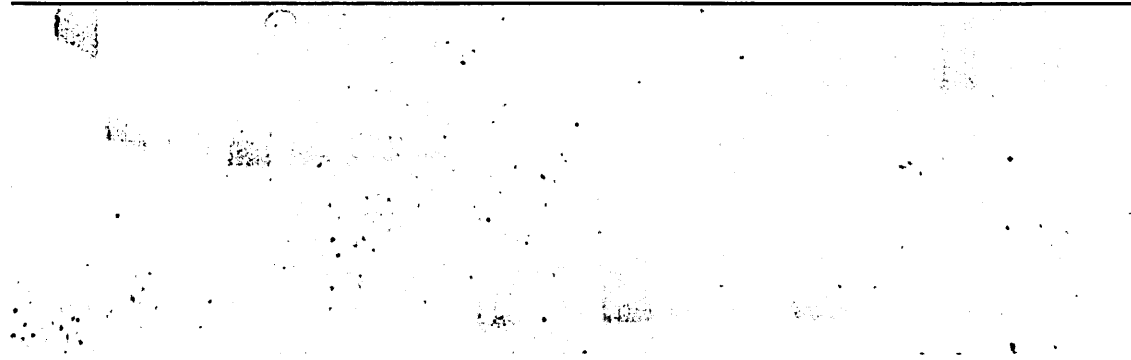


Fig 3.3.7.2 A Gel shows heteroduplex analysis of lymph node samples 13-18. bands have migrated as expected with no evidence of heteroduplex bands

lane 1: heteroduplex control, in lane 2-19: lymph node samples 13-18 exons 5, 7 and 8 respectively. lane 20: Φ X174/*Hinf*1 Ladder (7cm section of 50cm heteroduplex PagePlus[®] gel, Gelstar [®] stain, negative image).

Fig 3.3.7.2 B Gel shows heteroduplex analysis of stained bone marrow samples 1-6.

bands have migrated as expected with no evidence of heteroduplex bands lane 1: heteroduplex control, in lane 2-19: stained bone marrow samples 1-6 exons 5, 7 and 8 respectively. lane 20: Φ X174/*Hinf*1 Ladder. Lane 14 shows two bands with aberrant retarded migration patterns that were not reproduced when the PCR was repeated. (7cm section of 50cm heteroduplex PagePlus[®] gel, Gelstar [®] stain, negative image).

reproduced when the PCR was repeated, which suggests the presence of a non-specific amplification product in the initial reaction. Control band shows formation of heteroduplex.

Stained bone marrow samples 7-12 (Fig 3.3.7.3 A) show good resolution of exon 5, 7 and 8. All bands have migrated as expected with no evidence of heteroduplex bands. Control band shows formation of heteroduplex.

Stained bone marrow samples 13-18 in (Fig 3.3.7.3 B) show resolution of exon 5 and 7 and 8. Sample 16 shows a fainter products in exon 8 and heteroduplex generation would not be apparent. All bands have migrated as expected with no evidence of heteroduplex formation. Control band shows formation of heteroduplex.

Fig 3.3.7.3 Heteroduplex analysis of stained bone marrow samples 7-18

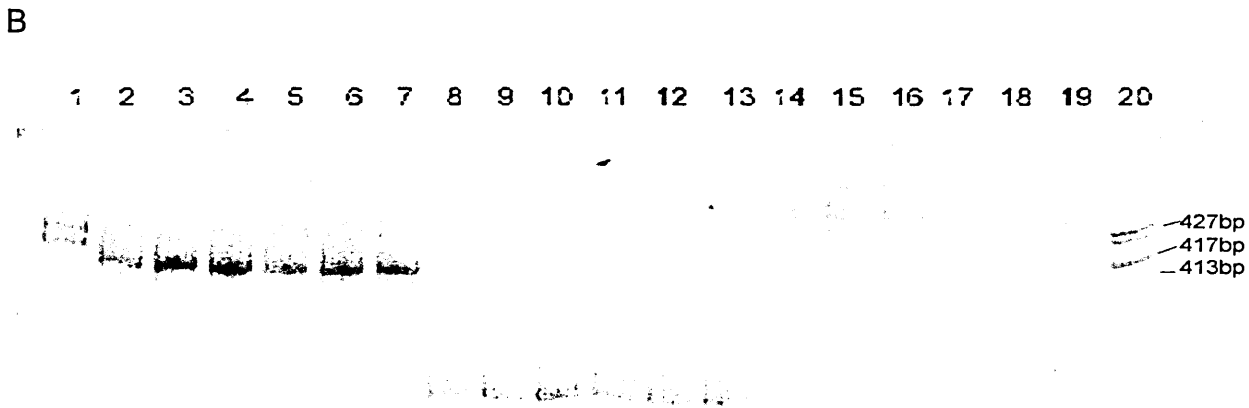
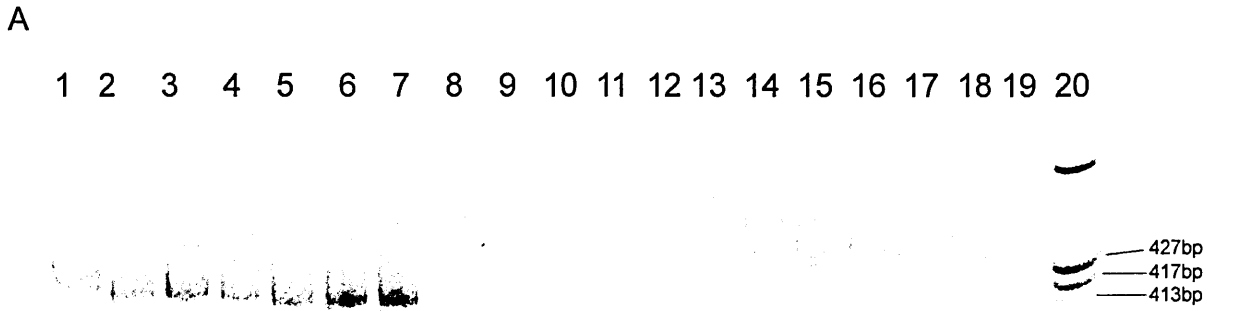


Fig 3.3.7.5 Gel shows heteroduplex analysis of stained bone marrow samples 7-12. Lane 1: heteroduplex control, in lane 2-19: stained bone marrow samples 7-12 exons 5, 7 and 8 respectively. lane 20: Φ X174/*Hinf*I Ladder (7cm section of 50cm heteroduplex PagePlus[®] gel, Gelstar [®] stain, negative image).

Fig 3.3.7.6 Gel shows heteroduplex analysis of stained bone marrow samples 13-18. lane 1: heteroduplex control, in lane 2-19 stained bone marrow samples 13-18 exons 5, 7 and 8 respectively. lane 20: Φ X174/*Hinf*I Ladder (7cm section of 50cm heteroduplex PagePlus[®] gel, Gelstar [®] stain, negative image).

3.4 SSCP analysis

3.4.1 PCR product specificity for SSCP analysis

Gel in Fig 3.4.1 shows all primers used in SSCP analysis which produce PCR products of around 300bp. Exon 1 primers showed some non-specific amplification products. Exon 2 primers produced a number of non-specific products that varied between 300 and 1000 bp. Results were highly variable for specificity of exon 2 PCR between batches of amplification (results not shown). This variability was similar to that obtained with the heteroduplex exon 2 primers despite a 120bp reduction in amplified fragment size. The unpredictability and lack of specificity in the exon 2 PCR led to its exclusion from the SSCP analysis as exon 2 is not identified as an area commonly subject to mutation (Bonneau and Longy 2000).

The PCR for SSCP analysis yielded higher levels of specific product than the heteroduplex reactions. The SSCP gels were also less susceptible to diffusion effects.

Fig 3.4.1 shows the product of each SSCP primer pair and demonstrates the continued lack of specificity of the exon 2 reaction.

Optimum separation of single strand amplicons was achieved at 12 W constant power for 16h at a plate temperature (measured in the centre of the plate) of 13⁰C, which corresponded to a coolant temperature of 10 ⁰C.

The SSCP analysis was performed on a 30cm or 50cm-long gel but, as shown in Fig 3.4.2, resolution of single stranded complexes was possible using a much smaller and more manageable 8cm format gel with higher concentration of PagePlus media. Lane 3 shows clearly the aberrant migration of PTEN exon 7 product obtained using NIH33 cells.

Fig 3.4.1 PCR products obtained using primers for SSCP analysis

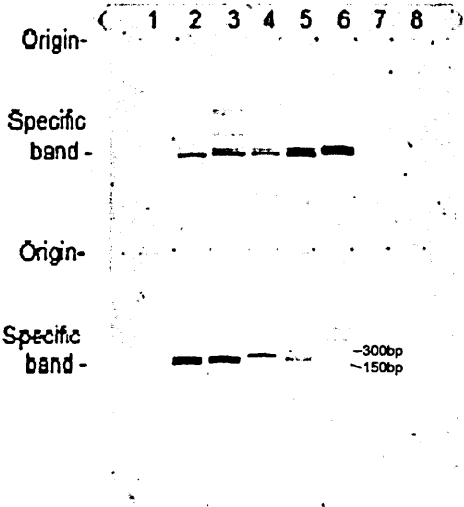
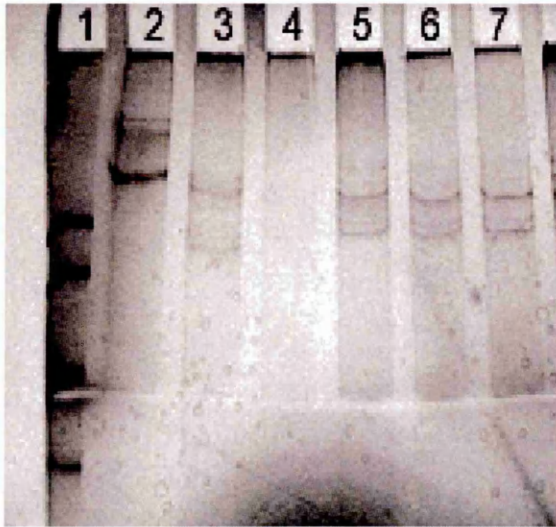


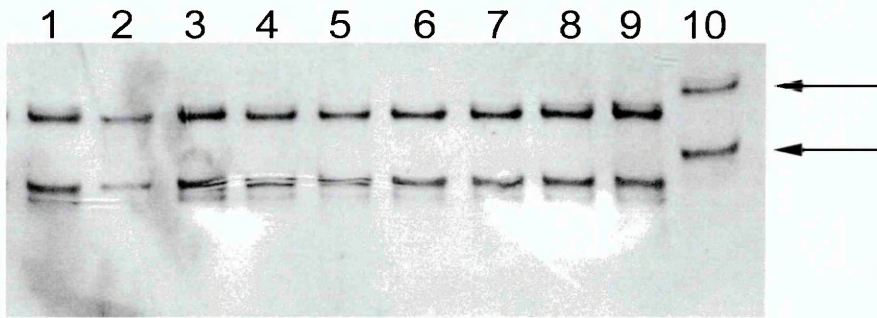
Fig 3.4.1 Gel shows PCR products obtained using primers for SSCP analysis with random normal DNA extract from fresh blood. Top row, Lane 2-6: PTEN SSCP 1-5 respectively. Bottom row, lane 2-5: PTEN SSCP 6-9 respectively.. Lane 6 100bp Ladder (8cm Agarose minigel, ethidium bromide stain, negative image)

Fig 3.4.2 SSCP electrophoresis on 8cm and 50cm Page Plus gels

A



B



A Gel shows SSCP electrophoresis on 8cm Page Plus® gel with 2x manufacturer's recommended concentration of PagePlus concentrate. PTEN exon 7 PCR. Differential migration is evident on small format gel using more concentrated medium but result is clearer using the 30 cm format gel shown in B
Lane 1 & 2 Ladders, Lane 3 positive control NIH 33 cells Lanes 4-7 Fresh bone marrow DNA..

B shows 30 cm gel with recommended concentration of PagePlus medium PTEN exon 7 PCR
Lanes 1-9 bone marrow samples, lane 10 (arrowed) positive control NIH 33 cells.

3.4.2 SSCP of bone marrow samples

3.4.2.1 SSCP PTEN Exon1

SSCP analysis of PTEN exon 1 showed good PCR product levels that yielded 4 main conformers on electrophoresis. The use of the cooling system greatly reduced band distortion and “smiling” in all the large format SSCP gels. Of the four bands, the individual band showing the strongest stain varied from sample to sample with no obviously dominant conformation. Some faint, background, slower-migrating bands were evident with silver staining, the staining intensity of these bands was proportional to the intensity of the four main conformers. No aberrant migrating bands that would suggest the presence of a mutation were identified in the 114 samples screened Samples 96-114 are not shown due to a mishap when handling the gel after silver staining.

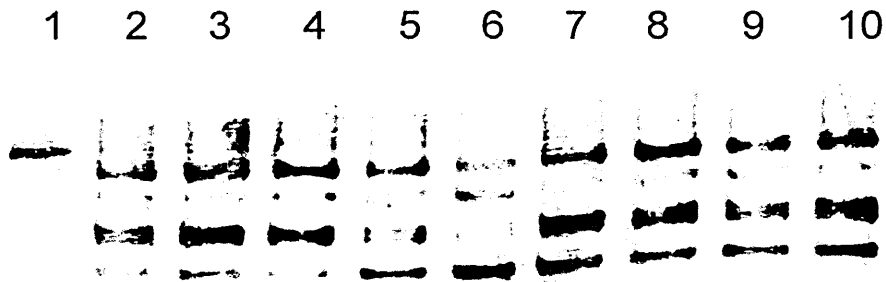


Fig 3.4.2.1.1 Gel shows PTEN exon1 SSCP analysis of fresh bone marrow samples 1-9. Lane 1: Φ X174/*Hinf*I Ladder, lane 2-10: fresh bone marrow samples 1-9 respectively. (5cm section of 50cm PagePlus[®] gel, Silver stain, positive enhanced image).

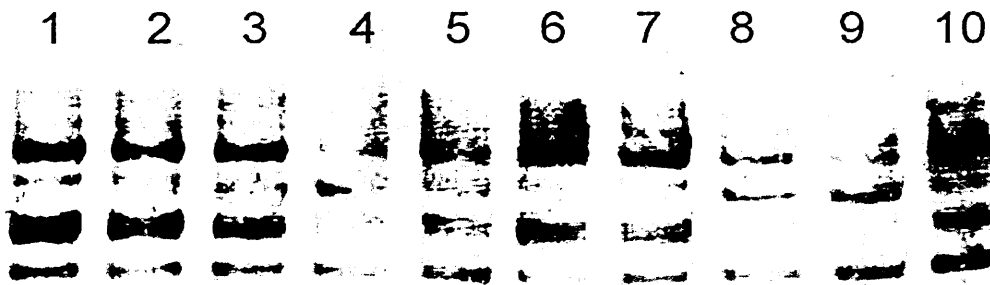


Fig 3.4.2.1.2 Gel shows PTEN exon1 SSCP analysis of fresh bone marrow samples 10-19. Lane 1-10: fresh bone marrow samples 10-19 respectively. (5cm section of 50cm PagePlus[®] gel, Silver stain, positive enhanced image).

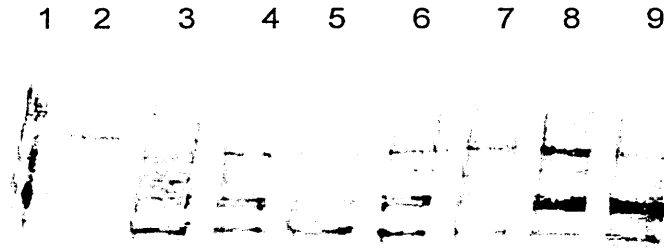


Fig 3.4.2.1.3 Gel shows PTEN exon1 SSCP analysis of fresh bone marrow samples 20-28. Lane 2: Φ X174/*Hinf*I Ladder, lane 1+ 3-9: fresh bone marrow samples 20-28 respectively. (5cm section of 50cm PagePlus[®] gel, Silver stain, positive enhanced image).

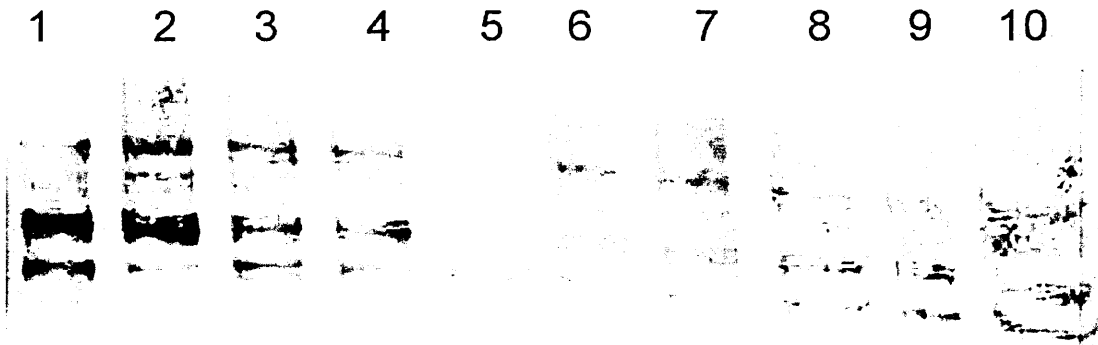


Fig 3.4.2.1.4 Gel shows PTEN exon1 SSCP analysis of fresh bone marrow samples 29-38. Lane 1-10: fresh bone marrow samples 29-38 respectively. (5cm section of 50cm PagePlus[®] gel, Silver stain, positive enhanced image).

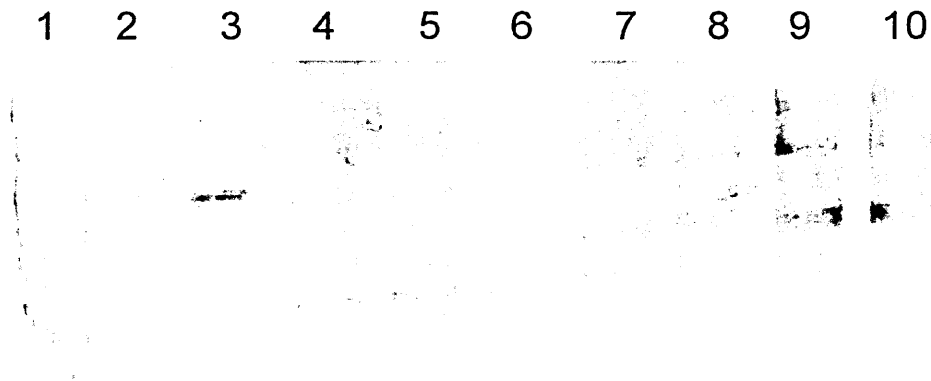


Fig 3.4.2.1.5 Gel shows PTEN exon1 SSCP analysis of fresh bone marrow samples 39-47. Lane 3: Φ X174/*Hinf*I Ladder, lane 1-2+ 4-10: fresh bone marrow samples 39-47 respectively. (5cm section of 50cm PagePlus[®] gel, Silver stain, positive enhanced image).

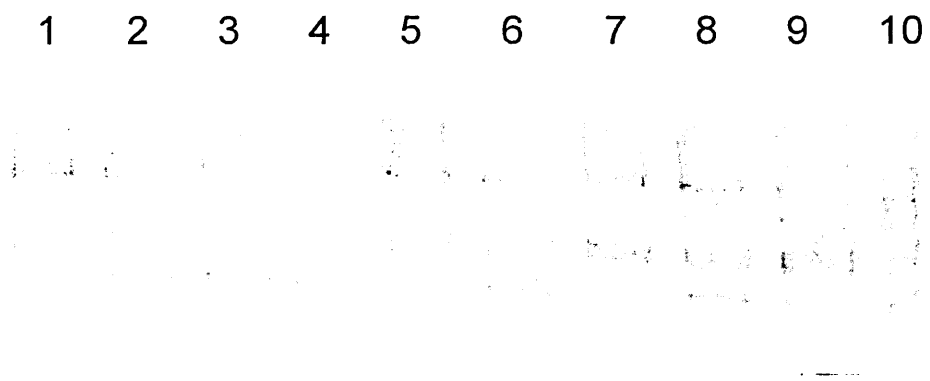


Fig 3.4.2.1.6 Gel shows PTEN exon1 SSCP analysis of fresh bone marrow samples 48-57. Lane 1-10: fresh bone marrow samples 48-57 respectively. (5cm section of 50cm PagePlus[®] gel, Silver stain, positive enhanced image).

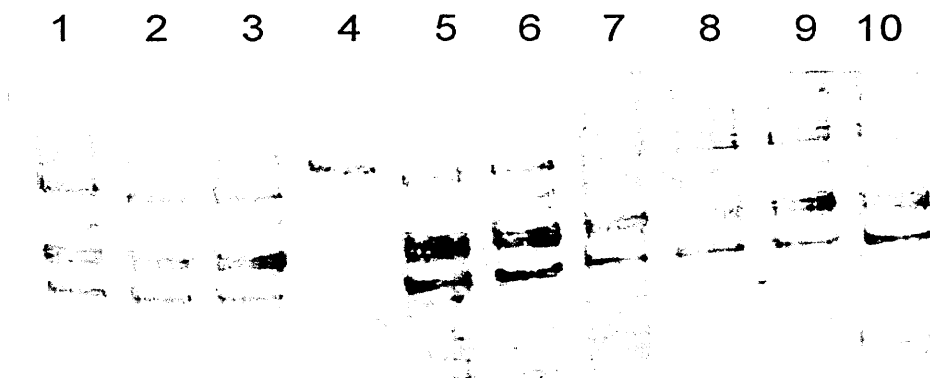


Fig 3.4.2.1.7 Gel shows PTEN exon1 SSCP analysis of fresh bone marrow samples 58-66. Lane 4: Φ X174/*Hinf*I Ladder, lane 1-3+ 4-10: fresh bone marrow samples 58-66 respectively. (5cm section of 50cm PagePlus[®] gel, Silver stain, positive enhanced image).

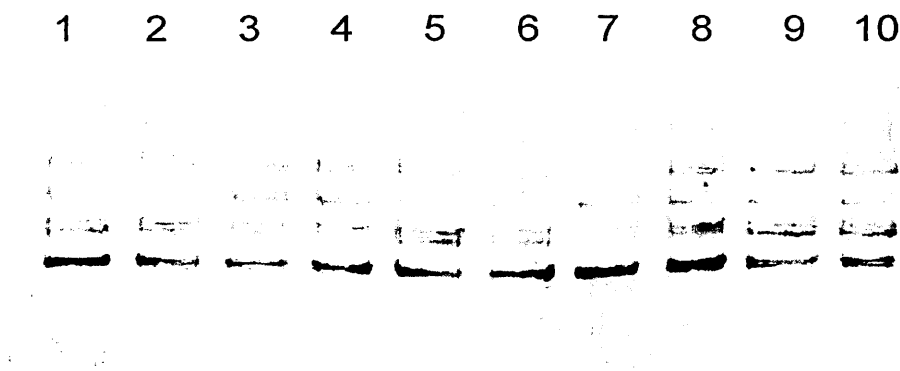


Fig 3.4.2.1.8 Gel shows PTEN exon1 SSCP analysis of fresh bone marrow samples 67-76. Lane 1-10: fresh bone marrow samples 67-76 respectively. (5cm section of 50cm PagePlus[®] gel, Silver stain, positive enhanced image).

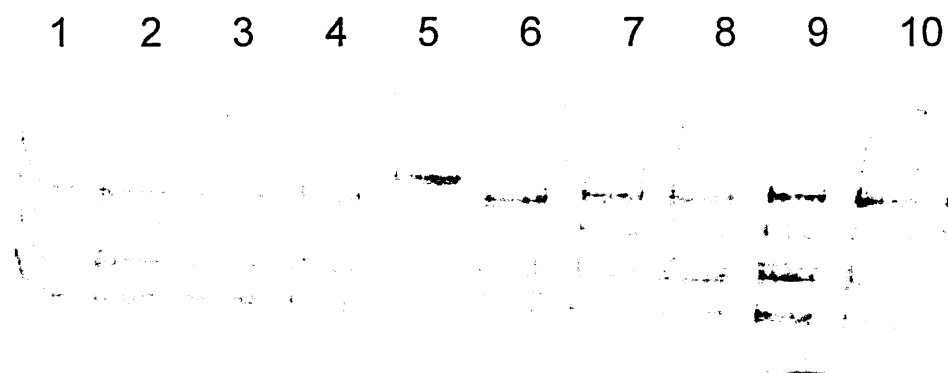


Fig 3.4.2.1.9 Gel shows PTEN exon1 SSCP analysis of fresh bone marrow samples 77-85. Lane 5: Φ X174/*Hinf*I Ladder, lane 1-4 + 5-10: fresh bone marrow samples 77-85 respectively. (5cm section of 50cm PagePlus[®] gel, Silver stain, positive enhanced image).

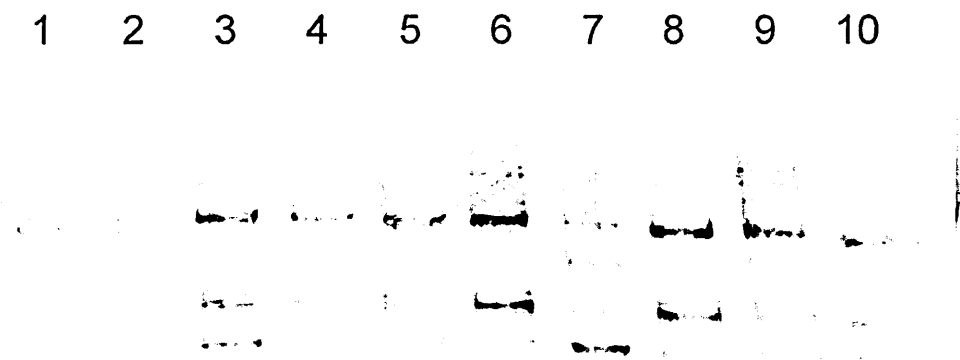


Fig 3.4.2.1.10 Gel shows PTEN exon1 SSCP analysis of fresh bone marrow samples 86-95. Lane 1-10: fresh bone marrow samples 86-95 respectively. (5cm section of 50cm PagePlus[®] gel, Silver stain, positive enhanced image).

3.4.2.2 SSCP PTEN Exon 2

Exon two was excluded from the SSCP analysis because no suitable specific PCR reaction could be developed. These findings mirror those of the heteroduplex analysis of PTEN exon 2, despite the fact that exon 2 SSCP PCR primers produce a fragment 150bp smaller than the PTGS exon two primers.

3.4.2.3 SSCP PTEN Exon 3

SSCP analysis of PTEN exon 3 showed good PCR product levels that yielded 4 main conformers on electrophoresis. Of the four bands, the individual band showing the strongest stain, like exon1, varied from sample to sample with the slowest migrating conformer usually being dominant. The first or second band of the three fastest migrating bands was the first to show fainter staining intensity. No faint background bands were evident with silver staining. No aberrant migrating bands that would suggest the presence of a mutation were identified in the 114 samples screened.

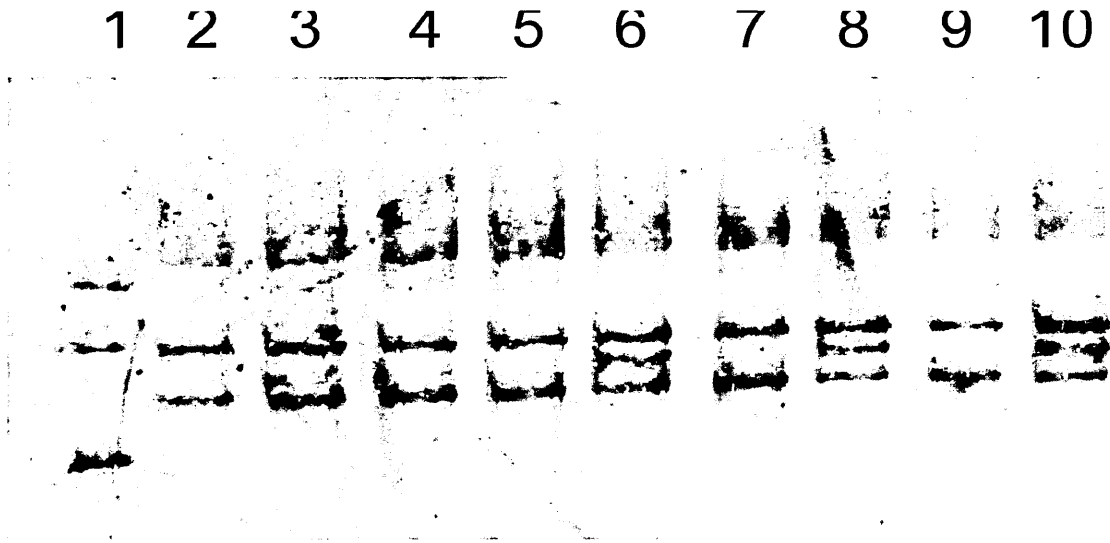


Fig 3.4.2.3.1 Gel shows PTEN exon 3 SSCP analysis of fresh bone marrow samples 1-9. Lane 1: Φ X174/*Hinf*I Ladder, lane 2-9: fresh bone marrow samples 1-9 respectively. (5cm section of 50cm PagePlus[®] gel, Silver stain, positive enhanced image).

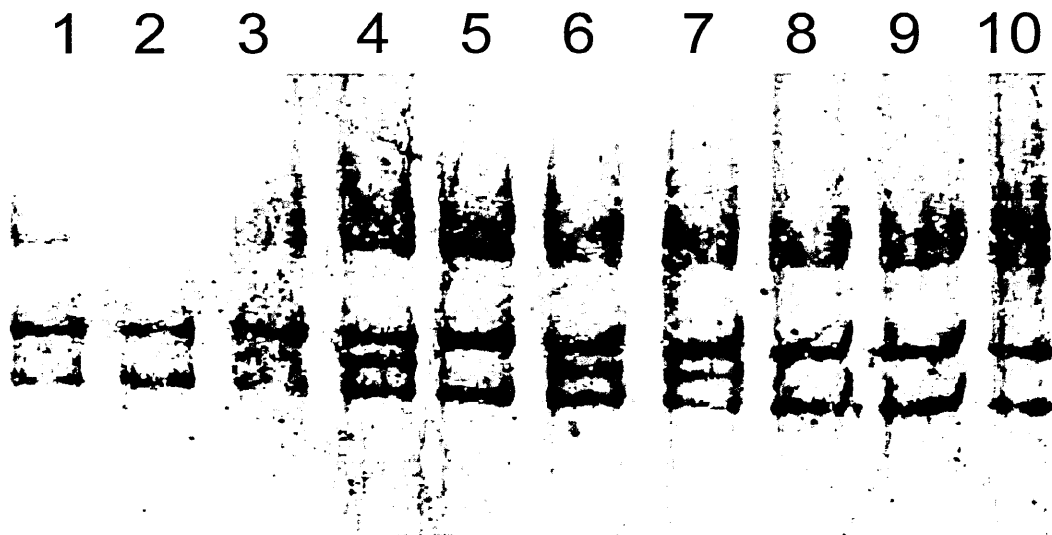


Fig 3.4.2.3.2 Gel shows PTEN exon 3 SSCP analysis of fresh bone marrow samples 10-19. Lane 1-10: fresh bone marrow samples 10-19 respectively. (5cm section of 50cm PagePlus[®] gel, Silver stain, positive enhanced image).

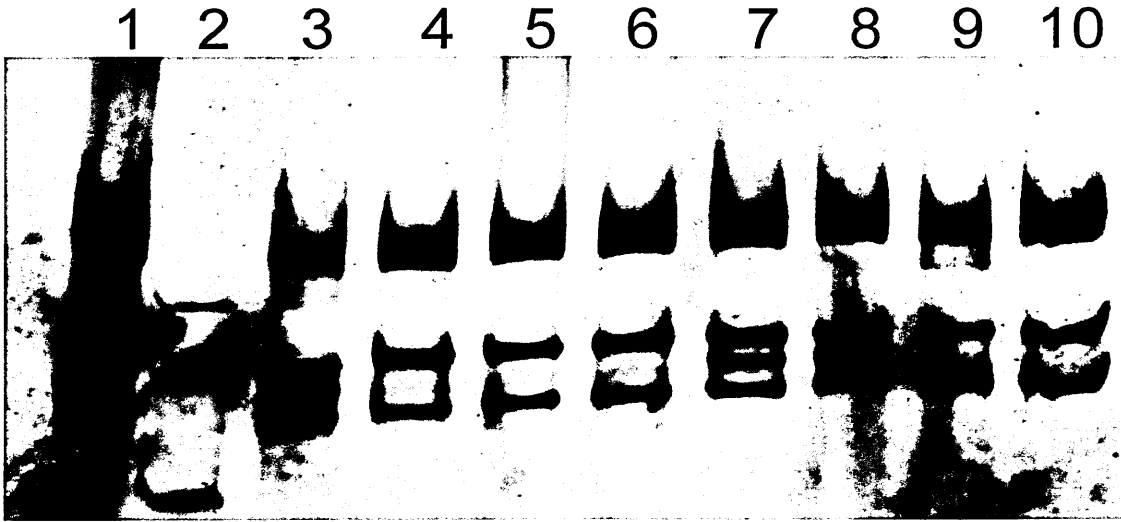


Fig 3.4.2.3.3 Gel shows PTEN exon 3 SSCP analysis of fresh bone marrow samples 20-28. Lane 2: Φ X174/*Hinf*I Ladder, lane 1+ 3-9: fresh bone marrow samples 20-28 respectively. (5cm section of 50cm PagePlus[®] gel, Silver stain, positive enhanced image).



Fig 3.4.2.3.4 Gel shows PTEN exon 3 SSCP analysis of fresh bone marrow samples 29-38. Lane 1-10: fresh bone marrow samples 29-38 respectively. (5cm section of 50cm PagePlus[®] gel, Silver stain, positive enhanced image).

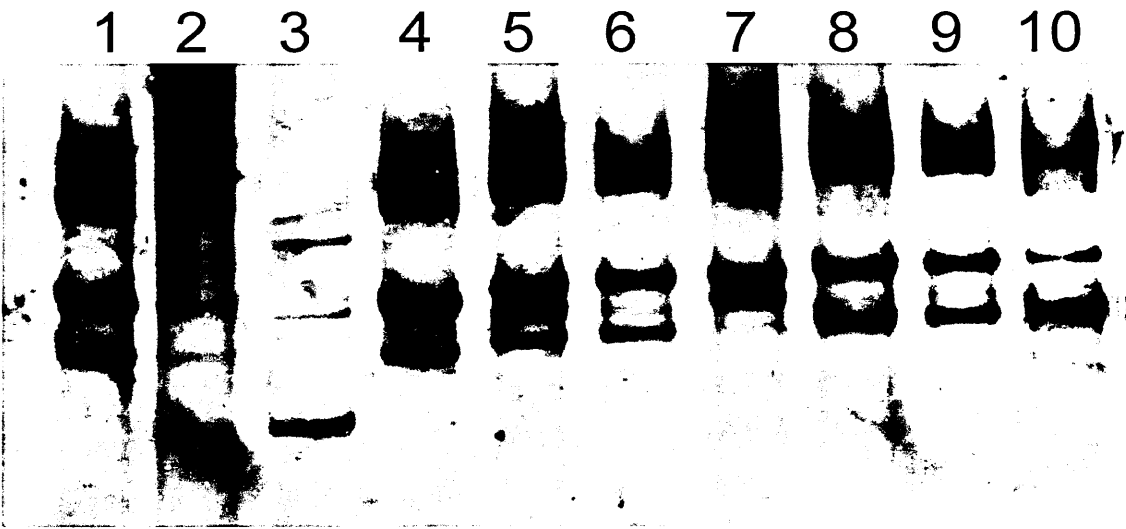


Fig 3.4.2.3.5 Gel shows PTEN exon 3 SSCP analysis of fresh bone marrow samples 39-47. Lane 3: Φ X174/*Hinf*I Ladder, lane 1-2+ 4-10: fresh bone marrow samples 39-47 respectively. (5cm section of 50cm PagePlus[®] gel, Silver stain, positive enhanced image).



Fig 3.4.2.3.6 Gel shows PTEN exon 3 SSCP analysis of fresh bone marrow samples 48-57. Lane 1-10: fresh bone marrow samples 48-57 respectively. (5cm section of 50cm PagePlus[®] gel, Silver stain, positive enhanced image).

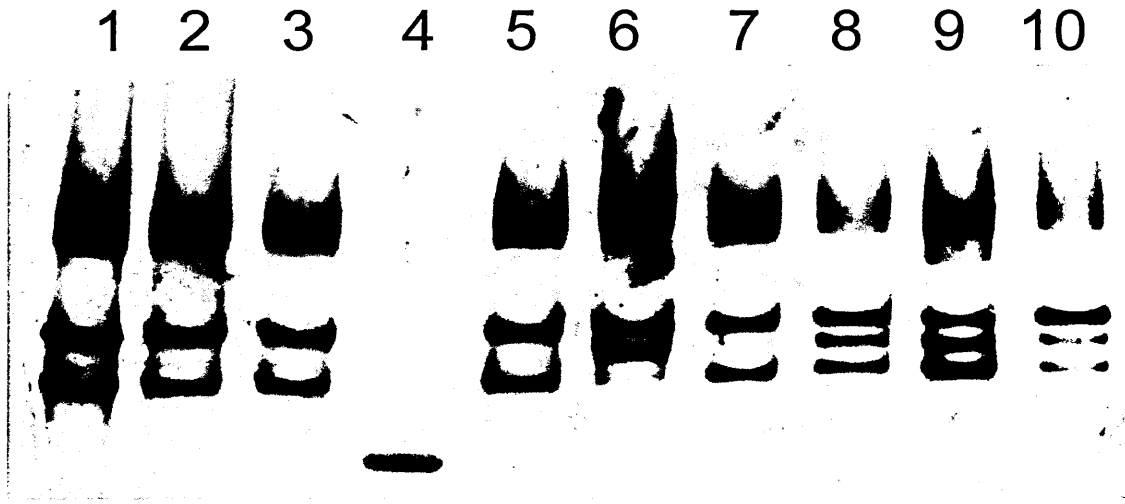
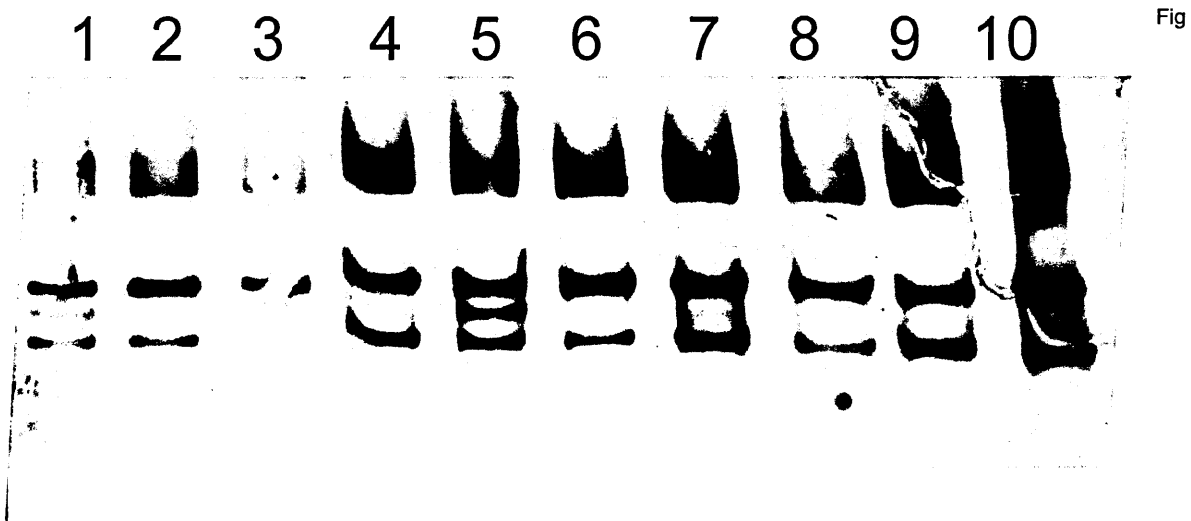


Fig 3.4.2.3.7 Gel shows PTEN exon 3 SSCP analysis of fresh bone marrow samples 58-66. Lane 4: Φ X174/*Hinf*I Ladder, lane 1-3+ 5-10: fresh bone marrow samples 58-66 respectively. (5cm section of 50cm PagePlus[®] gel, Silver stain, positive enhanced image).



3.4.2.3.8 Gel shows PTEN exon 3 SSCP analysis of fresh bone marrow samples 67-76. Lane 1-10: fresh bone marrow samples 67-76 respectively. (5cm section of 50cm PagePlus[®] gel, Silver stain, positive enhanced image).

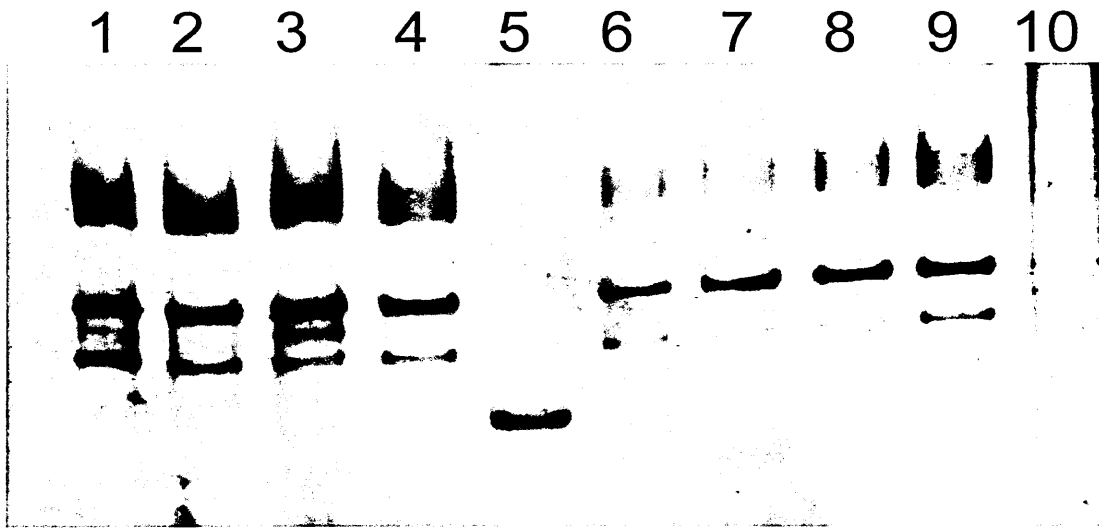


Fig 3.4.2.3.9 Gel shows PTEN exon 3 SSCP analysis of fresh bone marrow samples 77-85. Lane 5: Φ X174/*Hinf*I Ladder, lane 1-4 + 6-10: fresh bone marrow samples 77-85 respectively. (5cm section of 50cm PagePlus[®] gel, Silver stain, positive enhanced image).

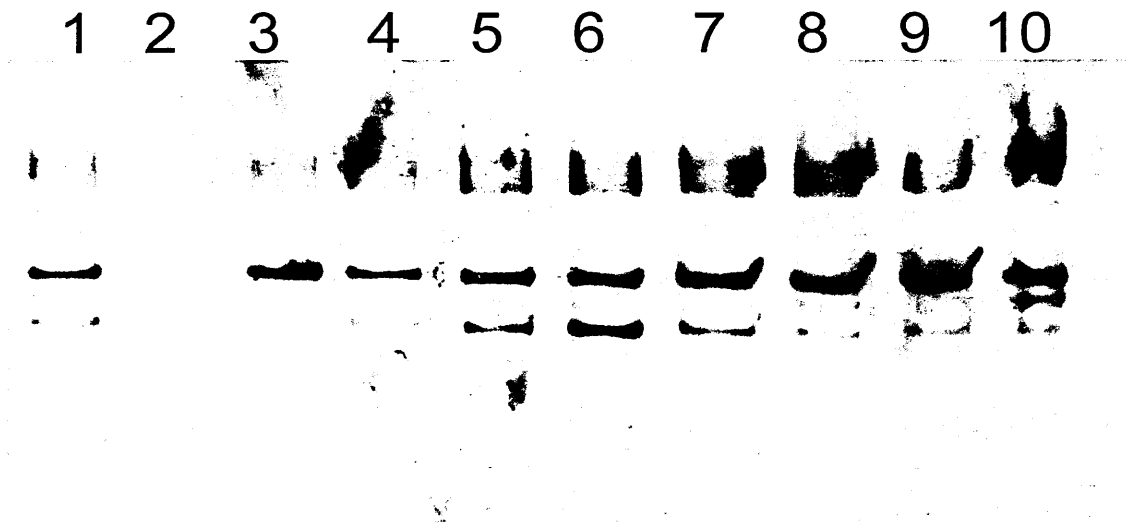


Fig 3.4.2.3.10 Gel shows PTEN exon 3 SSCP analysis of fresh bone marrow samples 86-95. Lane 1-10: fresh bone marrow samples 86-95 respectively. (5cm section of 50cm PagePlus[®] gel, Silver stain, positive enhanced image).

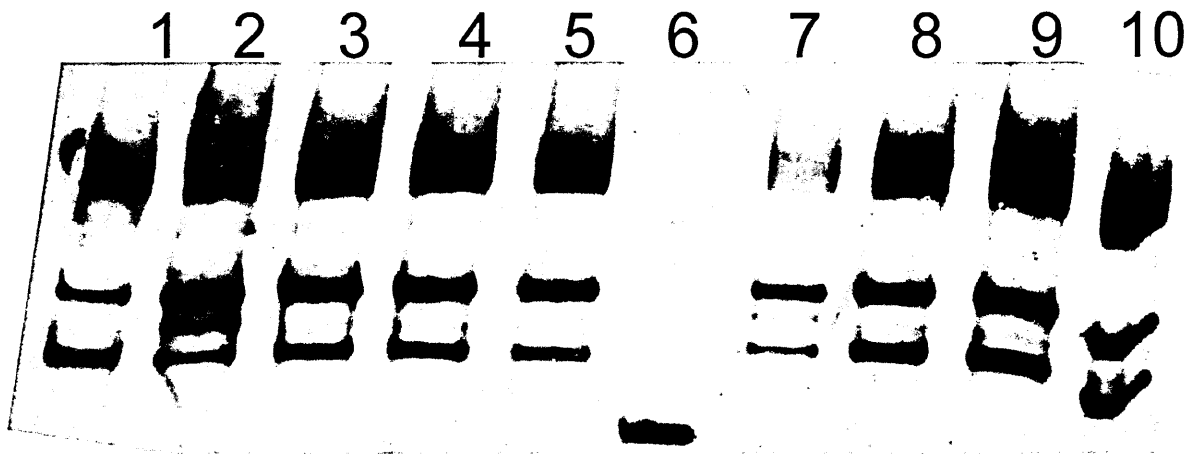


Fig 3.4.2.3.11 Gel shows PTEN exon 3 SSCP analysis of fresh bone marrow samples 96-104. Lane 6: Φ X174/*Hinf*I Ladder, lane 1-5 + 7-10: fresh bone marrow samples 96-104 respectively. (5cm section of 50cm PagePlus[®] gel, Silver stain, positive enhanced image).

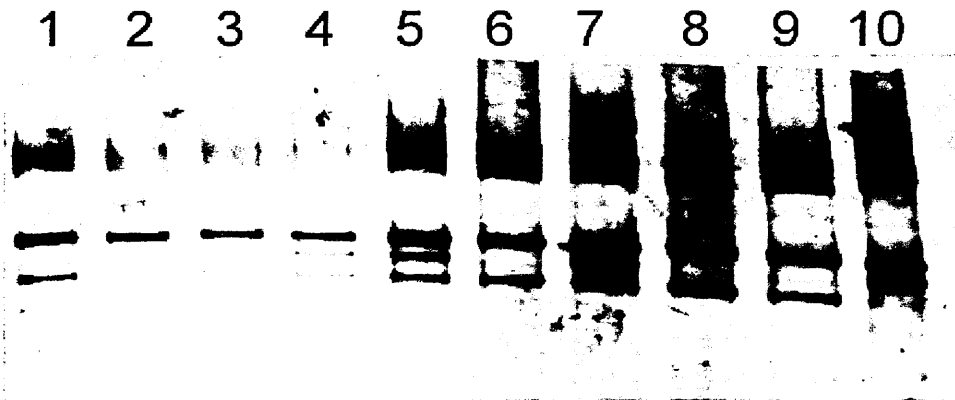


Fig 3.4.2.3.12 Gel shows PTEN exon 3 SSCP analysis of fresh bone marrow samples 105-114. Lane 1-10: fresh bone marrow samples 105-114 respectively. (5cm section of 50cm PagePlus[®] gel, Silver stain, positive enhanced image).

3.4.2.4 SSCP PTEN Exon 4

SSCP analysis of PTEN exon 4 showed good PCR product levels which yielded 2 or 3 main conformers on electrophoresis. The three main conformers were interspersed with a large number of faint bands, the staining intensity of these bands was proportional to the intensity of the three main conformers, the individual band showing the strongest stain varied from sample to sample with the two slowest migrating conformers usually the strongest. No aberrant migrating bands that would suggest the presence of a mutation were identified in the 114 samples screened but faint aberrant conformers could be masked by the background signal.

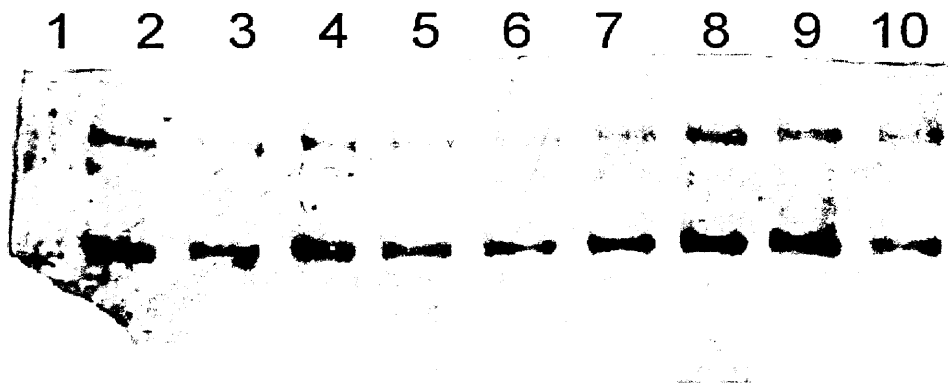


Fig 3.4.2.4.1 Gel shows PTEN exon 4 SSCP analysis of fresh bone marrow samples 1-9. Lane 1: Φ X174/*Hinf*I Ladder, lane 2-9: fresh bone marrow samples 1-9 respectively. (5cm section of 50cm PagePlus[®] gel, Silver stain, positive enhanced image).

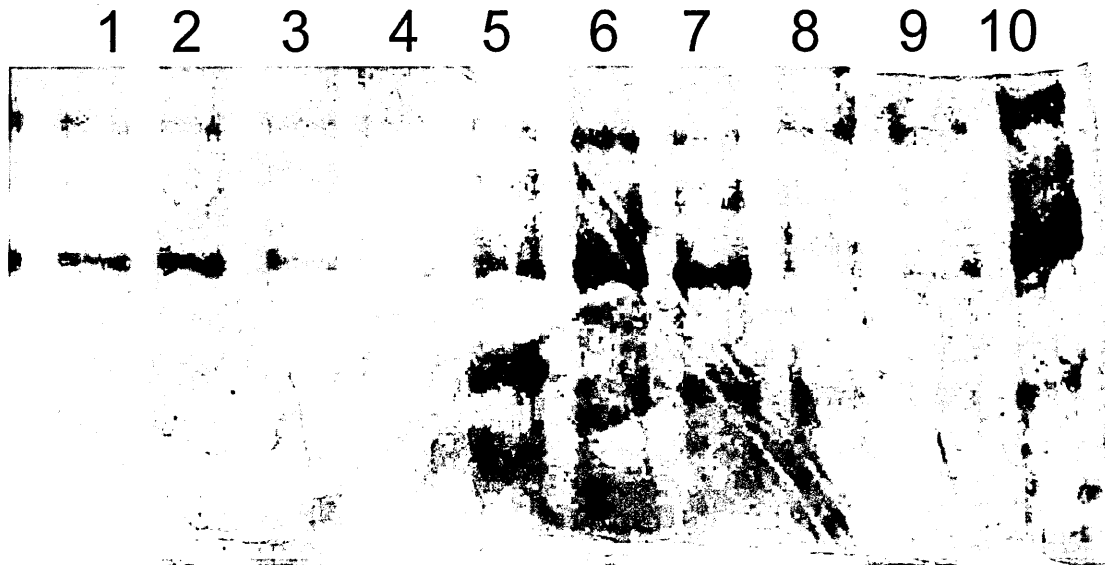


Fig 3.4.2.4.2 Gel shows PTEN exon 4 SSCP analysis of fresh bone marrow samples 10-19. Lane 1-10: fresh bone marrow samples 10-19 respectively. (5cm section of 50cm PagePlus[®] gel, Silver stain, positive enhanced image).

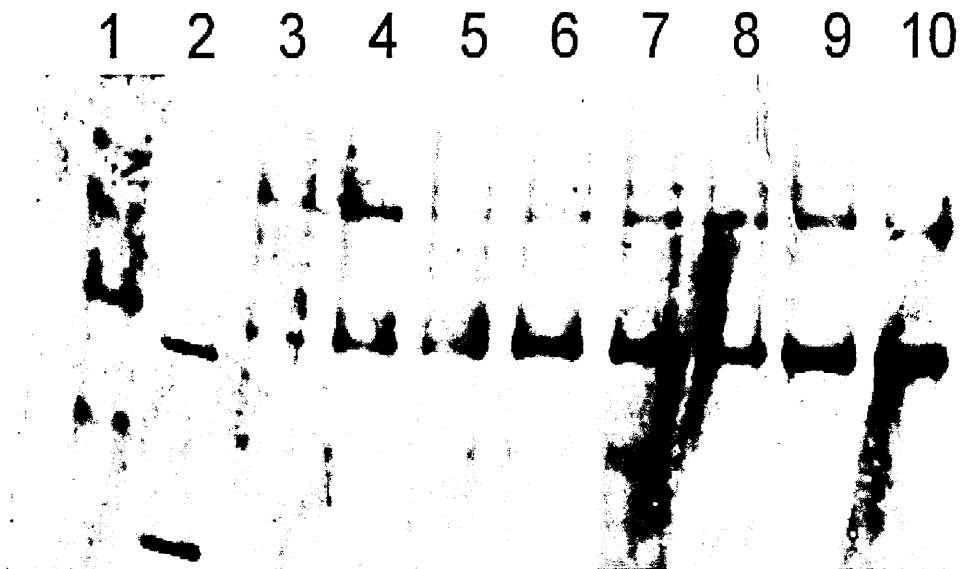


Fig 3.4.2.4.3 Gel shows PTEN exon 4 SSCP analysis of fresh bone marrow samples 20-28. Lane 2: Φ X174/*Hinf*I Ladder, lane 1+ 3-9: fresh bone marrow samples 20-28 respectively. (5cm section of 50cm PagePlus[®] gel, Silver stain, positive enhanced image).

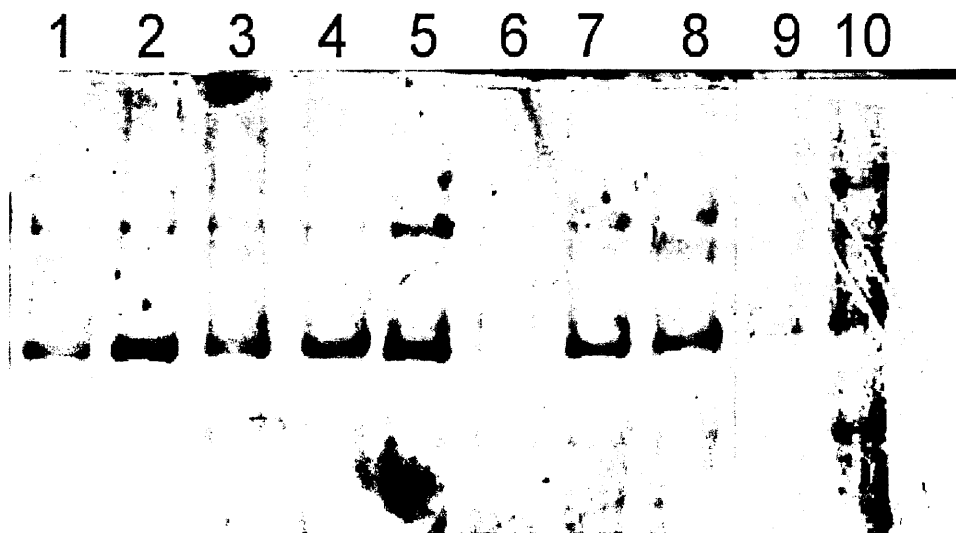


Fig 3.4.2.4.4 Gel shows PTEN exon 4 SSCP analysis of fresh bone marrow samples 29-38. Lane 1-10: fresh bone marrow samples 29-38 respectively. (5cm section of 50cm PagePlus[®] gel, Silver stain, positive enhanced image).

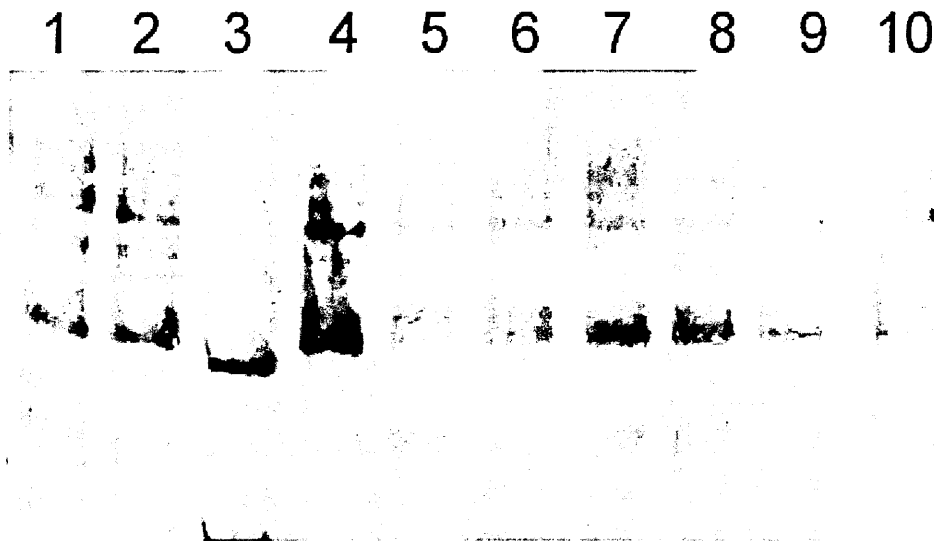


Fig 3.4.2.4.5 Gel shows PTEN exon 4 SSCP analysis of fresh bone marrow samples 39-47. Lane 3: Φ X174/*Hinf*I Ladder, lane 1-2+ 4-10: fresh bone marrow samples 39-47 respectively. (5cm section of 50cm PagePlus[®] gel, Silver stain, positive enhanced image).

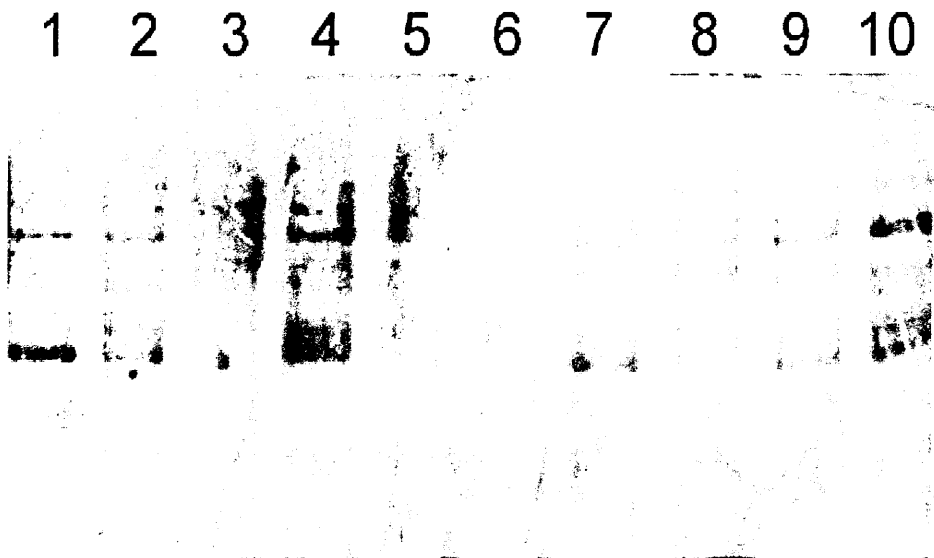


Fig 3.4.2.4.6 Gel shows PTEN exon 1 SSCP analysis of fresh bone marrow samples 48-57. Lane 1-10: fresh bone marrow samples 48-57 respectively. (5cm section of 50cm PagePlus[®] gel, Silver stain, positive enhanced image).



Fig 3.4.2.4.7 Gel shows PTEN exon 4 SSCP analysis of fresh bone marrow samples 58-66. Lane 4: Φ X174/*Hinf*I Ladder, lane 1-3+ 5-10: fresh bone marrow samples 58-66 respectively. (5cm section of 50cm PagePlus[®] gel, Silver stain, positive enhanced image).

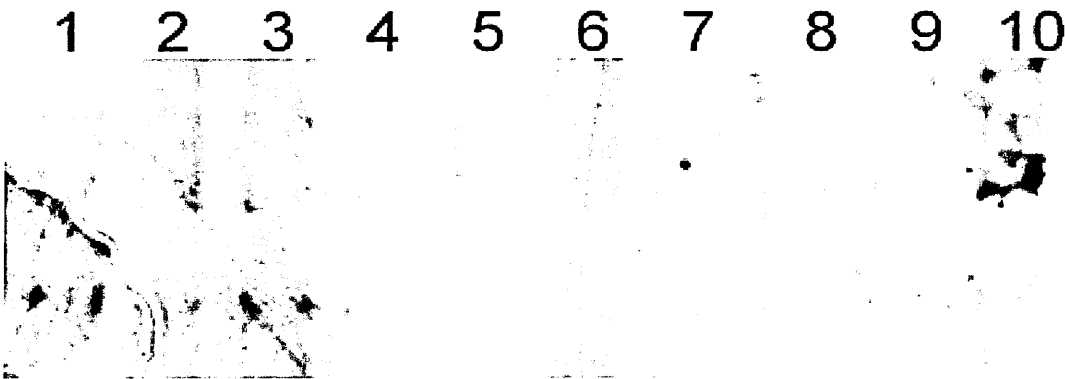


Fig 3.4.2.4.8 Gel shows PTEN exon 4 SSCP analysis of fresh bone marrow samples 67-76. Lane 1-10: fresh bone marrow samples 67-76 respectively. (5cm section of 50cm PagePlus[®] gel, Silver stain, positive enhanced image).

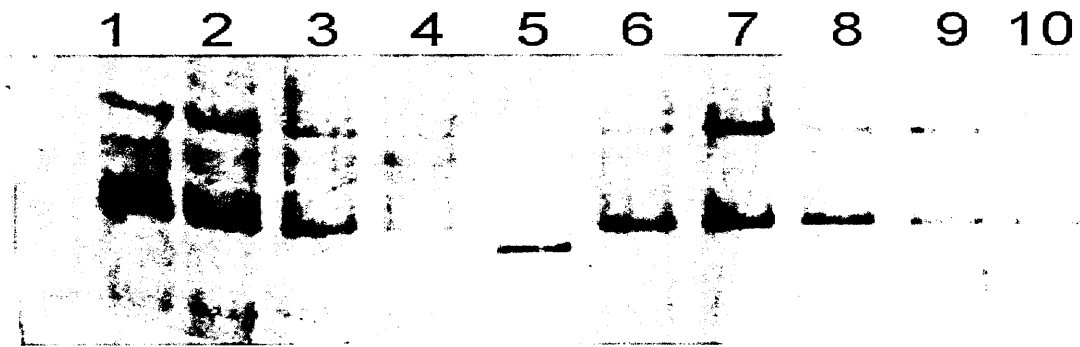


Fig 3.4.2.4.9 Gel shows PTEN exon4 SSCP analysis of fresh bone marrow samples 77-85. Lane 5: Φ X174/*Hinf*I Ladder, lane 1-4 + 5-10: fresh bone marrow samples 77-85 respectively. (5cm section of 50cm PagePlus[®] gel, Silver stain, positive enhanced image).

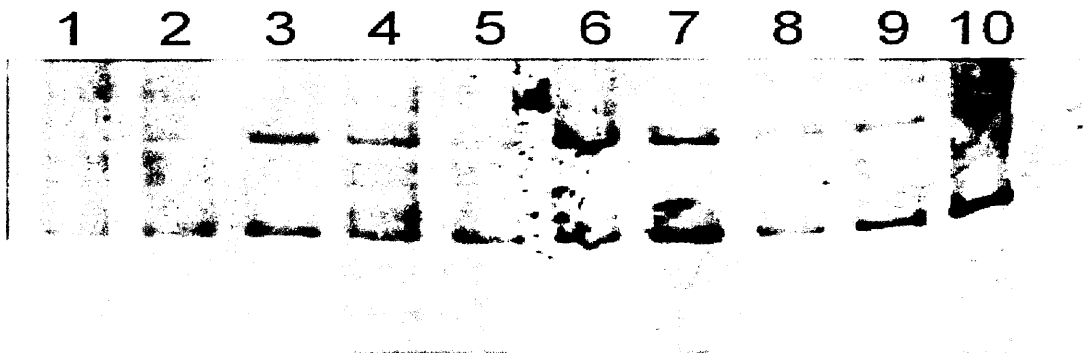


Fig 3.4.2.4.10 Gel shows PTEN exon 4 SSCP analysis of fresh bone marrow samples 86-95. Lane 1-10: fresh bone marrow samples 86-95 respectively. (5cm section of 50cm PagePlus[®] gel, Silver stain, positive enhanced image).



Fig 3.4.2.4.11 Gel shows PTEN exon 4 SSCP analysis of fresh bone marrow samples 96-104. Lane 6: Φ X174/*Hinf*I Ladder, lane 1-5 + 6-10: fresh bone marrow samples 96-104 respectively. (5cm section of 50cm PagePlus[®] gel, Silver stain, positive enhanced image).



Fig 3.4.2.4.12 Gel shows PTEN exon 4 SSCP analysis of fresh bone marrow samples 105-114. Lane 1-10: fresh bone marrow samples 105-114 respectively. (5cm section of 50cm PagePlus[®] gel, Silver stain, positive enhanced image).

3.4.2.5 SSCP PTEN Exon5

SSCP analysis of PTEN exon 5 showed good PCR product levels which yielded 6 conformers on electrophoresis. The conformers were composed of three clear bands interspersed with three fainter bands. As with previous exons, the staining intensity of these bands was proportional to the intensity of the three main conformers, the individual band showing the strongest stain was consistent from sample to sample with the two fastest and the slowest migrating conformers usually the strongest. Two aberrant migrating bands that would suggest the presence of a mutation were identified (Fig 3.4.2.5.13) in the 114 samples screened. Though six conformers were generated per sample, these were consistent throughout the samples and aberrant bands were easily identified. No faint background conformers were evident.

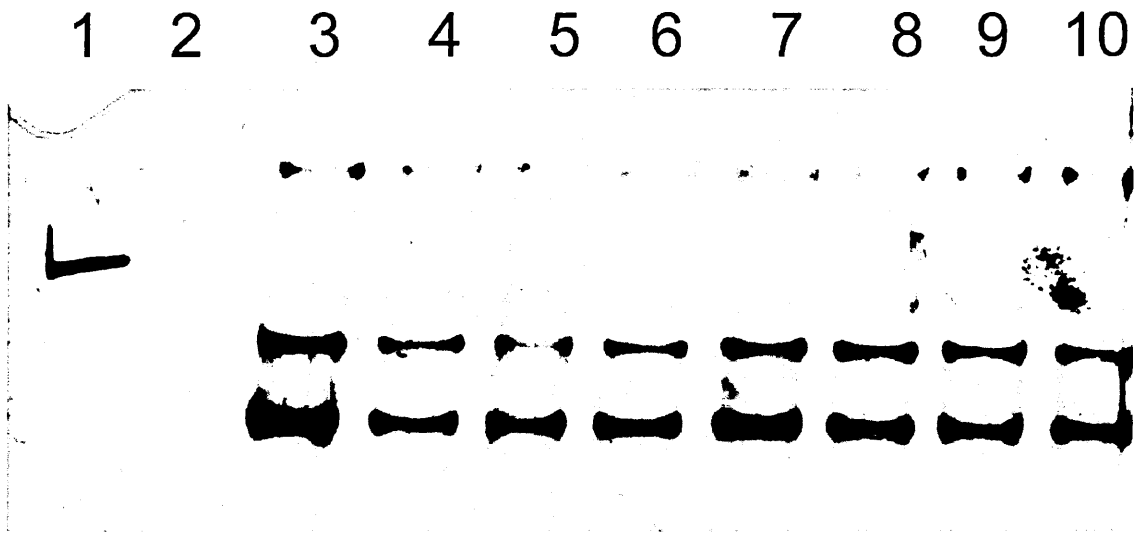


Fig 3.4.2.5.1 Gel shows PTEN exon 5 SSCP analysis of fresh bone marrow samples 1-9. Lane 1: Φ X174/*Hinf*I Ladder, lane 2-9: fresh bone marrow samples 1-9 respectively. (5cm section of 50cm PagePlus[®] gel, Silver stain, positive enhanced image).

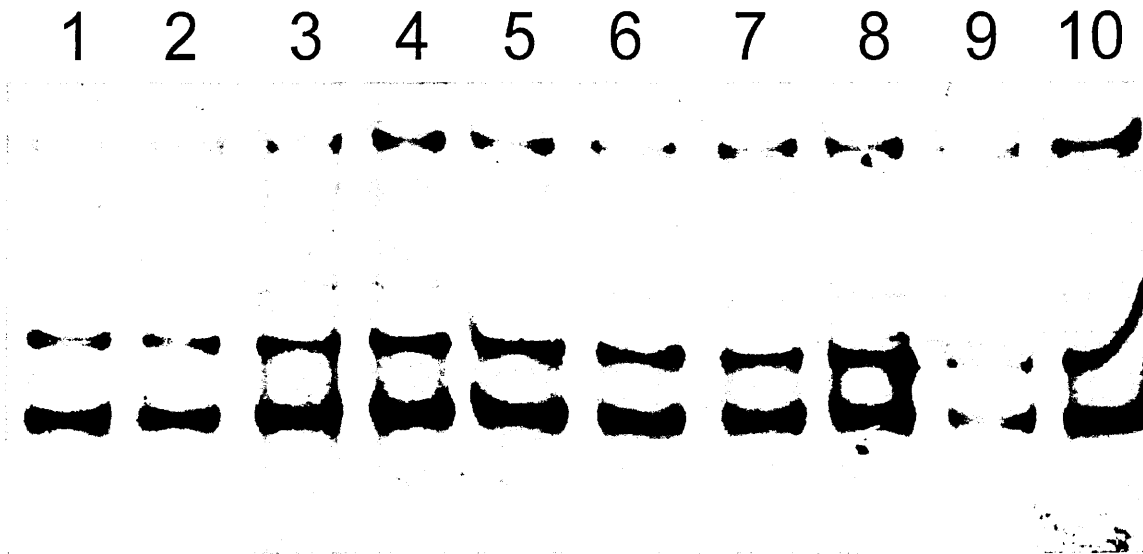
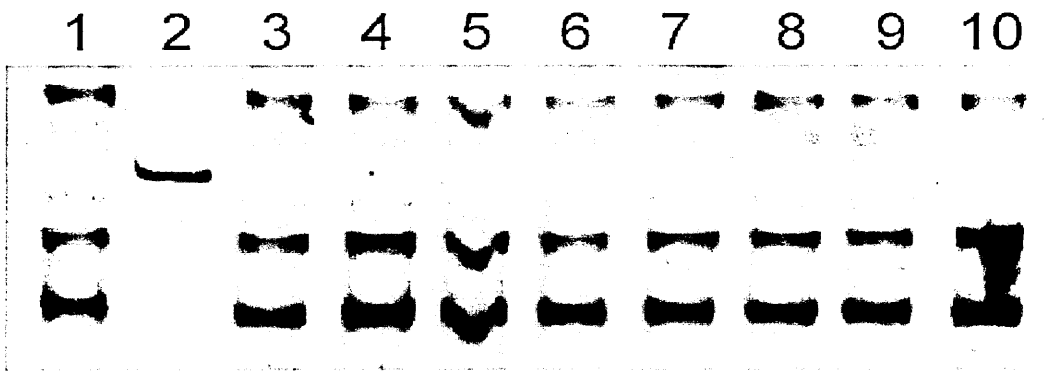


Fig 3.4.2.5.2 Gel shows PTEN exon 5 SSCP analysis of fresh bone marrow samples 10-19. Lane 1-10: fresh bone marrow samples 10-19 respectively. (5cm section of 50cm PagePlus[®] gel, Silver stain, positive enhanced image).



late 3.4.2.5.3 Gel shows PTEN exon 5 SSCP analysis of fresh bone marrow samples 20-28. Lane 2: Φ X174/*Hinf*I Ladder, lane 1+ 3-9: fresh bone marrow samples 20-28 respectively. (5cm section of 50cm PagePlus[®] gel, Silver stain, positive enhanced image).

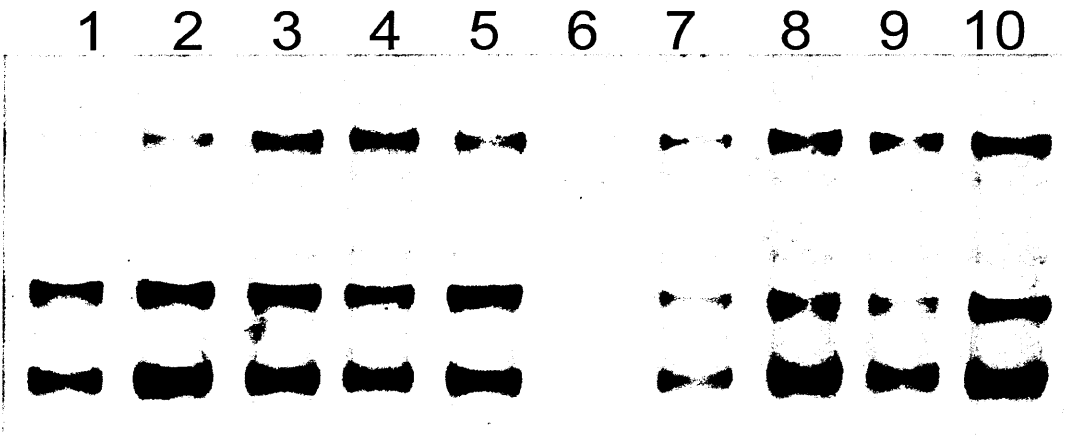


Fig 3.4.2.5.4 Gel shows PTEN exon 5 SSCP analysis of fresh bone marrow samples 29-38. Lane 1-10: fresh bone marrow samples 29-38 respectively. (5cm section of 50cm PagePlus[®] gel, Silver stain, positive enhanced image).

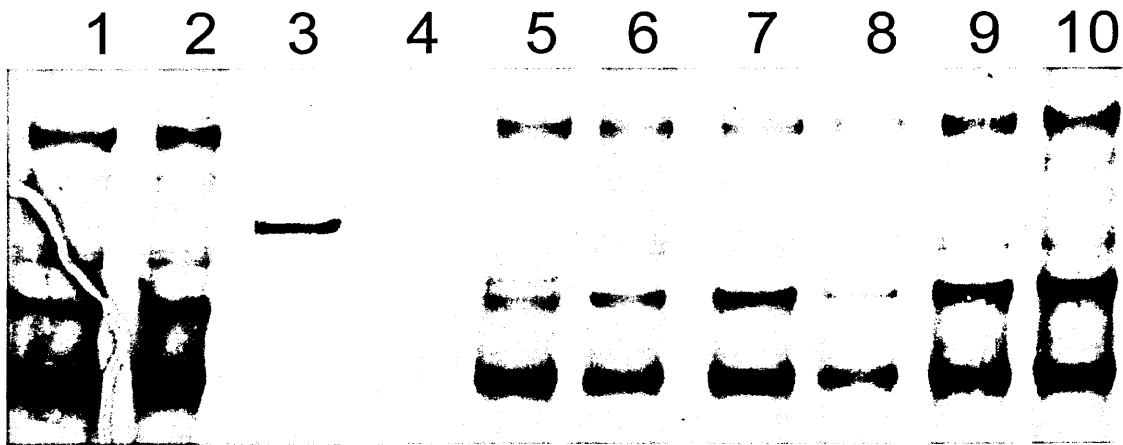


Fig 3.4.2.5.5 Gel shows PTEN exon 5 SSCP analysis of fresh bone marrow samples 39-47. Lane 3: Φ X174/*Hinf*I Ladder, lane 1-2+ 4-10: fresh bone marrow samples 39-47 respectively. (5cm section of 50cm PagePlus[®] gel, Silver stain, positive enhanced image).

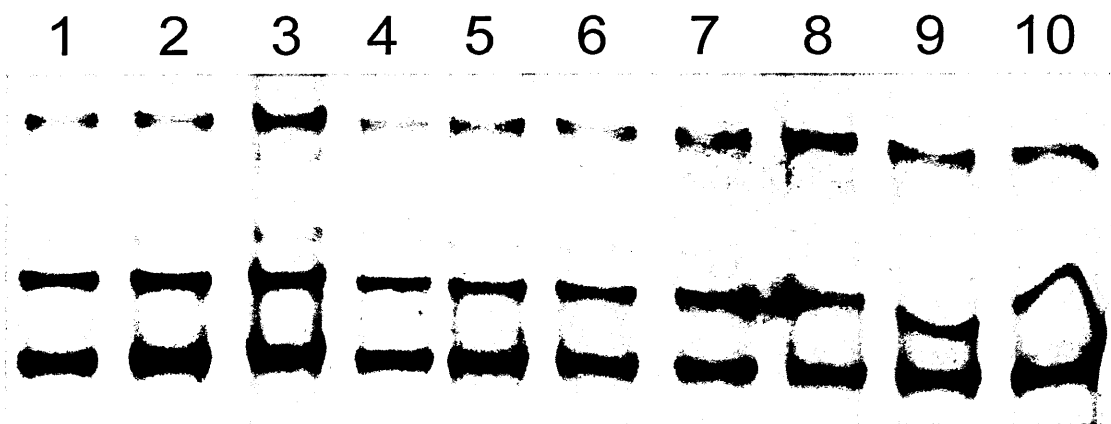


Fig 3.4.2.5.6 Gel shows PTEN exon 5 SSCP analysis of fresh bone marrow samples 48-57. Lane 1-10: fresh bone marrow samples 48-57 respectively. (5cm section of 50cm PagePlus[®] gel, Silver stain, positive enhanced image).

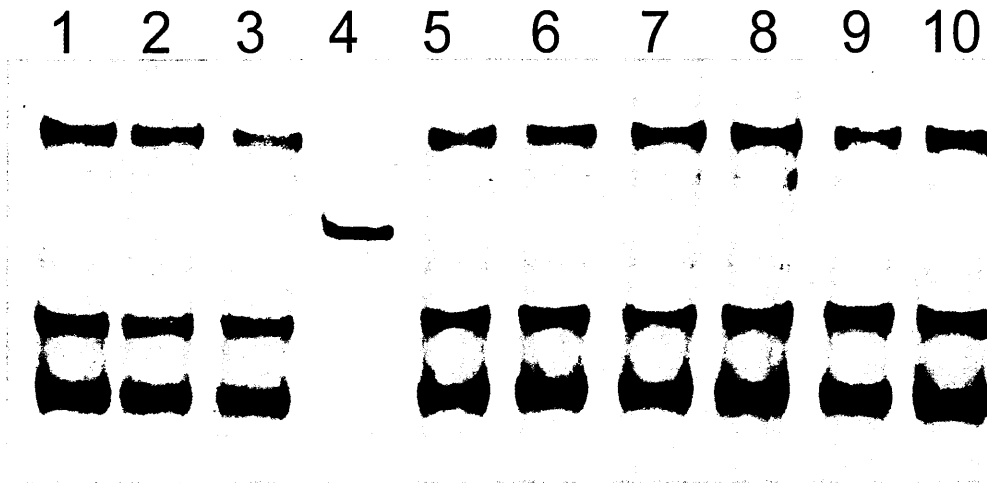


Fig 3.4.2.5.7 Gel shows PTEN exon 5 SSCP analysis of fresh bone marrow samples 58-66. Lane 4: Φ X174/*Hinf*I Ladder, lane 1-3+ 5-10: fresh bone marrow samples 58-66 respectively. (5cm section of 50cm PagePlus[®] gel, Silver stain, positive enhanced image).

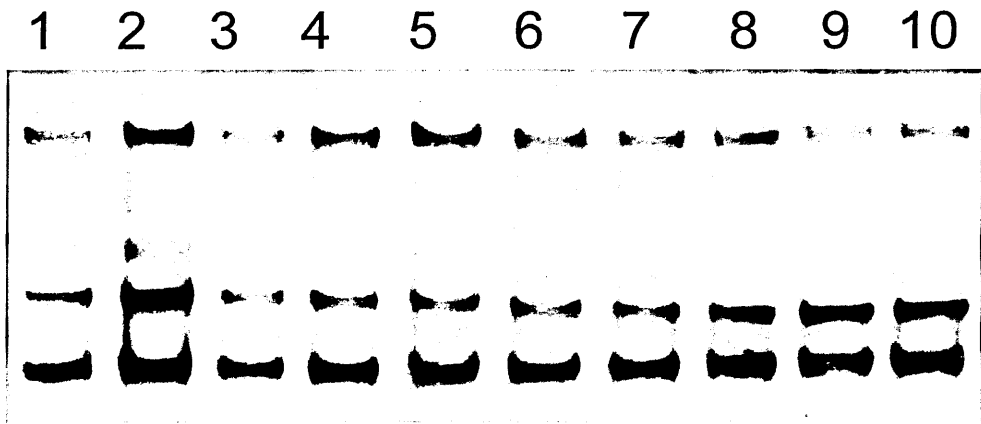


Fig 3.4.2.5.8 Gel shows PTEN exon 5 SSCP analysis of fresh bone marrow samples 67-76. Lane 1-10: fresh bone marrow samples 67-76 respectively. (5cm section of 50cm PagePlus[®] gel, Silver stain, positive enhanced image).

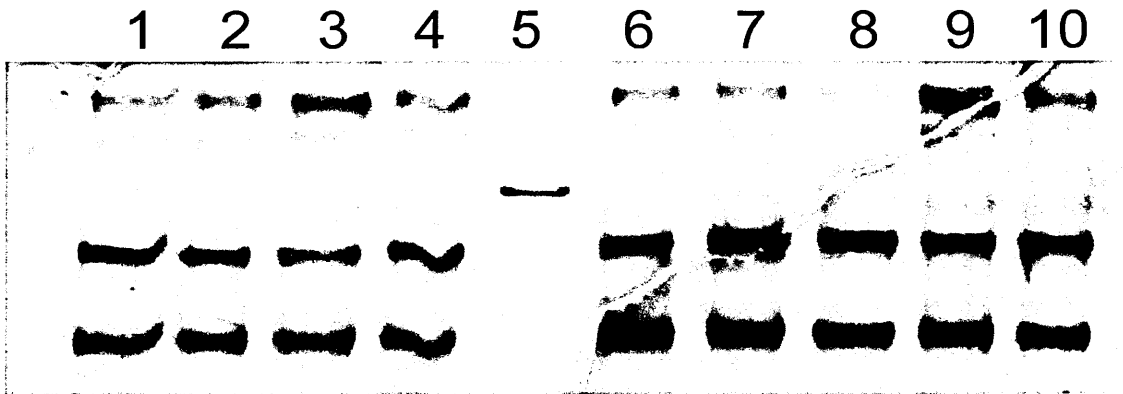


Fig 3.4.2.5.9 Gel shows PTEN exon 5 SSCP analysis of fresh bone marrow samples 77-85. Lane 5: Φ X174/*Hinf*I Ladder, lane 1-4 + 6-10: fresh bone marrow samples 77-85 respectively. (5cm section of 50cm PagePlus[®] gel, Silver stain, positive enhanced image).

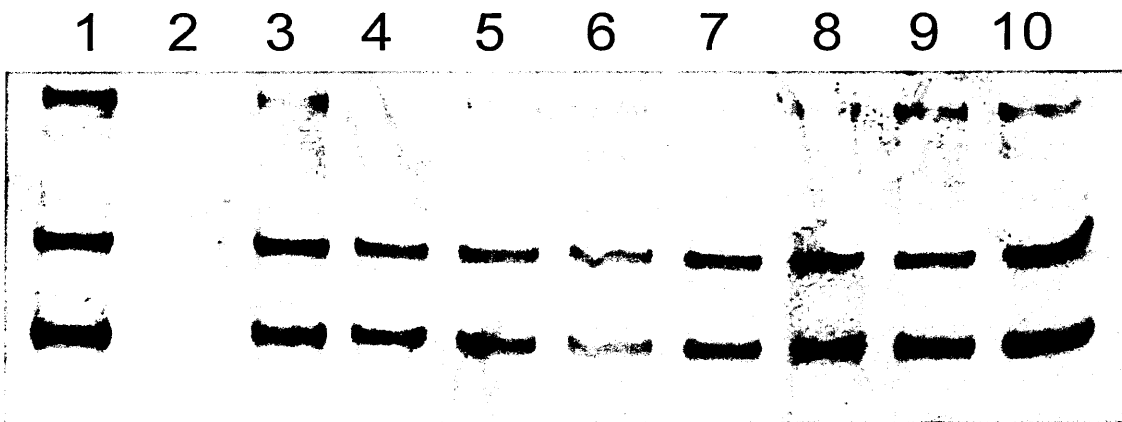


Fig 3.4.2.5.10 Gel shows PTEN exon 5 SSCP analysis of fresh bone marrow samples 86-95. Lane 1-10: fresh bone marrow samples 86-95 respectively. (5cm section of 50cm PagePlus[®] gel, Silver stain, positive enhanced image).

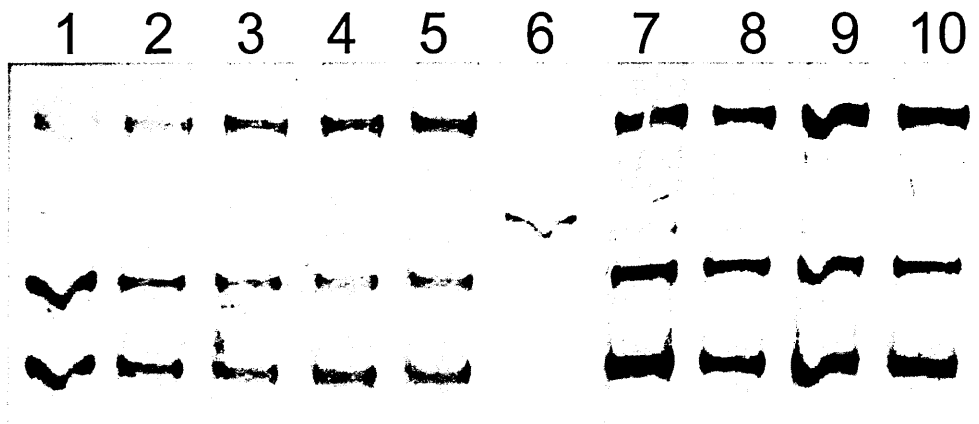


Fig 3.4.2.5.11 Gel shows PTEN exon 5 SSCP analysis of fresh bone marrow samples 96-104. Lane 6: Φ X174/*Hinf*I Ladder, lane 1-5 + 7-10: fresh bone marrow samples 96-104 respectively. (5cm section of 50cm PagePlus[®] gel, Silver stain, positive enhanced image).

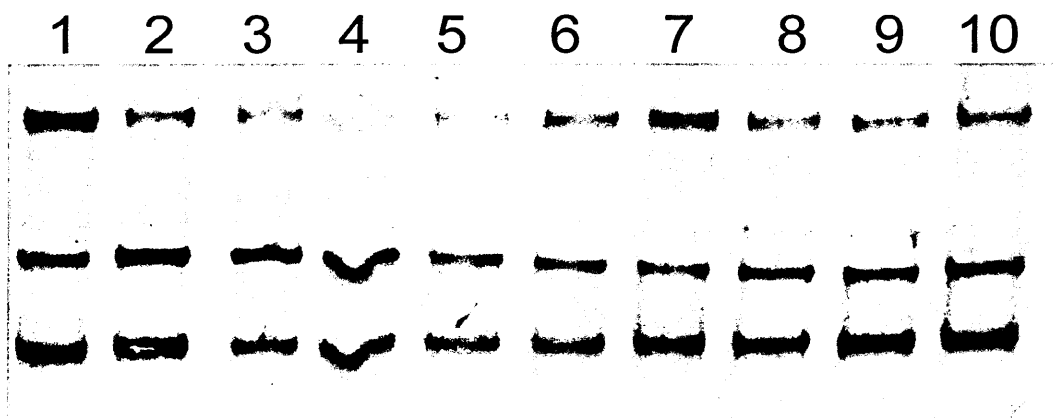


Fig 3.4.2.5.12 Gel shows PTEN exon 5 SSCP analysis of fresh bone marrow samples 105-114. Lane 1-10: fresh bone marrow samples 105-114 respectively. (5cm section of 50cm PagePlus[®] gel, Silver stain, positive enhanced image).

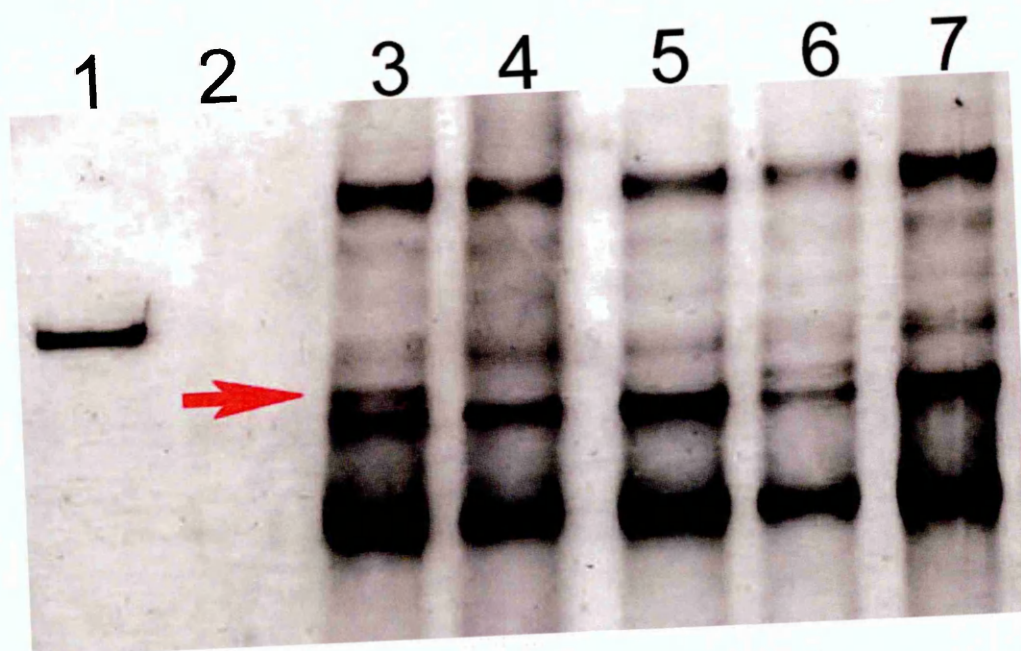


Fig 3.4.2.5.13 SSCP PTEN exon 5 samples 42 & 45, in lanes 3 and 6 respectively - detail of aberrant bands (arrowed)

3.4.2.6 SSCP PTEN Exon6

SSCP analysis of PTEN exon 6 showed good PCR product levels which yielded 2 conformers on electrophoresis. The conformers were composed of two clear bands occasionally interspersed with one fainter band in stronger staining samples. As with previous exons, the staining intensity of these bands was proportional to the intensity of the main conformers, The two main conformers were stained with equal intensity. No aberrant migrating bands that would suggest the presence of a mutation were identified in the 114 samples screened. The two conformers present with this exon were very clear and aberrant conformers would have been seen easily. No faint background conformers were evident.

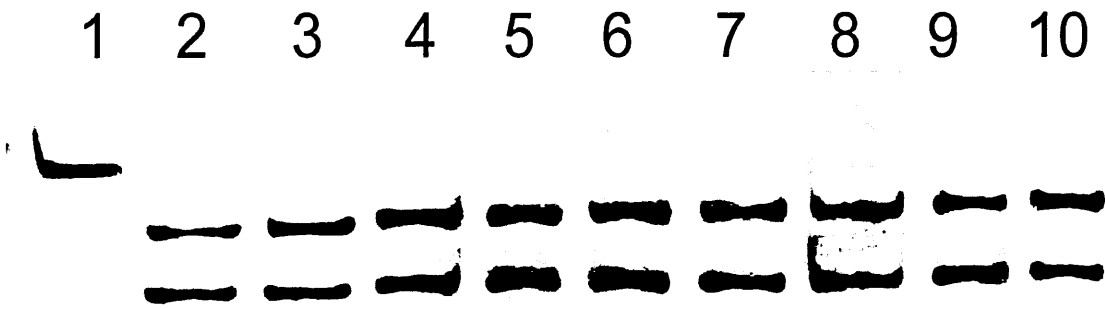


Fig 3.4.2.6.1 Gel shows PTEN exon 6 SSCP analysis of fresh bone marrow samples 1-9. Lane 1: Φ X174/*Hinf*I Ladder, lane 2-9: fresh bone marrow samples 1-9 respectively. (5cm section of 50cm PagePlus[®] gel, Silver stain, positive enhanced image).

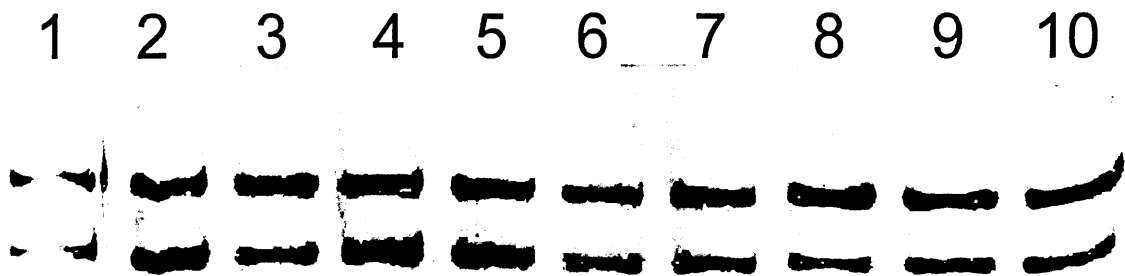


Fig 3.4.2.6.2 Gel shows PTEN exon 6 SSCP analysis of fresh bone marrow samples 10-19. Lane 1-10: fresh bone marrow samples 10-19 respectively. (5cm section of 50cm PagePlus[®] gel, Silver stain, positive enhanced image).

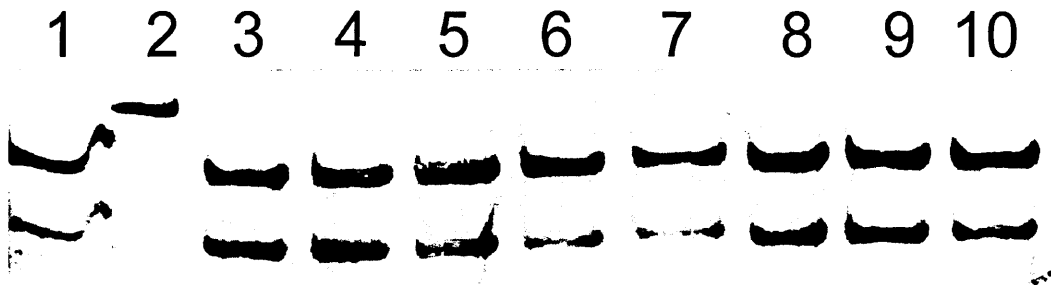


Fig 3.4.2.6.3 Gel shows PTEN exon 6 SSCP analysis of fresh bone marrow samples 20-28. Lane 2: Φ X174/*Hinf*I Ladder, lane 1+ 3-9: fresh bone marrow samples 20-28 respectively. (5cm section of 50cm PagePlus[®] gel, Silver stain, positive enhanced image).

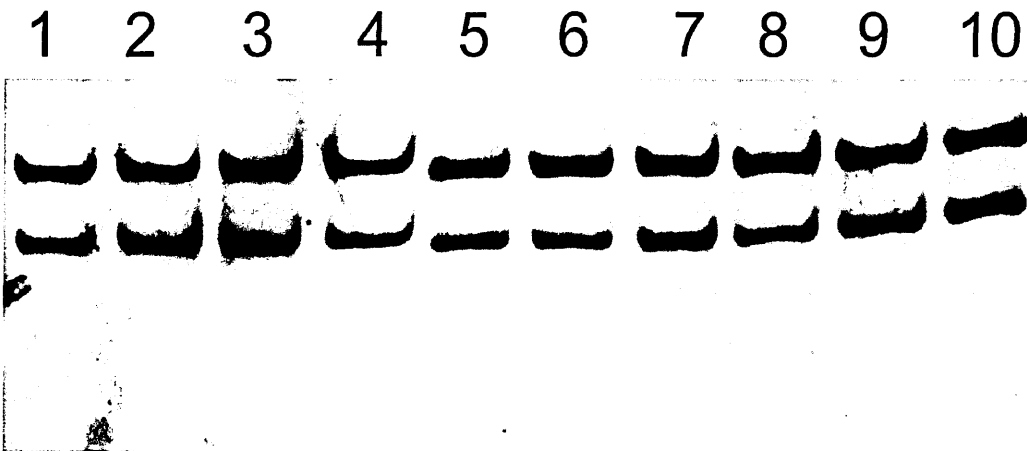


Fig 3.4.2.6.4 Gel shows PTEN exon 6 SSCP analysis of fresh bone marrow samples 29-38. Lane 1-10: fresh bone marrow samples 29-38 respectively. (5cm section of 50cm PagePlus[®] gel, Silver stain, positive enhanced image).

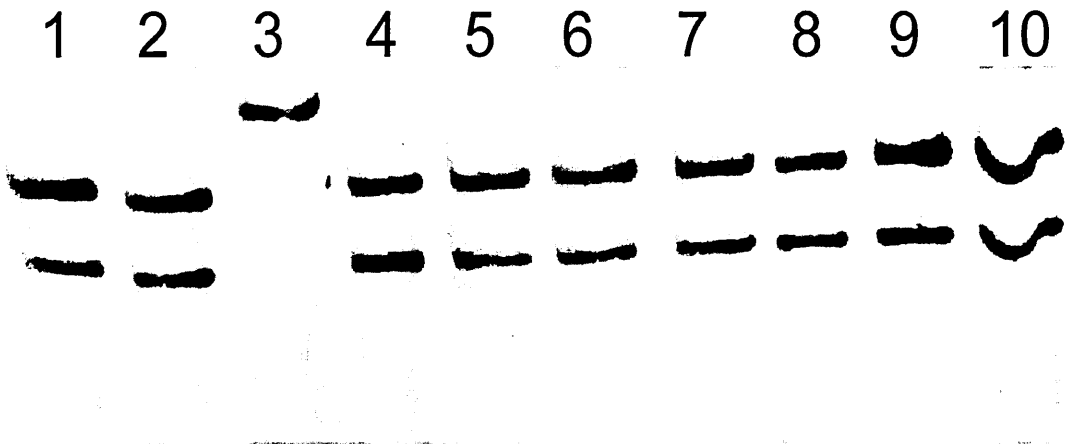


Fig 3.4.2.6.5 Gel shows PTEN exon 6 SSCP analysis of fresh bone marrow samples 39-47. Lane 3: Φ X174/*Hinf*I Ladder, lane 1-2+ 4-10: fresh bone marrow samples 39-47 respectively. (5cm section of 50cm PagePlus[®] gel, Silver stain, positive enhanced image).

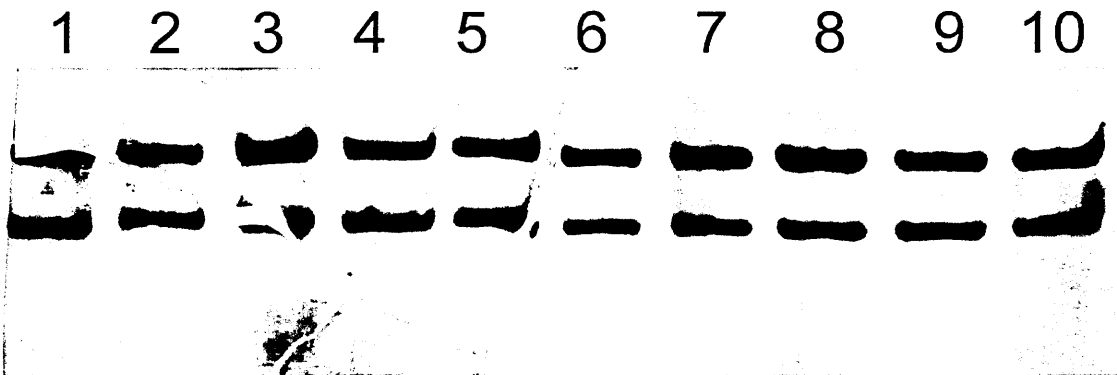


Fig 3.4.2.6.6 Gel shows PTEN exon 6 SSCP analysis of fresh bone marrow samples 48-57. Lane 1-10: fresh bone marrow samples 48-57 respectively. (5cm section of 50cm PagePlus[®] gel, Silver stain, positive enhanced image).

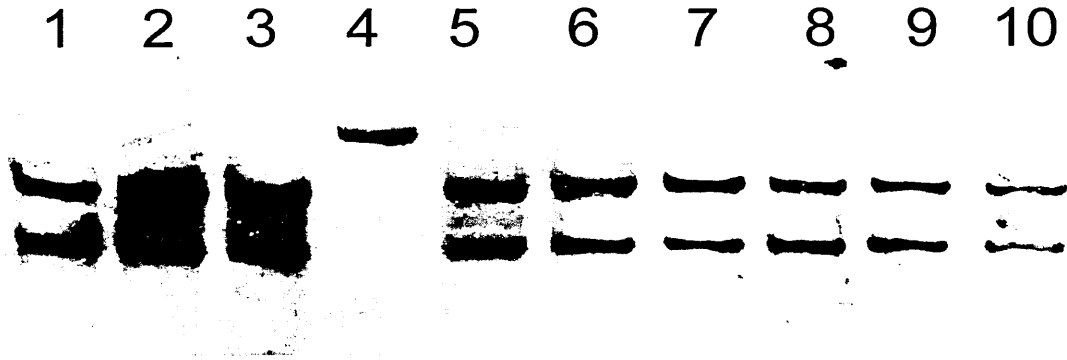


Fig 3.4.2.6.7 Gel shows PTEN exon 6 SSCP analysis of fresh bone marrow samples 58-66. Lane 4: Φ X174/*Hinf*I Ladder, lane 1-3+ 5-10: fresh bone marrow samples 58-66 respectively. (5cm section of 50cm PagePlus[®] gel, Silver stain, positive enhanced image).

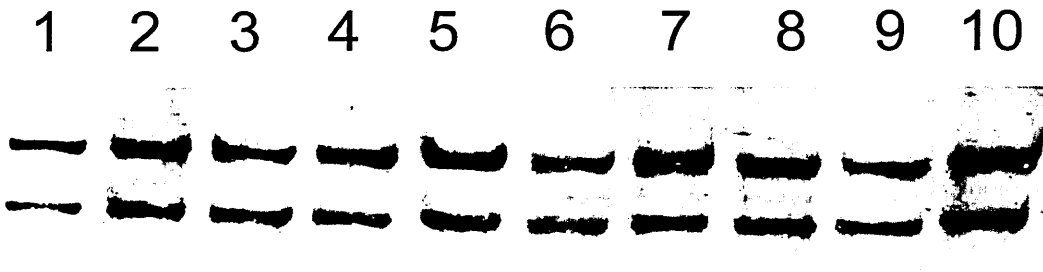


Fig 3.4.2.6.8 Gel shows PTEN exon 6 SSCP analysis of fresh bone marrow samples 67-76. Lane 1-10: fresh bone marrow samples 67-76 respectively. (5cm section of 50cm PagePlus[®] gel, Silver stain, positive enhanced image).

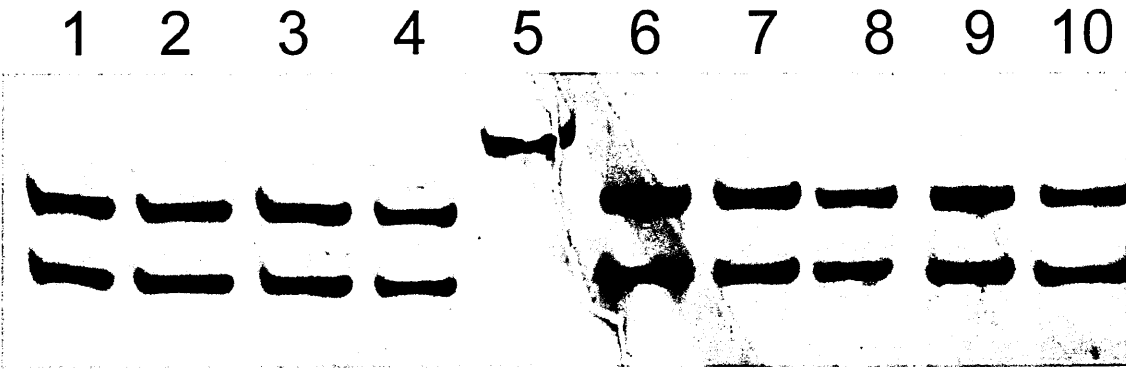


Fig 3.4.2.6.9 Gel shows PTEN exon 6 SSCP analysis of fresh bone marrow samples 77-85. Lane 5: Φ X174/*Hinf*I Ladder, lane 1-4 + 6-10: fresh bone marrow samples 77-85 respectively. (5cm section of 50cm PagePlus[®] gel, Silver stain, positive enhanced image).

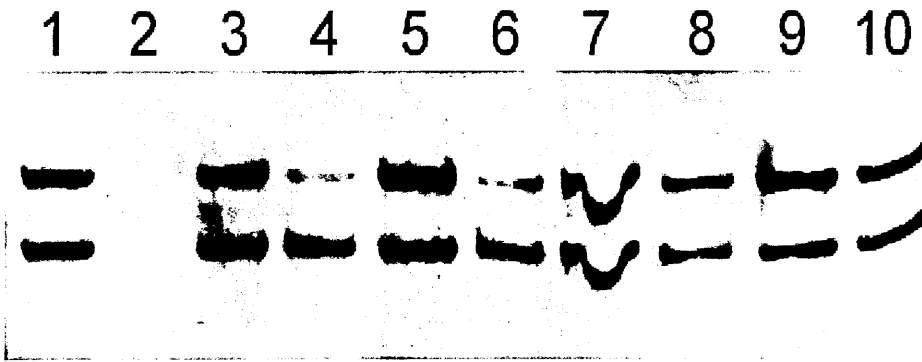


Fig 3.4.2.6.10 Gel shows PTEN exon 6 SSCP analysis of fresh bone marrow samples 86-95. Lane 1-10: fresh bone marrow samples 86-95 respectively. (5cm section of 50cm PagePlus[®] gel, Silver stain, positive enhanced image).

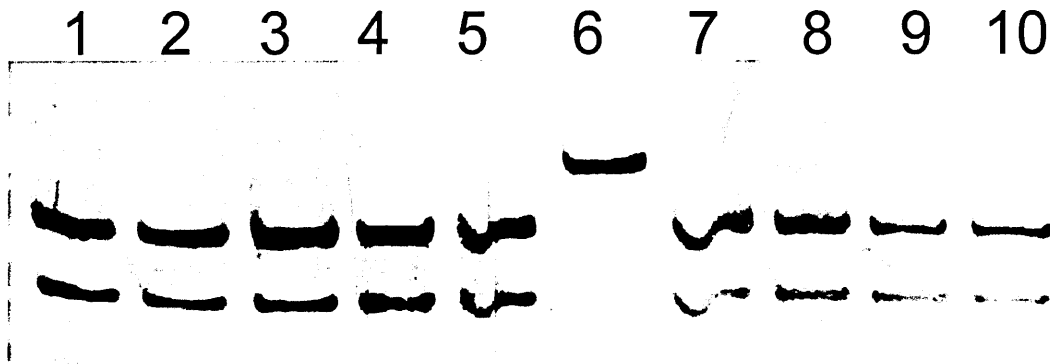


Fig 3.4.2.6.11 Gel shows PTEN exon 6 SSCP analysis of fresh bone marrow samples 96-104. Lane 6: Φ X174/HinI Ladder, lane 1-5 + 7-10: fresh bone marrow samples 96-104 respectively. (5cm section of 50cm PagePlus[®] gel, Silver stain, positive enhanced image).

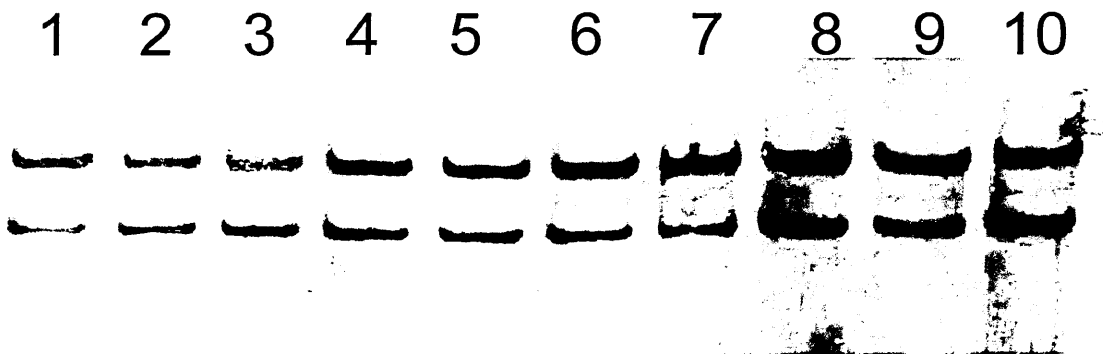


Fig 3.4.2.6.12 Gel shows PTEN exon 6 SSCP analysis of fresh bone marrow samples 105-114. Lane 1-10: fresh bone marrow samples 105-114 respectively. (5cm section of 50cm PagePlus[®] gel, Silver stain, positive enhanced image).

3.4.2.7 SSCP PTEN Exon 7

SSCP analysis of PTEN exon 7 showed good PCR product levels which yielded 4 conformers on electrophoresis. The conformers were composed of two clear bands sandwiched between with one faint, faster migrating band and one faint, slower migrating band. As with previous exons, the staining intensity of these bands was proportional to the intensity of the main conformers, The two main conformers were stained with equal intensity. No aberrant migrating bands that would suggest the presence of a mutation were identified in the 114 samples screened. The four conformers present with this exon were very clear and aberrant conformers would have been seen easily as shown by the positive control in Fig 3.4.2.7.10. No faint background conformers were evident outside of the four main bands.

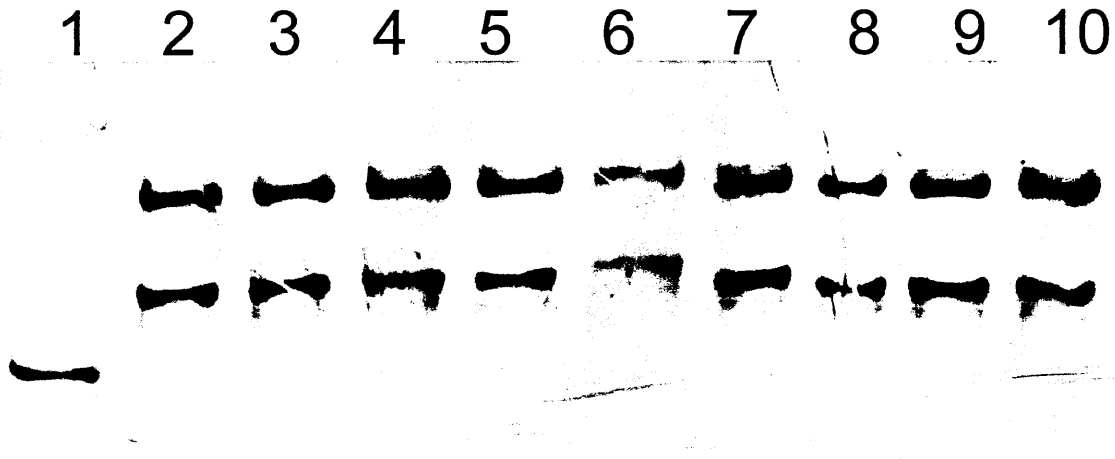


Fig 3.4.2.7.1 Gel shows PTEN exon 7 SSCP analysis of fresh bone marrow samples 1-9. Lane 1: Φ X174/*Hinf*I Ladder, lane 2-9: fresh bone marrow samples 1-9 respectively. (5cm section of 50cm PagePlus[®] gel, Silver stain, positive enhanced image).

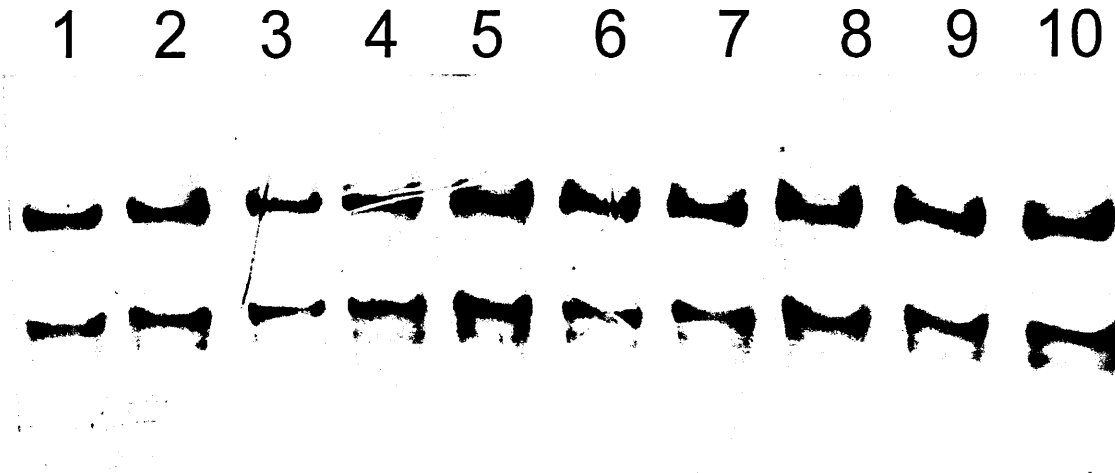


Fig 3.4.2.7.2 Gel shows PTEN exon 7 SSCP analysis of fresh bone marrow samples 10-19. Lane 1-10: fresh bone marrow samples 10-19 respectively. (5cm section of 50cm PagePlus[®] gel, Silver stain, positive enhanced image).

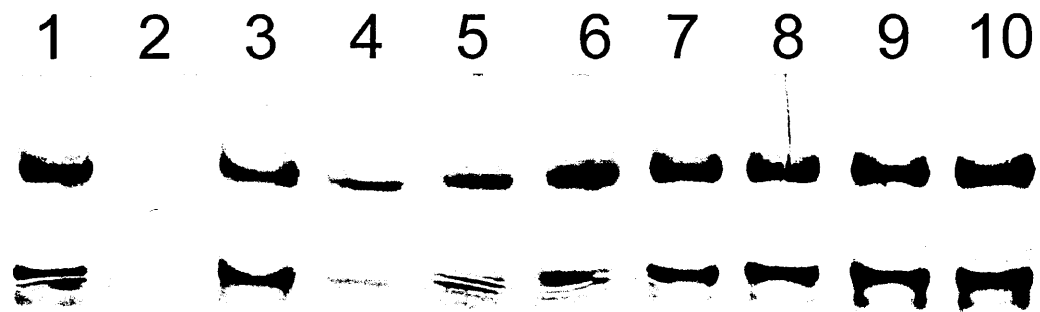


Fig 3.4.2.7.3 Gel shows PTEN exon 7 SSCP analysis of fresh bone marrow samples 20-28. Lane 2: Φ X174/*Hinf*I Ladder, lane 1+ 3-9: fresh bone marrow samples 20-28 respectively. (5cm section of 50cm PagePlus[®] gel, Silver stain, positive enhanced image).

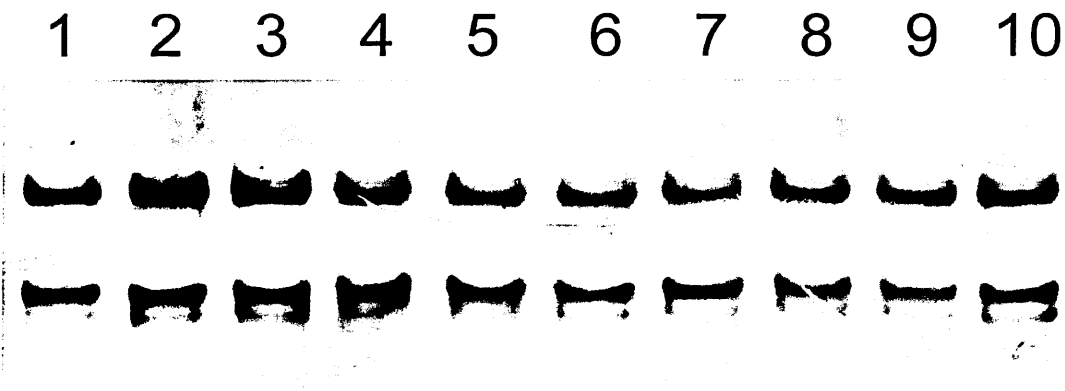


Fig 3.4.2.7.4 Gel shows PTEN exon 7 SSCP analysis of fresh bone marrow samples 29-38. Lane 1-10: fresh bone marrow samples 29-38 respectively. (5cm section of 50cm PagePlus[®] gel, Silver stain, positive enhanced image).

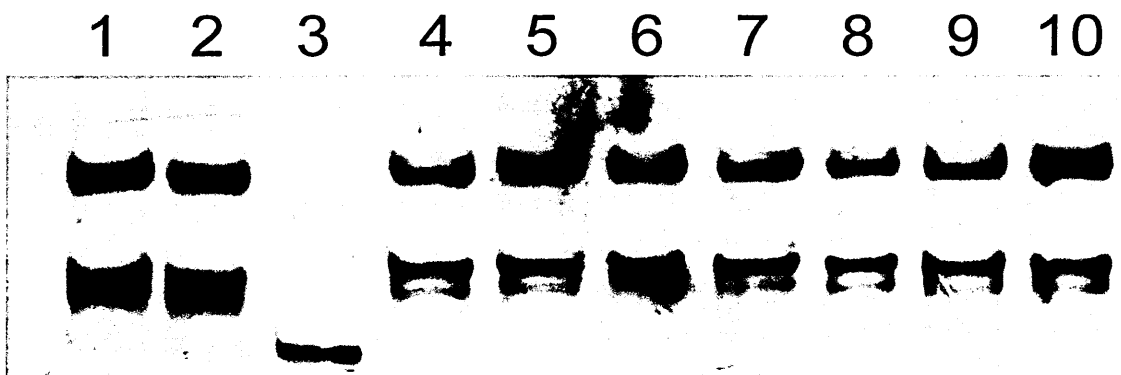


Fig 3.4.2.7.5 Gel shows PTEN exon 7 SSCP analysis of fresh bone marrow samples 39-47. Lane 3: Φ X174/*Hinf*I Ladder, lane 1-2+ 4-10: fresh bone marrow samples 39-47 respectively. (5cm section of 50cm PagePlus[®] gel, Silver stain, positive enhanced image).

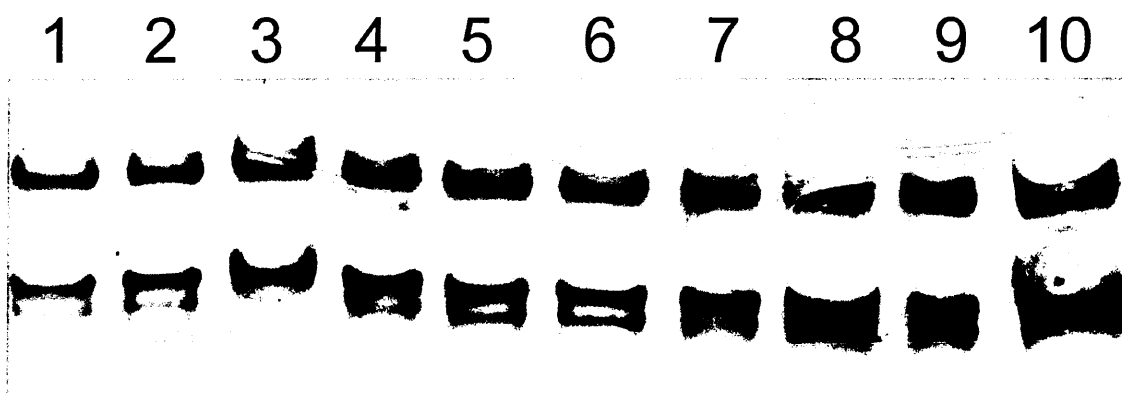


Fig 3.4.2.7.6 Gel shows PTEN exon 7 SSCP analysis of fresh bone marrow samples 48-57. Lane 1-10: fresh bone marrow samples 48-57 respectively. (5cm section of 50cm PagePlus[®] gel, Silver stain, positive enhanced image).

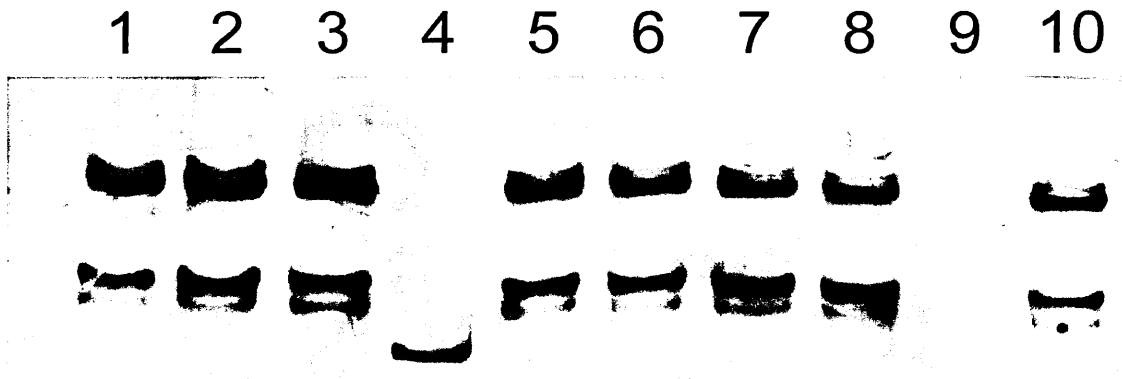


Fig 3.4.2.7.7 Gel shows PTEN exon 7 SSCP analysis of fresh bone marrow samples 58-66. Lane 4: Φ X174/*Hinf*I Ladder, lane 1-3+ 5-10: fresh bone marrow samples 58-66 respectively. (5cm section of 50cm PagePlus[®] gel, Silver stain, positive enhanced image).

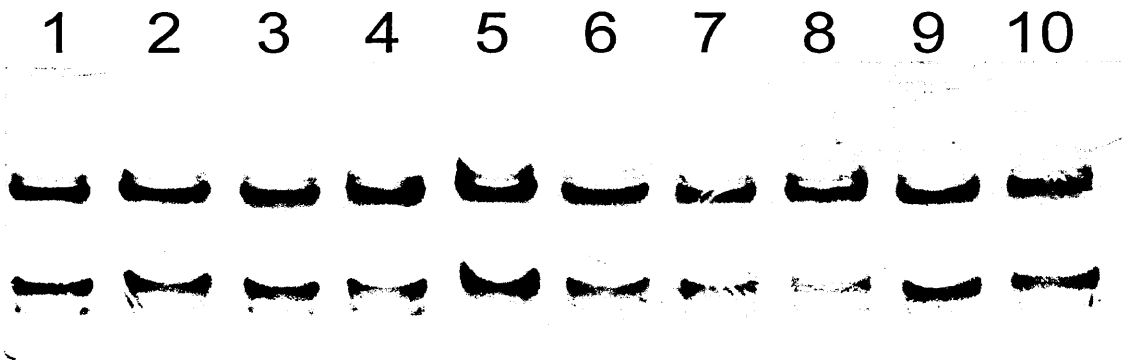


Fig 3.4.2.7.8 Gel shows PTEN exon 7 SSCP analysis of fresh bone marrow samples 67-76. Lane 1-10: fresh bone marrow samples 67-76 respectively. (5cm section of 50cm PagePlus[®] gel, Silver stain, positive enhanced image).

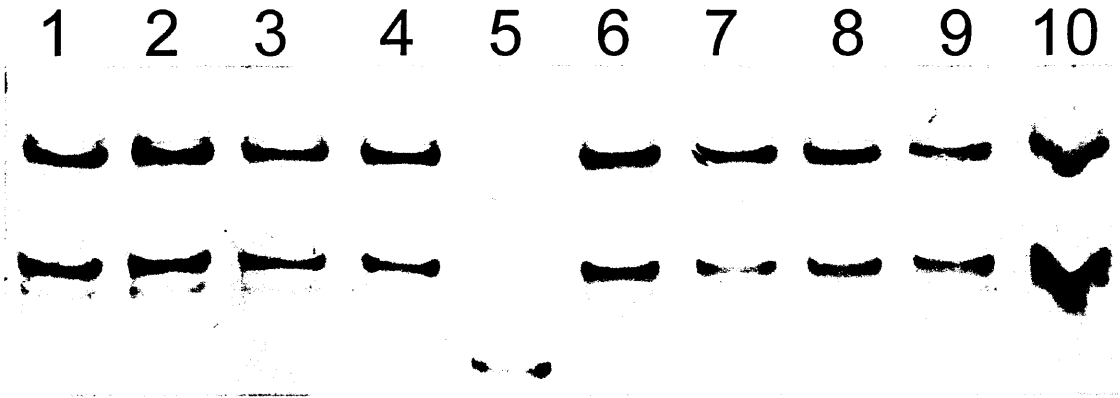


Fig 3.4.2.7.9 Gel shows PTEN exon 7 SSCP analysis of fresh bone marrow samples 77-85. Lane 5: Φ X174/*Hinf*I Ladder, lane 1-4 + 6-10: fresh bone marrow samples 77-85 respectively. (5cm section of 50cm PagePlus[®] gel, Silver stain, positive enhanced image).

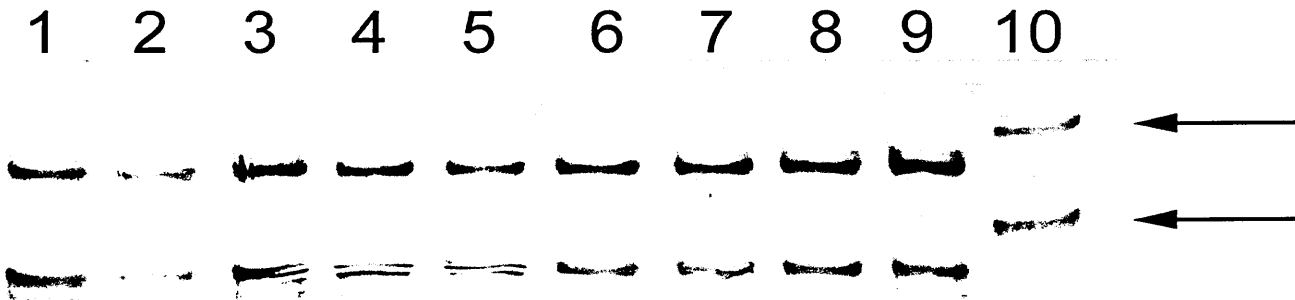


Fig 3.4.2.7.10 Gel shows PTEN exon 7 SSCP analysis of fresh bone marrow samples 86-94. Lane 1-9: fresh bone marrow samples 86-94 respectively. Lane 10: PTEN SSCP control (arrowed). (5cm section of 50cm PagePlus[®] gel, Silver stain, positive enhanced image). Note: sample 95 excluded from exon 7 study

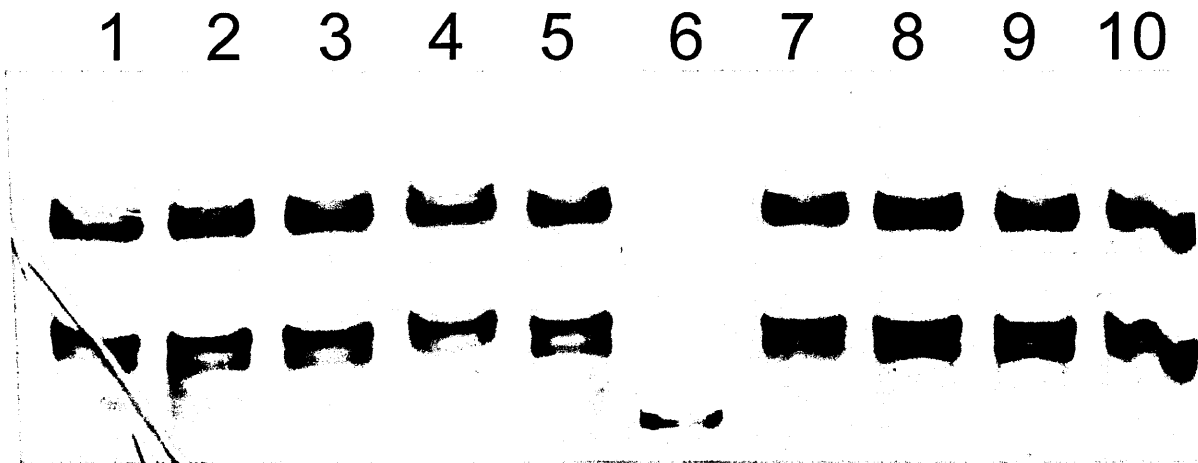


Fig 3.4.2.7.11 Gel shows PTEN exon 7 SSCP analysis of fresh bone marrow samples 96-104. Lane 6: Φ X174/*Hinf*I Ladder, lane 1-5 + 7-10: fresh bone marrow samples 96-104 respectively. (5cm section of 50cm PagePlus[®] gel, Silver stain, positive enhanced image).

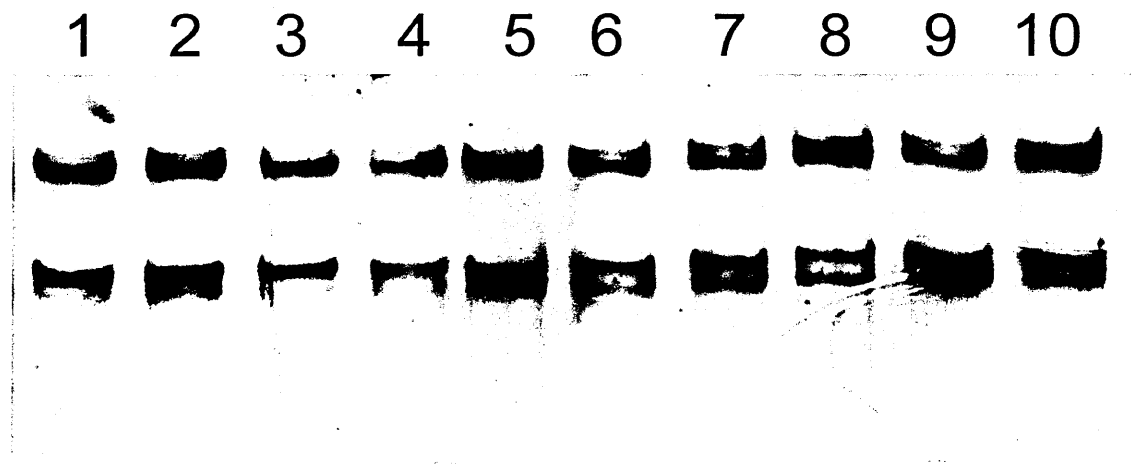


Fig 3.4.2.7.12 Gel shows PTEN exon 7 SSCP analysis of fresh bone marrow samples 105-114. Lane 1-10: fresh bone marrow samples 105-114 respectively. (5cm section of 50cm PagePlus[®] gel, Silver stain, positive enhanced image).

3.4.2.8 SSCP PTEN Exon 8

SSCP analysis of PTEN exon 8 showed good PCR product levels which yielded 2 conformers on electrophoresis. The conformers were composed of two clear bands with the slowest migrating band showing stronger staining. As with previous exons, the staining intensity of the fainter bands was proportional to the intensity of the main conformer. No aberrant migrating bands that would suggest the presence of a mutation were identified in the 114 samples screened. The two conformers present with this exon were very clear and aberrant conformers would have been seen easily though the slowest migrating conformer showed some streaking in the heaviest stained samples and this could have masked weakly stained aberrant conformers. No faint background conformers were evident

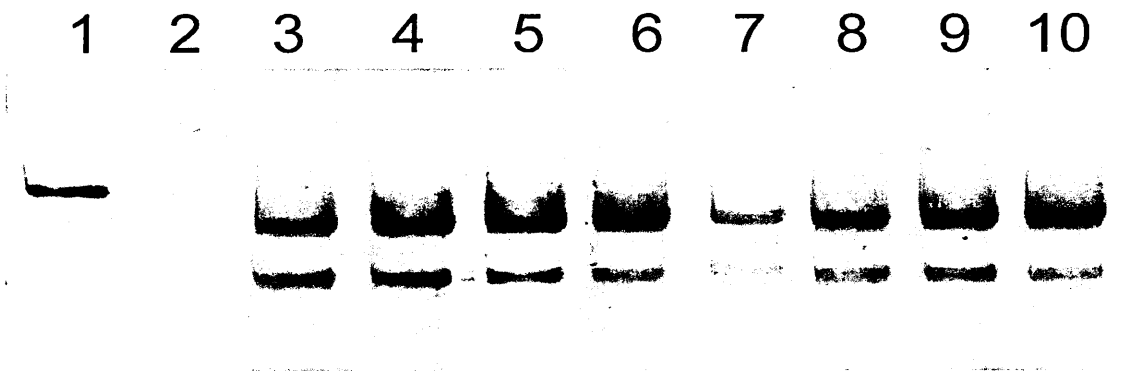


Fig 3.4.2.8.1 Gel shows PTEN exon 8 SSCP analysis of fresh bone marrow samples 1-9. Lane 1: Φ X174/Hinf1 Ladder, lane 2-9: fresh bone marrow samples 1-9 respectively. (5cm section of 50cm PagePlus[®] gel, Silver stain, positive enhanced image).

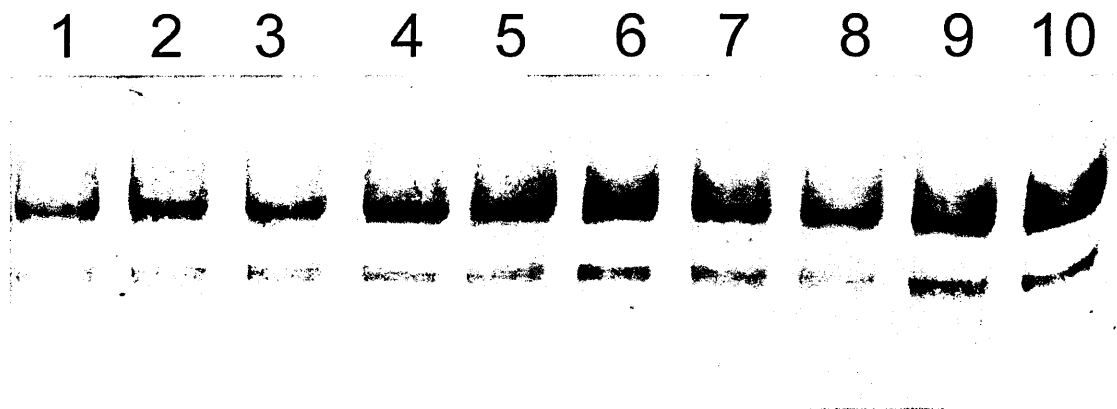


Fig 3.4.2.8.2 Gel shows PTEN exon 8 SSCP analysis of fresh bone marrow samples 10-19. Lane 1-10: fresh bone marrow samples 10-19 respectively. (5cm section of 50cm PagePlus[®] gel, Silver stain, positive enhanced image).

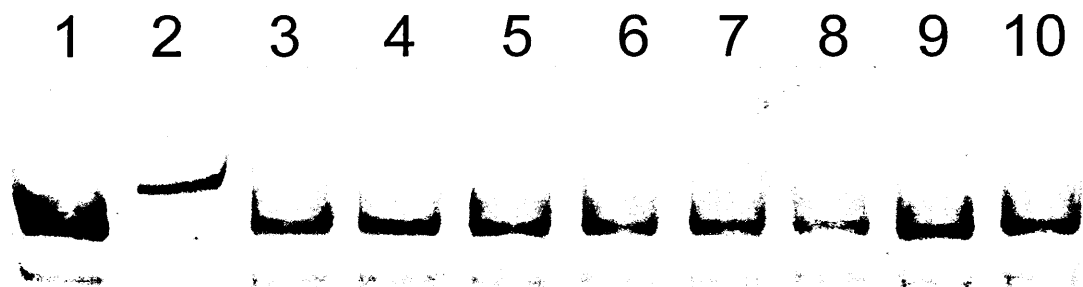


Fig 3.4.2.8.3 Gel shows PTEN exon 8 SSCP analysis of fresh bone marrow samples 20-28. Lane 2: Φ X174/*Hinf*I Ladder, lane 1+ 3-9: fresh bone marrow samples 20-28 respectively. (5cm section of 50cm PagePlus[®] gel, Silver stain, positive enhanced image).

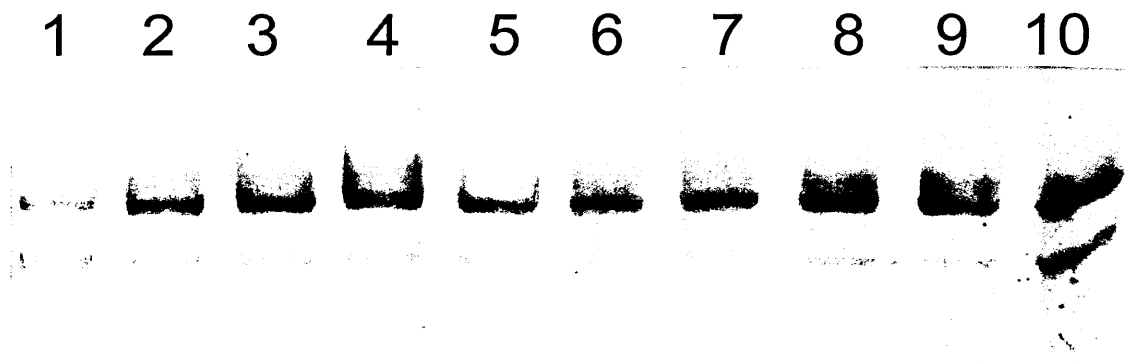


Fig 3.4.2.8.4 Gel shows PTEN exon 8 SSCP analysis of fresh bone marrow samples 29-38. Lane 1-10: fresh bone marrow samples 29-38 respectively. (5cm section of 50cm PagePlus[®] gel, Silver stain, positive enhanced image).

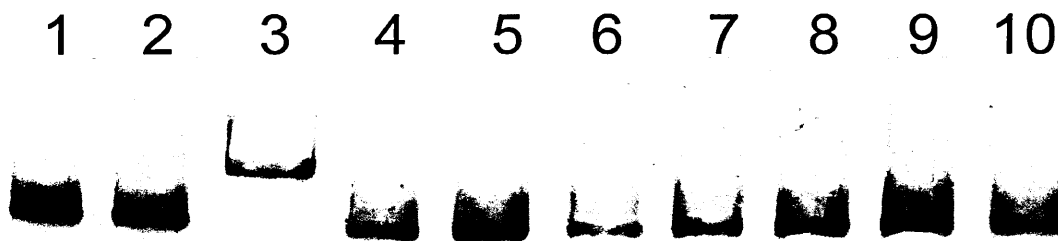


Fig 3.4.2.8.5 Gel shows PTEN exon 8 SSCP analysis of fresh bone marrow samples 39-47. Lane 3: Φ X174/*Hinf*I Ladder, lane 1-2+ 4-10: fresh bone marrow samples 39-47 respectively. (5cm section of 50cm PagePlus[®] gel, Silver stain, positive enhanced image).

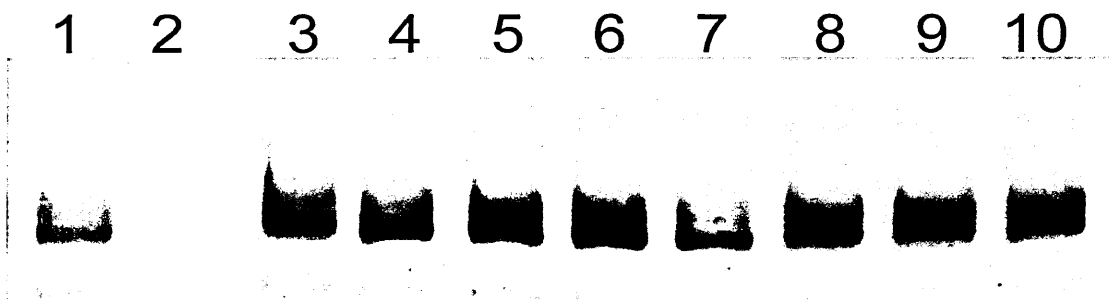


Fig 3.4.2.8.6 Gel shows PTEN exon 8 SSCP analysis of fresh bone marrow samples 48-57. Lane 1-10: fresh bone marrow samples 48-57 respectively. (5cm section of 50cm PagePlus[®] gel, Silver stain, positive enhanced image).

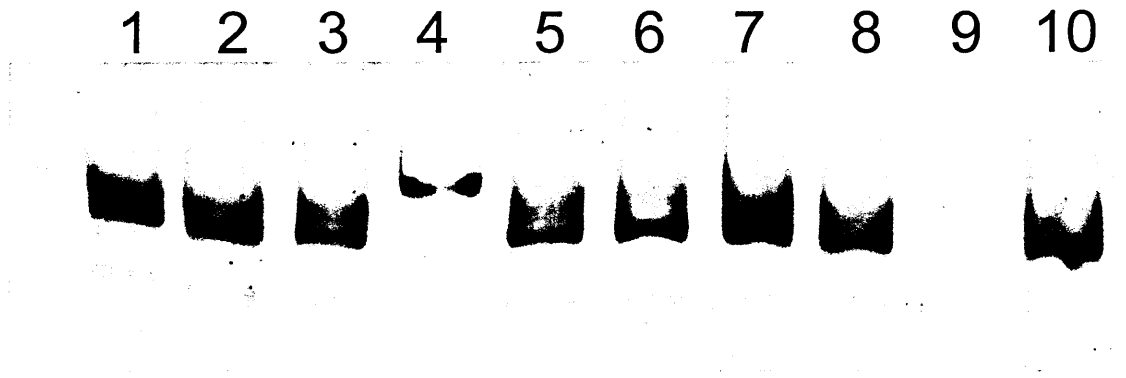


Fig 3.4.2.8.7 Gel shows PTEN exon 8 SSCP analysis of fresh bone marrow samples 58-66. Lane 4: Φ X174/*Hinf*I Ladder, lane 1-3+ 5-10: fresh bone marrow samples 58-66 respectively. (5cm section of 50cm PagePlus[®] gel, Silver stain, positive enhanced image).



Fig 3.4.2.8.8 Gel shows PTEN exon 8 SSCP analysis of fresh bone marrow samples 67-76. Lane 1-10: fresh bone marrow samples 67-76 respectively. (5cm section of 50cm PagePlus[®] gel, Silver stain, positive enhanced image).

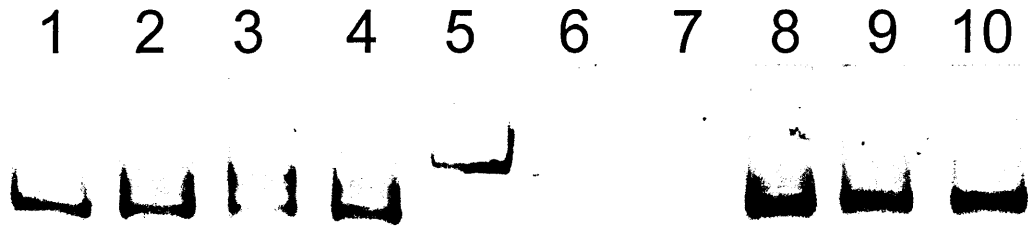


Fig 3.4.2.8.9 Gel shows PTEN exon 8 SSCP analysis of fresh bone marrow samples 77-85. Lane 5: Φ X174/*Hinf*I Ladder, lane 1-4 + 6-10: fresh bone marrow samples 77-85 respectively. (5cm section of 50cm PagePlus[®] gel, Silver stain, positive enhanced image).

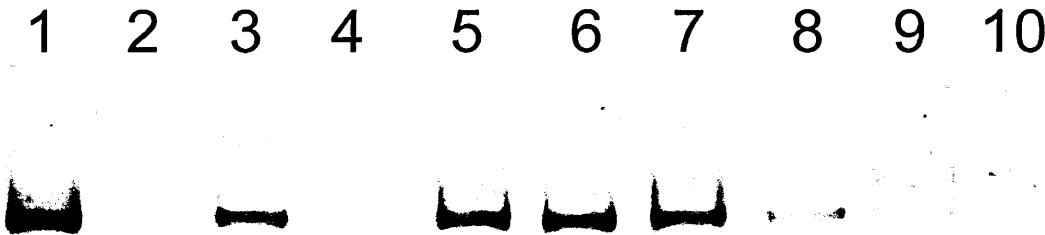


Fig 3.4.2.8.10 Gel shows PTEN exon 8 SSCP analysis of fresh bone marrow samples 86-95. Lane 1-10: fresh bone marrow samples 86-95 respectively. (5cm section of 50cm PagePlus[®] gel, Silver stain, positive enhanced image).



Fig 3.4.2.8.11 Gel shows PTEN exon 8 SSCP analysis of fresh bone marrow samples 96-104. Lane 6: $\Phi X174/Hinf1$ Ladder, lane 1-5 + 7-10: fresh bone marrow samples 96-104 respectively. (5cm section of 50cm PagePlus[®] gel, Silver stain, positive enhanced image).

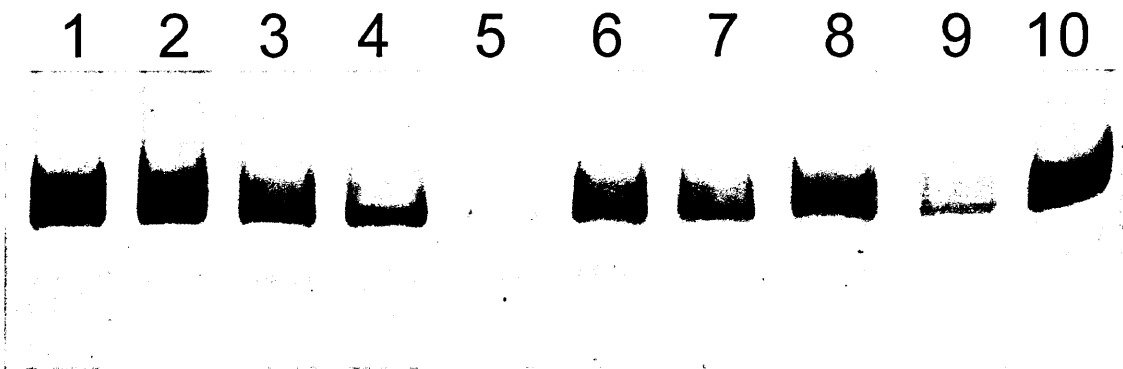


Fig 3.4.2.8.12 Gel shows PTEN exon 8 SSCP analysis of fresh bone marrow samples 105-114. Lane 1-10: fresh bone marrow samples 105-114 respectively. (5cm section of 50cm PagePlus[®] gel, Silver stain, positive enhanced image).

3.4.2.9 SSCP PTEN Exon 9

SSCP analysis of PTEN exon showed good PCR product levels which yielded 2 conformers on electrophoresis. These gels were subject to slight overdeveloping in the silver staining process and the main conformers are less clear in the Figs than when judgment was made regarding the presence of aberrant conformers. The conformers were composed of two clear bands with the fastest migrating band showing stronger staining. As with previous exons, the staining intensity of the fainter bands was proportional to the intensity of the main conformers. The heaviest stained samples show some background staining and faint aberrant bands that were not evident when the gel was examined initially after staining. No aberrant migrating bands that would suggest the presence of a mutation were identified in the 114 samples screened. The two conformers present with this exon were very clear and aberrant conformers would have been seen easily.

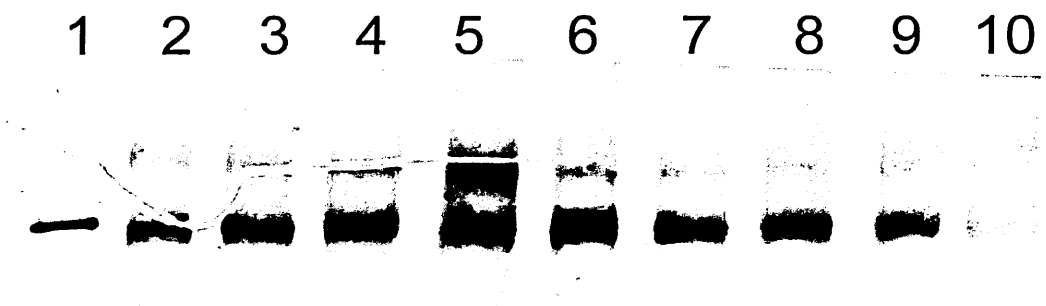


Fig 3.4.2.9.1 Gel shows PTEN exon 9 SSCP analysis of fresh bone marrow samples 1-9. Lane 1: Φ X174/*Hinf*I Ladder, lane 2-9: fresh bone marrow samples 1-9 respectively. (5cm section of 50cm PagePlus[®] gel, Silver stain, positive enhanced image).

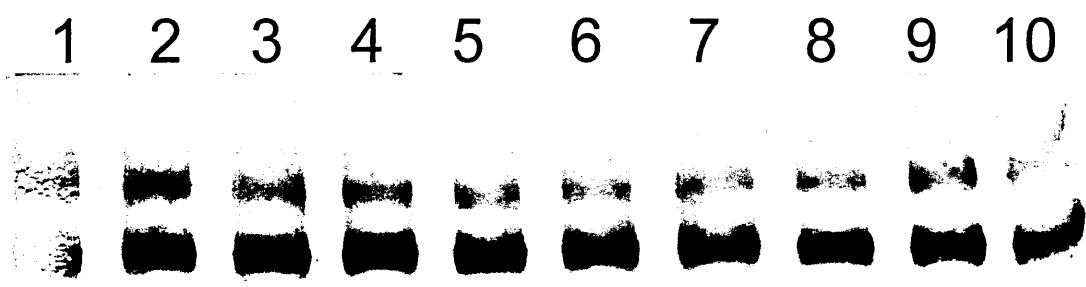


Fig 3.4.2.9.2 Gel shows PTEN exon 9 SSCP analysis of fresh bone marrow samples 10-19. Lane 1-10: fresh bone marrow samples 10-19 respectively. (5cm section of 50cm PagePlus[®] gel, Silver stain, positive enhanced image).

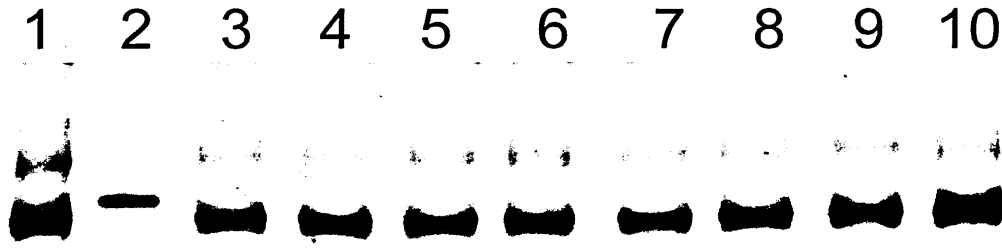


Fig 3.4.2.9.3 Gel shows PTEN exon 9 SSCP analysis of fresh bone marrow samples 20-28. Lane 2: Φ X174/*Hinf*I Ladder, lane 1+ 3-9: fresh bone marrow samples 20-28 respectively. (5cm section of 50cm PagePlus[®] gel, Silver stain, positive enhanced image).

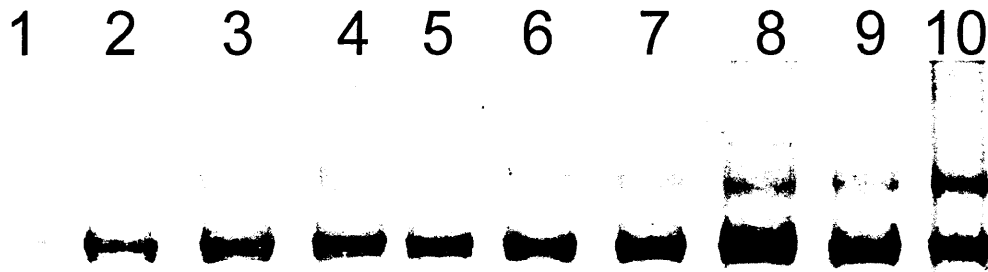


Fig 3.4.2.9.4 Gel shows PTEN exon 9 SSCP analysis of fresh bone marrow samples 29-38. Lane 1-10: fresh bone marrow samples 29-38 respectively. (5cm section of 50cm PagePlus[®] gel, Silver stain, positive enhanced image).



Fig 3.4.2.9.5 Gel shows PTEN exon 9 SSCP analysis of fresh bone marrow samples 39-47. Lane 3: Φ X174/*Hinf*I Ladder, lane 1-2+ 4-10: fresh bone marrow samples 39-47 respectively. (5cm section of 50cm PagePlus[®] gel, Silver stain, positive enhanced image).

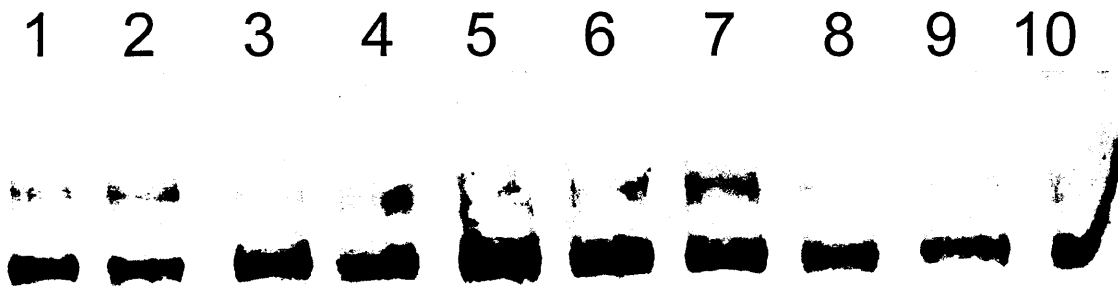


Fig 3.4.2.9.6 Gel shows PTEN exon 9 SSCP analysis of fresh bone marrow samples 48-57. Lane 1-10: fresh bone marrow samples 48-57 respectively. (5cm section of 50cm PagePlus[®] gel, Silver stain, positive enhanced image).

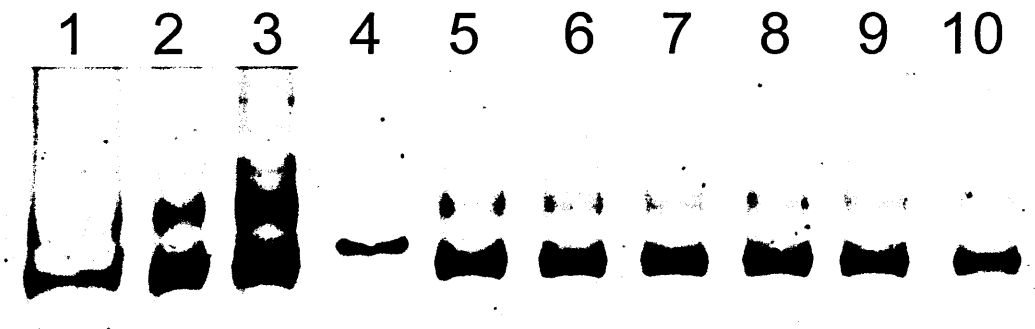


Fig 3.4.2.9.7 Gel shows PTEN exon 9 SSCP analysis of fresh bone marrow samples 58-66. Lane 4: Φ X174/*Hinf*I Ladder, lane 1-3+ 5-10: fresh bone marrow samples 58-66 respectively. (5cm section of 50cm PagePlus[®] gel, Silver stain, positive enhanced image).

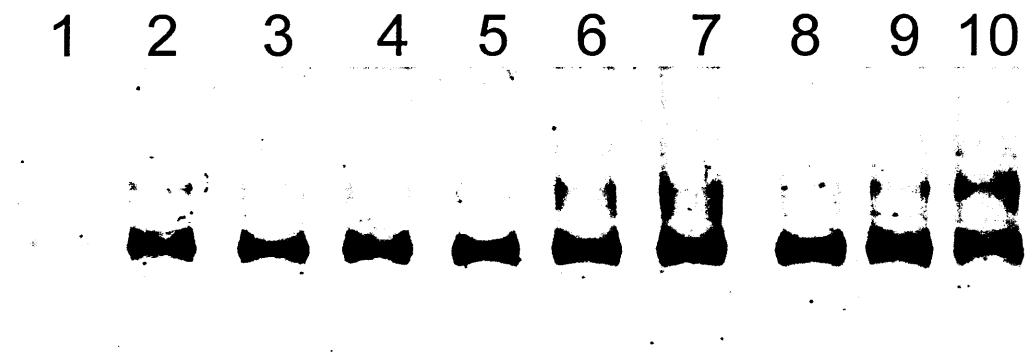


Fig 3.4.2.9.8 Gel shows PTEN exon 9 SSCP analysis of fresh bone marrow samples 67-76. Lane 1-10: fresh bone marrow samples 67-76 respectively. (5cm section of 50cm PagePlus[®] gel, Silver stain, positive enhanced image).

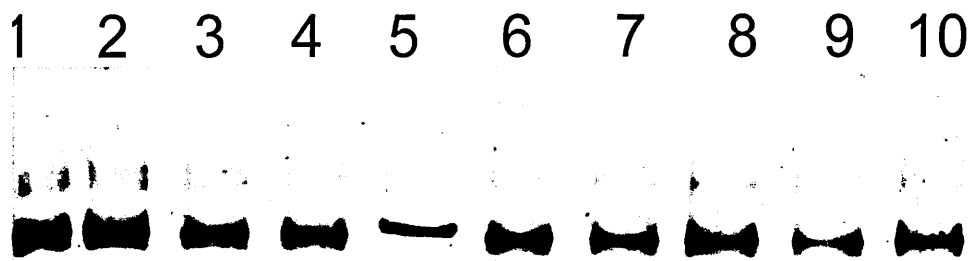


Fig 3.4.2.9.9 Gel shows PTEN exon 9 SSCP analysis of fresh bone marrow samples 77-85. Lane 5: Φ X174/*Hinf*I Ladder, lane 1-4 + 6-10: fresh bone marrow samples 77-85 respectively. (5cm section of 50cm PagePlus[®] gel, Silver stain, positive enhanced image).

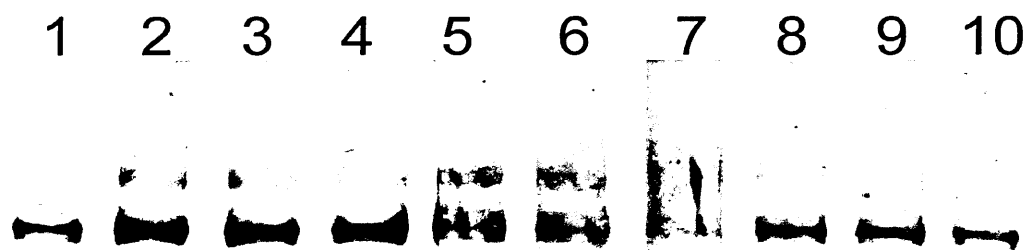


Fig 3.4.2.9.10 Gel shows PTEN exon 9 SSCP analysis of fresh bone marrow samples 86-95. Lane 1-10: fresh bone marrow samples 86-95 respectively. (5cm section of 50cm PagePlus[®] gel, Silver stain, positive enhanced image).

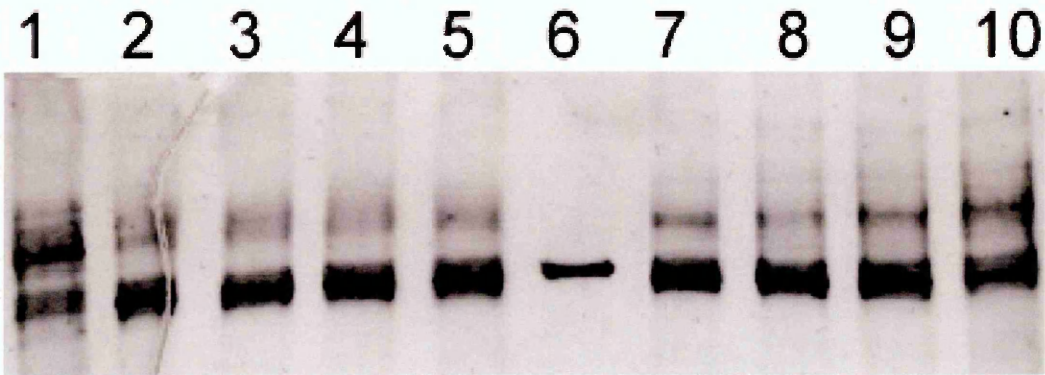


Fig 3.4.2.9.11 Gel shows PTEN exon 9 SSCP analysis of fresh bone marrow samples 96-104. Lane 6: Φ X174/*Hinf*I Ladder, lane 1-5 + 7-10: fresh bone marrow samples 96-104 respectively. (5cm section of 50cm PagePlus[®] gel, Silver stain, positive enhanced image).

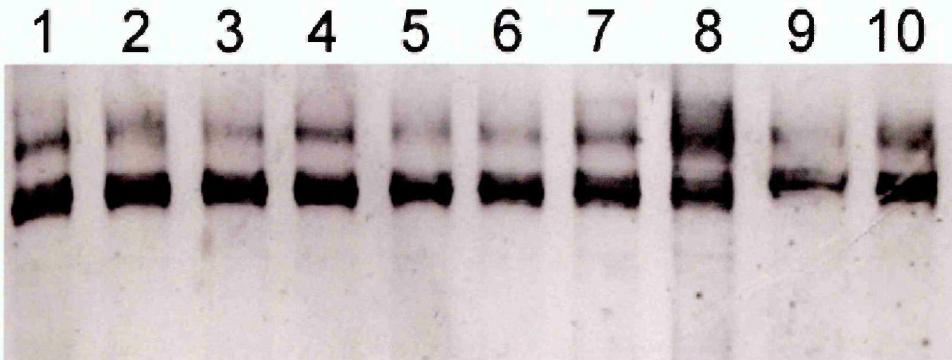


Fig 3.4.2.9.12 Gel shows PTEN exon 9 SSCP analysis of fresh bone marrow samples 105-114. Lane 1-10: fresh bone marrow samples 105-114 respectively. (5cm section of 50cm PagePlus[®] gel, Silver stain, positive enhanced image).

3.4.3 SSCP gels stained with GelStar

Fig 3.4.3.1 shows a composite image of all six gels in the SSCP exon 7 analysis stained with GelStar. This stain was used to identify the position of the unpredictable migration of single stranded conformers prior to excision for silver staining. Compared to the silver stained gels in Figs 2.5.2.7.1 – 2.4.2.7.12, GelStar shows less intense staining but does not resolve very faint conformers. Background staining was absent and aberrant migration in the SSCP control was apparent.

Fig 3.4.3.1 Composite picture of 114 PCR reactions of PTEN exon 7 SSCP gels

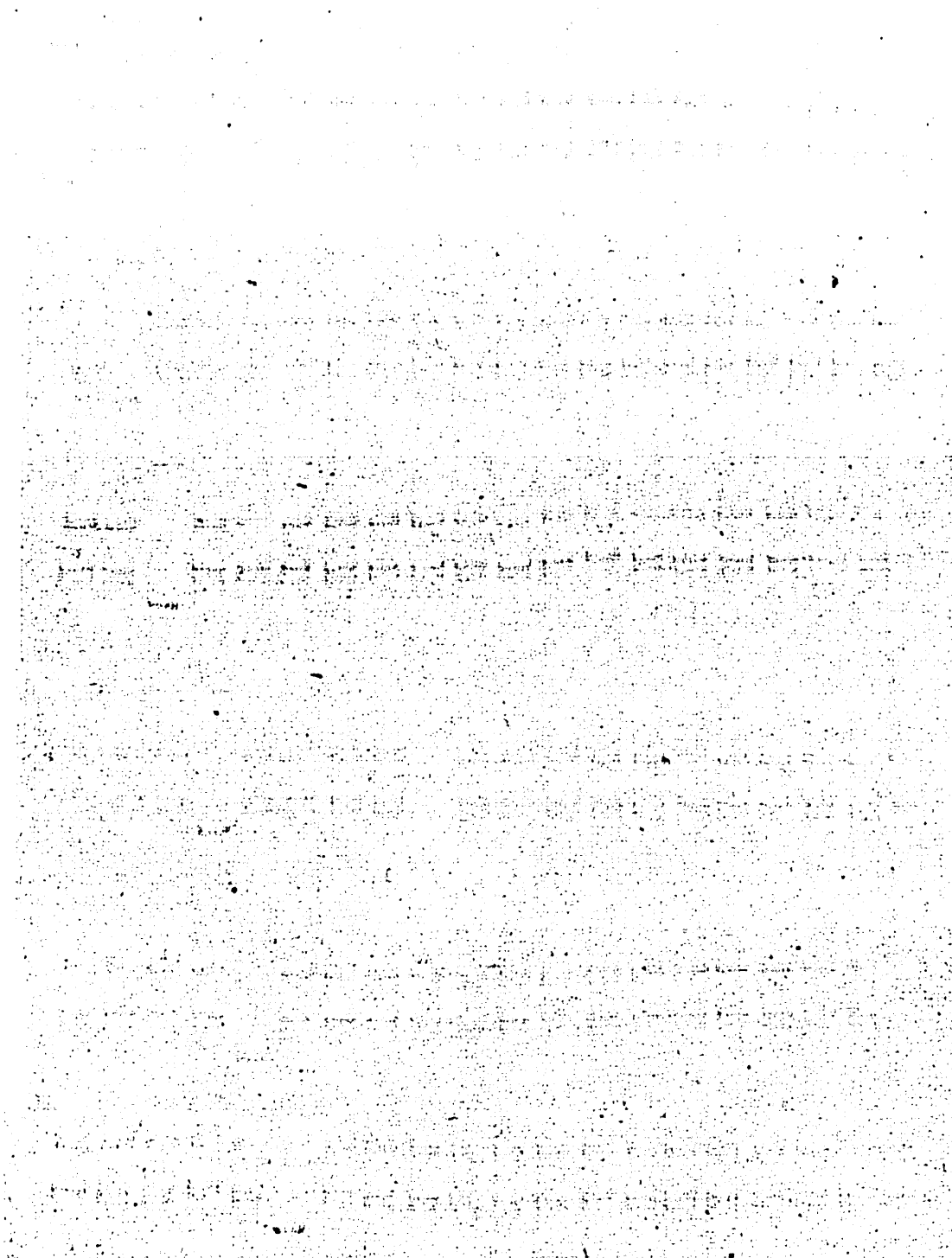


Fig 3.4.3.1 Composite picture of 114 PCR reactions of PTEN exon 7 SSCP gels stained with 2 x GelStar[®]. Each excised strip was approx 7 cm from top to bottom. DNA ladder occupies lane one to six in successive gels as an aid to identification. SSCP positive control was in the last lane of the fifth gel down (negative image, fluorescence obtained at 312 nm by transillumination)

3.4.4 SSCP analysis – summary of results

SSCP analysis carried out on frozen bone marrow samples showed a low rate of reaction failure compared to fixed cells (section 3.3) . Exon 8 reactions, as with heteroduplex analysis, showed a higher failure rate than other exons studied. The only aberrant migrating band in all exons studied were found in exon five. Resolution of bands was much clearer using SSCP with lower levels of product diffusion compared to Heteroduplex analysis

Exon Number	Failure Rate	Aberrant migration
1	2/114	0/114
2	Not screened	Not screened
3	0/114	0/114
4	0/114	0/114
5	1/114	2/114
6	0/114	0/114
7	0/113	0/113
8	8/114	0/114
9	0/114	0/114

Table 3.4.4 Table shows rate of failure of PCR reaction for each PTEN exon in the SSCP gel plus the number of lanes showing aberrant band migration.

3.5 DNA sequencing of PTEN exon 5 in samples with aberrant SSCP migration.

PTEN sequences were obtained for all 9 samples studied. Base calling was most accurate at the beginning of the electropherogram and deteriorated as noise became more pronounced later in the sequence. All sequenced exons corresponded to published sequences.

Electropherogram of sequence sample number 4 (JW4AR) showed a possible mismatch at nucleotide number 116 in the reverse sequencing (relative to published sequence data). Forward sequencing did not show a complementary mismatch and corresponded to the published sequence, so the anomaly was ignored.

Sequence of exon 5 for bone marrow samples 42 and 45 that produced aberrant bands in SSCP analysis (JW 3 and 5) corresponded to the published sequence.

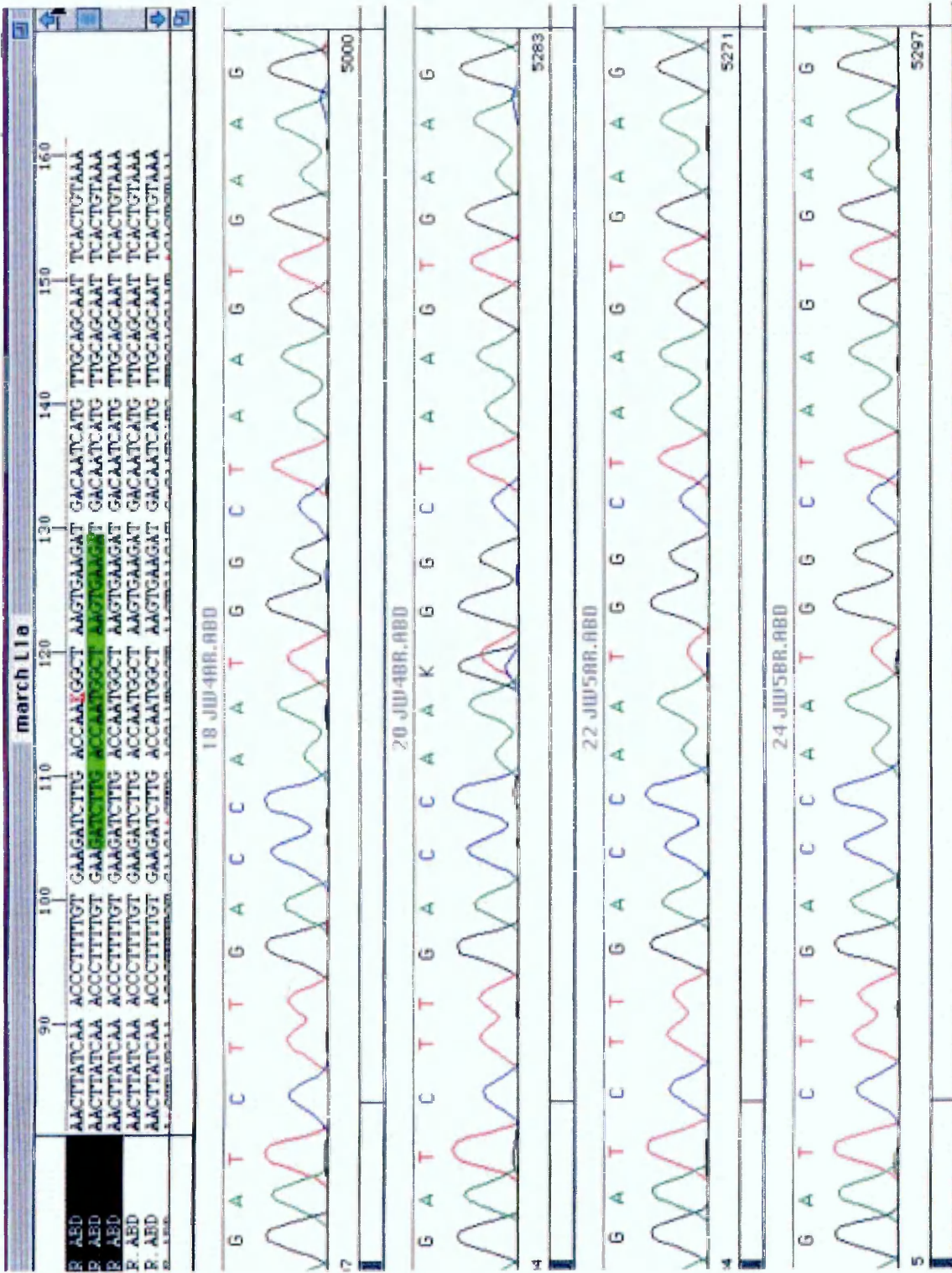


Fig 3.7.2.1 Electropherogram of sequence sample number 4 (JW4AR) forward and reverse sequencing, top two rows plus sample number 5, bottom two rows. A possible mismatch T>G was shown in sequence 20 (JW4BR) at nucleotide number 116 (relative to published sequence data). Forward sequencing does not show a complementary mismatch.

march L1a 25/11/2002 11:18

	10	20	30	40	50	60	70	80
1 JW10AF.ABD	T-----C	TLATCTGAG	GTATCTTTT	TACCACA ₂ TT	GCACAATATC	CTTTTGAAGA	CCATAACCCA	CCACAGCTAG
2 JW10AR.ABD	TTTTTTTTTC	TTATCTGAG	GTTATCTTTT	TACCACAGTT	GCACAATATC	CTTTTGAAGA	CCATAACCCA	CCACAGCTAG
3 JW10BF.ABD	-----C	TNAT-CT ₂ GAG	GT-AT ₂ TTTT	TACCACAGTT	GCACAATATC	CTTTTGAAGA	CCATAACCCA	CCACAGCTAG
4 JW10BR.ABD	TTTTTTTTTC	TTATCTGAG	GTTATCTTTT	TACCACAGTT	GCACAATATC	CTTTTGAAGA	CCATAACCCA	CCACAGCTAG
6 JW1AR.ABD	TTTTTTTTTC	TTATCTGAG	GTTATCTTTT	TACCACAGTT	GCACAATATC	CTTTTGAAGA	CCATAACCCA	CCACAGCTAG
8 JW1BR.ABD	TTTTTTTTTC	TTATCTGAG	GTTATCTTTT	TACCACAGTT	GCACAATATC	CTTTTGAAGA	CCATAACCCA	CCACAGCTAG
10 JW2AR.ABD	TTTTTTTTTC	TTATCTGAG	GTTATCTTTT	TACCACAGTT	GCACAATATC	CTTTTGAAGA	CCATAACCCA	CCACAGCTAG
12 JW2BR.ABD	TTTTTTTTTC	TTATCTGAG	GTTATCTTTT	TACCACAGTT	GCACAATATC	CTTTTGAAGA	CCATAACCCA	CCACAGCTAG
14 JW3AR.ABD	TTTTTTTTTC	TTATCTGAG	GTTATCTTTT	TACCACAGTT	GCACAATATC	CTTTTGAAGA	CCATAACCCA	CCACAGCTAG
16 JW3BR.ABD	TTTTTTTTTC	TTATCTGAG	GTTATCTTTT	TACCACAGTT	GCACAATATC	CTTTTGAAGA	CCATAACCCA	CCACAGCTAG
18 JW4AR.ABD	TTTTTTTTTC	TTATCTGAG	GTTATCTTTT	TACCACAGTT	GCACAATATC	CTTTTGAAGA	CCATAACCCA	CCACAGCTAG
20 JW4BR.ABD	TTTTTTTTTC	TTATCTGAG	GTTATCTTTT	TACCACAGTT	GCACAATATC	CTTTTGAAGA	CCATAACCCA	CCACAGCTAG
22 JW5AR.ABD	TTTTTTTTTC	TTATCTGAG	GTTATCTTTT	TACCACAGTT	GCACAATATC	CTTTTGAAGA	CCATAACCCA	CCACAGCTAG
24 JW5BR.ABD	TTTTTTTTTC	TTATCTGAG	GTTATCTTTT	TACCACAGTT	GCACAATATC	CTTTTGAAGA	CCATAACCCA	CCACAGCTAG
26 JW6AR.ABD	TTTTTTTTTC	TTATCTGAG	GTTATCTTTT	TACCACAGTT	GCACAATATC	CTTTTGAAGA	CCATAACCCA	CCACAGCTAG
28 JW6BR.ABD	TTTTTTTTTC	TTATCTGAG	GTTATCTTTT	TACCACAGTT	GCACAATATC	CTTTTGAAGA	CCATAACCCA	CCACAGCTAG
29 JW7AF.ABD	TTTTTT--C	TTATCTGAG	GTTATCTTTT	TACCACAGTT	GCACAATATC	CTTTTGAAGA	CCATAACCCA	CCACAGCTAG
30 JW7AR.ABD	TTTTTTTTTC	TTATCTGAG	GTTATCTTTT	TACCACAGTT	GCACAATATC	CTTTTGAAGA	CCATAACCCA	CCACAGCTAG
31 JW7BF.ABD	T----TT-C	TTATCTGAG	GTTATCTTTT	TACCACAGTT	GCACAATATC	CTTTTGAAGA	CCATAACCCA	CCACAGCTAG
32 JW7BR.ABD	TTTTTTTTTC	TTATCTGAG	GTTATCTTTT	TACCACAGTT	GCACAATATC	CTTTTGAAGA	CCATAACCCA	CCACAGCTAG
34 JW8AR.ABD	TTTTTTTTTC	TTATCTGAG	GTTATCTTTT	TACCACAGTT	GCACAATATC	CTTTTGAAGA	CCATAACCCA	CCACAGCTAG
36 JW8BR.ABD	TTTTTTTTTC	TTATCTGAG	GTTATCTTTT	TACCACAGTT	GCACAATATC	CTTTTGAAGA	CCATAACCCA	CCACAGCTAG
37 JW9AF.ABD	-----C	TTAT-CT ₂ GAG	GTTATCTTTT	TACCACAGTT	GCACAATATC	CTTTTGAAGA	CCATAACCCA	CCACAGCTAG
38 JW9AR.ABD	TTTTTTTTTC	TTATCTGAG	GTTATCTTTT	TACCACAGTT	GCACAATATC	CTTTTGAAGA	CCATAACCCA	CCACAGCTAG
39 JW9BR.ABD	-----C	TTAT-CT ₂ GAG	GTTATCTTTT	TACCACAGTT	GCACAATATC	CTTTTGAAGA	CCATAACCCA	CCACAGCTAG
40 JW9BR.ABD	TTTTTTTTTC	TTATCTGAG	GTTATCTTTT	TACCACAGTT	GCACAATATC	CTTTTGAAGA	CCATAACCCA	CCACAGCTAG
41 ex5 all	TTTTTTTTTC	TTATCTGAG	GTTATCTTTT	TACCACAGTT	GCACAATATC	CTTTTGAAGA	CCATAACCCA	CCACAGCTAG
42 ex5 align	-----	-----	-----	-----gtt	gcacaatatc	cttttgaaga	ccataaccca	ccacagctag
48	?????????	?????????	?????????	?????????	AlaGlnTyrP	roPheGluAs	pHisAsnPro	ProGlnLeuG
43	*****	*****	*****	*****	-----	-----	-----	-----

march L1a 25/11/2002 11:18

	90	100	110	120	130	140	150	160
1 JW10AF.ABD	AACCTATCAA	ACCCTTTTGT	GAAGATCTTG	ACCAATGGCT	AAGTGAAGAT	GACAATCATG	TTGCAGCAAT	TCACTGTAAA
2 JW10AR.ABD	AACCTATCAA	ACCCTTTTGT	GAAGATCTTG	ACCAATGGCT	AAGTGAAGAT	GACAATCATG	TTGCAGCAAT	TCACTGTAAA
3 JW10BF.ABD	AACCTATCAA	ACCCTTTTGT	GAAGALCTTG	ACCAALGGCT	AAGTGAAGAT	GACAATCATG	TTGCAGCAAT	TCACTGTAAA
4 JW10BR.ABD	AACCTATCAA	ACCCTTTTGT	G ₂ AG ₂ CTTG	ACCAALGGCT	AAGTGAAGAT	G ₂ CAATCATG	TTGCAGCAAT	TCACTGTAAA
6 JW1AR.ABD	AACCTATCAA	ACCCTTTTGT	GAAGATCTTG	ACCAATGGCT	AAGTGAAGAT	GACAATCATG	TTGCAGCAAT	TCACTGTAAA
8 JW1BR.ABD	AACCTATCAA	ACCCTTTTGT	GAAGATCTTG	ACCAATGGCT	AAGTGAAGAT	GACAATCATG	TTGCAGCAAT	TCACTGTAAA
10 JW2AR.ABD	AACCTATCAA	ACCCTTTTGT	GAAGATCTTG	ACCAATGGCT	AAGTGAAGAT	GACAATCATG	TTGCAGCAAT	TCACTGTAAA
12 JW2BR.ABD	AACCTATCAA	ACCCTTTTGT	GAAGATCTTG	ACCAATGGCT	AAGTGAAGAT	GACAATCATG	TTGCAGCAAT	TCACTGTAAA
14 JW3AR.ABD	AACCTATCAA	ACCCTTTTGT	GAAGATCTTG	ACCAATGGCT	AAGTGAAGAT	GACAATCATG	TTGCAGCAAT	TCACTGTAAA
16 JW3BR.ABD	AACCTATCAA	ACCCTTTTGT	GAAGATCTTG	ACCAATGGCT	AAGTGAAGAT	GACAATCATG	TTGCAGCAAT	TCACTGTAAA
18 JW4AR.ABD	AACCTATCAA	ACCCTTTTGT	GAAGATCTTG	ACCAATGGCT	AAGTGAAGAT	GACAATCATG	TTGCAGCAAT	TCACTGTAAA
20 JW4BR.ABD	AACCTATCAA	ACCCTTTTGT	GAAGATCTTG	ACCAATGGCT	AAGTGAAGAT	GACAATCATG	TTGCAGCAAT	TCACTGTAAA
22 JW5AR.ABD	AACCTATCAA	ACCCTTTTGT	GAAGATCTTG	ACCAATGGCT	AAGTGAAGAT	GACAATCATG	TTGCAGCAAT	TCACTGTAAA
24 JW5BR.ABD	AACCTATCAA	ACCCTTTTGT	GAAGATCTTG	ACCAATGGCT	AAGTGAAGAT	GACAATCATG	TTGCAGCAAT	TCACTGTAAA
26 JW6AR.ABD	AACCTATCAA	ACCCTTTTGT	GAAGATCTTG	ACCAATGGCT	AAGTGAAGAT	GACAATCATG	TTGCAGCAAT	TCACTGTAAA
28 JW6BR.ABD	AACCTATCAA	ACCCTTTTGT	GAAGATCTTG	ACCAATGGCT	AAGTGAAGAT	GACAATCATG	TTGCAGCAAT	TCACTGTAAA
29 JW7AF.ABD	A ₂ CTTATCAA	ACCCTTTTGT	GAAGALCTTG	ACCAATGGCT	AAGTGAAGAT	G ₂ CAATCATG	TTGCAGCAAT	LC ₂ ACTGTAAA
30 JW7AR.ABD	AACCTATCAA	ACCCTTTTGT	GAAGATCTTG	ACCAATGGCT	AAGTGAAGAT	GACAATCATG	TTGCAGCAAT	TCACTGTAAA
31 JW7BF.ABD	AACCTA ₂ CAA	ACCCTTTTGT	GAAGALCTTG	ACCAALGGCT	AAG ₂ GAAGAT	G ₂ CAALCATG	TTGCAGCAAT	LC ₂ ACTGTAAA
32 JW7BR.ABD	AACCTATCAA	ACCCTTTTGT	GAAGATCTTG	ACCAATGGCT	AAGTGAAGAT	GACAATCATG	TTGCAGCAAT	TCACTGTAAA
34 JW8AR.ABD	AACCTATCAA	ACCCTTTTGT	GAAGATCTTG	ACCAATGGCT	AAGTGAAGAT	GACAATCATG	TTGCAGCAAT	TCACTGTAAA
36 JW8BR.ABD	AACCTATCAA	ACCCTTTTGT	GAAGATCTTG	ACCAATGGCT	AAGTGAAGAT	GACAATCATG	TTGCAGCAAT	TCACTGTAAA
37 JW9AF.ABD	AACCTATCAA	ACCCTTTTGT	G ₂ AGATCTTG	ACCAATGGCT	AAGT ₂ AAGAT	GACAATCATG	TT ₂ CA ₂ CAAT	TCACTGTAAA
38 JW9AR.ABD	AACCTATCAA	ACCCTTTTGT	GAAG ₂ CTTG	ACCAATGGCT	AAGTGAAGAT	GACAATCATG	TTGCAGCAAT	TCACTGTAAA
39 JW9BR.ABD	AACCTATCAA	ACCCTTTTGT	GAAGATCTTG	ACCAATGGCT	AAGTGAAGAT	G ₂ CAALCATG	TTGCAGCAAT	TCACTGTAAA
40 JW9BR.ABD	AACCTATCAA	ACCCTTTTGT	GAAGATCTTG	ACCAATGGCT	AAGTGAAGAT	GACAATCATG	TTGCAGCAAT	TCACTGTAAA
41 ex5 all	AACCTATCAA	ACCCTTTTGT	GAAGATCTTG	ACCAATGGCT	aagtgaAGAT	GACAATCATG	TTGCAGCAAT	TCACTGTAAA
42 ex5 align	aaactatcaa	acccttttgt	gaagatcttg	accaatggct	aagtgaagat	gacaatcatg	ttgcagcaat	tcactgtaaa
48	luLeuIleLys	sProPheCys	GluAspLeuA	spGlnTrpLe	uSerGluAsp	AspAsnHisV	a1AlaAlaI1	eHisCysLys
43	-----	-----	-----	-----	-----	-----	-----	-----

Fig 3.7.2.2 PTEN exon 5 sequencing results- nucleotides 1-160. Forward (F) and Reverse (R) sequence output after interpretation of electropherogram JW4BR forward sequence shows possible mismatch at nucleotide116

march Lla 25/11/2002 11:18

	170	180	190	200	210	220	230	240
1 JW10AF.ABD	GCTGGAAAGG	GACGAAGTGG	TGTAATGATA	TGTGCATATT	TATTACATCG	GGGCAAAATTT	TTAAAGGCAC	AAGAGGCCCT
2 JW10AR.ABD	GCTGGAAAGG	GACGAAGTGG	TGTAATGATA	TGTGCATATT	TATTACATCG	GGGCAAAATTT	TTAAAGGCAC	AAGAGGCCCT
3 JW10BF.ABD	GCTGGAAAGG	GACGAAGTGG	TGTAATGATA	TGTGCATATT	TATTACATCG	GGGCAAAATTT	TTAAAGGCAC	AAGAGGCCCT
4 JW10BR.ABD	GCTGGAAAGG	GACGAAGTGG	TGTAATGATA	TGTGCATATT	TATTACATCG	GGGCAAAATTT	TTAAAGGCAC	AAGAGGCCCT
6 JW1AR.ABD	GCTGGAAAGG	GACGAAGTGG	TGTAATGATA	TGTGCATATT	TATTACATCG	GGGCAAAATTT	TTAAAGGCAC	AAGAGGCCCT
8 JW1BR.ABD	GCTGGAAAGG	GACGAAGTGG	TGTAATGATA	TGTGCATATT	TATTACATCG	GGGCAAAATTT	TTAAAGGCAC	AAGAGGCCCT
10 JW2AR.ABD	GCTGGAAAGG	GACGAAGTGG	TGTAATGATA	TGTGCATATT	TATTACATCG	GGGCAAAATTT	TTAAAGGCAC	AAGAGGCCCT
12 JW2BR.ABD	GCTGGAAAGG	GACGAAGTGG	TGTAATGATA	TGTGCATATT	TATTACATCG	GGGCAAAATTT	TTAAAGGCAC	AAGAGGCCCT
14 JW3AR.ABD	GCTGGAAAGG	GACGAAGTGG	TGTAATGATA	TGTGCATATT	TATTACATCG	GGGCAAAATTT	TTAAAGGCAC	AAGAGGCCCT
16 JW3BR.ABD	GCTGGAAAGG	GACGAAGTGG	TGTAATGATA	TGTGCATATT	TATTACATCG	GGGCAAAATTT	TTAAAGGCAC	AAGAGGCCCT
18 JW4AR.ABD	GCTGGAAAGG	GACGAAGTGG	TGTAATGATA	TGTGCATATT	TATTACATCG	GGGCAAAATTT	TTAAAGGCAC	AAGAGGCCCT
20 JW4BR.ABD	GCTGGAAAGG	GACGAAGTGG	TGTAATGATA	TGTGCATATT	TATTACATCG	GGGCAAAATTT	TTAAAGGCAC	AAGAGGCCCT
22 JW5AR.ABD	GCTGGAAAGG	GACGAAGTGG	TGTAATGATA	TGTGCATATT	TATTACATCG	GGGCAAAATTT	TTAAAGGCAC	AAGAGGCCCT
24 JW5BR.ABD	GCTGGAAAGG	GACGAAGTGG	TGTAATGATA	TGTGCATATT	TATTACATCG	GGGCAAAATTT	TTAAAGGCAC	AAGAGGCCCT
26 JW6AR.ABD	GCTGGAAAGG	GACGAAGTGG	TGTAATGATA	TGTGCATATT	TATTACATCG	GGGCAAAATTT	TTAAAGGCAC	AAGAGGCCCT
28 JW6BR.ABD	GCTGGAAAGG	GACGAAGTGG	TGTAATGATA	TGTGCATATT	TATTACATCG	GGGCAAAATTT	TTAAAGGCAC	AAGAGGCCCT
29 JW7AF.ABD	GCTGGAAAGG	GACGAAGTGG	TGTAATGATA	TGTGCATATT	TATTACATCG	GGGCAAAATTT	TTAAAGGCAC	AAGAGGCCCT
30 JW7AR.ABD	GCTGGAAAGG	GACGAAGTGG	TGTAATGATA	TGTGCATATT	TATTACATCG	GGGCAAAATTT	TTAAAGGCAC	AAGAGGCCCT
31 JW7BF.ABD	GCTGGAAAGG	GACGAAGTGG	TGTAATGATA	TGTGCATATT	TATTACATCG	GGGCAAAATTT	TTAAAGGCAC	AAGAGGCCCT
32 JW7BR.ABD	GCTGGAAAGG	GACGAAGTGG	TGTAATGATA	TGTGCATATT	TATTACATCG	GGGCAAAATTT	TTAAAGGCAC	AAGAGGCCCT
34 JW8AR.ABD	GCTGGAAAGG	GACGAAGTGG	TGTAATGATA	TGTGCATATT	TATTACATCG	GGGCAAAATTT	TTAAAGGCAC	AAGAGGCCCT
36 JW8BR.ABD	GCTGGAAAGG	GACGAAGTGG	TGTAATGATA	TGTGCATATT	TATTACATCG	GGGCAAAATTT	TTAAAGGCAC	AAGAGGCCCT
37 JW9AF.ABD	GCTGGAAAGG	GACGAAGTGG	TGTAATGATA	TGTGCATATT	TATTACATCG	GGGCAAAATTT	TTAAAGGCAC	AAGAGGCCCT
38 JW9AR.ABD	GCTGGAAAGG	GACGAAGTGG	TGTAATGATA	TGTGCATATT	TATTACATCG	GGGCAAAATTT	TTAAAGGCAC	AAGAGGCCCT
39 JW9BF.ABD	GCTGGAAAGG	GACGAAGTGG	TGTAATGATA	TGTGCATATT	TATTACATCG	GGGCAAAATTT	TTAAAGGCAC	AAGAGGCCCT
40 JW9BR.ABD	GCTGGAAAGG	GACGAAGTGG	TGTAATGATA	TGTGCATATT	TATTACATCG	GGGCAAAATTT	TTAAAGGCAC	AAGAGGCCCT
41 ex5 all	GCTGGAAAGG	GACGAAGTGG	TGTAATGATA	TGTGCATATT	TATTACATCG	GGGCAAAATTT	TTAAAGGCAC	AAGAGGCCCT
42 ex5 align	gctggaaagg	gacgaactgg	tgtaatgata	tgtgcatttt	tattacatcg	gggcaaatTT	ttaaaggcAC	aagagGCCCT
48	AlaGlyLysG	lyArgThrGl	yValMetIle	CysAlaTyrL	euLeuHisAr	gGlyLysPhe	LeuLysAlaG	lInGluAlaLe
43								

march Lla 25/11/2002 11:18

	250	260	270	280	290	300	310	320
1 JW10AF.ABD	AGATTTCCTAT	GGGgaagtaa	ggaccagaga	caaaaaggta	agttattttt	tgatgttttt	c	
2 JW10AR.ABD	AGATTTCCLAT	GGG						
3 JW10BF.ABD	AGATTTCCTAT	GGGgaagtaa	ggaccagaga	caaaaaggta	agttattttt	tgatgttttt	cctttctctc	
4 JW10BR.ABD	AGATTTCCTAT	GGG						
6 JW1AR.ABD	AGATTTCCTAT	GGGgaagtaa	ggaccagaga	caaaaaggta	ag			
8 JW1BR.ABD	AGATTTCCLAT	GGGgaagtaa	ggaccagaga	caaaaaggta	ag			
10 JW2AR.ABD	AGATTTCCTAT	GGGgaagtaa	ggaccagaga	caaaaaggta	a			
12 JW2BR.ABD	AGATTTCCTAT	GGGgaagtaa	ggaccagaga	caaaaaggta	agttat			
14 JW3AR.ABD	AGATTTCCLAT	GGG						
16 JW3BR.ABD	AGATTTCCTAT	GGG						
18 JW4AR.ABD	AGATTTCCTAT	GGG						
20 JW4BR.ABD	AGATTTCCTAT	GGG						
22 JW5AR.ABD	AGATTTCCTAT	GGG						
24 JW5BR.ABD	AGATTTCCLAT	GGG						
26 JW6AR.ABD	AGATTTCCTAT	GGG						
28 JW6BR.ABD	AGATTTCCTAT	GGG						
29 JW7AF.ABD	AGATTTCCTAT	GGGgaagtaa	ggaccagaga	caaaaaggta	agttattttt	tgatgttttt	cctt	
30 JW7AR.ABD	AGATTTCCLAT	GGG						
31 JW7BF.ABD	AGATTTCCTAT	GGGgaagtaa	ggaccagaga	caaaaaggta	agttattttt	tgatgtttt		
32 JW7BR.ABD	AGATTTCCTAT	GGG						
34 JW8AR.ABD	AGATTTCCTAT	GGG						
36 JW8BR.ABD	AGATTTCCTAT	GGG						
37 JW9AF.ABD	AGATTTCCTAT	GGGgaagtaa	ggaccagaga	caaaaaggta	agttattttt			
38 JW9AR.ABD	AGATTTCCLAT	GGG						
39 JW9BF.ABD	AGATTTCCTAT	GGG						
40 JW9BR.ABD	AGATTTCCTAT	GGG						
41 ex5 all	AGATTTCCTAT	GGGGAAGTAA	GGACCAGAGA	CAAAAAGGTA	AGTTATTTTT	TGATGTTTTT	CCTTTCCTCT	TCCTGGATCT
42 ex5 align	agatttctat	ggggaagtaa	ggaccagaga	caaaaagg				
48	uAspPheTyr	GlyGluValA	rgThrArgAs	pLysLys				
43								

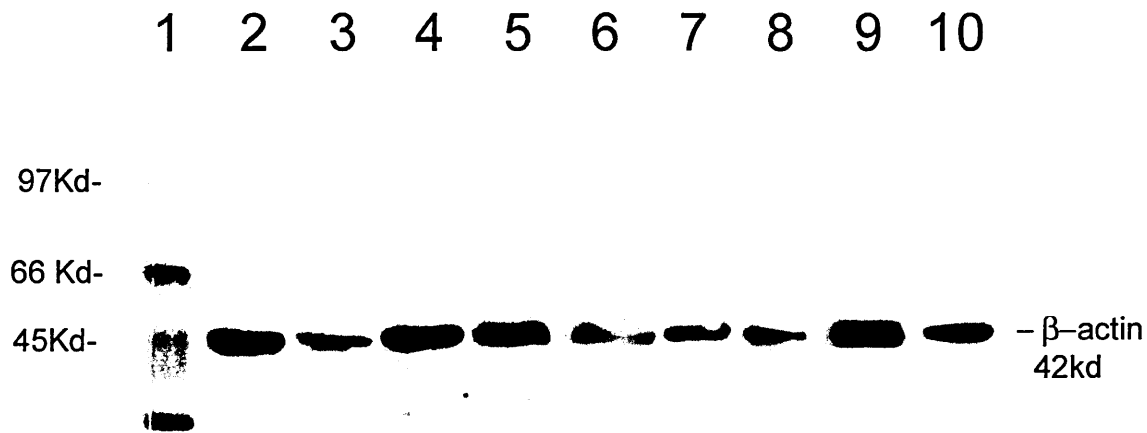
Fig 3.7.2.3 PTEN exon 5 sequencing results- nucleotides 170- 310. Forward (F) and Reverse (R) sequence output after interpretation of electropherogram

3.6 Western blotting of PTEN protein

The heteroduplex and SSCP screening tests suggested a very low rate of point mutations and small deletions in the samples studied. Western blots were performed on frozen bone marrow samples to detect protein expression in leukaemia cells and thus rule out abolition of PTEN protein expression by other mechanisms such as large scale gene deletion. Western blots for PTEN were performed using a normal control, two chronic granulocytic leukaemia, one chronic lymphocytic leukaemia, one acute myeloid leukaemia (FAB class M1), one acute myeloid leukaemia (FAB class M2) and one acute myeloid leukaemia (FAB class M3 variant), chronic granulocytic leukaemia acute phase samples. All showed the expected 55kd band plus a band of unknown specificity (upper band) present in each lane. Lane 6 AML shows some sample degradation. Lane 9 shows stronger signal from non-specific band compared to 55kd PTEN band and was probably a staining artefact as the upper band has a different shape to the lower specific PTEN band. All samples showed a signal corresponding to PTEN though at much lower levels than the β -actin control.

Figure 3.5.1 Western blotting of PTEN primary leukaemia samples

A.



B.

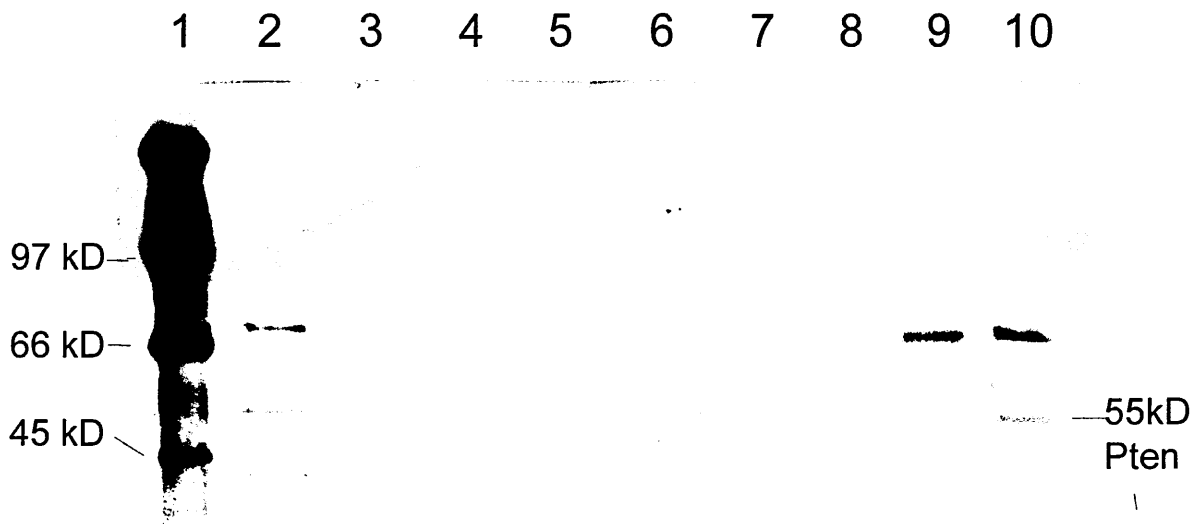


Fig 3.5.1 A and B. Lane 1, molecular weight marker. Lane 2 normal control, Lane 3 CGL, Lane 4 CLL, Lane 5 AML M1, Lane 6 AML M2, Lane 7 AML M3 variant, Lane 8 CGL acute phase. Lane 9 CGL
A. shows western blot of β -actin protein. B. shows western blot of PTEN protein. PTEN is expressed in all samples but staining is much reduced compared to β -actin. PTEN blot has been exposed to photographic film for longer, so the difference in expression is more pronounced than apparent from the photograph. This is evident from the increased level of background and molecular weight marker staining on the PTEN blot

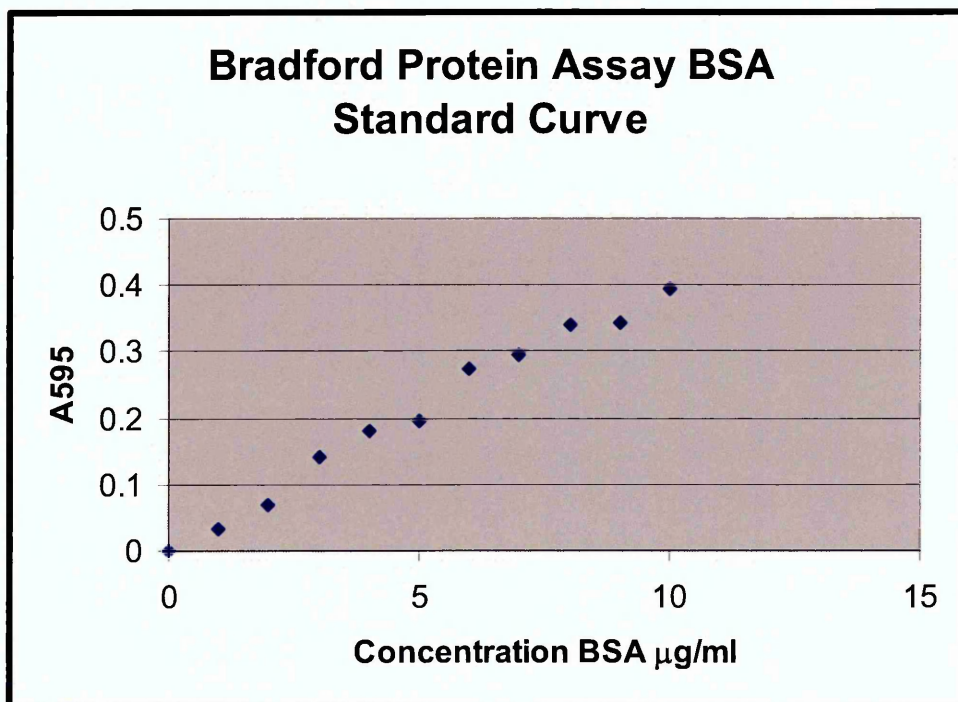


Fig 3.5.2 Bradford assay standard curve

Figure shows absorbance at 595nm of bovine serum albumin protein solutions at 0-10 $\mu\text{g ml}^{-1}$ Graph was used to interpolate the protein concentration of extracts for western blotting to achieve uniform loading quantities,

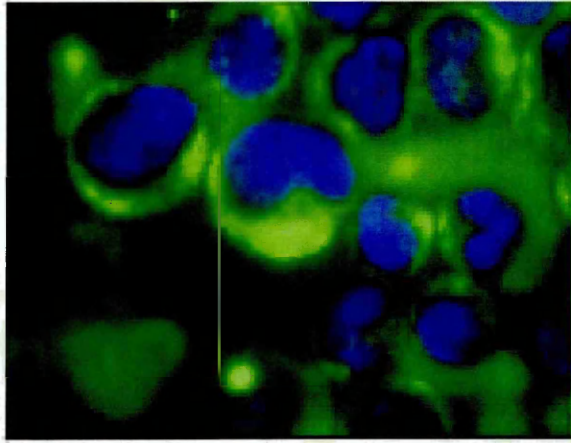
3.7 PTEN Immunocytochemistry and immunofluorescence

3.7.1 Immunofluorescence

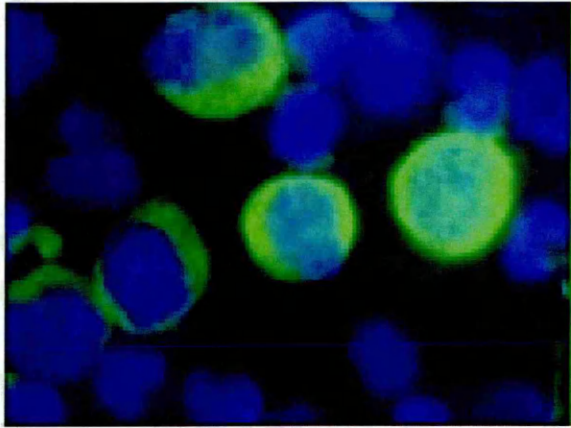
The western blot studies showed that PTEN protein was present in the samples studied but the samples represented a mix of tumour and normal cells. PTEN expression could be absent in the tumour cell population but present in the residual normal cell population. Immunofluorescence was performed to establish that PTEN expression was present in leukaemic cells and/or normal cells. Immunofluorescence showed PTEN expression in all leukaemias stained successfully. The proportion of failed samples was 55% (11 of 20) in which PTEN staining was absent in all cells within the bone marrow smear, not just the tumour cell population. Staining in leukaemia and normal bone marrow was stronger in immature cells with lesser intensity in mature cells. Staining was compartmentalised within the cytoplasm with low levels of nuclear staining in all smears except the CGL, which showed a diffuse distribution throughout the cytoplasm, which obscured possible nuclear staining.

Fig 3.6.1 immunofluorescence staining of PTEN protein

A



B



C

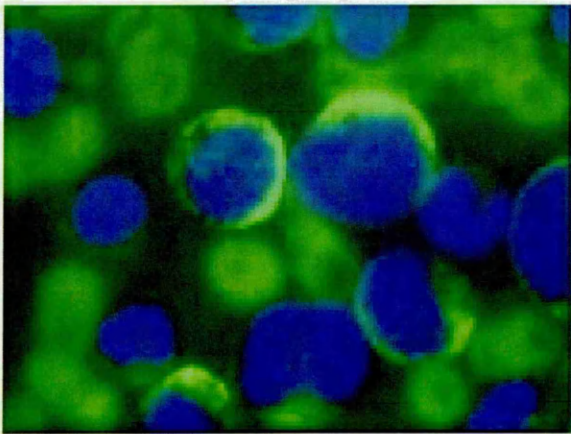


Fig 3.6.1 shows immunofluorescence staining of PTEN protein (green) in Normal Marrow (A), CGL (B) and M3 AML (C). UV induced fluorescence with DAPI nuclear stain (blue). Magnification 1000x.

3.7.2 Immunocytochemistry

Immunocytochemistry showed very slight staining compared to immunofluorescence. Staining was not obviously compartmentalised and showed, at best, weak signals with no apparent difference between control and leukaemia slides (not shown).

Chapter 4

Discussion and Conclusion

This study involved careful optimisation of methods used to identify mutations in PTEN in archival bone marrow smears, formalin fixed tissue samples and frozen bone marrow. The findings presented here show that extraction of PCR amplifiable DNA was possible from formalin-fixed, paraffin-embedded lymph node tissue and that simple heat treatment followed by proteinase K digestion led to better yield of PCR products than organic solvent extraction methods.

Amplification of 219 base pair sequences of β -globin was successful in 50% of extracts but amplification of longer sequences was more refractory. Zsikla *et al.* (2004) reported that the duration of fixation is the major factor affecting the preservation of DNA in formalin fixed tissue. They proposed that unbuffered formalin oxidises to formic acid and the subsequent acidic environment causes degradation of nucleic acids since the β -glycosidic bonds in the purine nucleotides are hydrolysed at pH 4. This group used a real-time PCR system to generate a 295 bp product of the β -actin gene and claimed that up to 50 times more β -actin DNA molecules could be extracted from small forceps biopsy samples fixed in buffered formalin when compared to unbuffered formalin. All the FFPE samples used in the current study were fixed overnight in buffered formalin and thus, should not have been subject to depurination by proton donors.

Dedhia *et al.* (2007) report that DNA extracted from formalin fixed tissues is highly degraded due to cross-linking between nucleic acid strands. They extracted DNA from FFPE sections using heat treatment and amplified by PCR using a real-time system with different primer sets that gave amplicons of different sizes when amplifying cyclin D1 and β -globin genes. PCR product was observed with shorter amplicon up to 250bp in length. Longer amplicons failed to amplify with paraffin

extracted DNA. Good results were seen with a primer concentration of 300nM and 5ng of template DNA. This group suggested that DNA obtained from formalin fixed paraffin embedded tissue is highly fragmented but can be used for successful amplification of shorter amplification products up to 250bp in length. The size of DNA amplified from FFPE in this study using a heat extraction and proteinase K method was similar to that reported by Rivero *et al.* (1997). They utilised a salting out method to extract DNA from FFPE tissue using 4M ammonium acetate followed by DNA precipitation using isopropanol. This group were able to amplify 167 and 268bp fragments of APC and β -globin genes respectively but had less success amplifying a 536bp fragment of β -globin gene. Coura *et al.* (1995) used a method based on xylene/ethanol de-waxing, followed by a long rehydration step prior to the DNA extraction step. In contrast to the findings presented in this thesis, which gave variable success rates, they reported 100% amplification success rate for fragments of 121bp to 227bp for FFPE tissue. Organic solvent extraction techniques were evaluated in this study but gave very poor levels of amplification compared to solvent free methods. Aviel-Ronen *et al.* (2006) used a quantitative PCR technique for whole genome amplification with a Bst DNA polymerase (described as Multiple-strand Displacement Amplification (MDA)) using proteinase K-extracted FFPE tissue. The amplified products obtained had amplicon sizes in excess of 23Kb. The MDA technique relies on the repeated random priming of large template DNA molecules rather than repeated cycling as in standard PCR, and generates only 1000 fold amplification. Nevertheless, this technique demonstrates its suitability for replication of DNA template obtained from FFPE and again contradicts the findings presented here that DNA amplification of products around 200 bp only is possible. The failure to amplify reliably products in excess of 200bp in this study

may be due to carry over of formalin in the DNA extraction process and subsequent degradation of the polymerase enzyme in the PCR mix. If formalin carry over was present, then it occurred despite careful washing of the nucleic acid sample.

Quach *et al.* (2004) questioned the fidelity of amplicons generated from FFPE extracted templates and reported that error prone trans-lesion synthesis across sites of damage produced *in vitro* artefactual mutations in their PCR products. Errors secondary to trans-lesion bypass were distinct from polymerase replication accuracy, reflecting incorporation of the wrong base opposite a damaged base rather than misincorporation of the wrong base opposite a normal base.

Amplification of DNA extracted by this method varied between PTEN exons 5, 7 and 8, with 8 being the most unreliable. Levels of amplification observed here are lower than those reported in other studies.

Court *et al.* (2001) extracted DNA from Giemsa stained smears using proteinase K digestion, treatment with saturated NaCl followed by DNA extracted from the supernatant by phenol/chloroform/isoamyl alcohol. Retrieved DNA was precipitated with ethanol at -20°C overnight then washed with 95% ethanol.

Comparison of this method with a technique using frozen cells demonstrated that the quality of extracted DNA isolated by the two methods was comparable. The technique used by this group was similar to that used in this study, but used a final phenol chloroform extraction step prior to precipitation of DNA. Similarly, Boyle *et al.* (1998) compared proteinase K and organic solvent techniques for DNA extraction from Giemsa stained bone marrow smears. They reported that, contrary to the work reported in this thesis, prior treatment with proteinase K had no effect on the yield of DNA extracted from smears using a phenol/chloroform method and that successive failure of PCR was not related to the quantity of DNA

isolated from the smears.

Tian *et al.* (2001) used BT549 cell line DNA samples with two mutations (16delAA and 822delG) in PTEN to assess the sensitivity of heteroduplex analysis coupled with capillary electrophoresis for detection of small deletion mutations. The group were able to identify a heterozygous mutation in PTEN in this cell line using this method.

Tsou *et al.* 1998 successfully used heteroduplex analysis to screen for novel germline mutations in PTEN using DNA isolated from individuals with Cowden syndrome. Two mutations in the PTEN gene were found: a transition (T→C) at nucleotide 335 in exon 5 and a novel splice site mutation (801+2 T→G) in intron 7. Hansen *et al.* (2001) used heteroduplex analysis and SSCP to screen for PTEN mutations. Nine exons of the PTEN gene, including intronic flanking regions were analysed in 62 patients with insulin-resistant type II diabetes. No mutations predicted to influence the expression or biological function of the PTEN protein but four intronic polymorphisms were identified.

Several groups used cell line or human wild type DNA for their analysis of PTEN using heteroduplex analysis (Tian *et al.* (2001), Tsou *et al.* (1998) and Hansen *et al.* (2001)). Their success suggests the technique is suitable for the detection of small deletions and point mutations. In the above studies, DNA was extracted from homogeneous cell types and in such cases, the heteroduplex pattern depends on whether the cells are heterozygous or homozygous for a specific allele. This contrasts with samples tested in the present study which consisted of a heterogeneous mix of tumour cells and normal cells. The relative percentage of each varied from 10% to over 90% between samples. Assuming that mutant and normal sequences are amplified with the same efficiency, and that hetero- and homoduplexes are formed with the same efficiency, the intensity of the PTEN

homoduplex bands generated from the normal cell sequences would obscure a heteroduplex band generated from a small percentage of tumour cells. Even with the use of silver staining and its associated sensitivity, it may not be sufficient to demonstrate a small proportion of heteroduplex bands. The problems associated with heterogeneous cell types would be addressed by using a viable microdissection technique to select tumour cells for nucleic acid extraction that yielded high levels of amplified product. The loss of heteroduplex bands against a background of homoduplex bands would be exacerbated by the generalised loss of band intensity reported here. The degree of diffusion in the heteroduplex bands varied between exons, with exon 8 showing high levels, making resolution of heteroduplex bands more difficult.

The current findings of the SSCP screening presented show that SSCP using sequences amplified from fresh or frozen cells is preferable to archived, fixed and stained cells. The technique using frozen cells generated bands in all reactions, even when very low levels of extracted DNA were present, which appeared to separate well using modified cross linking agents in the commercial polyacrylamide-based gels. The issue of heterogeneous tumour and normal cell populations and the sensitivity of mutation screening methods addressed by Fan *et al.* (2001). This group compared the sensitivity of non-isotopic PCR-SSCP to direct sequencing of PTEN exons. The group extracted DNA from leukocytes derived from healthy donors as well as from the glioblastoma cell line LN319 and mixed these in differing proportions from 0 to 100%. (The LN319 cell line contains a point mutation at codon 15 exon 1 of the PTEN gene). The PCR-SSCP demonstrated mutations in samples containing as little as 10% tumour DNA. Direct DNA sequencing experiments were less sensitive, requiring 30-70% of tumour DNA in the sample, depending on the DNA strand sequenced. They

concluded that PCR-SSCP based detection of PTEN point mutations was more sensitive than automated sequencing and recommended sequencing of both strands, and that samples containing less than 30% tumour cells should be studied by PCR-SSCP in order to discriminate false negative results obtained by sequencing reactions. The 10% tumour cell detection limit suggested by Fan *et al.* (2001) is the same as that used as a cut-off point in this study.

Mutation screening by heteroduplex analysis and SSCP failed to demonstrate point mutations or small deletions in any exon of the primary leukaemia and lymphoma samples studied here. This was supported by the DNA sequence analysis results even though all positive control reactions in the screening tests were successful. This suggests that small deletions and mutations are rare in the leukaemia and lymphoma groups examined in this study. The SSCP technique employed here may not have been sensitive to large heterozygous or homozygous deletions of PTEN in the tumour cell population as the tissue samples contained varying levels of normal cells which would express wild type PTEN, which would be amplified in the PCR step.

cDNA or genomic DNA from all primary malignancies and cell lines was analysed successfully by Dahia *et al.* (1998) for the presence of mutations in the whole coding region of PTEN. DGGE analysis revealed no mutations in the cDNA of 43 myeloid and 31 lymphoid primary leukaemia PTEN coding regions studied but a IVS4+42C→T mutation in an intron of one transformed myelodysplastic syndrome (secondary acute myeloid leukaemia).

Using SSCP and DNA sequencing, Sakai *et al.* (1998) examined 27 haematopoietic cell lines (representing a variety of lymphoid lineages), 65 primary lymphoid tumours (including 24 lymphoblastic leukaemia/lymphoma), 30 large B-cell lymphoma, 7 Burkitt's lymphoma, 4 anaplastic large cell lymphoma, and 25

non-malignant lymph node controls. Six of the 27 cell lines and 3 of 65 primary lymphomas contained alterations of PTEN. The group reported a large homozygous deletion spanning exons 2 through 5 in one lymphoblastic leukaemia cell line, two insertions potentially resulting in premature termination in a second lymphoblastic leukaemia cell line. Non-conservative nucleotide variations were found in two other cell lines (one large B-cell lymphoma and one Burkitt's lymphoma) and in one primary case of LBCL. In addition, two other cell lines (one BL and one myeloma) and two primary lymphomas, both LBCL, contained small deletions within intron 7. No point mutations were reported in the PTEN gene which supports the findings of this thesis

Grønbaek *et al.* (1998) studied 14 malignant and 4 benign lymphoid cell lines for deletions and mutations in all exons of the PTEN gene by combining PCR, DGGE and direct sequence analysis. The group reported mutations of *PTEN* in two of the malignant cell lines (a deletion of exons 2 to 5 in a T-cell ALL cell line and a C → T transition at the first base of codon 17 in the myeloma cell line HS-Sultan) but none in the benign cell lines. Grønbaek *et al.* (1998) also examined all exons of the PTEN gene by PCR/DGGE analysis in 170 primary lymphoid malignancies and detected two point mutations, both in large B-cell lymphomas cases.

Nakahara *et al.* (1998) examined 29 cases of primary NHL for mutations in the PTEN gene. One case of diffuse large B cell lymphoma had an 11bp deletion, but the remaining 28 cases showed no mutations in the gene. Butler *et al.* (1999) carried out a study of PTEN mutations in lymphoma, based on their observation that deletions and rearrangements of 10q22-25 have been reported in approximately 5%-10% of NHL, raising the possibility of PTEN involvement in these tumours. The group analysed cell lines and primary tumours in a panel of

74 NHLs (which were representative of the main histological subtypes) for mutations and homozygous deletions of PTEN. They reported somatic coding/splice site variants in 20% (2 of 10) of Burkitt's lymphoma cell lines and in 3% (2 of 64) of primary NHL cases analyzed. No homozygous deletions were detected. The group reported that all NHL cases with 10q22-q25 abnormalities displayed neither biallelic deletions nor mutations of PTEN. They also suggested that a tumour suppressor gene distinct from PTEN may be involved in 10q deletions in the subgroup of NHL cases.

Scarlsbrick *et al.* (2000) examined 54 tumour DNA samples from patients with cutaneous T-cell lymphoma (CTCL) for loss of heterozygosity on 10q. Allelic loss was identified in 10 samples, all of which were from the 44 patients with mycosis fungoides (a T-cell malignancy). Samples with allelic loss on 10q were analyzed for abnormalities of the PTEN gene. No tumour-specific mutations in PTEN were detected. The group suggested that their data imply that this gene is rarely inactivated by small deletions or point mutations.

Aggerholm *et al.* (2000) screened 13 leukaemia cell lines for mutations and homozygous deletions in PTEN using PCR and DGGE. They identified an intragenic deletion including PTEN exons 2-5 in an acute myelocytic leukaemia cell line, HL-60 blast, and an insertion of four nucleotides in exon 5 in an acute monocytic leukaemia cell line, U937. The group screened 59 patients with AML, 26 patients with MDS and 10 patients CML and only revealed a polymorphic base substitution in codon 44 in one AML patient. The group suggested that mutations in the PTEN gene are infrequent genetic aberrations in myeloid leukaemia.

Leupin *et al.* (2003) found 20% of B-CLL patients exhibit loss of heterozygosity (LOH) at 10q23.3. Microsatellite markers mapped complete LOH to 10q23.3 in 2/41 B-CLL (5%) and allelic imbalances in 6/41 (15%). No PTEN gene mutations

were found. PTEN protein expression was not detected in 11 B-CLL (28%), and was reduced in eight patients (20%). LOH or allelic imbalances at 10q23.3 were fairly frequent in B-CLL, but did not encompass the PTEN gene. The group suggested that PTEN protein may be absent in B-CLL with a normal PTEN genotype, suggesting a role of this phosphatase in the molecular pathology of B-CLL. Liu *et al.* (2000) screened 62 AML patients for DNA mutations in all PTEN exons by PCR-SSCP and direct sequencing. No mutations were observed in any of the coding regions and none of the AML cases had LOH.

Chang *et al.* (2006) analysed clonal plasma cells from patients with MM and plasma cell leukaemia for deletions/mutations of the PTEN gene by using interphase fluorescent *in situ* hybridisation (FISH). PTEN deletions were detected in 4 of 71 myeloma clones and 2 of 10 plasma cell leukaemia. DNA sequencing analysis did not detect PTEN mutations in 11 primary myeloma and 5 plasma cell leukaemia cases. The group concluded that alterations of PTEN are uncommon in myeloma patients, and PTEN deletions tend to occur in advanced disease suggesting that they are secondary rather than primary events in the pathogenesis of MM.

Thus, all groups referenced above have reported that point mutations and small deletions are rare in primary haematological malignancy and support the findings of this study (Sakai *et al.* (1998), Grønbaek *et al.* (1998), Nakahara *et al.* (1998), Butler *et al.* (1999), Scarisbrick *et al.* (2000), Aggerholm *et al.* (2000), Liu *et al.* (2000), Leupin *et al.* (2003), and Chang *et al.* (2006)). PTEN is reported to be mutated at a higher frequency in solid tumours than in haematological malignancy. Bonneau and Longy (2000) reviewed somatic mutations in primary tumours and reported the majority of PTEN mutations in endometrial carcinomas and glioblastomas. 130 out of 145 cases of informative tumours had bi-allelic

inactivation of PTEN through loss of heterozygosity by deletion of one allele and point mutations in the remaining allele. 23% of somatic mutation occurred in exon 5 (encoding the phosphatase domain), particularly at arginine residues 130, 233 and 335. A difference in location of mutations was noted between endometrial carcinoma (predominantly exons 7 and 8) and glioblastoma (predominantly exon 6).

Kurose *et al.* (2002) demonstrate high frequencies of somatic mutations in the PTEN gene and p53 tumour protein in breast neoplasms using DGGE. Mutations in p53 and PTEN were mutually exclusive in either compartment. 15 of 50 (30%) breast carcinomas had somatic mutations in PTEN in either neoplastic epithelium or stroma. Mutations in PTEN were not accompanied by LOH. Kolasa *et al.* (2006) reported PTEN mutations in 5/100 cases of primary cervical carcinoma and there was a reverse association of p53 and PTEN mutations.

Weng *et al.* (2001) examined 10 thyroid cancer cell lines and found a hemizygous PTEN deletion with a splice variant in the remaining allele in a single follicular thyroid carcinoma line. Four lines, including the FTC line, expressed PTEN mRNA at low levels. Transient expression of PTEN in 7 thyroid cancer cell lines resulted in G1 arrest in 2 well-differentiated papillary thyroid cancer lines. Cairns *et al.* (1997) screened 80 prostate tumours by microsatellite analysis and found chromosome 10q23 to be deleted in 23 cases; sequence analysis of cases showing loss of heterozygosity. 10 tumours, (43%) demonstrated a second mutation, thus establishing PTEN as a main inactivation target of 10q loss in sporadic prostate cancer. PTEN mutations occur in up to 60% of primary prostate cancers an LOH as a single defect is reported more frequently than LOH followed by mutational inactivation of the remaining allele. LOH is more common in metastatic prostate tumours, indicating an association of PTEN dysfunction and

tumour progression. (Wang *et al.* (1998), Vlietstra *et al.* (1998), Pesche *et al.* (1998), Feilotter *et al.* (1998), Dong JT *et al.* (1998), and Bar-Shira *et al.* (2006)). The coding region of the PTEN gene was examined in malignant melanoma from 16 primary and 61 metastatic tumours from 67 patients. (Birck *et al.* 2000). Mutations were identified in 4 of the metastatic samples (7%) and analysis of 2 intragenic polymorphisms showed allelic loss in 3 of 8 primary tumours (38%) and in 18 of 31 metastatic tumours (58%). One of the mutant cases showed allelic loss, suggesting that both PTEN alleles were inactivated in this tumour. The group proposed that mutation and deletion of PTEN may contribute to the development and progression of malignant melanoma. Celebi *et al.* (2000) examined 21 metastatic melanoma samples and found LOH at 10q23 in 7 of 21 samples and identified sequence alterations in the PTEN gene in four of the samples.

Neither Cowden syndrome or Bannayan-Zonana syndrome predispose to cervical cancer, LOH of markers on chromosome 10q is however frequently observed in cervical cancers. To determine the potential role that PTEN mutation plays in cervical tumourigenesis, Kurose *et al.* (2000) screened 20 primary cervical cancers for LOH of polymorphic markers within and flanking the PTEN gene, and for intragenic mutations in the entire coding region and exon-intron boundaries of the PTEN gene. LOH was observed in 7 of 19 (36.8%) cases. Three (15%) intragenic mutations were found: two were somatic missense mutations in exon 5 and the third was an occult germline intronic sequence variant in intron 7 and was shown to be associated with aberrant splicing. All 3 samples with the mutations also had LOH of the wildtype allele. In cervical cancer, unlike some other human primary carcinomas biallelic structural PTEN defects seem necessary for carcinogenesis.

Somatic genetic inactivation of PTEN is involved in as high as 93% of sporadic endometrial carcinomas (EC) and can occur in the earliest precancers. Zhou *et al.* (2002) obtained 41 endometrial carcinomas and analysed PTEN expression and undertook mutation analysis. Mutation analysis of 20 aberrant PTEN-expressing tumours revealed that 17 (85%) harboured 18 somatic PTEN mutations. All were frameshift mutations, 10 (56%) of which involved the 6(A) tracts in exon 7 or 8.

Other researchers have reported primary endometrial cancers with PTEN mutations approaches 80% to 90% in the endometrioid class of tumour, making PTEN mutation the most common finding in EC mutation screening (Risinger *et al.* (1997), Tashiro *et al.* (1997), Lin *et al.* (1998), Maxwell *et al.* (1998), Mutter *et al.* (2000) Oda *et al.* (2005)).

Mutation of PTEN is seen in the earliest stages of EC including endometrial hyperplasia. This suggests that PTEN loss is an early event in this disease. In contrast to brain tumours (Wen *et al.* (2001)), loss of PTEN in EC is associated with increased survival rates Risinger *et al.* (1998).

The role of PTEN in head and neck squamous cell carcinomas in correlation to mutation and methylation of the p16 gene and to previous studies concerning loss of chromosomes 9 and 10 was examined by Poetsch *et al.* (2002). They screened for alterations in PTEN and p16 in 52 HNSCC of different sites and found mutations in 12 (23%) tumour samples; PTEN missense mutations were found in 7 carcinomas (13%), and a loss of chromosome 10 was detected in 5 (71%) of these.

In their original description of PTEN, Li *et al.* (1997) screened genomic DNA from 18 primary glioblastomas for mutations in three exons. Mutations in PTEN were found in three of these tumours: a 2-bp insertion at codon 15 (534 T); a point

mutation resulting in a Gly → Arg change at codon 129 (132T), and a 4-bp frameshift mutation at codon 337 (134T). The mutation at codon 129 is within the signature sequence for tyrosine phosphatases. All three tumours displayed LOH in the PTEN region. In addition, the tumour mutations were not detected in DNA from paired blood samples.

Wen *et al.* (2001) reported data indicating that PTEN regulates tumour-induced angiogenesis and the progression of gliomas to a malignant phenotype via the regulation of phosphoinositide-dependent signals. Mutation in the PTEN gene accompanies progression of brain tumours from benign to the most malignant forms. Tumour progression, particularly in aggressive and malignant tumours, is associated with the induction of angiogenesis, a process termed the angiogenic switch. Biallelic inactivation of PTEN has been reported in 30% to 40% of glioblastoma multiforme, in anaplastic astrocytoma, and rarely in lower-grade glioma and glioneuronal tumours (Liu *et al.* (1997); Rasheed *et al.* (1997); Wang *et al.* (1997); Duerr *et al.* 1998) and Smith *et al.* (2001))

From the above findings, it is clear that though PTEN is not commonly subject to mutation in haematological malignancy, it is frequently mutated in other solid tumours. Sansall and Sellers (2004) commented on the discordance between the rate of LOH and the rate of mutation of the second PTEN allele, which has led some to suggest that a second tumour suppressor gene is harboured in the 10q23 region (as suggested in haematological malignancy by Butler *et al.* (1999)). However, this difference could also result from the technical inability to detect second mutational events in the remaining functional PTEN allele.

Passegué *et al.* (2003) observed the low number of mutations necessary to induce leukaemia compared with solid tumours and commented on the pre-existing immortalised character that HSCs have in common with leukaemic cells.

It may be the case that the rapid proliferation of the stem cell compartment associated with turnover of HSC (1 trillion cells per day in an adult (Ogawa 1995)), coupled with a small number of critical oncogenic mutations is enough to cause neoplasia, by passing PTEN and the downstream PI3/AKT pathway which modulates cell cycling. Kurose *et al.* (2002) have reported mutually exclusive occurrence of p53 and PTEN mutation in breast neoplasia, suggesting that the presence of either mutation is capable of inducing tumour formation. Also, PTEN is not the only phosphatase involved in modulation of the PI3/AKT pathway. The SH2 domain-containing inositol 5'-phosphatase (SHIP) group of proteins also modulate the AKT pathway but reports of its involvement in haematological malignancy are contradictory. Luo *et al.* (2003) reported that the SHIP is crucial in haematopoietic development. They examined primary leukaemia cells from 30 AML patients, together with eight myeloid leukaemia cell lines. A somatic mutation at codon 684, replacing Val with Glu, was detected in one patient, lying within the signature motif 2, which is the phosphatase active site. Leukaemia cells with this mutation showed enhanced Akt phosphorylation following IL-3 stimulation. K562 cells transfected with the mutated SHIP-V684E cDNA showed a growth advantage even at lower serum concentrations and resistance to apoptosis induced by serum deprivation and exposure to etoposide. The authors suggested that these results are evidence of possible role of the mutated *SHIP* gene in the development of acute leukaemia and chemotherapy resistance through the deregulation of the PI3/Akt signalling pathway.

The findings of Luo *et al.* (2003) contrast with an earlier study by Choi *et al.* (2002) who found loss of PTEN expression in OPM2 and $\Delta 47$ human myeloma cell lines, which led to high Akt activity toward insulin-like growth factor. Down-regulation and over-expression of SHIP in myeloma, PCT and NIH3T3 cell lines

did not affect Akt activity in all systems analysed (unlike PTEN), despite its ability to dephosphorylate a PI3K product. Expression of SHIP and SHIP2 in a PTEN-null myeloma line did not suppress Akt activity. Biologically, expression of only PTEN, but not SHIP and SHIP2, resulted in growth inhibition. Horn *et al.* (2004) analyzed the effects of SHIP on the lymphoid Jurkat cell line in which expression of endogenous SHIP (and PTEN) protein was not detectable. Restoration of SHIP expression in Jurkat cells with an inducible expression system caused a 69% reduction of PI3K and a 65% reduction of Akt kinase activity. This was associated with increased transit time through the G1 phase of the cell cycle. Restoration of SHIP expression did not cause a complete cell cycle arrest or apoptosis. It is noteworthy that Jurkat cells show abolition of PTEN and SHIP expression - both mechanisms that control PI3K.

If the HSC compartment is proliferating constantly to maintain homeostasis, then PTEN expression and an associated brake on proliferation might be reduced in normal haemopoetic systems. Any subsequent disruption of PTEN by mutation might not confer a selective growth advantage if PTEN is not an important regulator of proliferation in this system, particularly if the SHIP pathway is still intact. However, this theory is not supported by the fact that SHIP^{-/-} mice are viable and are not reported to be predisposed to develop leukaemia (Luo *et al.* 2003).

As reported in chapter 1 (1.7.1.3), BCR/ABL in CML cases might be able to mimic the physiologic IL-3 survival signal in a PI3K-dependent manner. Ship and Ship-2 are activated in response to growth factor signals and by BCR/ABL. BCR/ABL interacts indirectly with the p85 regulatory subunit of PI3K via GRB-2/Gab2 and this appears pathologically relevant because Gab2-deficient marrow cells are resistant to BCR/ABL transformation (Sattler *et al.* 2002)

RT-PCR analysis of cell lines in this study showed amplification of full-length cDNA in all haemopoietic cell lines studied apart from Jurkat cells, suggesting that expression of full-length mRNA resulted from at least one PTEN allele. Jurkat, a lymphoid cell line, has expression of both PTEN alleles abolished by mutation. Shan *et al.* (2000) described the defect in expression of PTEN in Jurkat T cells as leading to unregulated pleckstrin homology (PH) domain interactions with the plasma membrane. Inhibition of phosphoinositide phosphorylation by PI3K inhibitors, or by expression of PTEN, blocked constitutive phosphorylation of Akt on Ser-473 and caused Itk (a PH domain-containing kinase) to redistribute from the plasma membrane to the cytosol. The PTEN-deficient cells were also hyper-responsive to T-cell receptor (TCR) stimulation, which suggested a negative regulatory role for PTEN in TCR stimulation. Cell cycle arrest and release assays in Jurkat cells showed that PTEN expression reduced proliferation by slowing progression through all phases of the cell cycle. This was associated with reduced levels of cyclins A, B1 and B2, cdk4, and cdc25A and increased p27^{KIP1} expression. Apoptosis played no role in the antiproliferative effect of PTEN, since only marginal increases in the rate of apoptosis were detected upon PTEN expression, and inhibitors of effector caspases did not restore proliferative capacity. Active Akt blocked the antiproliferative effects of PTEN, indicating that PTEN mediates its effects through conventional PI3K-linked signalling pathways (Seminario *et al.* 2003). The results presented in this thesis are in line with the findings of Dahia *et al.* (1999) who found the level of PTEN expression varied widely amongst the cell lines in their study: B15, BLIN1, DHL4, DHL10, NALM6, HT, RS4;11 and RAJI showed high transcript levels, whereas BV173, HL60 and U937 had very low transcript levels and the remaining samples (207, DHL7, DHL8 and K562) showed an intermediate level of PTEN transcription. Jurkat cells

were not included in their study. Epigenetic silencing of PTEN by methylation was reported in 5% of malignant melanoma primary tumours (Zhou *et al.* 2000), but none of 58 primary gastric cancers (Sato *et al.* 2006).

Zysman *et al.* (2002) commented on the difficulty of assessing methylation status in PTEN due to extensive methylation of the nearby pseudogene and reported that PTEN promoter methylation is rare in primary malignancy.

Western blot analysis in this study showed expression of PTEN in all of the primary leukaemia bone marrow samples, but at low levels compared to the β -actin control. Protein isolated from the primary leukaemia samples will reflect both the leukaemic and normal cell population in the bone marrow compartment, thus total abolition of PTEN expression can not be ruled out. These results are in agreement with Min *et al.* (2004) who correlated Skp2 protein expression (PTEN regulates Skp2-mediated degradation of cell cycle inhibitor p27Kip1) with PTEN expression in 99 consecutive adults patients with *de novo* AML, with 4 M0; 20 M1; 33 M2; 19 M4; 21 M5 and 2 M6 subtypes. Constitutive expression of phosphorylated PTEN protein was demonstrated in the majority of AML cases with high correlation with Skp2 expression. Zouh *et al.* (2003) found that expression of PTEN assessed by western blotting was absent in 3 of 9 ALL cell lines. Leupin *et al.* (2003) reported that PTEN protein expression was not detected in 11 of 41 B-CLL cases (28%), and was reduced in eight patients (20%).

Liu *et al.* (2004) found that PTEN protein was decreased in 18 of 30 (60%) JMML patients, and these patients had significantly lower RNA expression of PTEN than normal controls.

Shen *et al.* (2005) explored PTEN gene expression and its clinical significance in acute leukaemia comprising 5 leukaemia cell lines, 87 patients with acute

leukaemias including 59 AML, 26 ALL, and 2 acute hybrid leukaemia, 21 ALL in complete remission (ALL-CR), 31 CML and 14 normal controls were assayed. The expression ratio of PTEN mRNA between CML and normal control had no statistical difference. The expression ratios of PTEN mRNA in ALL and ALL-CR were significantly lower than that in normal control ALL also has a lower expression ratio than that of ALL-CR ($P < 0.05$). The decreased level of PTEN mRNA had a positive correlation with poor-prognostic factors. The group concluded that there was a down-regulated expression of PTEN gene in ALL. The immunofluorescence staining of PTEN in primary leukaemias in this study demonstrated an increased level of staining in immature cells. Two of eleven cases (CGL and M3 AML) show high levels of cytoplasmic expression, which supports the observation by Liu *et al.* (2005) that wild-type PTEN shows preferential nuclear localization in differentiated or resting cells and cytoplasmic localisation in immature cells. The visualisation of PTEN signal in leukaemic cells removes any possibility of a false positive signal generated by normal cells within the tumour cell sample. Cytoplasmic expression of PTEN by immunofluorescence staining was reported by: Furnari *et al.* (1997) in glioma cell lines; by Li and Sun (1997) in transfected HepG2 and NIH3T3 cells and by Georgescu *et al.* (2000) in transfected U87-MG cells.

Conclusion

Deletion of PTEN causes the generation of transplantable leukaemia-initiating cells in a murine model and causes the depletion of normal haemopoetic stem cells (Yimaz *et al.* 2006). If these findings translate to the human system, is PTEN mutated in leukaemia? The findings presented here show that the PTEN gene is not mutated in any stages of primary haematological malignancy and the protein is expressed in most primary leukaemias. Epigenetic mechanisms of PTEN activation have not been reported. These findings assume that the mutation detection techniques used in this study present an accurate picture of mutation status. The only possible source of error is contamination of the leukaemic cell population with normal cells, but the high percentage of tumour cells in the samples analysed make this unlikely. The use of cell sorting and laser capture dissection techniques would remove contamination as a source of error. It is also possible (but improbable) that small mutations of PTEN in exon 2 are more common in haematological malignancy. The exon was not screened in this study due to technical difficulty. Bonneau and Longy (2000) catalogue 332 somatic PTEN mutations in primary tumours; only 18 (5%) occur in PTEN exon 2, mostly in EC cases - none are reported in haematological malignancy.

PTEN is essential for haemopoetic stem cell function in at least two critical areas associated with the malignant transformation process: control of cell cycle and proliferation, plus chemotaxis and localisation within the bone marrow compartment. PTEN therefore, would be a candidate for mutation to facilitate the transformation of normal cells. The PI3-kinase/Akt pathway is constitutively active in primary AML cells and blocking PI3-kinase has direct anti-leukaemic effects in AML progenitor subsets (Grandage *et al.* 2005). Defects in PTEN co-operate with complex somatic mutations in solid tumours at multiple stages (with the loss of

other tumour suppressors and/or activation of oncogenes) to promote malignancy (Yamada and Araki 2002). However, the work presented in this thesis showed no evidence of PTEN mutation in leukaemia. Melo and Deininger (2004) demonstrated that p53 is genetically or functionally inactivated in a large fraction of CML blast crisis cases. In line with the mutually exclusive presence of p53TP and PTEN mutations reported in solid tumours, it may be the case that with the small number of oncogenic mutations required to initiate leukaemia, the function of PTEN, aberrant or otherwise, is not a critical factor in promoting the leukaemic phenotype.

4.3 Further Work

The intrinsic involvement of PTEN with the proliferation status of haemopoetic stem cells demands further investigation, particularly the levels of phosphorylated PTEN and Akt in leukaemic and normal cells and the effect of other oncogenic mutations on PTEN function. Flow cytometry would be an ideal means of correlating phenotypic markers associated with leukaemia class with levels of PTEN and Akt expression and phosphorylation. The tumour cells of haematological malignancy are particularly suitable for this method as they are usually discrete, single cells. The technique would be limited in the study of primary haematological malignancy by its requirement for very fresh cellular material.

The weak, poorly-characterised protein phosphatase activity of PTEN towards proteins such as PDGF deserves further exploration. A search for other substrates of PTEN may reveal an undiscovered function which may be important in the promotion of the leukaemic phenotype. Finally, the frequent deletion of 10q sequences in B-cell lymphoma that exclude the PTEN gene suggest the presence of a further tumour suppressor element in this region. The exon trapping technique used by Steck *et al.* (1997) in the original identification of PTEN would be useful if the element is a tumour suppressor gene.

References

- ALBERTS, B., *et al.* 2000. *Molecular Biology of the Cell*. Garland Science New York and London.
- AGARWAL, S. K., 2004. Molecular pathology of the MEN1 gene. *Ann N Y Acad Sci.*, 1014, 189-98
- AGGERHOLM, A. *et al.* 2000. Mutational analysis of the tumour suppressor gene MMAC1/PTEN in malignant myeloid disorders. *Eur J Haematology*, 65(2),109-13.
- ALGECIRAS-SCHIMNICH, A. *et al.* 2006. Apoptosis Dependent and Independent Functions of Caspases. *Apoptosis*. Landes Bioscience USA
- ALLEN, R.T. *et al.* 1998. Mechanisms controlling cellular suicide role of Bcl-2 and caspases. *Cell Mol Life Sci.*, 54(5), 427-45
- AVIEL-RONEN, S. 2006. Large fragment Bst DNA polymerase for whole genome amplification of DNA from formalin-fixed paraffin-embedded tissues. *BMC Genomics.*, 12 (7), 312
- BAI, F. *et al.* 2003. Haploinsufficiency of p18(INK4c) sensitizes mice to carcinogen-induced tumorigenesis. *Mol Cell Biol.*, 23(4), 1269-77
- BARILA, D. AND SUPERTI-FURGA, G. 1998. An intramolecular SH3-domain interaction regulates c-Abl activity. *Nat Genet.*, 18(3), 280-2
- BAR-SHIRA, A. *et al.* 2006. Mutation screening and association study of the candidate prostate cancer susceptibility genes MSR1, PTEN, and KLF6. *Prostate*. 66(10), 1052-60
- BIRCK, A. *et al.* 2000. Mutation and allelic loss of the PTEN/MMAC1 gene in primary and metastatic melanoma biopsies. *J. Invest. Derm.*, 114, 277-280,
- BIRLE, D, *et al.* 2002. Negative Feedback Regulation of the Tumor Suppressor PTEN by Phosphoinositide-Induced Serine Phosphorylation¹. *Journal of*

Immunology, 169, 286-291.

BONNEAU, D. AND LONGY, M. 2000. Mutations of the human PTEN gene.

Hum Mutat, 16(2), 109-22.

BOYLE, E.B. *et al.* , 1998. Accuracy of DNA amplification from archival hematological slides for use in genetic biomarker studies. *Cancer Epidemiol Biomarkers*, 7(12),1127-31.

BUTLER, M.P. *et al.* 1999 Analysis of PTEN mutations and deletions in B-cell non-Hodgkin's lymphomas. *Genes Chromosomes Cancer*. 24(4), 322-7.

BROWN, T.A. 2002. *Genomes* Garland Science, New York and London

CAIRNS, P. 1997. Frequent inactivation of PTEN/MMAC1 in primary prostate cancer. *Cancer Res.*, 57, 4997-5000,

CALABRETTA, B. AND PERROTTI, D. 2004. The biology of CML blast crisis. *Blood*, 103(11), 4010-22

CALLADINE, C.R. AND DREW, H.R. 1997. *Understanding DNA; The Molecule and How It Works*. Academic Press Inc.,U.S.

CAMPIONI, M. *et al.* 2005. Role of Apaf-1, a key regulator of apoptosis, in melanoma progression and chemoresistance. *Exp Dermatol.*, 14(11), 811-8.

CELEBI, J. T. 2000. Identification of PTEN mutations in metastatic melanoma specimens. *J. Med. Genet.*, 37, 653-657

CHANG, H. *ET AL* 2006. Analysis of PTEN deletions and mutations in multiple myeloma. *Leuk Res.*, 30(3), 262-5

CHEN, P.L. *et al.* 1989. Phosphorylation of the retinoblastoma gene product is modulated during the cell cycle and cellular differentiation. *Cell*, 58(6), 1193-8

CHEN, Y. AND STRUHL, G. 1996. Dual roles for patched in sequestering and transducing Hedgehog. *Cell.*, 87(3), 553-63

CHEONG, J.W. *et al.* 2003. Phosphatase and tensin homologue phosphorylation

in the C-terminal regulatory domain is frequently observed in acute myeloid leukaemia and associated with poor clinical outcome. *Br J Haematol.*, 122(3), 454-6.

CHOI, Y. *et al.* 2002. PTEN, but not SHIP and SHIP2, suppresses the PI3K/Akt pathway and induces growth inhibition and apoptosis of myeloma cells. *Oncogene*, 21(34), 5289-5300

CLARKSON, B.D.*et al.* 1997. New understanding of the pathogenesis of CML a prototype of early neoplasia. *Leukemia*, 11(9), 1404-28.

COFFIN, J. *et al.* 1997. *Retroviruses*. Cold Spring Harbor Laboratory Press, USA

COOPER, G.M. 2000. *The Cell - A Molecular Approach*, Sinauer Associates, Inc. USA

COURA, R. *et al.* 2005. An alternative protocol for DNA extraction from formalin fixed and paraffin wax embedded tissue. *J Clin Pathol.*, 58(8), 894-5

COURT, E.L. *et al.* 2001. C-kit mutation screening in patients with acute myeloid leukaemia adaptation of a Giemsa-stained bone-row smear DNA extraction technique. *Br J Biomed Sci.*, 58(2), 76-84.

CRINO, P.B. *et al.* 2006. The tuberous sclerosis complex. *N Engl J Med.*, 355(13), 1345-56.

DAHIA, P.L. *et al.* 1999. PTEN is inversely correlated with the cell survival factor Akt/PKB and is inactivated via multiple mechanisms in haematological malignancies. *Hum Mol Genet.*, 8(2), 185-93.

DAY, D.A. AND TUIITE, M.F. 1998. Post-transcriptional gene regulatory mechanisms in eukaryotes an overview. *J Endocrinol.*, 157(3), 361-71.

DEDHIA, P. *et al.* 2007. Evaluation of DNA extraction methods and real time PCR optimization on formalin-fixed paraffin-embedded tissues. *Asian Pac J Cancer Prev.*, 8(1), 55-9

DEININGER, M.W. *et al.* 2000. BCR-ABL tyrosine kinase activity regulates the expression of multiple genes implicated in the pathogenesis of chronic myeloid leukemia. *Cancer Res.*, 60(7), 2049-55

DEININGER, M.W. *et al.* 2001. Direct relation between BCR-ABL tyrosine kinase activity and cyclin D2 expression in lymphoblasts. *Cancer Res.*, 61(21), 8005-13

DONG, J.T. *et al.* 1998. PTEN/MMAC1 is infrequently mutated in pT2 and pT3 carcinomas of the prostate. *Oncogene*, 17, 1979-1982,

DUERR, E.M. *et al.* 1998
PTEN mutations in gliomas and glioneuronal tumors. *Oncogene* 16 2259-2264,

EAVES, A.C. *et al.* 1986. Unregulated proliferation of primitive chronic myeloid leukemia progenitors in the presence of normal row adherent cells. *Proc Natl Acad Sci USA.*, 83(14), 5306-10

EAVES, C. J. *et al.* 2003. New models to investigate mechanisms of disease genesis from primitive BCR-ABL(+) hematopoietic cells. *Ann N Y Acad Sci.*, 996, 1-9

FADERL, S. *et al.* 1999. Chronic myelogenous leukemia biology and therapy *Ann Intern Med.*, 131(3), 207-19

FAN, X. *et al.* 2001. Non-isotopic silver-stained SSCP is more sensitive than automated direct sequencing for the detection of PTEN mutations in a mixture of DNA extracted from normal and tumor cells. *Int J Oncol.*, 5, 1023-6.

FEILOTTER, H.E. *et al.* 1998. Analysis of PTEN and the 10q23 region in primary prostate carcinomas. *Oncogene*, 16, 1743-1748,

FIALKOW, P.J. *et al.* 1977 Chronic myelocytic leukemia clonal origin in a stem cell common to the granulocyte, erythrocyte, platelet and monocyte/macrophage. *Am J Med.*, 63(1), 125-30.

- FRIEDENAUER, S. AND BERLET, H.H.1989. Sensitivity and variability of the Bradford protein assay in the presence of detergents. *Anal Biochem.*, 178(2), 263-8
- FRIEDMAN, J.M. *et al.* 2002. Cardiovascular disease in neurofibromatosis 1 report of the NF1 *Cardiovascular Task Force*. *Genet Med.*, 4(3), 105-11.
- FRIEDMAN, J. M. 2006. *Neurofibromatosis 1 Seattle (WA) University of Washington 1993-2007 Gene reviews* NCBI books. Available from: <http://www.ncbi.nlm.nih.gov/books/bv.fcgi?rid=gene.TOC>
- FURNARI, F.B. *et al.* 1997. Growth suppression of glioma cells by PTEN requires a functional phosphatase catalytic domain. *Acad. Sci. USA*, 94, 12479-12484
- GANGULY, A. *et al.* 1993. Conformation-sensitive gel electrophoresis for rapid detection of single-base differences in double stranded PCR products and DNA fragments evidence for solvent induced bends in DNA heteroduplexes. *Proc Natl Acad Sci U S A*, 90, 10325–10329
- GANGULY, A. AND PROCKOP, D. J. (1995). *Electrophoresis*, 16, 1830–1835.
- GARCÍA, Z. *et al.* 2006. Phosphoinositide 3-kinase controls early and late events in mammalian cell division. *EMBO J.*, 25(4), 655-61.
- GARCÍA-CAO, M. *et al.* 2002. A role for the Rb family of proteins in controlling telomere length. *Nat Genet.*, 32(3), 415-9.
- GEARY, C. G. 2000. The story of chronic myeloid leukaemia. *British Journal of Haematology*, 110 (1), 2-11
- GEORGESCU, M.M. *et al.* 2000. Stabilization and Productive Positioning Roles of the C2 Domain of PTEN Tumor Suppressor. *Cancer Research* 60, 7033-7038,
- GILBERT, S. F. 2000. *Developmental Biology*. *Sinauer Associates, Inc USA*

GRANDAGE, V.L. 2005. PI3-kinase/Akt is constitutively active in primary acute myeloid leukaemia cells and regulates survival and chemoresistance via NF-kappaB, Mapkinase and p53 pathways. *Leukemia*. 19(4), 586-94.

GRØNBAEK, K. *et al.* 1998. Alterations of the MMAC1/PTEN gene in lymphoid malignancies. *Blood*, 91(11), 4388-90.

HABER, D.A. *et al.* 1991. Alternative splicing and genomic structure of the Wilms tumor gene WT1. *Proc Natl Acad Sci U S A*, 88(21), 9618-22

HADLIE, J.L. and Howe JR 2006. Juvenile polyposis syndrome. *Gene reviews* NCBI books. Available from [http //www.ncbi.nlm.nih.gov/books/ncbi books](http://www.ncbi.nlm.nih.gov/books/ncbi%20books).

HANSEN, L. *et al.* 2001. Studies of variability in the PTEN gene among Danish caucasian patients with Type II diabetes mellitus. *Diabetologia*, 44(2), 237-40.

HAO, S.X. AND REN, R. 2000. Expression of interferon consensus sequence binding protein (ICSBP) is downregulated in Bcr-Abl-induced murine chronic myelogenous leukemia-like disease, and forced coexpression of ICSBP inhibits Bcr-Abl-induced myeloproliferative disorder. *Mol Cell Biol.*, 20(4), 1149-61

HILL, R. *et al.* 2005. Heterogeneous tumor evolution initiated by loss of pRb function in a preclinical prostate cancer model. *Cancer Res.*, 65(22), 10243-54.

HOFFBRAND, V. (ed) *et al.* 2006. *Essential Haematology* Blackwell Publishing, 5 Rev Ed.

HOLLAND, J. 2003. *Cancer Medicine* NCBI books. Available at: [http //www.ncbi.nlm.nih.gov/books/bv.fcgi?rid=cmed6.TOC&depth=2](http://www.ncbi.nlm.nih.gov/books/bv.fcgi?rid=cmed6.TOC&depth=2)

HORITA, M. *et al.* 2000. Blockade of the Bcr-Abl kinase activity induces apoptosis of chronic myelogenous leukemia cells by suppressing signal transducer and activator of transcription 5-dependent expression of Bcl-xL. *J Exp Med.*, 191(6), 977-84

HOSSAIN, A. AND SAUNDERS, G.F. 2001. The human sex-determining gene

SRY is a direct target of WT1. *J Biol Chem.*, 276(20), 16817-23

HORN, S. *et al.* 2004. Restoration of SHIP activity in a human leukemia cell line downregulates constitutively activated phosphatidylinositol 3-kinase/Akt/GSK-3 beta signaling and leads to an increased transit time through the G1 phase of the cell cycle. *Leukemia*, 18(11), 1839-49

ILIAKIS, G. 1997. Cell cycle regulation in irradiated and nonirradiated cells. *Semin Oncol.*, 24(6), 602-15

JENA, N. *et al.* 2002. Critical role for cyclin D2 in BCR/ABL-induced proliferation of hematopoietic cells. *Cancer Res.* 62(2), 535-41

JENNE, D.E. *et al.* 1998. Peutz-Jeghers syndrome is caused by mutations in a novel serine threonine kinase *Nat Genet.* 18(1), 38-43

JIN, Y. *et al.* 1997. Cell cycle-dependent colocalization of BARD1 and BRCA1 proteins in discrete nuclear domains. *Proc Natl Acad Sci U S A.* 94(22), 12075-80

JOHNSON, R.L. *et al.* 1996. Human homolog of patched, a candidate gene for the basal cell nevus syndrome. *Science*, 272(5268), 1668-71

JOU, T.S. *et al.* 1995. Genetic and biochemical dissection of protein linkages in the cadherin-catenin complex. *Proc Natl Acad Sci U S A*, 92(11), 5067-71

KAELIN, W.G. 2002. Molecular basis of the VHL hereditary cancer syndrome. *Nat Rev Cancer.*, 2(9), 673-82

KARTI, S.S. *et al.* 2002. Effect of interferon-alpha(2a) on neutrophil adhesion and phagocytosis in chronic myeloid leukemia and Behcet's disease. *Clin Rheumatol.*, 21(3), 211-4

KASHIGE, N. *et al.* 2000. Tyrosine phosphorylation of p62dok by p210bcr-abl inhibits RasGAP activity. *Proc Natl Acad Sci U S A*, 97(5), 2093-8

KEESHAN, K. *et al.* 2002. High Bcr-Abl expression prevents the translocation of

Bax and Bad to the mitochondrion. *Leukemia*, 16(9), 1725-34

KIMBALL, J. 2006. *Kimball's Biology Pages*. Available at:

<http://home.comcast.net/~john.kimball1/BiologyPages/>

KING, M. W. 2006. *Classification of proto-oncogenes* Available at: [http](http://www.dentistry.leeds.ac.uk/biochem/thcme/oncogene.html)

[//www.dentistry.leeds.ac.uk/biochem/thcme/oncogene.html](http://www.dentistry.leeds.ac.uk/biochem/thcme/oncogene.html)

KNUDSON, A.G. 1971. Mutation and cancer statistical study of retinoblastoma.

Proc. Natl Acad. Sci. USA, 68, 820–823

KOLASA, I.K, *et al.* 2006. PTEN mutation, expression and LOH at its locus in ovarian carcinomas. Relation to TP53, K-RAS and BRCA1 mutations. *Gynecol Oncol.*, 103(2), 692-7.

KORKKO, J. *et al.* 1998. Conformation sensitive gel electrophoresis for simple and accurate detection of mutations comparison with denaturing gradient gel electrophoresis and nucleotide sequencing. *Proc Natl Acad Sci U S A*, 95(4), 1681-5

KRALOVICS, R. *et al* 2005. A gain-of-function mutation of JAK2 in myeloproliferative disorders. *N Engl J Med.*, 352(17), 1779-90

KRAMER, A. *et al.* 2001. Proliferating status of peripheral blood progenitor cells from patients with BCR/ABL-positive chronic myelogenous leukemia. *Leukemia*, 15(1), 62-8

KUDLA, G. *et al.* , 2004. Gene Conversion and GC-Content Evolution in Mammalian Hsp70. *Mol Biol Evol.*, 21(7), 1438-44

KUFE, D. W. *et al.* (eds) 2006. *Cancer Medicine*. NCBI books Hamilton (Canada)

BC ker Inc. Available at: [http](http://www.ncbi.nlm.nih.gov/books/bv.fcgi?rid=cmed6.TOC&depth=2)

[//www.ncbi.nlm.nih.gov/books/bv.fcgi?rid=cmed6.TOC&depth=2](http://www.ncbi.nlm.nih.gov/books/bv.fcgi?rid=cmed6.TOC&depth=2)

KUROSE, K. *et al.* 2000. Biallelic inactivating mutations and an occult germline mutation of PTEN in primary cervical carcinomas. *Genes Chromosomes Cancer*,

29166-172,.

KUROSE, K. *et al.* 2002. Frequent somatic mutations in PTEN and TP53 are mutually exclusive in the stroma of breast carcinomas. *Nat Genet.*, 32(3), 355-7.

LEE, W.H. *et al.* 1987. The retinoblastoma susceptibility gene encodes a nuclear phosphoprotein associated with DNA binding activity *Nature*, 329, 642 - 645.

LEE, J.O. 1999. Crystal structure of the PTEN tumor suppressor implications for its phosphoinositide phosphatase activity and membrane association. *Cell*, 99(3), 323-34

LEHMANN, U. *et al.* 2001. Demonstration of light chain restricted clonal B-lymphoid infiltrates in archival bone row trephines by quantitative real-time polymerase chain reaction. *Am J Pathol.*, 159(6), 2023-9.

LESLIE, N.R. *et al.* 2007. PtdIns(3,4,5)P(3)-dependent and -independent roles for PTEN in the control of cell migration. *Curr Biol.*, 17(2), 115-25.

LESLIE, N.R. AND DOWNES, C.P. 2004. PTEN function how normal cells control it and tumour cells lose it. *Biochem J.* 382(1), 1-11

LEUPIN, N. *et al.* 2003. Disparate expression of the PTEN gene a novel finding in B-cell chronic lymphocytic leukaemia (B-CLL). *Br J Haematol.*, 121(1), 97-100.

LI, J. *et al.* 1997. PTEN, a putative protein tyrosine phosphatase gene mutated in human brain, breast, and prostate cancer. *Science*, 275, 1943-1946,

LIN, W.M. *et al.* 1998. Loss of heterozygosity and mutational analysis of the PTEN/MMAC1 gene in synchronous endometrial and ovarian carcinomas. *Clin Cancer Res* 4 2577-2583.

LIU, J.L. *et al.* 2005. Nuclear PTEN-Mediated Growth Suppression Is Independent of Akt Down-Regulation. *Molecular and Cellular Biology*, 25(14), 6211–6224

LIU, T.C. *et al.* 2000. Mutation analysis of PTEN/MMAC1 in acute myeloid

leukemia. *Am J Hematol*, 63, 170-5

LIU, W. *et al.* 1997. PTEN/MMAC1 mutations and EGFR amplification in glioblastomas. *Cancer Res.*, 57, 5254-5257

LIU, Y.L. *et al.* 2004. Evidence for PTEN Deficiency in Juvenile Myelomonocytic Leukemia. *Blood (ASH Annual Meeting Abstracts,)* 104, 3428

LODISH, H. *et al.* 2003. *Molecular Cell Biology* New York W. H. Freeman & Co., NCBI books. Available at: <http://www.ncbi.nlm.nih.gov/books/bv.fcgi?rid=mcb.TOC>

LUKAS, J. *et al.* 1995. Oncogenic aberrations of p16INK4/CDKN2 and cyclin D1 cooperate to deregulate G1 control. *Cancer Res.*, 55(21), 4818-23

LUO, J.M. *et al.* 2003. Possible dominant-negative mutation of the SHIP gene in acute myeloid leukemia. *Leukemia*,. 17(1), 1-8.

MARSH, D. J. *et al.* 1997. Differential Loss of Heterozygosity in the Region of the Cowden Locus within 10q22–23 in Follicular Thyroid Adenomas and Carcinomas. *Cancer Research*. 57, 500-503

MARU, Y. AND WITTE, O. N. 1991. The BCR gene encodes a novel serine/threonine kinase activity within a single exon. *Cell*, 67, 459-468,

MAXWELL, G.L. *et al.* 1998. Mutation of the PTEN tumor suppressor gene in endometrial hyperplasias. *Cancer Res.*, 58, 2500-2503.

MELO, J.V. 1996. The molecular biology of chronic myeloid leukaemia. *Leukemia*, 10(5), 751-6

MELO, J.V. AND DEININGER, M.W. 2004. Biology of chronic myelogenous leukemia--signaling pathways of initiation and transformation. *Hematol Oncol Clin North Am.*, 18(3), 545-68

MICHAEL, N. *et al.* 2004. *Cell Growth Control of Cell Size*. Cold Spring Harbour Press USA

MIN, Y.H. *et al.* 2004. Elevated S-phase kinase-associated protein 2 protein

expression in acute myelogenous leukemia its association with constitutive phosphorylation of phosphatase and tensin homologue protein and poor prognosis. *Clin Cancer Res.* 10(15), 5123-30

MUTTER, G.L. *et al.* 2000. Altered PTEN expression as a diagnostic marker for the earliest endometrial precancers. *J Natl Cancer Inst.*, 92, 924-930.

NAGAMINE, C. M. *et al.* 1989. A PCR artefact - generation of heteroduplexes, *Am J Hum Genet.*, 45(2), 337-339.

NAKAHARA, Y. *et al.* 1998. Mutational analysis of the PTEN/MMAC1 gene in non-Hodgkin's lymphoma. *Leukemia*, 12(8), 1277-80

NARITA, M. *et al.* 2003. Rb-mediated heterochromatin formation and silencing of E2F target genes during cellular senescence. *Cell*, 113(6), 703-16

NATHKE, I. 2004. APC at a glance. *J Cell Sci.*, 117(21), 4873-5.

NESHAT, M.S. *et al.* 2000. The survival function of the Bcr-Abl oncogene is mediated by Bad-dependent and -independent pathways roles for phosphatidylinositol 3-kinase and Raf. *Mol Cell Biol.*, 20(4), 1179-86.

NIEBOROWSKA-SKORSKA, M. *et al.* 1999. Signal transducer and activator of transcription (STAT)5 activation by BCR/ABL is dependent on intact Src homology (SH)3 and SH2 domains of BCR/ABL and is required for leukemogenesis. *J Exp Med.*, 189(8), 1229-42

NIGG, E. A. 1995. Cyclin-dependent protein kinases key regulators of the eukaryotic cell cycle. *Bioessays*, 17(6), 471-80

NIKSIC, M. *et al.* 2004. The Wilms' tumour protein (WT1) shuttles between nucleus and cytoplasm and is present in functional polysomes. *Hum Mol Genet.*, 13(4), 463-71

NISHIO, M. *et al.* 2007. Control of cell polarity and motility by the PtdIns(3,4,5)P3 phosphatase SHIP1. *Nat Cell Biol.*, 9(1), 36-44.

NOWELL, P.C. AND HUNGERFORD, D.A. 1960. Chromosome studies on normal and leukemic human leukocytes. *J Natl Cancer Inst.* 25, 85-109

ODA K *et al.* 2005. High Frequency of Coexistent Mutations of PIK3CA and PTEN Genes in Endometrial Carcinoma. *Cancer Research* 65, 10669-10673,

ODRIOZOLA, L. *et al.* 2007. Regulation of PTEN activity by its carboxyl-terminal autoinhibitory domain. *J Biol Chem.* 12 (Published on line ahead of print)
Available from [http //www.jbc.org/cgi/doi/10.1074/jbc.M611240200](http://www.jbc.org/cgi/doi/10.1074/jbc.M611240200)

OGWA 1993. Differentiation and Proliferation of Hematopoietic Stem Cells *Blood*, 81, 2844-2853

PANE, F. *et al.* 2002. BCR/ABL genes and leukemic phenotype from molecular mechanisms to clinical correlations. *Oncogene*, 21(56), 8652-67

PASSEGUÉ, E. *et al.* 2003. Normal and leukemic hematopoiesis are leukemias a stem cell disorder or a reacquisition of stem cell characteristics? *Proc Natl Acad Sci U S A*, 100 (Suppl 1), 11842-9

PAYNE, S. R. AND KEMP, C.J. 2005. Tumor suppressor genetics. *Carcinogenesis*, 26 (12), 2031-2045.

PESCHE, S. *et al.* 1998. PTEN/MMAC1/TEP1 involvement in primary prostate cancers. *Oncogene*, 16, 2879-2883,

PETRUCCELLI, N. *et al.* 2005. BRCA1 and BRCA2 Hereditary Breast/Ovarian Cancer. *GeneReviews* NCBI books. Available from [http //www.ncbi.nlm.nih.gov/books/bv.fcgi?rid=gene.TOC](http://www.ncbi.nlm.nih.gov/books/bv.fcgi?rid=gene.TOC).

POETSCH, M. *et al.* 2002. Detection of new PTEN/MMAC1 mutations in head and neck squamous cell carcinomas with loss of chromosome 10. *Cancer Genet. Cytogenet.*, 132, 20-24,

QUACH, N. *et al.* 2004. In vitro mutation artefacts after formalin fixation and error prone translesion synthesis during PCR *BMC Clinical Pathology*, 4(1) 1 Available

from [http](http://www.pubmedcentral.nih.gov/articlerender.fcgi?tool=pubmed&pubmedid=150281)

[//www.pubmedcentral.nih.gov/articlerender.fcgi?tool=pubmed&pubmedid=150281](http://www.pubmedcentral.nih.gov/articlerender.fcgi?tool=pubmed&pubmedid=150281)

25

RAFTOPOULOU, M. *et al.* 2004. Regulation of cell migration by the C2 domain of the tumor suppressor PTEN. *Science*, 303(5661), 1179-81

RASHEED, B.K. *et al.* 1997. PTEN gene mutations are seen in high grade but not in low-grade gliomas. *Cancer Res* 57, 4187- 4190,

RISINGER, J.I. *et al.* 1997. PTEN/MMAC1 mutations in endometrial cancers. *Cancer Res.*, 57, 4736-4738.

RISINGER, J.I. 1998 *et al.* PTEN mutation in endometrial cancers is associated with favorable clinical and pathologic characteristics. *Clin Cancer Res* 4, 3005-3010,

RIVERO, E.R. *et al.* 2006. Simple salting-out method for DNA extraction from formalin-fixed, paraffin-embedded tissues. *Pathol Res Pract.*, 202(7), 523-529.

ROBERTSON, K.D. 2005. DNA methylation and human disease. *Nat Rev Genet.*, 6(8), 597-610.

ROWLEY, D. 1973. A New Consistent Chromosomal Abnormality in Chronic Myelogenous Leukaemia identified by Quinacrine Fluorescence and Giemsa Staining. *Nature*, 243, 290 - 293

ROZEN, S. AND SKALETSKY, H.J. 2000. *Steve Rozen and Helen J. Skaletsky (2000) Primer3 on the WWW for general users and for biologist programmers. In: Krawetz S, Misener S (eds) Bioinformatics Methods and Protocols: Methods in Molecular Biology. Humana Press, Totowa, NJ, pp 365-386.* Available from, http://frodo.wi.mit.edu/cgi-bin/primer3/primer3_www.cgi

SAKAI, A. *et al.* 1998. PTEN gene alterations in lymphoid neoplasms. *Blood*, 92(9), 3410-5

SALMENA, L. AND PANDOLFI, P.P. 2007. Changing venues for tumour suppression balancing destruction and localization by monoubiquitylation *Nat Rev Cancer*, 7(6), 409-13..

SAMBROOK, J. *et al.* 2000. *Molecular Cloning (3-volume set) A Laboratory Manual* Cold Spring Harbor Laboratory Press USA.

SATO, K. *et al.* 2002. Analysis of genetic and epigenetic alterations of the PTEN gene in gastric cancer. *Virchows Arch.*, 440(2), 160-5.

SATTLER, M. *et al.* 2002. Critical role for Gab2 in transformation by BCR/ABL. *Cancer Cell*, 1(5), 479-92

SAVAGE, D.G. *et al.* 1997. Clinical features at diagnosis in 430 patients with chronic myeloid leukaemia seen at a referral centre over a 16-year period. *Br J Haematol.*, 96(1), 111-6

SAWYERS, C.L. *et al.* 1995. Genetic requirement for Ras in the transformation of fibroblasts and hematopoietic cells by the Bcr-Abl oncogene. *J Exp Med.*, 181(1), 307-13.

SAWYERS, C.L. 1999. Chronic myeloid leukemia. *N Engl J Med.*, 340(17), 1330-40

SCARISBRICK, J.J. *et al.* 2000. Loss of heterozygosity on 10q and microsatellite instability in advanced stages of primary cutaneous T-cell lymphoma and possible association with homozygous deletion of PTEN. *Blood*, 95(9), 2937-42

SCHMALE, G. A. *et al.* Hereditary Multiple Exostoses *Gene reviews* 2006. NCBI books Available from <http://www.ncbi.nlm.nih.gov/books/bv.fcgi?rid=gene.TOC>

SEMB, H. AND CHRISTOFORI, G. 1998. The tumor-suppressor function of E-cadherin. *Am J Hum Genet.*, 63(6), 1588-93

SEMINARIO, M-C. *et al.* 2003. PTEN expression in PTEN-null leukaemic T cell lines leads to reduced proliferation via slowed cell cycle progression. *Oncogene*,

SHAN, X. *et al.* 2000. Deficiency of PTEN in Jurkat T Cells Causes constitutive Localization of Itk to the Plasma Membrane and Hyperresponsiveness to CD3 Stimulation *Molecular And Cellular Biology*, 20(18), 6945–6957

SHEN, Q. *et al.* 2005. Expression of PTEN mRNA in acute leukemia and its clinical significance *Zhonghua Xue Ye Xue Za Zhi*, 26(8), 493-6.

SHEN, W.H. *et al.* 2007. Essential role for nuclear PTEN in maintaining chromosomal integrity. *Cell*, 128(1), 157-70

SOLOMON, C. AND BURT, R. W. APC-Associated Polyposis Conditions. *Gene Reviews* NCBI books 2005. Available from <http://www.ncbi.nlm.nih.gov/books/bv.fcgi?rid=gene.TOC>

STAMBOLIC, V. *et al.* 1998. Negative regulation of PKB/Akt-dependent cell survival by the tumor suppressor PTEN. *Cell*, 95(1), 29-39

STAMBOLIC, V. *et al.* 2001. Regulation of PTEN transcription by p53. *Mol Cell*, 8(2), 317-25

STECK, P.A. *et al.* 1997. Identification of a candidate tumour suppressor gene, MMAC1, at chromosome 10q23.3 that is mutated in multiple advanced cancers. *Nat Genet.*, 15(4), 356-62

STEHELIN, D. 1976. The transforming gene of avian tumor viruses. *Pathol Biol.*, 24(8), 513-5. STOTT, F.J. *et al.* 1998. The alternative product from the human CDKN2A locus, p14(ARF), participates in a regulatory feedback loop with p53 and MDM2 *EMBO J.*, 17, 5001-14

STRACHAN, T. AND READ, A. 2003. *Human Molecular Genetics*. Garland Science UK.

SUBRAMANIAN, K.K. *et al.* 2007. Tumor suppressor PTEN is a physiologic suppressor of chemoattractant-mediated neutrophil functions. *Blood*, 109(9),

TAKEDA, N. AND SHIBUYA, M. 1999. The BCR-ABL oncoprotein potentially interacts with the xeroderma pigmentosum group B protein. *Proc Natl Acad Sci U S A*, 96(1), 203-7

TAMURA, M. *et al.* 1998. Inhibition of cell migration, spreading, and focal adhesions by tumor suppressor PTEN. *Science*, 280(5369), 1614-7

TASHIRO, H. *et al.* 1997. Mutations in PTEN are frequent in endometrial carcinoma but rare in other common gynaecological malignancies. *Cancer Res.*, 57, 3935-3940,

THEIN, S. AND WALLACE, R. 1986. The use of synthetic oligonucleotides as specific hybridization probes in the diagnosis of genetic disorders. *Human Genetic Diseases A Practical Approach*. Herndon, Vancouver. IRL Press,.

THOMAS, D.M. *et al.* 2001. The retinoblastoma protein acts as a transcriptional coactivator required for osteogenic differentiation. *Mol Cell.*, 8(2), 303-16.

THOMPSON, M. E. *et al.* 1995. Decreased expression of BRCA1 accelerates growth and is often present during sporadic breast cancer progression. *Nature Genetics*, 9, 444 - 450

TIAN, H. *et al.* 2001. Capillary and microchip electrophoresis for rapid detection of known mutations by combining allele-specific DNA amplification with heteroduplex analysis. *Clin Chem.*, 47(2), 173-85.

TOLKACHEVA, T. *et al.* 2001. Regulation of PTEN binding to MAGI-2 by two putative phosphorylation sites at threonine 382 and 383. *Cancer Res.* 61(13), 4985-9

TORRES, J. and Pulido R. 2001. The tumor suppressor PTEN is phosphorylated by the protein kinase CK2 at its C terminus. Implications for PTEN stability to

proteasome-mediated degradation. *J Biol Chem.*, 276(2), 993-8

TROTMAN, L.C. *et al.* 2007. Ubiquitination regulates PTEN nuclear import and tumor suppression. *Cell.*, 128(1), 141-56.

TSOU, H.C. *et al.* 1998. The genetic basis of Cowden's syndrome three el mutations in PTEN/MMAC1/TEP1. *Hum Genet.*, 102(4), 467-73.

TUCKER, K.L. *et al.* 1996. Complementation of methylation deficiency in embryonic stem cells by a DNA methyltransferase minigene. *Proc Natl Acad Sci USA*, 93, 12920-5

VARDIMAN, J.W. *et al.* 2002. The World Health Organization (WHO) classification of the myeloid neoplasms. *Blood*, 100(7), 2292-2302

VAZQUEZ, F. *et al.* 2000. Phosphorylation of the PTEN tail regulates protein stability and function. *Mol Cell Biol.*, 20(14), 5010-8

VAZQUEZ, F. *et al.* 2001. Phosphorylation of the PTEN tail acts as an inhibitory switch by preventing its recruitment into a protein complex. *J Biol Chem.*, 276(52), 48627-30

VERSTEEGE, I. *et al.* 1998. Truncating mutations of hSNF5/INI1 in aggressive paediatric cancer. *Nature*. 394(6689) 203-6

VIROLLE, T. *et al.* 2001. The Egr-1 transcription factor directly activates PTEN during irradiation-induced signalling. *Nat Cell Biol.*, 3(12), 1124-8.

VLIETSTRA, R.J. *et al.* 1998. Frequent inactivation of PTEN in prostate cancer cell lines and xenografts. *Cancer Res* 58 ,2720-2723

VOGELSTEIN, B. AND KINZLER, K.W. 2004. Cancer genes and the pathways they control. *Nat Med.*, 10(8), 789-99

WALKER, S.M. *et al.* 2004. The tumour-suppressor function of PTEN requires an N-terminal lipid-binding motif. *Biochem J.*, 379(Pt 2), 301-7

WANG, S.I. *et al.* 1998. Homozygous deletion of the PTEN tumor suppressor

gene in a subset of prostate adenocarcinomas. *Clin Cancer Res.*, 4, 811-815,

WANG, J.Y. 2000. Regulation of cell death by the Abl tyrosine kinase. *Oncogene*, 19(49), 5643-50

WANG, X.W. 1999. Role of p53 and apoptosis in carcinogenesis. *Anticancer Res.* 19(6A), 4759-71.

WEINBERG, R.A. 1994. Oncogenes and tumor suppressor genes. *CA Cancer J Clin.* 44(3), 160-70

WEN, S. *et al.* 2001. PTEN controls tumor-induced angiogenesis. *Proc. Nat. Acad. Sci.*, 98, 4622-4627,

WENG, L.P. *et al.* 1999. PTEN suppresses breast cancer cell growth by phosphatase activity-dependent G1 arrest followed by cell death. *Cancer Res.*, 59, 5808-5814,

WENG, L.P. *et al.* 2001a. PTEN coordinates G(1) arrest by down-regulating cyclin D1 via its protein phosphatase activity and up-regulating p27 via its lipid phosphatase activity in a breast cancer model. *Hum Mol Genet.*, 10(6), 599-604

WENG, L.P. *et al.* 2001b. PTEN induces apoptosis and cell cycle arrest through phosphoinositol-3-kinase/Akt-dependent and -independent pathways. *Hum Mol Genet.*, 10(3), 237-42

WILCOCKSON, J. 1973. The use of sodium perchlorate in deproteinization during the preparation of nucleic acids. *Biochem J.*, 135(3), 559-61.

WU, H. *et al.* 2003. PTEN signaling pathways in melanoma. *Oncogene*, 22(20), 3113-22

YAMADA, K. M. and Araki M 2002. Tumor suppressor PTEN modulator of cell signaling, growth, migration and apoptosis. *Journal of Cell Science*, 114, 2375-2382

YAP, D.B. *et al* 1999. mdm2 a bridge over the two tumour suppressors, p53 and

Rb. *Oncogene*, 18(53), 7681-9.

YILMAZ, O.H. *et al.* 2006. PTEN dependence distinguishes haematopoietic stem cells from leukaemia-initiating cells. *Nature*, 441(7092), 475-82

YOU, M.J. *et al.* 2002. Genetic analysis of PTEN and Ink4a/Arf interactions in the suppression of tumorigenesis in mice. *Proc Natl Acad Sci U S A*, 99(3), 1455-60

ZHANG, J. *et al.* 2006. PTEN maintains haematopoietic stem cells and acts in lineage choice and leukaemia prevention. *Nature*, 441(7092), 518-22.

ZHOU, X-P. *et al.* 2000. Epigenetic PTEN Silencing in Malignant Melanomas without *PTEN* Mutation. *American Journal of Pathology*, 157, 1123-1128

ZHOU, X-P. *et al.* 2002. Distinct PTEN mutational spectra in hereditary non-polyposis colon cancer syndrome-related endometrial carcinomas compared to sporadic microsatellite unstable tumors. *Hum. Molec. Genet.* 11, 445-450,

ZHOU, M. *et al.* 2003. PTEN Reverses MDM2-mediated Chemotherapy Resistance by interacting with p53 in Acute Lymphoblastic Leukemia Cells *Cancer Research*, 63, 6357–6362,

ZSIKLA, V. *et al.* 2004. Effect of buffered formalin on amplification of DNA from paraffin wax embedded small biopsies using real-time PCR. *Journal of Clinical Pathology*, 57, 654-656

ZYSMAN, A. *et al.* 2002. Considerations When Analyzing the Methylation Status of PTEN Tumor Suppressor Gene *American Journal of Pathology*, 160, 795-800.

Appendix I

World Health Organisation Classification of Haematological Malignancy (Vardiman *et al.* 2002.)

WHO classification of acute myeloid leukemia

Acute myeloid leukemia with recurrent genetic abnormalities

Acute myeloid leukemia with t(8;21)(q22;q22), (*AML1/ETO*)

Acute myeloid leukemia with abnormal bone marrow eosinophils and inv(16)(p13q22) or t(16;16)(p13;q22), (*CBF β /MYH11*)

Acute promyelocytic leukemia with t(15;17)(q22;q12), (*PML/RAR α*) and variants

Acute myeloid leukemia with 11q23 (*MLL*) abnormalities

Acute myeloid leukemia with multilineage dysplasia

Following MDS or MDS/MPD

Without antecedent MDS or MDS/MPD, but with dysplasia in at least 50% of cells in 2 or more myeloid lineages

Acute myeloid leukemia and myelodysplastic syndromes, therapy related

Alkylating agent/radiation-related type

Topoisomerase II inhibitor-related type (some may be lymphoid)

Acute myeloid leukemia, not otherwise categorized Classify as:

Acute myeloid leukemia, minimally differentiated

Acute myeloid leukemia without maturation

Acute myeloid leukemia with maturation

Acute myelomonocytic leukemia

Acute monoblastic/acute monocytic leukemia

Acute erythroid leukemia (erythroid/myeloid and pure erythroleukemia)

Acute megakaryoblastic leukemia

Acute basophilic leukemia

Acute panmyelosis with myelofibrosis

Myeloid sarcoma

WHO classification of the myelodysplastic/myeloproliferative diseases

Chronic myelomonocytic leukemia

Atypical chronic myeloid leukemia

Juvenile myelomonocytic leukemia

Myelodysplastic/myeloproliferative disease, unclassifiable

WHO classification and criteria for the myelodysplastic syndromes

Disease	Blood findings	Bone marrow findings
Refractory anemia (RA)	Anemia No or rare blasts	Erythroid dysplasia <i>only</i> < 5% blasts < 15% ringed sideroblasts
Refractory anemia with ringed sideroblasts (RARS)	Anemia No blasts	Erythroid dysplasia <i>only</i> ≥ 15% ringed sideroblasts < 5% blasts
Refractory cytopenia with multilineage dysplasia (RCMD)	Cytopenias (bicytopenia or pancytopenia) No or rare blasts No Auer rods < 1 × 10 ⁹ /L monocytes	or Dysplasia in ≥ 10% of cells in 2 or more myeloid cell lines < 5% blasts in marrow No Auer rods < 15% ringed sideroblasts
Refractory cytopenia with multilineage dysplasia and ringed sideroblasts (RCMD-RS)	Cytopenias (bicytopenia or pancytopenia) No or rare blasts No Auer rods < 1 × 10 ⁹ /L monocytes	or Dysplasia in ≥ 10% of cells in 2 or more myeloid cell lines ≥ 15% ringed sideroblasts < 5% blasts No Auer rods
Refractory anemia with excess blasts-1 (RAEB-1)	Cytopenias < 5% blasts No Auer rods < 1 × 10 ⁹ /L monocytes	Unilineage or multilineage dysplasia 5% to 9% blasts No Auer rods
Refractory anemia with excess blasts-2 (RAEB-2)	Cytopenias 5% to 19% blasts Auer rods ± < 1 × 10 ⁹ /L monocytes	Unilineage or multilineage dysplasia 10% to 19% blasts Auer rods ±
Myelodysplastic syndrome, unclassified (MDS-U)	Cytopenias No or rare blasts No Auer rods	Unilineage dysplasia in granulocytes or megakaryocytes < 5% blasts No Auer rods
MDS associated with isolated	Anemia < 5% blasts Platelets normal or increased	Norm to inc megakaryocytes with del(5q) hypolobated nuclei < 5% blasts No Auer rods

WHO classification Diagnostic criteria for CMML

Persistent peripheral blood monocytosis greater than $1 \times 10^9/L$

No Philadelphia chromosome or *BCR/ABL* fusion gene

Fewer than 20% blasts* in the blood or bone marrow

Dysplasia in one or more myeloid lineages. If myelodysplasia is absent or minimal, the diagnosis of CMML may still be made if the other requirements are present and:

an acquired, clonal cytogenetic abnormality is present in the marrow cells, or

the monocytosis has been persistent for at least 3 months and all other causes of monocytosis have been excluded

Diagnose CMML-1 when blasts fewer than 5% in blood and fewer than 10% in bone marrow

Diagnose CMML-2 when blasts are 5% to 19% in blood, or 10% to 19% in marrow, or if Auer rods are present and blasts are fewer than 20% in blood or marrow

Diagnose CMML-1 or CMML-2 with eosinophilia when the criteria above are present and when the eosinophil count in the peripheral blood is greater than $1.5 \times 10^9/L$

*In this classification of CMML, blasts include myeloblasts, monoblasts, and promonocytes.

WHO classification of chronic myeloproliferative diseases

Chronic myelogenous leukemia [Ph chromosome, t(9;22)(q34;q11), *BCR/ABL*-positive]

Chronic neutrophilic leukemia

Chronic eosinophilic leukemia (and the hypereosinophilic syndrome)

Polycythemia vera

Chronic idiopathic myelofibrosis (with extramedullary hematopoiesis)

Essential thrombocythemia

Chronic myeloproliferative disease, unclassifiable

WHO classification - Criteria for accelerated and blast phases of CML

CML, accelerated phase (AP)

Diagnose if one or more of the following is present:

Blasts 10% to 19% of peripheral blood white cells or bone marrow cells

Peripheral blood basophils at least 20%

Persistent thrombocytopenia ($< 100 \times 10^9/L$) unrelated to therapy, or persistent thrombocytosis ($> 1000 \times 10^9/L$) unresponsive to therapy

Increasing spleen size and increasing WBC count unresponsive to therapy

Cytogenetic evidence of clonal evolution (ie, the appearance of an additional genetic abnormality that was not present in the initial specimen at the time of diagnosis of chronic phase CML)

Megakaryocytic proliferation in sizable sheets and clusters, associated with marked reticulin or collagen fibrosis, and/or severe granulocytic dysplasia, should be considered as suggestive of CML-AP. These findings have not yet been analyzed in large clinical studies, however, so it is not clear if they are independent criteria for accelerated phase. They often occur simultaneously with one or more of the other features listed.

CML, blast phase (BP)

Diagnose if one or more of following is present:

Blasts 20% or more of peripheral blood white cells or bone marrow cells

Extramedullary blast proliferation

Large foci or clusters of blasts in bone marrow biopsy

Appendix II

French/American/British Classification of leukaemia (Vardiman *et al.* 2002.)

Acute myeloid leukaemia

M0 (undifferentiated AML)
M1 (myeloblastic, without maturation)
M2 (myeloblastic, with maturation)
M3 (promyelocytic), or acute promyelocytic leukemia (APL)
M4 (myelomonocytic)
M4eo (myelomonocytic together with bone marrow eosinophilia)
M5 monoblastic leukemia (M5a) or monocytic leukemia (M5b)
M6 (erythrocytic), or erythroleukemia
M7 (megakaryoblastic)

Acute lymphoblastic leukaemia

ALL-L1:small uniform cells
ALL-L2: large varied cells
ALL-L3: large varied cells with vacuoles (bubble-like features)

Myelodysplastic syndromes

RA Refractory anemia - less than 5% primitive blood cells (myeloblasts) in the bone marrow and pathological abnormalities primarily seen in red cell precursors
RARS Refractory anemia with ringed sideroblasts less than 5% myeloblasts in the bone marrow, 15% or greater "ringed sideroblasts";
RAEB Refractory anemia with excess blasts - 5-19% myeloblasts in the marrow;
RAEB-T Refractory anemia with excess blasts in transformation - 20-29% myeloblasts in the marrow (30% blasts is defined as acute myeloid leukemia);
CMML Chronic myelomonocytic leukemia -

Appendix III

Manual Staining Procedure For Blood Films

1 PRINCIPLE

The acidic groupings of the nucleic acids and proteins of the cell nuclei and cytoplasm determine the uptake in varying intensities of the basic dye Azure B whilst the presence of any basic groupings are indicated by the Eosin Y, for example:

- Neutrophil granules are weakly stained by the azure complexes.
 - Eosinophilic granules containing alkaline groups stain strongly with Eosin.
 - Basophil granules stain heavily with Azure due to its heparin content.
- Cells that have both groupings take up both stains in varying intensities, eg.

reticulocytes.

2 COSHH and HEALTH & SAFETY REQUIREMENTS

Blood films are still a biohazard until they are fixed.

Methanol – toxic by ingestion and is inflammable.

May Grunwald stain –contains methanol

Giemsa stain

see COSHH file

3 REAGENTS

Absolute Methanol

Giemsa stain

May Grunwald stain

Sorensen's buffer concentrate

Buffered water pH (6.8 – 7.0)

4 PREPARATION OF STAINS

BUFFER

1 x 25ml bottle Sorensen's buffer concentrate to 5 litres deionised water. Mix well.

MAY GRUNWALD

100ml May Grunwald stain

200ml Buffer

GIEMSA

20ml Giemsa stain

280ml Buffer

5 METHOD

METHANOL	5 minutes
MAY GRUNWALD	6minutes
GIEMSA	12 minutes
BUFFERED WATER	2minutes

Appendix IV

Immunocytochemistry using Shandon Sequenza staining system

1. Place wax sections in a metal staining rack. Dewax sections in three consecutive changes of xylene - five minutes each, then take to alcohol in three changes of industrial ethanol five minutes each. Do not allow slides to dry at any time during entire staining process
2. Immerse in 0.5% hydrogen peroxide in methanol (Appendix 2) for ten minutes to inhibit endogenous peroxidase activity, and wash in tap water.
3. Place slides requiring trypsinisation in distilled water for 10 mins at 37°C. Place slides not requiring trypsinisation in TRIS buffered saline (TBS) pH 7.6 at room temp.
4. Incubate trypsinisation samples in 0.1% trypsin in 0.1% calcium chloride at pH 7.8 (Appendix 2) at 37°C for 30 mins then wash in cold water and transfer to TBS.
5. Place samples for microwave treatment in a polypropylene slide rack and immerse in 250 ml of citrate buffer (Appendix 2) in a polypropylene 1000 ml beaker. Place slides in a 750 Watt Toshiba microwave oven and microwave for twenty minutes at 80% power. Cool slowly in running tap water then placed in TBS.
6. Load sections onto a Shandon Sequenza staining rack and wash with TBS for five mins.
7. Incubate all sections with normal goat serum (1:5 with TBS) for 20 mins to block non specific binding of primary antibodies.

8. Treat with relevant dilution of primary antibody for 60 mins at room temp.
9. Wash in TBS for five mins.
10. Incubated in "Biogenex" Streptavidin Multilink diluted 1:60 in TBS for 30 mins.
11. Wash in TBS for five mins.
12. Incubate in "Biogenex" StrepABC/horse radish peroxidase label diluted 1:60 in TBS for 30 mins
13. Wash in TBS for five mins.
14. Incubated in DAB solution (Appendix 2) for 5 mins.
15. Wash in tap water 5mins.
16. Counterstain with Harris's Haematoxylin for 10 seconds and blue in tap water.
17. Dehydrate through consecutive changes of ethanol, clear in xylene and mount in non aqueous mounting media.

(Internal Standard Operating Procedure, Dept of Histopathology, Arrowe Park Hospital.2003)